

# 9. Early Performance Analysis of Conceptual Flight Vehicles with Multiple Types of Effectors

---

## Background

Designs of conceptual flight vehicles must meet, among many other things, controllability, stability, and maneuverability performance requirements in order to be certified for operation. However, a flight vehicle's ability to meet these requirements is often limited by performance, stability, or control authority availability. Thus, it is essential for designers to evaluate the overall performance and control authority of candidate concepts in a static sense, early in the design process, and prior to dynamic analysis.

Designers normally consider numerous possible vehicle configurations before stability and control system groups begin their analysis and design. However, there is no existing framework for conducting sophisticated and systematic analysis of early designs controlled with multiple types of effectors. There is a need, therefore, for a quick and methodical tool for examining new flight vehicle concepts and providing a more efficient design process by analyzing a number of important static performance parameters calculated from preliminary vehicle data. The methodology presented in this document is intended to bridge the gap between concept and realism and to simplify the task of the flight control systems engineer in evaluating new vehicle concepts in terms of satisfying mission and meeting performance expectations.

**Eric T. Falangas**  
**Flixan Engineering Services**  
**Web Site: [Flixan.com](http://Flixan.com)**  
**Email: [info@flixan.com](mailto:info@flixan.com)**

---

<b>Table of Contents</b>	<b>Page</b>
Background	1
Introduction	4
1.0 Methodology Overview	7
1.1 Control Effectors	11
1.2 Dynamic Modeling and Effector Mixing Logic	12
2.0 Trimming the Effectors for Balancing the Flight Vehicle Moments and Forces	13
2.1 Basic Aerodynamic Moments and Forces	16
2.2 Moments and Forces Produced by a Control Surface Deflection	17
2.3 Moments and Forces due to an Engine Gimbaling in Pitch and Yaw	18
2.4 Numerical Solution for Calculating the Effector Trim Deflections and Throttles	21
2.5 Running the Effector Trimming Program	23
2.6 Graphically Adjusting the Trim History	29
2.7 Trimming with a Modified Trajectory	33
2.8 Trimming with a Faulty Effector	35
3.0 Static Performance Analysis Along a Trajectory	38
3.1 Transforming the Aero Moment Coefficients	39
3.2 Converting FCS Demands to Vehicle Moments and Forces	40
3.3 Vehicle Moments and Forces Generated by a Double-Gimbaling Engine	42
3.4 Vehicle Moments and Forces Generated by an Engine Gimbaling in Single Direction	43
3.5 Vehicle Moments and Forces Generated by a Throttling Engine	44
3.6 Vehicle Moments and Forces Generated by Control Surfaces	44
3.7 Total Vehicle Moments and Forces due to All Effectors Combined	45
3.8 Performance Parameters	47
3.8.1 Aerodynamic Center	47
3.8.2 Static Margin	47
3.8.3 Center of Pressure	47
3.8.4 Pitch Static Stability/ Time to Double Amplitude (T2) Parameter	48
3.8.5 Directional Stability ( $C_n\beta_{dynamic}$ )	49
3.8.6 Lateral Time to Double Amplitude/ Stability Parameter (T2)	50
3.8.7 Control Authority of Effectors	50
3.8.8 Biased Effectors	53
3.8.9 Control to Disturbance Partial (Ma/Md)	53
3.8.10 Pitch Control Authority against an Angle of Attack Variation	54
3.8.11 Pitch Control Authority against Velocity Variation	56
3.8.12 Lateral Control Authority against Angle of Sideslip Dispersions	57
3.8.13 Lateral Control Authority against Velocity Variations	58
3.8.14 Normal and Lateral Loads	59
3.8.15 Bank Angle and Side-Force during a Steady Sideslip	60
3.8.16 Engine-Out or $Y_{CG}$ Offset Situations	61
3.8.17 Lateral Control Departure Parameter (LCDP)	61
3.8.18 Examples Showing the Effects of LCDP Sign Reversal on Stability	65
3.8.19 Effector Capability to Provide Rotational and Translational Accelerations	68
3.8.20 Steady Pull-Up Maneuverability	69
3.8.21 Pitch Inertial Coupling due to Stability Roll	71
3.8.22 Yaw Inertial Coupling due to Loaded Roll	72
3.8.22 Moments at the Hinges of the Control Surfaces	73
4.0 Aero Data, Trajectory Analysis and Plotting	74
4.1 Plotting the Aero Data	74
4.2 Plotting the Trajectory Data	76
4.3 Modifying the Trajectory Data for Dispersion Analysis	78
4.4 Adjusting the Effector Trim Data	81

4.5	Plotting and Comparing Data	85
5.0	Effector Combination Logic	87
5.1	Input Data	88
5.2	Creating a Mixing Logic Matrix from "Trim"	89
5.3	Derivation of an Effector Combination Matrix	95
5.3.1	Forces and Moments Generated By a Single Engine	97
5.3.2	Moments and Forces Generated by a Single Engine Gimbaling in Pitch and Yaw	99
5.3.3	Moments and Forces of an Engine Gimbaling in a Single Skewed Direction	100
5.3.4	Moments and Forces Generated by a Throttling Engine or an RCS Jet	101
5.3.5	Moments and Forces Generated by a Control Surface Deflection	102
5.3.6	Change in Vehicle Rate due to the Combined Effect from All Actuators	102
6.0	Generating State-Space Models for Linear Control Analysis	105
7.0	Contour Plots of Performance Parameters Plotted Against (Mach and Alpha)	113
7.1	Running the Flixan Contour Plots Program	117
8.0	Static Analysis Using Vector Diagrams	128
8.1	Maximum Moment and Force Vector Diagrams	132
8.2	Maximum Acceleration Vector Diagrams	138
8.2.1	Maximum Accelerations due to Air-Speed Variation $v_{max}$	141
8.3	Moment and Force Vector Partial	142
8.3.1	Control versus Airspeed Variation Partial	146
8.4	Acceleration per Acceleration Demand Vector Partial	148
8.5	Converting the Aero Uncertainties from Individual Aerosurface Panels to Vehicle Axes	150
8.6	Running the Vector Diagrams Program from Flixan	154
9.0	Data Files and Description	162
9.1	Trajectory Data Files	163
9.2	Mass Properties Data File	164
9.3	Propulsion Data File	165
9.4	Base Aero Data File	166
9.5	Control Surface Aero Data File	167
9.6	Hinge Moment Coefficients File	170
9.7	Damping Derivatives File	171
9.8	Aerodynamic Uncertainties File	172
9.9	Fuel Sloshing Data File	173
9.10	Output Data Files	174
10.0	Design Examples	175
10.1	Hypersonic Rocket-Plane Analysis during Ascent and Descent phases	1-1
10.2	F-16 Fighter Aircraft Analysis, Control Design, and 6-dof Simulation	2-1
10.3	Air-Launched Vehicle with Wings and Tails Design in Multiple Phases	3-1
10.4	Re-Usable Launch Vehicle with Multiple-Engines During Ascent and Descent	4-1
10.5	Lifting-Body Aircraft Descent from Space, Vertical Take-Off, and 6-dof Simulation	5-1
10.6	Re-Entry Vehicle Design and Analysis Using Aero-Surfaces and RCS Jets	6-1



## Introduction

Flight vehicles must meet controllability and maneuverability performance requirements in order to be certified for operations. A vehicle's ability to meet these requirements is often limited by the amount of control authority available. Thus, it is essential for designers to assess the control authority of candidate concepts early in the conceptual design phase. Designers normally consider numerous possible vehicle configurations before structures and control system groups begin their dynamic analysis. An early performance evaluation before detailed control design begins is necessary. In this document we are presenting a methodology for quick evaluation of controllability and performance of conceptual vehicle designs, in a static sense, against the requirements imposed by the vehicle purpose and mission at critical flight conditions.

In the early phase of a new flight vehicle the design team must define the purpose, missions, and hardware configuration of the vehicle. This determines its initial shape and the aerodynamic lift and drag coefficients. From the lift and drag coefficients trajectories are created by means of point-mass or 6-DOF simulations that achieve the mission goals and the critical flight conditions are identified. This design cycle, however, is an iterative process and there is a need for rapid re-evaluation of vehicle performance in terms of static-stability,

maneuverability, control authority, and the effector capability to trim in order to balance the moments and forces which are specified in the trajectory environment. This static evaluation of a vehicle concept must be performed prior to any linear analysis, flight control system design, and time domain simulations which are considerably more time consuming.

Sometimes you take a look at flight vehicle design concept and you instinctively suspect that there is something wrong with it, and wished that you had a logical way of proving it. The shape tells you something about its aerodynamics, the weight distribution about stability, the effectors location and size about control authority and maneuverability. Sometimes you suspect that the CG is either too far back or too close to the front or that the effectors are too small or too big and you are not sure if the engines or aerosurfaces can provide the forces and moments to maneuver it. There are also situations where you would like to trade control authority in one direction against other directions by adjusting the effectors and positions, or trying other types of effectors in different locations, or that you may want to quantify the effectors control authority necessary to survive the expected flight environment, or to trade control authority among multiple effectors. There are also times when the designer would like to know the consequences of losing an aerosurface, RCS jet, thrust or an actuator from a TVC engine, or to analyze the effects of CG variations due to payload shifts. An optimized trajectory does not provide any information about the vehicle performance and its ability to survive the expected trajectory environment, dispersions due to winds, and effector failures, mainly because it is missing the effector information. The vehicle may be unable to follow the trajectory, either because it does not have sufficient control authority to trim, to counteract dispersions in aerodynamic angles, or it may be too divergent or too stable and unable to maneuver. An analysis process is necessary between trajectory optimization and control design to predict the vehicle performance and its capability to track the proposed trajectory.

All these capabilities and more are addressed by the methodology presented in this document that provides a systematic approach and the necessary tools to rapidly evaluate an early vehicle concept. It uses aerodynamic data, trajectory, propulsion, and mass properties data to evaluate if the flight vehicle concept possesses adequate control power, static stability and maneuverability qualities to satisfy the requirements defined at critical flight conditions along a trajectory, without getting involved in simulations, dynamic modeling and control design. In addition, the method provides guidelines on how to take a corrective action in case the vehicle concept does not meet the required performance. This methodology is implemented in a software tool that is integrated as an option of the Flixan program. We call it "Trim" for short, although it performs a lot more functions other than trimming the control effectors. Trim is an interactive, user friendly, Windows based program that employs graphics, menus, and dialogs to rapidly assess the overall performance and controllability of conceptual vehicle designs. It is not only limited to aircraft or rockets but it can be applied to any flight vehicle configuration that uses aerosurfaces, gimbaling engines, thrust varying engines, reaction control jets, or any combination of the above.

Trim is not intended to replace the stability and control analysis but rather to improve and to simplify the evaluation of conceptual vehicles by helping the analyst to decide which ideas should be rejected or pursued further. In fact, it integrates nicely with other Flixan tools because it generates input data for the flight vehicle dynamic modeling program at selected flight conditions, and also for the effectors mixing-logic program.

The main features of the Trim program are as follows: to efficiently combine multiple types of effectors together, to calculate the effector trim angles and thrusts along a required trajectory, and also to analyze the vehicle performance in terms of some critical performance parameters which are described in chapter 3. The performance parameters are calculated as a function of time by processing the vehicle data along the trajectory. Trim also provides interactive tools for visually analyzing the maneuverability and controllability of the vehicle against wind-shear disturbances at selected flight conditions by means of vector diagrams. Contour plots are also used for visually analyzing vehicle stability and controllability in the entire Mach versus alpha envelope. Graphic utilities are included for plotting and comparing various trajectories and performance parameters against time. There are also options for generating dynamic models and effector mixing matrices at selected flight conditions along the trajectory. The Trim algorithm is very versatile because it allows the designer to perform a thorough and systematic analysis and examine different off-nominal situations, which include: aerodynamic uncertainties, parameter variations, "what if" analysis that help improve the design by graphically modifying some vehicle parameters and evaluating its robustness to trajectory alterations, modified trimming conditions, or by introducing external disturbances. All these features lead to designs that satisfy mission requirements in adverse situations.

The Trim program is not intended only for aircraft but it is designed to accommodate various types of atmospheric vehicle concepts with blended features, including missiles, launch vehicles, rocket-planes, or reentry glider type vehicles. It integrates and generalizes various stability and performance analytic criteria developed separately for aircraft and for launch vehicles and extends their applicability to generic vehicle concepts controlled by multiple effector types. Almost any type of flight vehicle can be implemented in a short time from its data, analyze static performance, evaluate the effects of parameter variations, perform disturbance analysis, model the effector types, their location, thrusts, etc. The flight vehicles are controlled either by aerosurfaces, thrust vectoring engines, thrust varying engines, reaction control jets, or any combination of the above effectors. The effectors are combined together as a system and the performance criteria are calculated based on the combined system and not the aerosurfaces separately or the TVC engines alone. The Trim algorithm, therefore, uses an effective method of combining the various types of effectors together which attempts to optimize performance in the controlled directions. Finally, the Trim program also provides a good starting point for a detailed control design and dynamic analysis work by coordinating with the Flixan Vehicle Modeling program and preparing input data for generating dynamic models at selected flight conditions along the trajectory.

# 9.1 Methodology Overview

The design of a new flight vehicle from the flight control point of view undergoes through various phases of design and analysis, as shown in Figure 1.1. The designer begins by collecting the vehicle data base, which initially is poor and some of the numbers may have to be roughly estimated or guessed. As the design progresses, however, and new numbers become available the database gradually becomes more refined. This is, obviously, an iterative process.

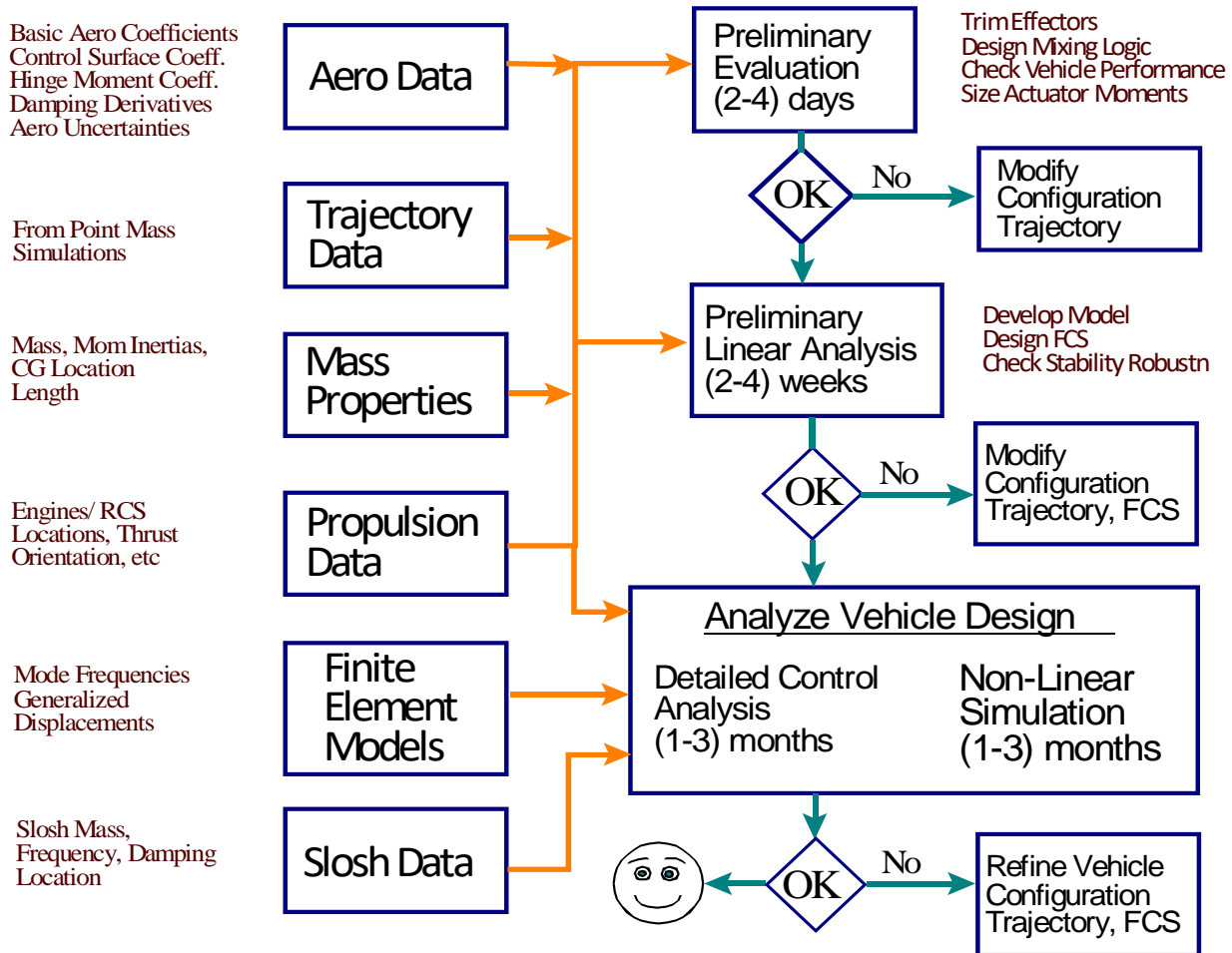


**Figure 1.1 Three Phases of Flight Vehicle Design from the Controls Point of View**

The control analyst begins by collecting the vehicle mass properties: weights, inertias, center of mass as a function of vehicle weight, geometry, locations of the vehicle sensors, engines, jets, control surfaces, etc. Then he or she must request aero data from the aerodynamics group consisting of aerodynamic coefficients for the base body, control surface increment coefficients, aero uncertainties, damping derivatives, and hinge-moment coefficients. Propulsion data for the engines and the reaction control jets are also needed, such as thrusts, directions, thruster locations, etc. A preliminary point-mass trajectory is also needed, such as one created by the POST program, optimized to achieve certain terminal-time criteria, such as maximizing payload weight, altitude or minimizing heating. The trajectories consist of several variables, such as: alpha, beta, weight, velocity, altitude, Mach number, acceleration, dynamic

pressure, thrust, etc. calculated as a function of time. The trajectory variables define the vehicle mission and the environment that it must tolerate during flight. A trajectory, however, does not include the vehicle rotational dynamics and its interaction with the control system. The first function of the Trim program is to trim the effectors, that is, to calculate the effector deflections that will balance the moments along the trajectory. Then it analyzes static controllability, stability, and overall performance. Although the analysis is static, it predicts some dynamic characteristics of the vehicle, such as: time to double amplitude, short period resonances, in addition to maneuverability, control authority, and robustness to uncertainties and disturbances.

The next step (or second phase) in this iterative process is to create dynamic models at critical flight conditions, design a preliminary control system and analyze dynamic stability, robustness to uncertainties, and dynamic performance in response to gusts and guidance commands. In the next phase, a 6-DOF simulation is created that includes preliminary control laws interpolated between the design cases. A 6-DOF includes the vehicle rotational dynamics and it can create more efficient trajectories than POST for Trim analysis and control system redesign. The linear analysis models are augmented with more detail dynamics, such as tail-wags-dog, fuel sloshing, and flexibility. This time the control laws are better refined and more details are included, such as: lead-lag, low-pass, flex filters, logic, etc. The 6-DOF simulation is also continuously refined. This modeling/ design/ analysis/ simulation process is repeated several times until the control design and the trajectories converge. Possibly multiple trajectories are processed. The user is referred to read the control design and simulation examples presented in Section 10.

In the preliminary phase of the Trim analysis, however, we are not yet concerned with the flight control system and simulations. In fact we don't even need a control system because all we are doing is finding out how stable or unstable the vehicle is and if the proposed effectors are strong enough to maneuver it in the trajectory environment. An FCS design for dynamic analysis is performed in the second phase. If the vehicle concept is stabilizable and maneuverable then it will be trivial to design a control system that satisfies some reasonable performance criteria. You can learn a lot about the vehicle dynamic behavior and maneuverability from static analysis before getting into the dynamics, control design, and simulations. If a vehicle does not have acceptable stability and maneuverability properties, then, even if you are able to design a control system that stabilizes it dynamically, it will probably be susceptible to noise, variations and uncertainties. So this preliminary process helps the designer to converge towards a well behaved airframe and mission environment without getting involved into detailed dynamic analysis. This is important because at an early phase some key decisions have to be made regarding the placement of sensors and the location and size of the vehicle effectors, typically: the control surfaces, TVC engines, and the reaction control jets, which determine the control authority. With increasing demand for agility and use of advanced FCS with relaxed static stability, consideration of control power has become an important issue in modern flight designs.



Excessive control authority can translate into increased weight and drag, while inadequate control power can result in a failed design. Thus, the designer's goal when sizing and placing thrusters or control surfaces is to provide sufficient, yet not excessive, control power to meet the required controllability and maneuvering performance requirements. Having a methodology, therefore, for analyzing performance and to properly size the control power is essential for optimizing conceptual flight vehicle configurations.

To summarize this overview, the Trim program is an important tool for rapid phase-1 type performance evaluation of a new flight vehicle concept without requiring flight control system design and a 6-DOF simulation. A simple static performance analysis is created after trimming to predict the vehicle performance and its dynamic characteristics in presence of disturbances, uncertainties and parameter variations, and to provide corrective actions in the event where the requirements are not satisfied. In the second and third phases of the design a preliminary rigid-body dynamic analysis of the flight vehicle is performed at critical flight conditions. The analyst selects some critical flight conditions to create dynamic models along the trajectory, and the Trim program generates the input data which are used by the Flight Vehicle Modeling Program (FVMP) to generate state-space systems at the selected flight conditions. The dynamic models are then used to design control laws, design effector combination logic, perform linear analysis, and eventually develop 6-DOF simulations.

Figure 1.2 shows the inputs and outputs of the Trim program which initially calculates the positions of the vehicle effectors. The effectors must rotate at a certain angle or to vary their thrust in order to produce moments and forces that balance the base vehicle moments and forces. The input files to the program are: a trajectory file, aero data consisting of basic vehicle aero plus aero-surface increments, damping and hinge moment coefficients, mass properties consisting of inertias and CG location as a function of weight, and slosh data which are optional and they are only used when there is fuel sloshing in order to generate inputs for the FVMP. The data files in Trim must be shaped in standard formats in order to be accessible by the program and this may take several hours to complete. Afterwards, the analysis process is straightforward and it should not take more than a few minutes to analyze the performance characteristics of new vehicles and to provide some recommendations for improvements, as it is demonstrated in the examples. In addition to trimming the effectors the program performs several other functions which are essential for preliminary analysis of flight vehicles.

1. Evaluates the overall capability of the conceptual vehicle with its effectors to meet the mission requirements by calculating some critical performance parameters along the flight trajectory that characterize stability, maneuverability and controllability in the presence of wind disturbances. These parameters are described in Section 3.
2. Plots of the trajectory data as a function of time and provides the graphic capability for the analyst to modify graphically some of the trajectory variables, such as: the angle of attack, sideslip, CG location, etc. by means of dialogs and interactive graphics. The user re-trims and reevaluates the vehicle performance using the modified trajectory. This is useful for analyzing parameter variations, CG shifts, and other "what if" type of studies.

3. When the vehicle has multiple effectors and types of effectors, after trimming the user can graphically reshape the deflection angles or the thrusts of some effectors. This is done by limiting their deflections and, therefore, trading the deflections of some effectors against others. The constraints are adjusted graphically by means of dialogs and interactive graphics. It can be used, for example, when trading elevon versus body-flap and speed-brake deflections, since they all affect pitching moment and longitudinal dynamics.
4. Provides graphical utilities for visualizing the basic aerodynamic and the aerosurface coefficients by plotting the coefficients and their derivatives as a function of alpha, beta, Mach number, and aerosurface deflection ( $\delta$ ).
5. Uses Contour Plots to display some of the important performance parameters, such as, pitch and lateral stability parameters, the LCDP and control authority, as a function of Mach versus alpha. Contour plots provide a wider perspective of performance in the entire Mach versus alpha range (rather than in the vicinity of the trajectory). They help locating undesirable or favorable flight conditions and provide direction on how to reshape the trajectory in order to improve performance and to avoid undesirable flight conditions.
6. Creates an effector mixing logic matrix for combining multiple types of effectors. The mixing matrix receives the flight control acceleration demands and calculates the effector positions that will produce the demanded acceleration changes. It uses pseudo-inversion based on geometry and the individual control authority of each effector. It optimizes controllability because it allocates control authority proportionally to the individual effector capability in the demanded directions. It also provides some form of open-loop decoupling between the control axes. The mixing logic matrix is used for analyzing the static performance characteristics of a vehicle. It is either constant, calculated at a fixed flight condition, or time-varying calculated at every time point along the trajectory.
7. Generates dynamic models for control design and simulations at critical points along the trajectory. The user selects the analysis points and the Trim program generates the input data at the selected flight conditions. The Flixan "*Flight Vehicle Modeling*" program generates various types of state-space systems and matrices required for control analysis and simulations at the selected trajectory points, as it is shown in the examples section 10.
8. Generates Vector Diagrams which are used for analyzing vehicle controllability against wind disturbances at specific flight conditions. They compare the control moments or forces in two directions against the moments and forces produced due to angles of attack and sideslip dispersions from trim. There are four types of vector diagrams, presented in Section 9.8, for analyzing moments, forces, accelerations, and partials.
9. Calculates the control moments at the hinges of the control surfaces as a function of the trajectory parameters and the aerosurface trim angles. This option is only available when a hinge moment coefficients file (.HMco) is included in the database.
10. Provides additional data visualization utilities for plotting and overlaying previously calculated data, such as: effector trim positions, performance parameters, multiple trajectories and aero-surface hinge moments.

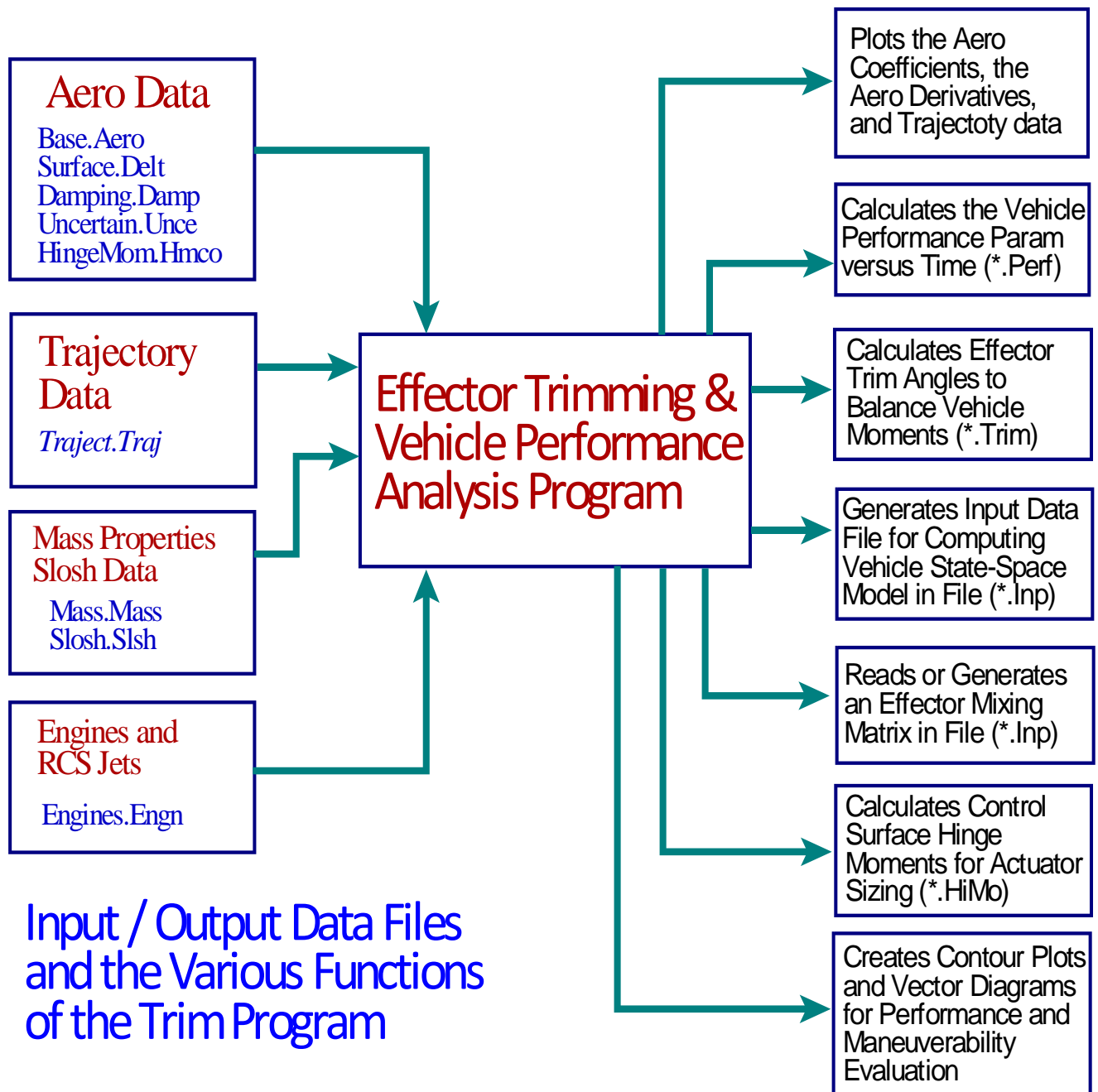


Figure 1.2 Inputs and Outputs of the Trim Program

### 1.1 Control Effectors

The effectors are the devices that provide the "muscle" power to maneuver the vehicle. The Trim program provides the capability for the user to select between four different types of effectors: (a) thrust vector control (TVC) consisting of engines that pivot either in two directions (pitch and yaw) or in a single (skewed) direction ( $\gamma$ ), (b) engines of variable thrust (throttling), (c) reaction control jets (RCS), and (d) control aerosurfaces that rotate about a constant hinge.

A throttling engine has a nominal thrust  $T_e$ , and it provides control forces on the vehicle by varying its thrust by a certain amount above and below nominal. The amount of thrust variation above and below  $T_e$  is defined by the throttle parameter in the engine data file ( $0 < T_h < 1$ ), which must be between zero and less than one. The actual thrust during trimming is determined by the trimming algorithm which calculates the engine throttle control input  $\delta_{Thro}(t)$  required to balance the acceleration, and it varies between -1 to +1. The actual engine thrust at any point along the trajectory is:  $T_e(1 + T_h \delta_{Thro})$ . When the throttle control is zero it corresponds to the nominal thrust value  $T_e$  and the thrust remains always positive. An engine may be defined to be both: gimbaling and throttling.

The RCS jets in Trim are also variable thrust devices but they are defined slightly different. They are continuous thrusters with zero nominal thrust. They can generate either positive or negative forces at a location on the vehicle along a specified direction. They represent a pair of back-to-back firing jets that can generate positive or negative forces. In the propulsion data file an RCS jet is defined by its maximum thrust  $T_{max}$  and by the throttle parameter which is set exactly to 1. This is the parameter that differentiates between a thrust varying propulsion engine and an RCS jet. The actual thrust during trimming is defined by the jet throttle control input  $\delta_{Thro}$  which varies between -1 to +1 and corresponds to jet thrust variation between  $-T_{max}$  to  $+T_{max}$ .

Aircraft engines and reaction control jets are defined as thrust varying engines. A re-entry glider vehicle can be controlled by control surfaces and RCS jets. Commercial aircraft use both, control surfaces and engine throttling. Launch vehicles use mainly thrust vector control (TVC) engines and sometimes in combination with differential throttling and RCS jets. Notice that in Trim the RCS jets are treated as analog and not as "on-off" devices because the purpose of the Trim program is for sizing the jets and not for simulations. "On-off" RCS jet firing is typically implemented in closed-loop simulations using dynamic models generated by the Flixan Vehicle Modeling program (FVMP). For further details see the examples in Section 10.

## 1.2 Dynamic Modeling and Effector Mixing Logic

When the initial vehicle evaluation is complete, in terms of calculating the effector trim angles, determining the vehicle stability, performance, maneuverability, calculating the actuator hinge moments, etc, and if the initial analysis is acceptable, the next step is to start generating dynamic models for analyzing dynamic performance at critical flight conditions. These models are used for designing flight control laws, and for performing dynamic analysis to evaluate the control system stability, closed-loop performance, and robustness to parameter uncertainties. The Trim program generates input data at specific flight conditions that can be processed by the FVMP. The initial models created by Trim are simple rigid-bodies but later they can be augmented by the user in the FVMP environment by including additional features, such as structural bending, tail-wags-dog, fuel sloshing, dynamic coupling with actuator models, etc. The Trim program also generates an effector mixing logic matrix at specific flight conditions. The mixing logic converts the flight control demands (mainly 3 rotational plus some translational accelerations) to actuator commands. It is included in the flight control system logic.

## 9.2 Trimming the Effectors for Balancing the Flight Vehicle Moments and Forces

---

Trimming is the process of balancing the moments and forces on a flight vehicle base generated by aerodynamics and propulsion, with moments and forces which are generated by the control effectors, such as the engines and aerosurfaces. We are mainly interested in trimming the three moments (roll, pitch and yaw) along a pre-defined trajectory. Sometimes we also trim along the axial and normal accelerations ( $A_x$  and  $A_z$ ), and rarely include the side acceleration ( $A_y$ ) in trimming.

The data needed for trimming are: the basic aerodynamic coefficients, the aero-surface increment coefficients, thrust vector control (TVC) and throttling engine data, and a trajectory. A trajectory is a table of flight variables calculated as a function of time. It is typically an Excel file of column data starting with time in the leftmost column, and consisting of a list of flight variables, such as: altitude, vehicle mass, angle of attack, sideslip, dynamic pressure, Mach number, velocity, acceleration, thrust etc. A trajectory characterizes the flight vehicle mission, its flight environment, and the maneuvering requirements. Trajectories are typically created by trajectory specialists, initially from point mass 3-dof trajectory optimization programs such as "POST" which calculates the trajectory based on thrust, weight, lift and drag aerodynamics, and atmospheric models, but it neglects the rotational dynamics. If we don't have a trajectory we can begin by creating our own at flight conditions near the critical missions. Some of the criteria for shaping a trajectory are: heating, fuel efficiency, payload weight maximization, and structural loading.

The primary concern of the flight control analyst is to make sure that the vehicle possesses the control authority to trim along the required trajectory in the static sense, and that the vehicle stability (or instability) is within acceptable limits, in both static and dynamic sense. In this section, however, we are dealing with static stability and in having the control authority to produce the required accelerations against the predicted aerodynamic disturbances. The moments and forces acting on the base vehicle are caused by aerodynamics and propulsion. The aerodynamic moments and forces are generated by the angles of attack and sideslip, as specified in the trajectory. They must be balanced with the control moments and forces generated by the vehicle effectors, that must have the control authority to trim and also to retain some extra capability for other functions. If the effectors do not have the required authority to trim, then either the trajectory has to be modified, or the effectors, or the vehicle shape and aerodynamics, or all of the above must be modified until an acceptable trimming condition can be achieved. This is usually an iterative process that requires several attempts and perhaps changes in the vehicle shape and size of the surfaces or the TVC. As a guideline, the control authority required for trimming should not exceed half of the maximum control capability of each effector. There should be some control capability reserved for maneuvering the vehicle and for reacting against wind gusts and other disturbances. Also, the uncertainties in the vehicle parameters and CG location may cause further uncertainty in the trim angles.

Balancing the three vehicle moments is usually the main objective when trimming the vehicle along the trajectory. Sometimes it is also necessary for the effectors system to have the capability to trim along some of the linear accelerations, mainly along the x and z directions. For example, it may be necessary to balance the axial acceleration and control speed independently of the pitch moment prior to landing by means of a speed brake or by varying the engine thrust. Also, to trim the normal acceleration independently of pitching when separating from another vehicle, by simultaneously using the Elevon, Body-Flap and vertical thrusters. This would prevent it from over-pitching and colliding after separation. Trimming is also important for sizing the effectiveness of the control surfaces, the TVC gimbaling capability, the engine thrusts, throttling capability, and the RCS jet thrusts. It is also used to analyze engine thrust failures, actuator hard-over failures, determining optimal installation angles for the TVC engines, RCS jets, zero positions for the aero-surfaces, wind-shear disturbances, and the maximum weight and CG variations that can be tolerated when carrying payloads.

In this section we are presenting a method for calculating the optimal effector trim positions along a trajectory for a vehicle that includes multiple types of effectors. This method is based on pseudo-inversion of a matrix and it attempts to allocate control authority to effectors according to their control capability in specific directions. It calculates the trim position of each effector at each point along the trajectory, as a function of time. In the ideal situation, when the trajectory is calculated correctly and trimming is perfect, the moments and forces applied on the vehicle from the propulsion and base aerodynamics (angles of attack and sideslip), should perfectly match the accelerations which are defined in the trajectory, and the control deflections should be zero because no correction is needed. Otherwise, if the rotational and translational accelerations on the vehicle (calculated due to  $\alpha$ ,  $\beta$ , and thrust) do not match the trajectory's accelerations, the control effectors must be used to provide the additional moments and forces required to match the accelerations defined in the trajectory. The purpose of trimming is to properly adjust the aerosurfaces, the TVC deflection angles, and thrusts, as necessary according to their capabilities, in order to provide the additional aerodynamic and propulsion forces and moments on the vehicle and to achieve the angular and linear accelerations defined in the trajectory along specific trim directions.

Equation (2.1) is a "Force=Mass x Acceleration" type of equation. On its right hand side there is a 6-dimensional vector consisting of three rotational and three translational accelerations which are defined in the trajectory. They are multiplied with the vehicle mass and moments of inertia to convert them to three moments and three forces. The moments and forces on the left side of the equation are due the aerodynamics, propulsion, and known disturbance forces, and in order to trim, they must balance the terms on the right hand side, at each point along the trajectory. Note that in equation (2.1) the aerodynamic and propulsion moments and forces on the LHS consist of both, base vehicle plus effector moments and forces.

$$\begin{bmatrix} M(aero) \\ F(aero) \end{bmatrix} + \begin{bmatrix} M(thrust) \\ F(thrust) \end{bmatrix} + \begin{bmatrix} M(disturb) \\ F(disturb) \end{bmatrix} = \begin{bmatrix} Inertia \times \dot{\omega}(traject) \\ Mass \times Accelerat(traject) \end{bmatrix} \quad (2.1)$$

In order to solve this equation we must separate the base terms from the effector terms on the left side of equation (2.1). The base terms cannot be modified by the effectors because they are caused by the aerodynamic forces due to the angles of attack and sideslip, and also by the constant propulsion forces of the engine thrusts applied on the base body. The only moments and forces that can be adjusted on the left side of this equation, in order to match the terms on the right side, are the contributions from the effector deflections and the thrust variations. They determine the trim positions of the control surfaces or TVC deflections and the thrust variations. The trim deflections are measured relative to the installation (or zero) position and the thrust variations are relative to the nominal thrust.

The effectors should not only be capable of providing the control authority to balance the equation but they must also have sufficient controllability left for maneuvering and overcoming unexpected disturbances, such as wind shear. In a typical trajectory derived from a point mass simulation the angular accelerations in the trajectory are zero because it assumes that the vehicle moments are perfectly balanced and the effector trimming boils down to zeroing the moments on the left side of equation 2.1. When the rotational accelerations are available, however, either from a 6-DOF simulation or test data, they can be included to provide a more efficient trimming. In equation 2.1 the translational accelerations from the trajectory on the RHS are multiplied with the vehicle mass to calculate the total force on the vehicle along  $x$ ,  $y$ , and  $z$ . The linear accelerations ( $A_x$  and  $A_z$ ) in a typical trajectory are not zero, and in some cases we may want to use the effectors in order to trim along those directions and to match the translational accelerations, because the axial acceleration affects the range and the normal acceleration affects the altitude. When trimming along the translational directions we may have to use additional effector activity such as propulsion, TVC, and aerosurfaces in order to balance the forces.

In this section we will present a trimming algorithm for a flight vehicle with multiple types of effectors. The number of effectors must be greater than or equal to the number of DOF that must be balanced, plus all directions to be trimmed and eventually controlled should be accessible by at least one effector. When the number of effectors exceeds the number of DOFs or trim directions the solution is overdetermined. The more effectors the better the controllability because they can be combined more efficiently to control the directions they can influence. Having an abundance of effectors is also good for redundancy. The trimming algorithm uses pseudo-inversion that gives preference to the effectors that are more capable in the demanded directions by allocating them bigger control authority and hence increased activity, than the effectors which are less capable along those directions and are, therefore, less active. All four types of effectors: gimbaling engines (pitch and yaw), throttling engines, RCS jets, and aerosurfaces, are combined by the trim algorithm and used as a system.

The trimming algorithm requires aerodynamic increment coefficients for each aerosurface and the orientation of each engine with respect to the vehicle. The direction of the engine thrust is defined by two angles (elevation and azimuth or simply pitch and yaw) which are measured relative to the  $-x$  axis. An engine is either mounted at a fixed position relative to the vehicle or it can be gimbaled in the pitch and yaw directions with respect to its mounting position and capable to provide TVC. The thrust is either constant or it can be modulated up and down relative to the nominal thrust to provide throttle control. An engine may also be able to gimbal and throttle simultaneously.

Aircraft engines, for example, are modeled as throttling engines having a nominal thrust ( $T_e$ ), with a certain amount of thrust variation about  $T_e$ . Reaction control jets (RCS) are also considered to be throttling engines. They are mounted at fixed angles relative to the vehicle axes and their thrust can vary between zero and  $\pm T_{\max}$ . For trimming purposes the RCS jets are not considered to be “on/off” devices, but they are continuous (analog) thrusters and negative thrusting is allowed. After all, the purpose of trimming is to size the thrusters and not to perform a dynamic simulation. A single thruster can be used to model a pair of back-to-back firing jets producing positive or negative forces as a function of the throttle control input. It is not necessary for all surfaces to be used for trimming and for flight control. Some of the aero surfaces can be defined in the aero-surfaces data file as fixed with zero max and min deflections and at a non-zero bias position (such as for example a fixed body flap).

In order to solve the trimming equation numerically we must rewrite equation 2.1 by separating the moments and forces produced by each effector as consisting of two parts: a fixed part and an adjustable part. In the equations that follow we will write in detail the moments and forces produced by the engines, jets, and the aerosurfaces and separate them into two parts: (a) the steady-state part that is produced when the effector is at trim position or nominal thrust, and (b) the adjustable part due to the deflection or throttle that is used for controlling and trimming the vehicle.

## 2.1 Basic Aerodynamic Moments and Forces

The aerodynamic moments and forces on the vehicle consist of two parts: (a) the aero moments and forces on the base body resolved along the body axes, assuming that the control surfaces are at zero or bias position, and (b) the moment and force increments produced by the control surface deflections, equation 2.4. The base aero moment and forces are defined in equations 2.2,

$$\begin{aligned}
 L_{BX} &= \bar{Q}S_{ref} b C_l(M, \alpha, \beta) & F_{BX} &= -\bar{Q}S_{ref} C_A(M, \alpha, \beta) \\
 M_{BY} &= \bar{Q}S_{ref} \bar{c} C_m(M, \alpha, \beta) & F_{BY} &= \bar{Q}S_{ref} C_Y(M, \alpha, \beta) \\
 N_{BZ} &= \bar{Q}S_{ref} b C_n(M, \alpha, \beta) & F_{BZ} &= \bar{Q}S_{ref} C_Z(M, \alpha, \beta)
 \end{aligned} \tag{2.2}$$

Where:

- $\bar{Q}$  is the dynamic pressure,
- $S_{ref}$  is the reference area,
- $\bar{c}$  is the reference length or mean aero-chord, and
- $b$  is the wing span.

The six basic aero coefficients (three moments and three forces) are non-linear functions of Mach number  $M$ , the angle of attack  $\alpha$ , and the angle of sideslip  $\beta$ .



## 2.2 Moments and Forces Produced by an Aerosurface Deflection

The control surfaces generate additional moments and forces that are used to balance the moments and forces on the base vehicle along the trajectory. The aerodynamic moments and forces are functions of the aero-surface increment coefficients, the dynamic pressure, and the reference length, as shown in equation (2.3). The surface coefficients are non-linear functions of four variables: the surface deflection from zero position ( $\Delta_{asi}$ ), the angles of attack and sideslip ( $\alpha$  and  $\beta$ ), and the Mach number  $M$ , for example,  $C_m(\alpha, \beta, M, \Delta_{asi})$ .

$$\begin{aligned}
 L_{xSi} &= \bar{Q}S_{ref} b \{C_l(\alpha, \beta, M, \Delta)\} & F_{xSi} &= -\bar{Q}S_{ref} \{C_A(\alpha, \beta, M, \Delta)\} \\
 M_{ySi} &= \bar{Q}S_{ref} \bar{c} \{C_m(\alpha, \beta, M, \Delta)\} & F_{ySi} &= \bar{Q}S_{ref} \{C_Y(\alpha, \beta, M, \Delta)\} \\
 N_{zSi} &= \bar{Q}S_{ref} b \{C_n(\alpha, \beta, M, \Delta)\} & F_{zSi} &= \bar{Q}S_{ref} \{C_Z(\alpha, \beta, M, \Delta)\}
 \end{aligned} \tag{2.3}$$

In order to trim we must solve equation (2.3) for the surface deflections ( $\Delta_{asi}$ ) which are needed to balance the base moments and forces. It is not easy, however, to solve directly for the surface deflections ( $\Delta_{asi}$ ) because the equations are non-linear and not explicitly available, but they are usually defined by wind-tunnel data. The equations are solved numerically by linearizing them at fixed ( $\alpha, \beta, \Delta_{asi}, M$ ) for each control surface, and using the control surface derivatives ( $C_{m\delta_{asi}}$ ) etc, to propagate the solution towards a deflection that will balance the vehicle moments and forces. The derivatives are calculated at each iteration and are also functions of ( $\alpha, \beta, \Delta_{asi}, M$ ).

In addition to the base aerodynamic moments and forces in equation 2.2, the moment/force increment from each aerosurface is calculated by separating equation 2.3 into two parts, as shown in equation 2.4: (a) a steady-state part  $M_{SOi}$  representing the moments and forces at a fixed aerosurface deflection ( $\Delta_{SOi}$ ), and (b) a linear term representing additional moments/ forces due to small deflection increment  $\delta_{asi}$  relative to the nominal deflection  $\Delta_{SOi}$ . These terms are in addition to the base aero forces described in equation (2.2).

In the aero-data base, the surface coefficients are measured or calculated at fixed discrete angles, and  $\Delta_{SOi}$  represents the deflection of surface (i) that is nearest to the expected trim angle ( $\Delta_{asi}$ ). The second term in the moment/force equation 2.4 is a linear derivative term that represents an increment relative to the first term. It is scaled by dividing the deflection increment  $\delta_{asi}$  with the max surface deflection ( $\delta_{asiMax}$ ). We must also multiply the coefficients in the second term with the max deflection ( $\delta_{asiMax}$ ). The input ( $\delta_{asi}/\delta_{asiMax}$ ) in the normalized second term in equation 2.4 becomes non-dimensional and it can only vary between zero and  $\pm 1$ . It is this increment that we must solve for, during each iteration, in order to calculate the new aerosurface deflection ( $\Delta_{SOi}$ ) that will eventually converge to the trim angle ( $\Delta_{asi}$ ).

$$\begin{aligned}
M_{Si} &= M_{SOi} + [DM_{Si}] \left( \frac{\delta_{asi}}{\delta_{asiMAX}} \right) \\
M_{Si} &= \bar{Q}S_{ref} \begin{bmatrix} bC_l(M, \alpha, \beta, \Delta_{SOi}) \\ \bar{c}C_m(M, \alpha, \beta, \Delta_{SOi}) \\ bC_n(M, \alpha, \beta, \Delta_{SOi}) \\ -C_A(M, \alpha, \beta, \Delta_{SOi}) \\ C_Y(M, \alpha, \beta, \Delta_{SOi}) \\ C_Z(M, \alpha, \beta, \Delta_{SOi}) \end{bmatrix}_{(i)} + \bar{Q}S_{ref} \delta_{asiMAX} \begin{bmatrix} bC_{l\delta as} \\ \bar{c}C_{m\delta as} \\ bC_{n\delta as} \\ -C_{A\delta as} \\ C_{Y\delta as} \\ C_{Z\delta as} \end{bmatrix}_{(i)} \left( \frac{\delta_{asi}}{\delta_{asiMAX}} \right) \quad (2.4)
\end{aligned}$$

### 2.3 Moments and Forces due to an Engine Gimbaling in Pitch and Yaw

The moments and forces on the vehicle generated by a single engine (i) are also non-linear functions of the pitch and yaw deflection angles and they also depend on its thrust variation. We will linearize the force equation produced by an engine (i) and separate it in three parts: (a) the nominal moments and forces generated due to its nominal thrust  $T_{0i}$  and at fixed deflections ( $D_{Zi}$  and  $D_{Yi}$ ) that correspond to the engine mounting positions, (b) the moment and force increments generated due to small engine deflections in pitch and yaw ( $\delta_{yei}$ ,  $\delta_{zei}$ ) relative to the engine mounting positions, and (c) the additional moment and force increments due to the variation  $D_{Thr(i)}$  in engine thrust from its nominal value. Each term in equation (2.5) is a 6-dimensional vector consisting of 3 moments and 3 forces. The pitch and yaw engine deflections ( $\delta_{yei}$ ,  $\delta_{zei}$ ) in equation (2.5) are normalized by dividing with the maximum engine deflections. Similarly, the thrust variation inputs ( $D_{Thr(i)}$ ) are normalized by dividing with the maximum thrust variation of each engine  $D_{ThrMax(i)}$ .

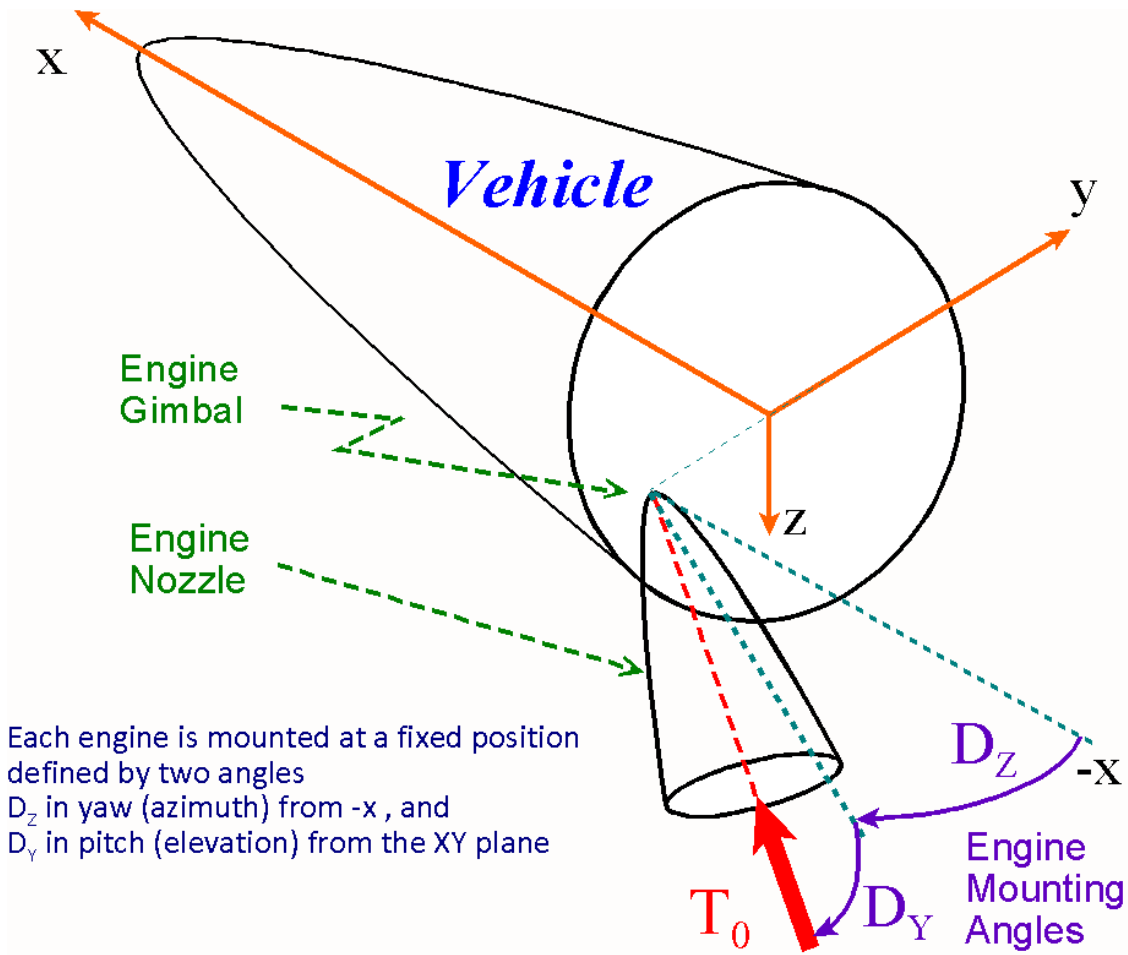
$$M_{E(i)} = M_{EO(i)} + [DM_{E(i)}] \left\{ \frac{\delta_{Y(i)}}{\delta_{YMAX(i)}} \right\} + [DM_{T(i)}] \left\{ \frac{D_{Thr(i)}}{D_{ThrMax(i)}} \right\} \quad (2.5)$$

Equation 2.6 calculates the forces at the gimbal along the vehicle body axes generated by a single engine, where  $\Delta_{Ei}$  is the pitch (elevation angle with respect to the x-y plane), and  $\Delta_{Zi}$  is the yaw (azimuth angle about the body z-axis), see Figure.

$$\begin{aligned}
F_{XO(i)} &= T_O(i) \cos(\Delta_{Yi}) \cos(\Delta_{Zi}) \\
F_{YO(i)} &= T_O(i) \cos(\Delta_{Yi}) \sin(\Delta_{Zi}) \\
F_{ZO(i)} &= -T_O(i) \sin(\Delta_{Yi})
\end{aligned} \quad (2.6)$$

The moment arms distances between an engine (i), and the vehicle CG is:

$$\begin{aligned}
l_{Xei} &= X_{ei} - X_{CG} \\
l_{Yei} &= Y_{ei} - Y_{CG} \\
l_{Zei} &= Z_{ei} - Z_{CG}
\end{aligned} \quad (2.7)$$



Equation (2.8) calculates the nominal moments and forces without variations generated by a single engine (i) at its nominal trim deflection angles ( $\Delta_{Ei}$  and  $\Delta_{Zi}$ ), which is the first term  $M_{EO(i)}$  in equation (2.5). This term assumes that the engine thrust is at its nominal value  $T_{e(i)}$ , and it does not include the small angle gimbaling terms.

$$M_{EO(i)} = \left\{ \begin{array}{l} \left[ \begin{array}{ccc} 0 & -l_{zei} & l_{yei} \\ l_{zei} & 0 & -l_{xei} \\ -l_{yei} & l_{xei} & 0 \end{array} \right] \left[ \begin{array}{c} F_{XO} \\ F_{YO} \\ F_{ZO} \end{array} \right]_{(i)} \\ \left[ \begin{array}{c} F_{XO} \\ F_{YO} \\ F_{ZO} \end{array} \right]_{(i)} \end{array} \right\} \quad (2.8)$$

The additional moments and forces on the vehicle generated by the small pitch and yaw angle deflections  $\delta_{Y(i)}$  and  $\delta_{Z(i)}$  of an engine (i) from its trim positions ( $\Delta_{Ei}$  and  $\Delta_{Zi}$ ), are shown in equation (2.9). The deflection inputs to the equation are normalized by dividing with the maximum pitch and yaw engine deflection capability ( $\delta_{YMAX(i)}$  and  $\delta_{ZMAX(i)}$ ). This normalization makes the inputs to equation (2.9) vary between zero and  $\pm 1$ . The elements inside the matrix are also scaled accordingly. Equation (2.9) represents the second term in equation (2.5).

$$\begin{aligned}
& \left[ DM_{E(i)} \right] \left\{ \begin{array}{l} \delta_{Y(i)} / \delta_{YMAX(i)} \\ \delta_{Z(i)} / \delta_{ZMAX(i)} \end{array} \right\} = \\
& T_e(i) \left\{ \begin{array}{l} \left[ \begin{array}{ccc} 0 & -l_{zei} & l_{yei} \\ l_{zei} & 0 & -l_{xei} \\ -l_{yei} & l_{xei} & 0 \end{array} \right] \left[ \begin{array}{cc} -\cos(\Delta_Z) \sin(\Delta_E) \delta_{YMAX} & -\cos(\Delta_E) \sin(\Delta_Z) \delta_{ZMAX} \\ -\sin(\Delta_Z) \sin(\Delta_E) \delta_{YMAX} & \cos(\Delta_E) \cos(\Delta_Z) \delta_{ZMAX} \\ -\cos(\Delta_E) \delta_{YMAX} & 0 \end{array} \right] \\ \left[ \begin{array}{cc} -\cos(\Delta_Z) \sin(\Delta_E) \delta_{YMAX} & -\cos(\Delta_E) \sin(\Delta_Z) \delta_{ZMAX} \\ -\sin(\Delta_Z) \sin(\Delta_E) \delta_{YMAX} & \cos(\Delta_E) \cos(\Delta_Z) \delta_{ZMAX} \\ -\cos(\Delta_E) \delta_{YMAX} & 0 \end{array} \right]_{(i)} \end{array} \right\} \left\{ \begin{array}{l} \delta_{Y(i)} / \delta_{YMAX(i)} \\ \delta_{Z(i)} / \delta_{ZMAX(i)} \end{array} \right\} \\
\end{aligned} \tag{2.9}$$

Similarly, equation 2.10 calculates the moments and forces on the vehicle generated by thrust variations  $D_{Thr(i)}$  of an engine (i). The throttle control input  $D_{Thr(i)}$  has no units, and it can be made to vary between zero and  $\pm 1$  maximum. The actual engine thrust is defined as:  $T(i) = T_e(i) \{1 + D_{Thr(i)}\}$  where  $T_e(i)$  is the nominal engine thrust. It means that the engine thrust can be varied between zero and  $2T_e(i)$ . However, the maximum throttle capability a throttling engine is typically less than one. The throttle parameter  $D_{ThrMax(i)}$  of a throttling engine is used to define the maximum thrust variation from nominal and it is less than one. For example, if the value of the throttling parameter  $D_{ThrMax} = 0.3$ , it means that the engine thrust can only vary  $\pm 30\%$  from nominal  $T_e$ . In equation 2.10, we must normalize the throttle control input the same way we normalized the deflection inputs of the aerosurfaces and the gimbaling engines. We scale the input by dividing it with the throttling parameter  $D_{ThrMax(i)}$ , and the normalized throttle input now varies between zero and  $\pm 1$ , representing  $\pm 30\%$  thrust variation relative to  $T_e$ . Equation (2.10) is the third term in equation 2.5 and calculates the moment and force variations due to throttling.

$$\begin{aligned}
& \left[ DM_{T(i)} \right] \left\{ \frac{D_{Thr(i)}}{D_{ThrMax}} \right\} = \\
& T_e(i) D_{ThrMax} \left\{ \begin{array}{l} \left[ \begin{array}{ccc} 0 & -l_{zei} & l_{yei} \\ l_{zei} & 0 & -l_{xei} \\ -l_{yei} & l_{xei} & 0 \end{array} \right] \left[ \begin{array}{c} \cos(\Delta_E) \cos(\Delta_Z) \\ \cos(\Delta_E) \sin(\Delta_Z) \\ -\sin(\Delta_E) \end{array} \right]_{(i)} \\ \left[ \begin{array}{c} \cos(\Delta_E) \cos(\Delta_Z) \\ \cos(\Delta_E) \sin(\Delta_Z) \\ -\sin(\Delta_E) \end{array} \right]_{(i)} \end{array} \right\} \left\{ \frac{D_{Thr(i)}}{D_{ThrMax}} \right\} \\
\end{aligned} \tag{2.10}$$

By scaling the control inputs when solving the trimming equation numerically, it adjusts the trim angles proportionally according to the control capability of each effector. For example, when a vehicle has three engines the combined moments and forces due to gimbaling and throttling is given by equation (2.11).

$$\begin{aligned}
M_{3TVC} = & \sum_{i=1}^{N_{eng}=3} M_{EO(i)} + \begin{bmatrix} DM_{E1} & DM_{E2} & DM_{E3} \end{bmatrix} \begin{bmatrix} \delta_{y1}/\delta_{y1Max} \\ \delta_{z1}/\delta_{z1Max} \\ \delta_{y2}/\delta_{y2Max} \\ \delta_{z2}/\delta_{z2Max} \\ \delta_{y3}/\delta_{y3Max} \\ \delta_{z3}/\delta_{z3Max} \end{bmatrix} \\
& + \begin{bmatrix} DM_{T1} & DM_{T2} & DM_{T3} \end{bmatrix} \begin{bmatrix} D_{Thr1}/D_{Thr1Max} \\ D_{Thr2}/D_{Thr2Max} \\ D_{Thr3}/D_{Thr3Max} \end{bmatrix}
\end{aligned} \tag{2.11}$$

## 2.4 Numerical Solution for Calculating the Effector Trim Deflections and Throttles

Now that we have derived the equations for calculating the moments and forces on the vehicle generated by each effector separately, that is, aerosurfaces, TVC, and engine throttling, we will combine all the effectors together in a single moment/ force balance equation as shown in 2.12.

$$\begin{aligned}
M(basic) + \sum_{i=1}^{N_{eng}} M_{EOi} + \sum_{i=1}^{N_{surf}} M_{SOi} + M(disturb) - M_v \times acceleration = -M(residual) = \\
-\delta M(aero\ surface) - \delta M(gimbaling) - \delta M(throttling)
\end{aligned} \tag{2.12}$$

Equation 2.12 is nonlinear and it must be solved numerically at each point along the trajectory. The residual terms on the left side of the equation must converge to zero at the completion of the iterations. The left-hand side consists of the base vehicle moments and forces which are eventually balanced by the effectors as they converge toward their trim positions. The effector increments are calculated from the RHS, after each iteration, and the increments are added to the trim estimate from the previous iteration, and the iterations continue until the trim estimate converges to the trim angle. There is also a term included on the LHS for adding external disturbances. It helps in analyzing the vehicle capability to trim against known disturbances. If the vehicle is capable to trim perfectly without requiring any assistance from the effectors, the forces and moments on the left side of the equation 2.12 would perfectly match the ( $M \times acceleration$ ) term which is also on the left side of the equation without any additional assistance from the ( $\delta M$ ) control terms which are on the RHS of the equation. But this is rarely the case. The ( $\delta M$ ) terms are the contributions from the three types of control effectors, which are normalized as already described and calculated after each iteration, that is:

- (a) Aerosurface deflections ( $\delta_{asi}$ ) from their nominal trim positions ( $\Delta_{SOi}$ ),
- (b) Pitch and Yaw TVC engine deflections ( $\delta_{yei}$ ,  $\delta_{zei}$ ) from their nominal installation angles ( $\Delta_{Eei}$ ,  $\Delta_{zei}$ ), and
- (c) Additional moments and forces due to engine thrust variations ( $D_{thri}$ ) from their nominal thrust  $T_{0i}$ .

During each iteration, if the moments and forces on the left side of the equation do not balance with the  $M \times$  acceleration terms, in which case the  $M(\text{residual})$  term is not equal to zero, then we must solve for the  $(\delta M)$  terms on the RHS to calculate how much additional deflections or thrust variations are needed in order to balance the LHS of equation 2.12. The deflection increments are then added to the deflections from the previous iteration to calculate the new trim positions and to adjust the residual terms. This is repeated until the  $M(\text{residual})$  term converges to zero. The non-linear matrix equation 2.12 is solved for the unknown effector increments on the RHS which are stacked together in a single column vector, as shown in the two aerosurfaces/two engines illustration in equation 2.13.

$$M(\text{resid}) = \left[ DM_{S1} \quad DM_{S2} \quad | \quad DM_{E1} \quad DM_{E2} \quad | \quad DM_{T1} \quad DM_{T2} \right] \begin{bmatrix} \delta_{as1} / \delta_{as1Max} \\ \delta_{as2} / \delta_{as2Max} \\ \text{-----} \\ \delta_{y1} / \delta_{y1Max} \\ \delta_{z1} / \delta_{z1Max} \\ \delta_{y2} / \delta_{y2Max} \\ \delta_{z2} / \delta_{z2Max} \\ \text{-----} \\ D_{Thr1} / D_{Thr1Max} \\ D_{Thr2} / D_{Thr2Max} \end{bmatrix}$$

*In\_Matrix\_Form:* 
$$M(\text{resid}) = [DM] \left( \frac{\delta_T}{\delta_{MAX}} \right) \tag{2.13}$$

This shapes equation (2.12) to a matrix equation form in (2.13) that is solved numerically for the effector trim positions vector  $(\delta_T)$  which is needed to balance the residual forces and moments  $M(\text{residual})$ , assuming of course that the matrix  $[DM]$  is pseudo-invertible. This happens when the rank of  $[DM]$  is greater than or equal to the number of vehicle direction dofs that must be trimmed. Notice that the normalized deflections obtained by the pseudo-inversion are multiplied by the max deflections because the inputs of equation (2.13) are already divided by the max deflections and the matrix  $DM$  was properly scaled. This scaling allows the effectors that have greater control authority in certain directions to be used more than others which are less capable in those directions.

$$\delta_T = \text{diag}(\delta_{MAX}) * \text{Pseudo Inverse}[DM] \times M(\text{resid}) \tag{2.14}$$

The equation (2.14) is solved numerically at each trajectory point as follows:

1. Starting with the first trajectory time point at time=T(0). The control surface positions are initialized at zero or bias angles ( $\delta_{s0i}$ ), the engines are initialized at the pitch and yaw mounting angles ( $\Delta_{Ee0i}$ ,  $\Delta_{Ze0i}$ ), and the thrusts at nominal  $T_{e(i)}$ . Then we calculate the initial matrix  $[DM]^0$  of equation (2.13), and the residual moment/ force vector  $M^0(\text{residual})$  from the LHS of equation (2.12) using the Mach number, the angles of attack and sideslip, and the engine positions.

2. Solve the pseudo-inverse equation (2.14) for the trim angle increments (first trajectory point, first iteration).

$$\delta_T^1 = \text{diag}(\delta_{MAX}) * \text{Pseudo Inverse}[DM]^0 \times M^0(\text{residual})$$

3. Calculate new values for the control surface deflections, engine gimbal deflections, and thrusts by adding the effector increments and throttle values (obtained from the first iteration step-2) to their corresponding previous trim values, as shown.

$$\begin{aligned} \Delta_{E(i)}^1 &= \Delta_{E(i)}^0 + \delta_{y(i)}^1 & \Delta_{Z(i)}^1 &= \Delta_{Z(i)}^0 + \delta_{z(i)}^1 \\ \Delta_{S(i)}^1 &= \Delta_{S(i)}^0 + \delta_{s(i)}^1 & T_{(i)}^1 &= T_{(i)}^0 (1 + D_{Thr(i)}^1) \end{aligned}$$

4. Obtain new values for matrices  $[DM]^1$  and  $M^1(\text{residual})$  from equations (2.13) and (2.12), repeat step-2 for the same trajectory time point and solve for the new trim variables using equation (2.14), and repeat the iterations in steps 2 and 3, still for the same trajectory point until the trim angles converge to steady-state values.

$$\delta_T^2 = \text{diag}(\delta_{MAX}) * \text{Pseudo\_Inverse}[DM]^1 \times M^1(\text{residual})$$

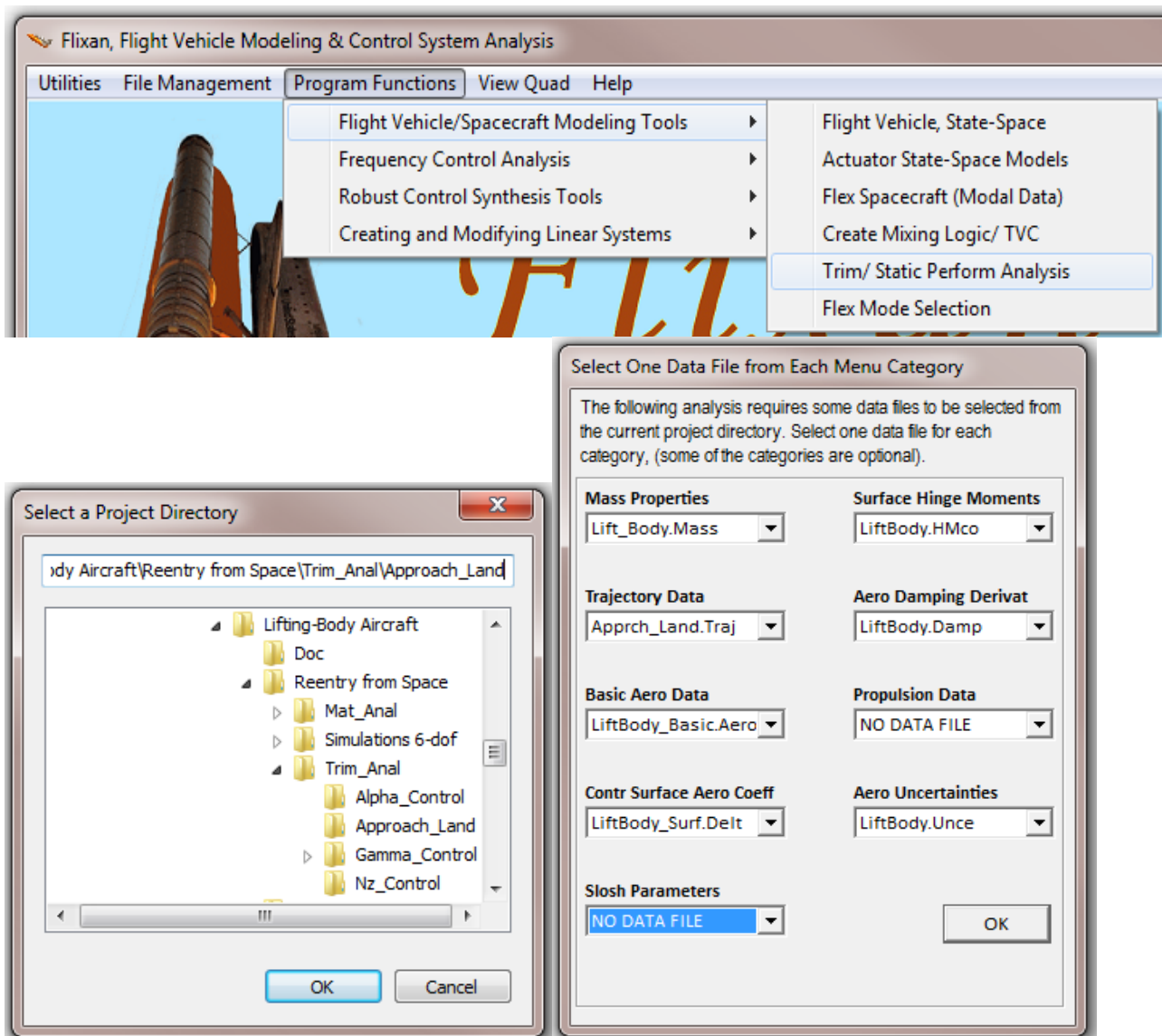
5. Select the next trajectory point at time=T(1) and repeat the same iterative process described in steps (1 - 4). Initialize using the trim angles from the previous trajectory time point and solve for the trim angles and throttle values at this point. Continue this process with the remaining trajectory points, all the way to T=T(n), and obtain a time history of the effector trim angles and throttle values as a function of trajectory time.

## 2.5 Running the Effector Trimming Program

The effector trimming program calculates the effector trim angles and throttle values as a function of the trajectory time by adjusting the effector deflections and thrusts as necessary to balance the moments and forces on the vehicle, as already described. The initial trim is calculated without any adjustments from the user. The algorithm is allocating control authority to each effector and calculating their position along the trajectory by taking into consideration their capability and their maximum deflections. The deflections and throttles are initialized at zero. Further adjustments by the analyst of the effector trim positions by trading-off the activity of some effectors against others may be possible when the vehicle has multiple effectors. This is accomplished by biasing the initial position and by adjusting the maximum capability of each effector as a function of the trajectory time, and re-trimming with new initial conditions.

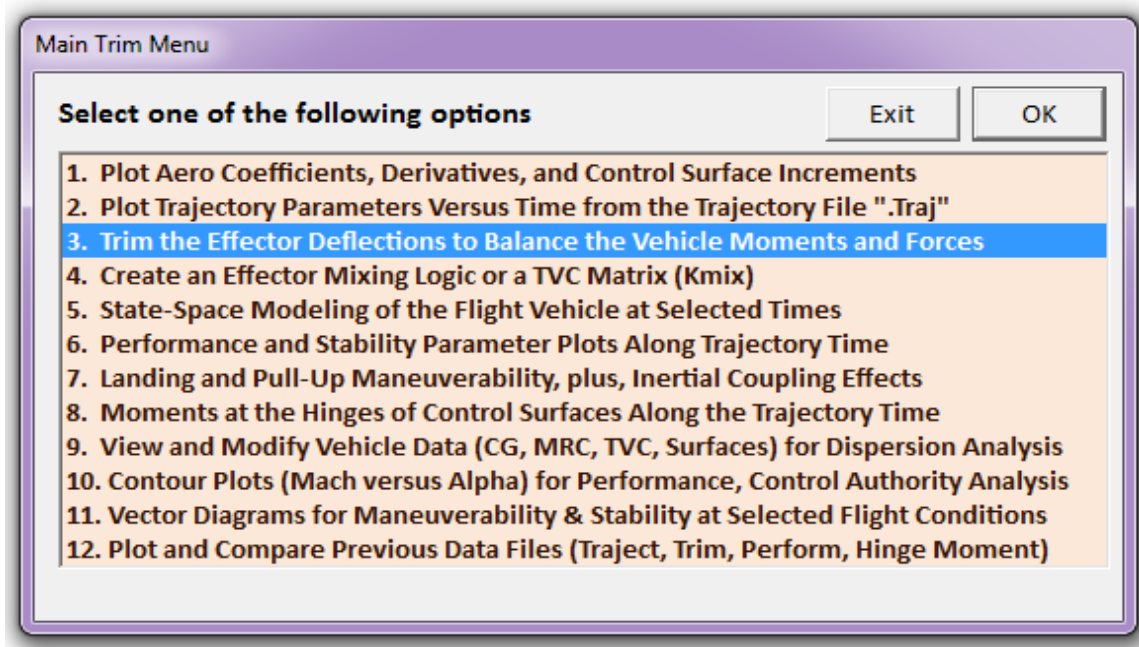
Trimming is also used to evaluate the vehicle effectors capability to tolerate variations in the trajectory variables. The program provides the capability for the user to modify some of the trajectory parameters graphically, re-trim with the variations and compare results, in order to check, for example, how much CG variation or sideslip due to wind-shear the vehicle is able to stand. Trimming can also be used to analyze if the vehicle is able to handle the loss of an engine thrust, situations where an actuator or aerosurface is stuck and unable to rotate, or RCS thruster failure (either on or off).

The trimming and static performance analysis program can be selected from the Flixan main menu as shown below. The user must select the project directory and the proper filenames which are located in this directory, such as the mass properties, the trajectory file, aero-data coefficients for both: vehicle and aerosurfaces, damping derivatives, hinge moment coefficients, engine and RCS data, aerodynamic uncertainties, and slosh parameters. Some of the data files such as slosh and uncertainties are optional and not necessary included in all applications. In fact for trimming you only need the mass properties, trajectory data, base aero, aerosurface data, and propulsion data.



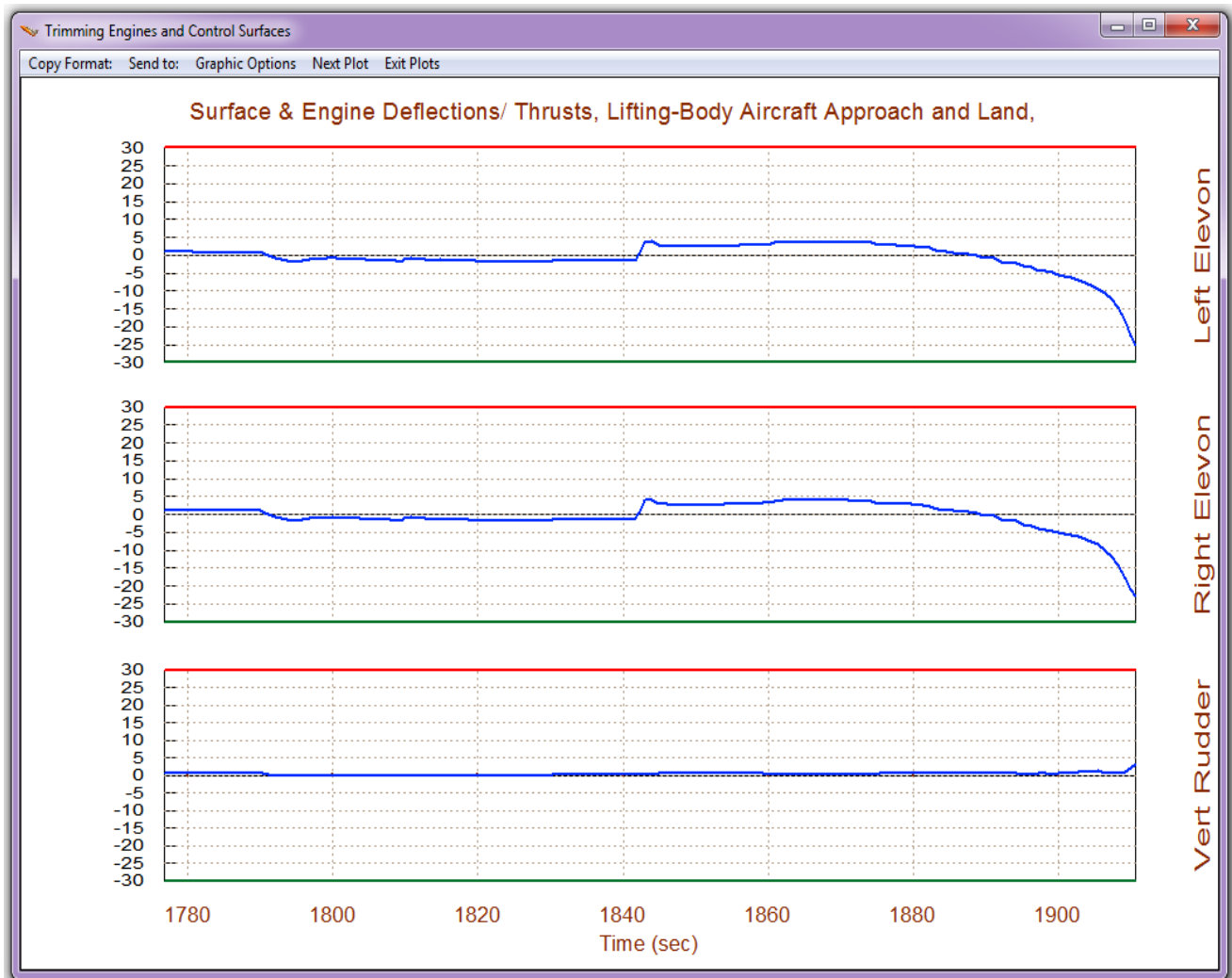
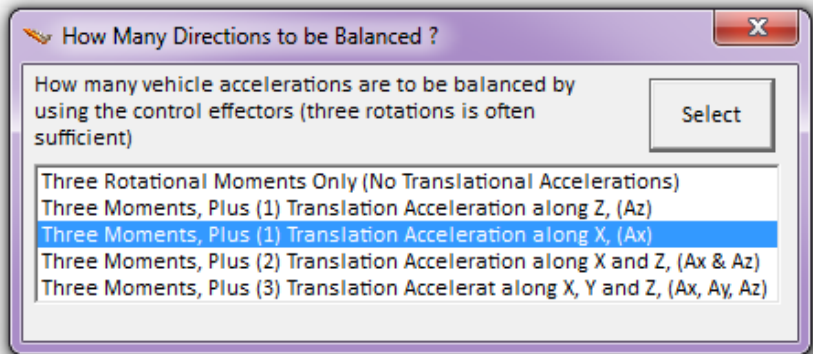
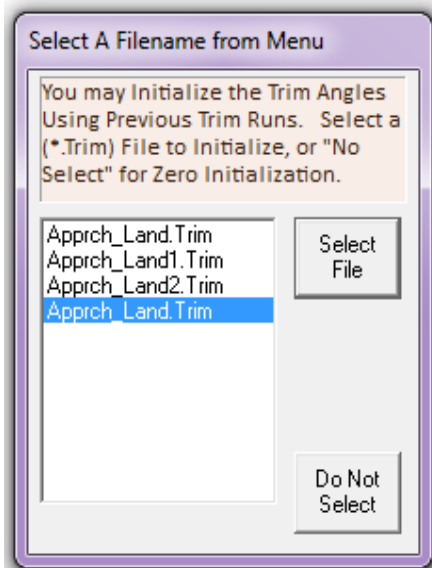


The trimming program can be selected from the main menu of the “Trim and Static Performance Analysis” program. It is the third option, as shown below. Before trimming the program needs to know how to initialize the trimming process and in which directions to trim. The effectors are initialized from a filename selection menu, either at zero, or from an already prepared trim file. This initialization (.Trim) file may be calculated from a previous trim run, in which case we select the trim file from the menu and click on “*Select File*”. Otherwise, to initialize from zero deflections, click on “*Do Not Select*” a file. The advantage of selecting a previous trim file is that it may include previous deflection modifications that were made interactively by the user and to continue with further trimming adjustments, like for example, when we trade the activity of one effector versus others. Up to 3 previous trim files are saved by the program.

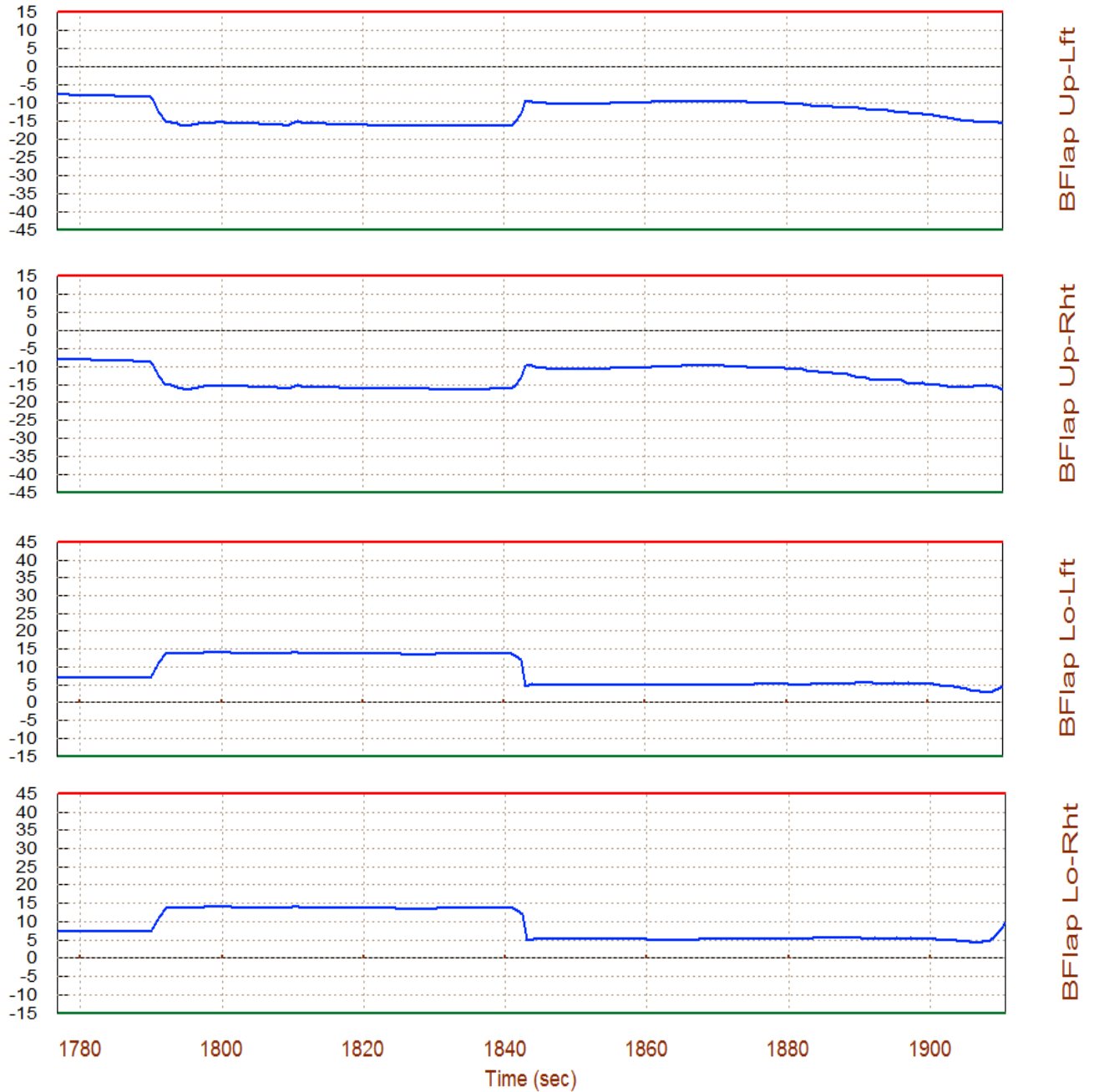


The program also needs to know along which axes or degrees-of-freedom the vehicle must be trimmed. From the menu below the user must define the directions along which to trim the vehicle moments and forces. The minimum is 3 rotational moments. However, some translational accelerations may also be included if the vehicle has the force effectors necessary to achieve the specified translational accelerations. In the example below, in addition to the 3 rotations we would also like to trim along the vehicle x-axis, and use the force effectors to achieve the x-acceleration as defined in the trajectory. This means that the vehicle must have at least one effector that controls the x axis, which may be a speed-brake or a thrust varying engine.

The Trim program calculates the effector trim angles and engine throttle positions and plots the data in a dialog-window that has a menu above the plot, similar to the one shown below. In this example we have 7 aerosurfaces, no engines or RCS. The upper and lower limits of each aerosurface are also shown by the red and green lines. They are limited to  $\pm 30^\circ$ . In this example the Elevon, Aileron, and Rudder aerosurfaces are used to trim: pitch, roll, and yaw moments.

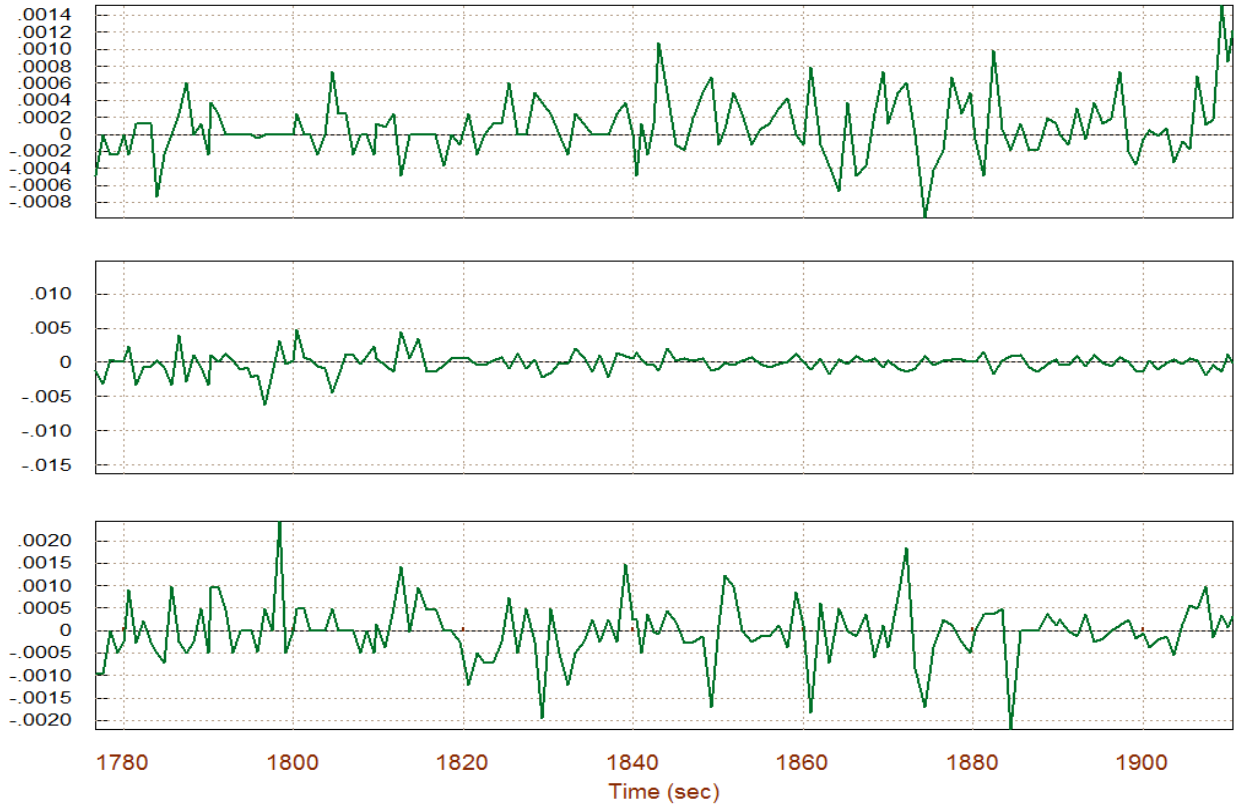


Surface & Engine Deflections/ Thrusts, Lifting-Body Aircraft Approach and Land,

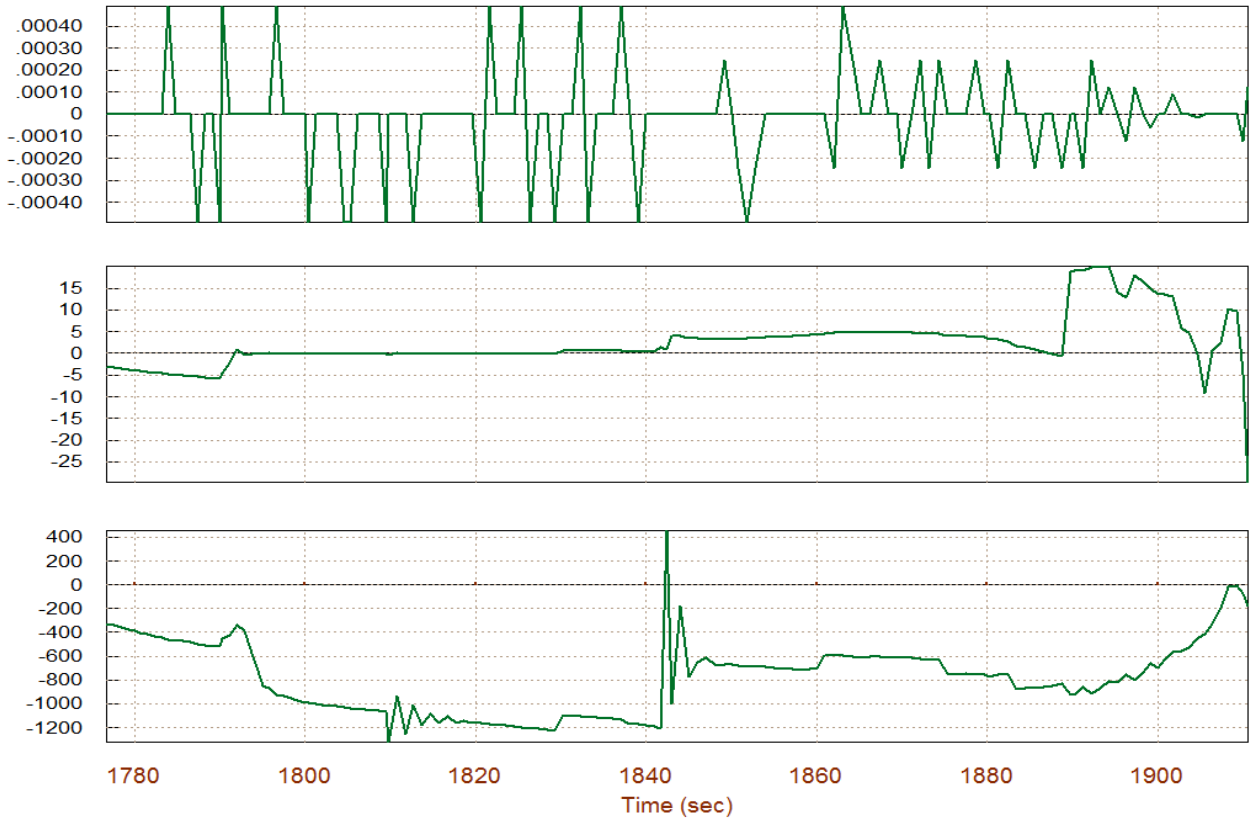


The four Body-Flaps (shown above) are partially opened and used to adjust drag in order to trim the x-axis acceleration and to match the trajectory acceleration. The next plots show the residual moments and forces after trimming which are zero in the 4 trimming directions (roll, pitch, yaw, and along the x-axis). It means that the program was successful in trimming along the 4 selected directions. The residuals in the Y and Z directions are not zero.

Residual Moments After Trimming (ft-lb) Lifting-Body Aircraft Approach and Land,



Residual Forces After Trimming (lb) Lifting-Body Aircraft Approach and Land, wit



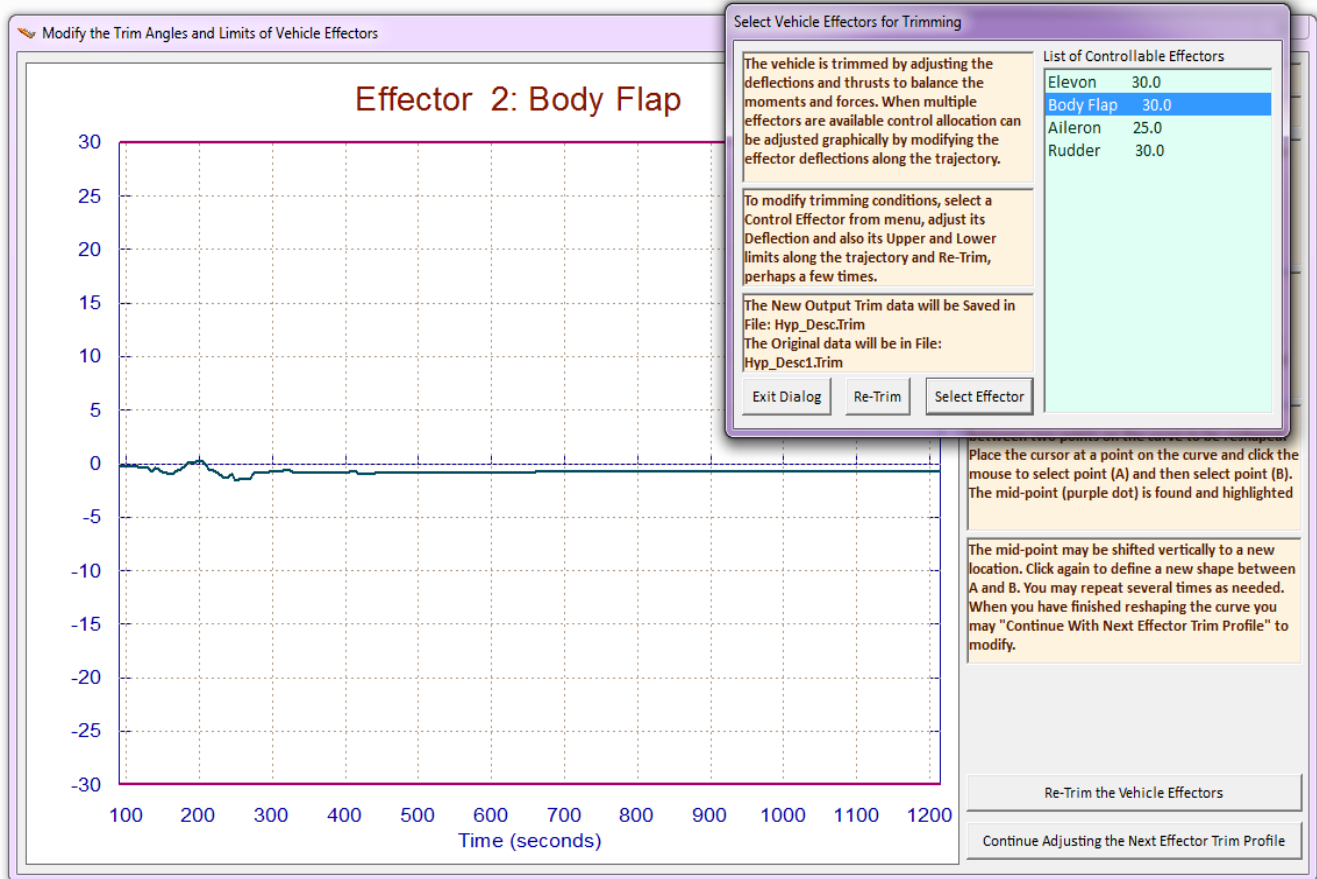
## 2.6 Graphically Adjusting the Trim History

The effector trimming algorithm calculates the effector trim angles and throttle values as a function of the trajectory time by adjusting the effector deflections and thrusts as necessary to balance the moments and forces on the vehicle. The utilization of each effector depends on its control authority along the trim directions which also depends on its maximum deflection or throttling capability. The algorithm calculates the trim positions by taking into consideration the effector's control authority as we have already described. The analyst has the capability of trading-off between effector utilization. Obviously, when there is a multiplicity of effectors, the better the flexibility of trading-off among them. The effector trimming is an iterative process and adjustments in the trimming parameters are often used in order to improve the trimming condition. A previous effector trim history versus trajectory time can also be used for initializing a new trim under different trimming conditions. The initialization trim history can also be manually adjusted as needed in order to bias the next trim results. For example, the designer may wish to reduce the reaction jet usage against allowing bigger aerosurface deflections in order to save fuel. In this case, the designer can adjust the trimming conditions by constraining the jet throttle values and opening up the max deflections on the aerosurfaces. Initializing the jet throttle values at lower magnitudes also helps reducing their activity after re-trimming. This of course is only possible when the vehicle has other effectors that can provide sufficient authority to trim along the required directions in the entire trajectory.

The initial trimming is performed based on the maximum effector deflections provided without imposing any additional limitations on the effector deflections or throttles. Then adjustments can be made on the effector initialization trim profile to constrain usage of some effectors at the expense of increasing the contributions from others. This trade-off can be performed graphically by adjusting the initial effector positions and their maximum deflections, as a function of time, and re-trimming. Consider, for example, a vehicle that may have an Elevon, a Body Flap, a Speed-Brake, and thruster engines. It may be possible to eliminate or to reduce activity in some of the effectors during trimming, like for example, the Body-Flap, by keeping it at a fixed position or scheduling its deflection versus time, and allow the other effectors to be adjusted by trimming. This of course is only possible when the vehicle has other effectors that can provide sufficient authority to span the control directions required to trim. If the vehicle configuration does not have sufficient or it has barely enough effectors to trim with the limitations imposed, the program will not be able to converge and modify its default trimming positions or it will allow very small amounts of effector adjustments from the original trim.

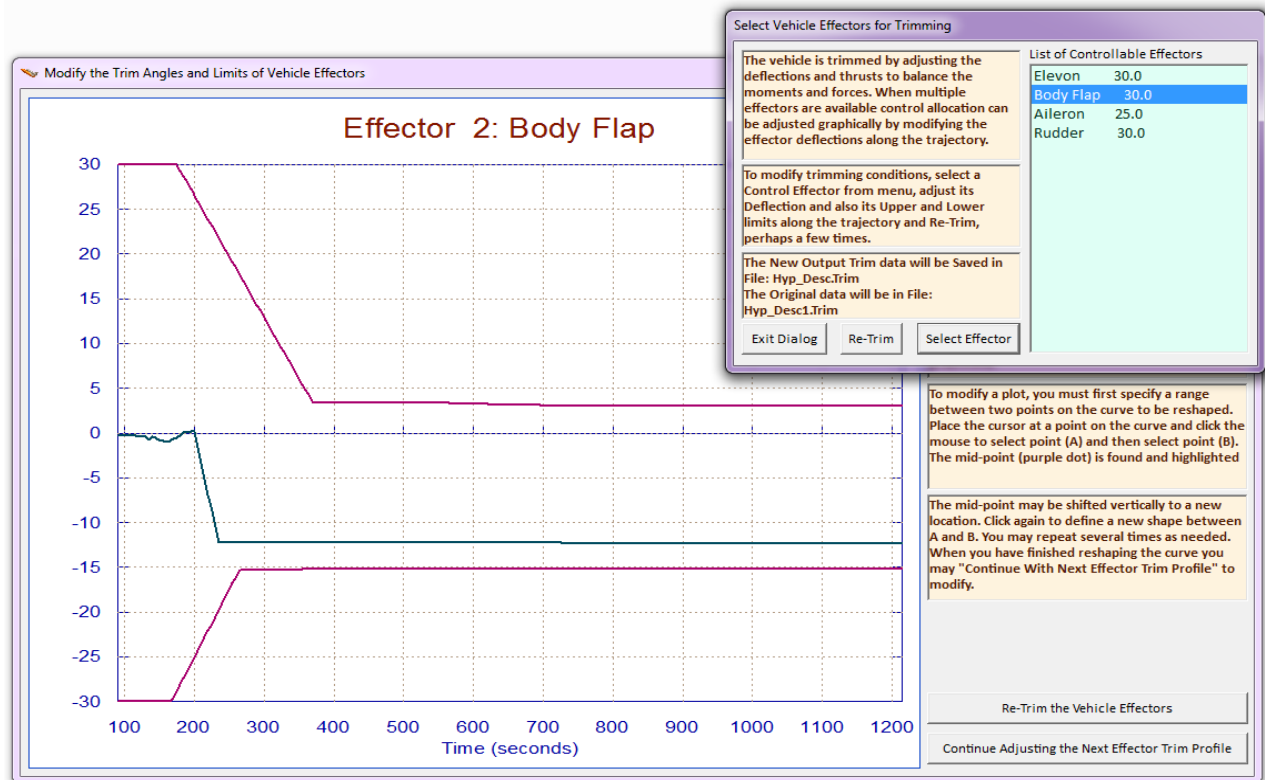
After the first trimming, the user may be allowed to adjust the trim positions of some effectors using the mouse driven interactive graphics of the Trim program. Above every trim plot there is a horizontal menu bar that includes various options. Go to the "*Graphic Options*" and from the vertical pop-up menu select: "*Modify a Trajectory Plot*", the same way you modify a vehicle trajectory plot but this time it is for effector trajectories. A menu comes up with a list of the vehicle effectors. Select one of them and a dialog-plot comes up showing the trim history of the effector as a function of the trajectory time, as it was calculated from the previous trim.

For example, let us choose the Body-Flap and click on the "Select Effector" button. The top dialog/plot in the next page shows the original trim history of the Body-Flap (green line) as it was calculated by Trim. It also shows its upper and lower limits (magenta) which are initially  $\pm 30^\circ$ .

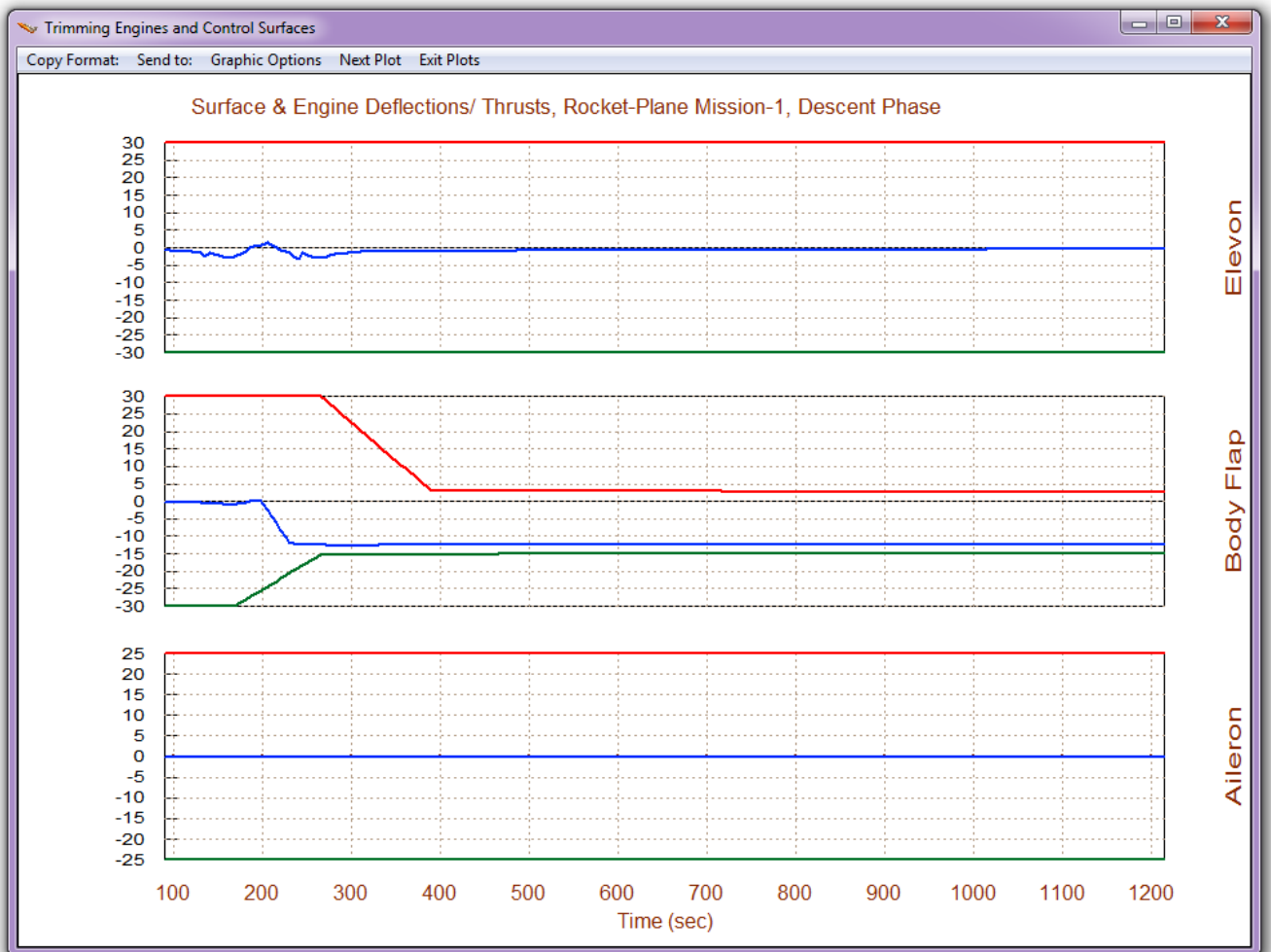
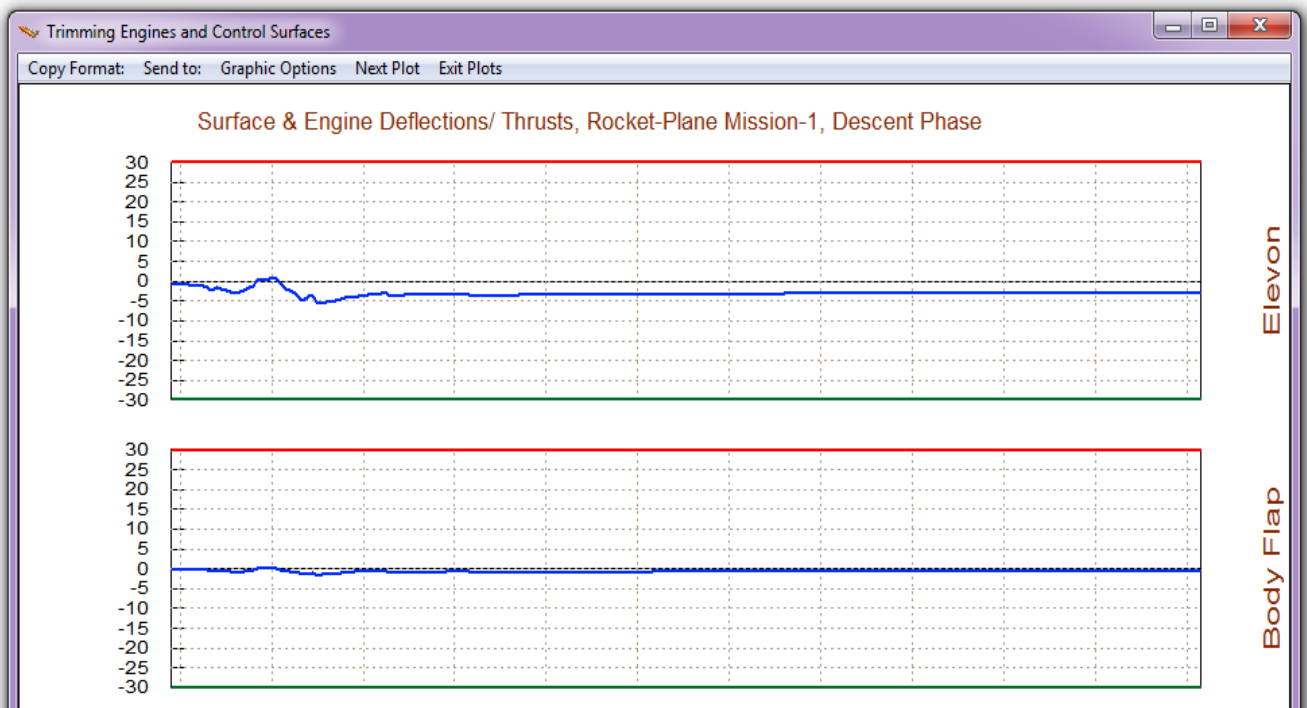


The maximum deflections limits determine the amount of aerosurface utilization at each trajectory point during trim. Notice that the body flap trim angle is very close to zero. The Elevon, however, is biased in the negative direction during most of the time in order to balance the pitching moment. However, in this particular vehicle the Elevon is meant to be used for flight control, but not the Body-Flap which is supposed to be only a trimming device. We would rather prefer to trim the pitching moment using the Body-Flap and keep the Elevon closer to zero in order to allow greater deflection capability for maneuvering.

The plot below shows the modified Body-Flap deflection after being reshaped by the user's mouse for the next trim. It is initialized at constant negative value  $-12^\circ$ . We would like to keep it at  $-12^\circ$  after  $t=200$  seconds. We must also reduce the upper and lower Body-Flap limits from  $\pm 30^\circ$  to smaller values, because lowering the deflection limits de-emphasizes the effector's authority during the next trim and reduces its capability to change from the  $-12^\circ$  initialization value in that range. The limits are reduced a few seconds later to allow for the dynamic pressure to increase. The Elevon max deflections were not reduced prior to re-trimming in order to allow it more authority to adjust. When the user modifications are complete, click on "Re-Trim" from either dialog, and the program will generate a new trim history.



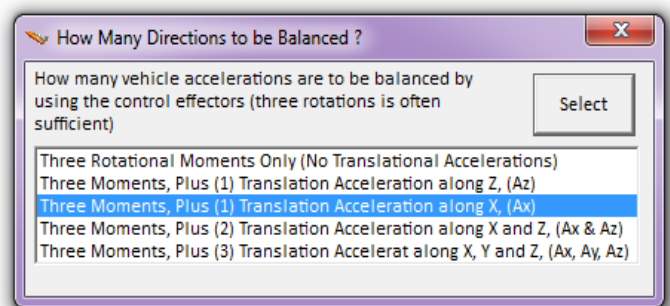
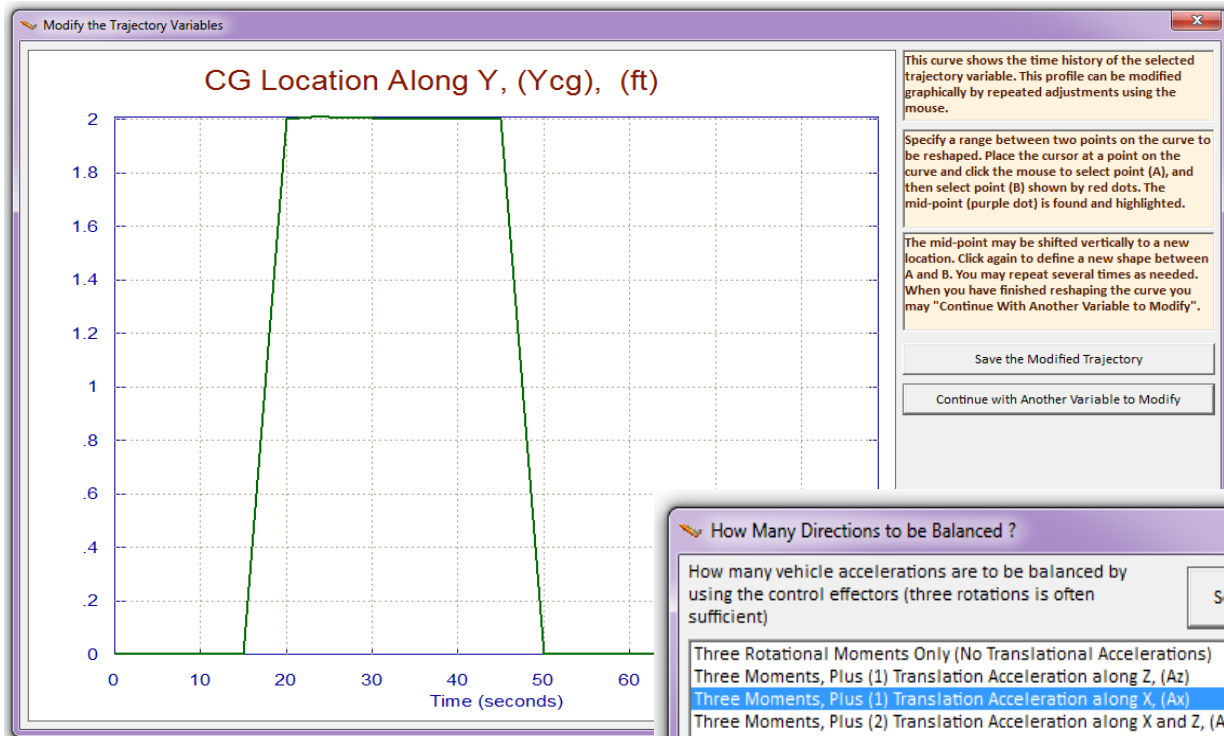
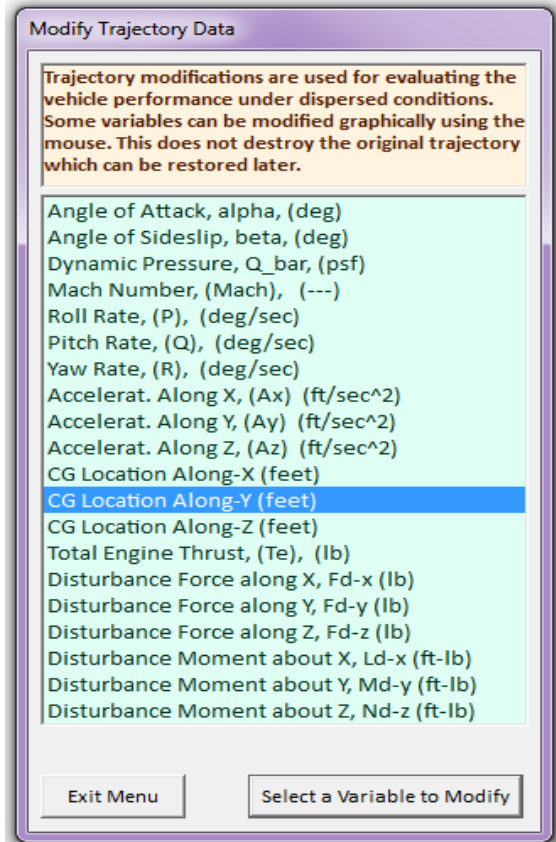
The plots in the next page show the effector deflections before and after trimming. The adjustments made by the user in the Body-Flap trajectory were processed by re-trimming and the Body-Flap was repositioned further down. It remained close to the  $-12^\circ$  initialization position that was set because it was constrained by the reduced limits. The Elevon, however, that had unconstrained limits was allowed to adjust from its initial position and it is now trimming very close to zero as we would like it to be. There are more trimming examples presented in Section 10.





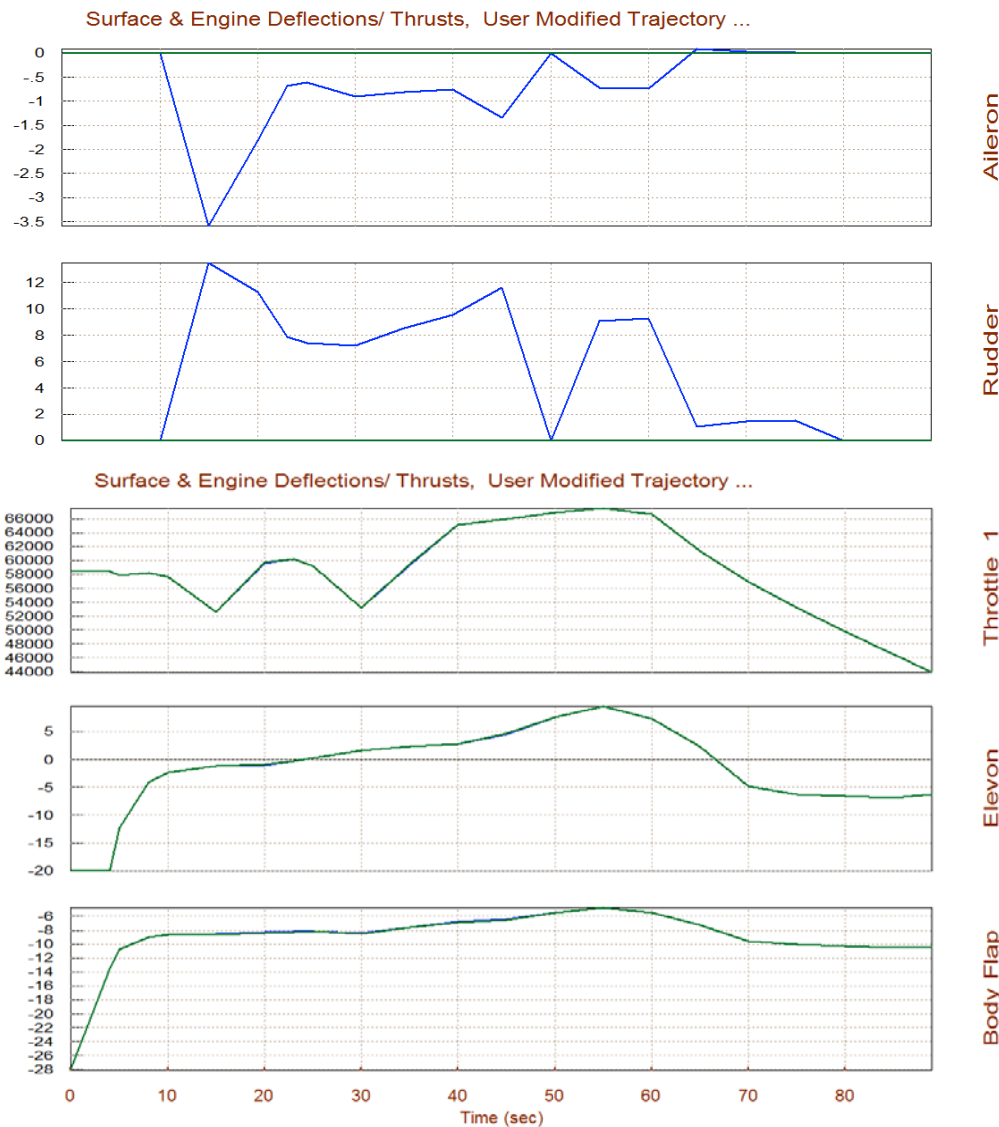
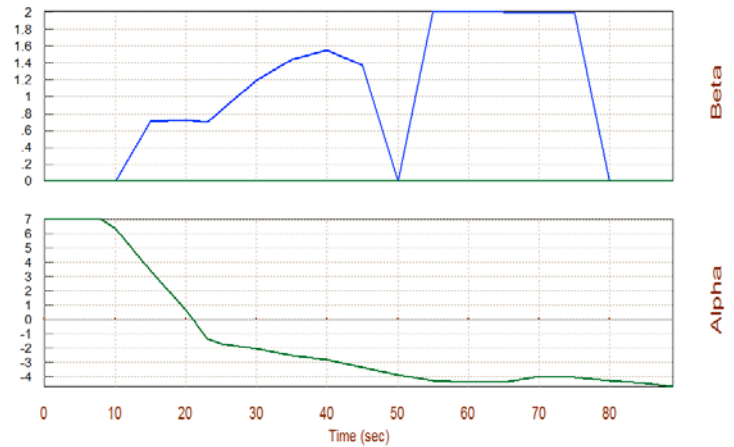
## 2.7 Trimming with a Modified Trajectory

It is also possible to trim along a trajectory that has been graphically modified by the user. This helps us to check the effector's robustness against parameter variations, such as: CG, angles of attack and sideslip, dynamic pressure, thrust, accelerations, etc. You must first trim using the original trajectory for reference. Then plot the original trajectory and from the menu bar above the trajectory plot, click on "Graphic Options", and select to modify the trajectory data. The menu on the right shows the trajectory parameters that can be manipulated by the user. Select one of the parameters to modify, such as, the  $Y_{CG}$  location, and click on "Select a Variable to Modify". You can now graphically modify this trajectory variable versus time in this window-plot below, using the mouse interactive graphics, and change the  $Y_{CG}$  location from zero to 2 feet, in this time range. Click on "continue with another variable", and select another variable to modify, such as the angle of sideslip and modify beta from zero to  $2^\circ$  over a different time period between 50 and 80 sec. Then save the modified trajectory under a different name for reference and re-trim with the modified trajectory.



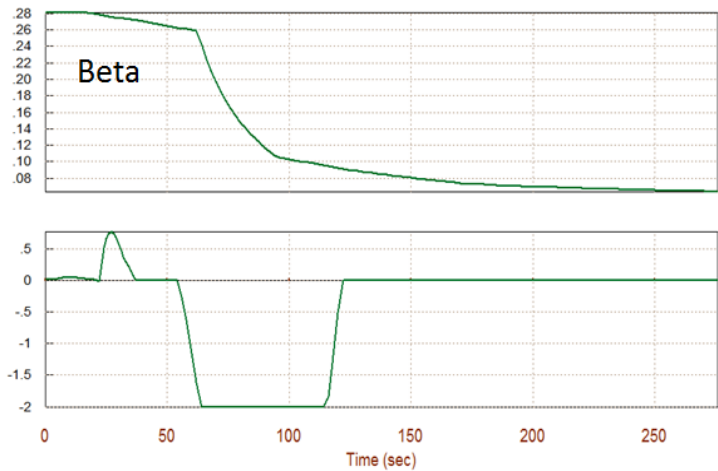
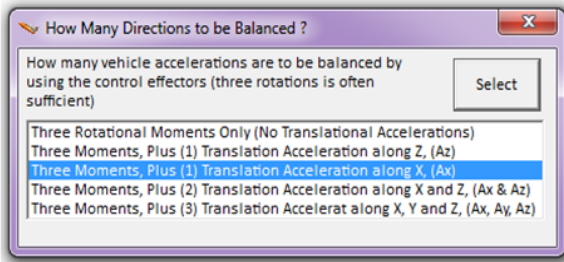
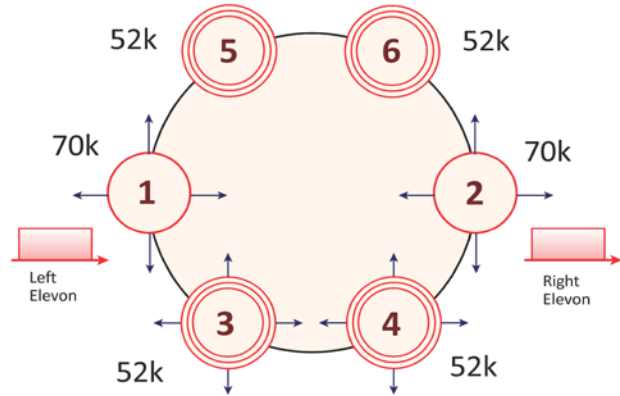
The menu is for selecting the trim directions. In this example the trim was performed in four directions, 3-moments plus X-acceleration. This plot shows the effector trim positions before and after the trajectory modification. It shows that the  $Y_{CG}$  offset causes the vehicle to develop a sideslip angle beta.

Since the variations affect the lateral directions, the longitudinal effectors which are the Elevon, the Body-Flap, and the main engine thrust, remained the same, before and after trajectory modifications, The aileron and rudder, however, that were zero when trimming along the original trajectory (shown in green), are now deflecting in order to provide the roll and yaw torques necessary to counteract the disturbances produced by the variations in the  $Y_{CG}$  and Beta.



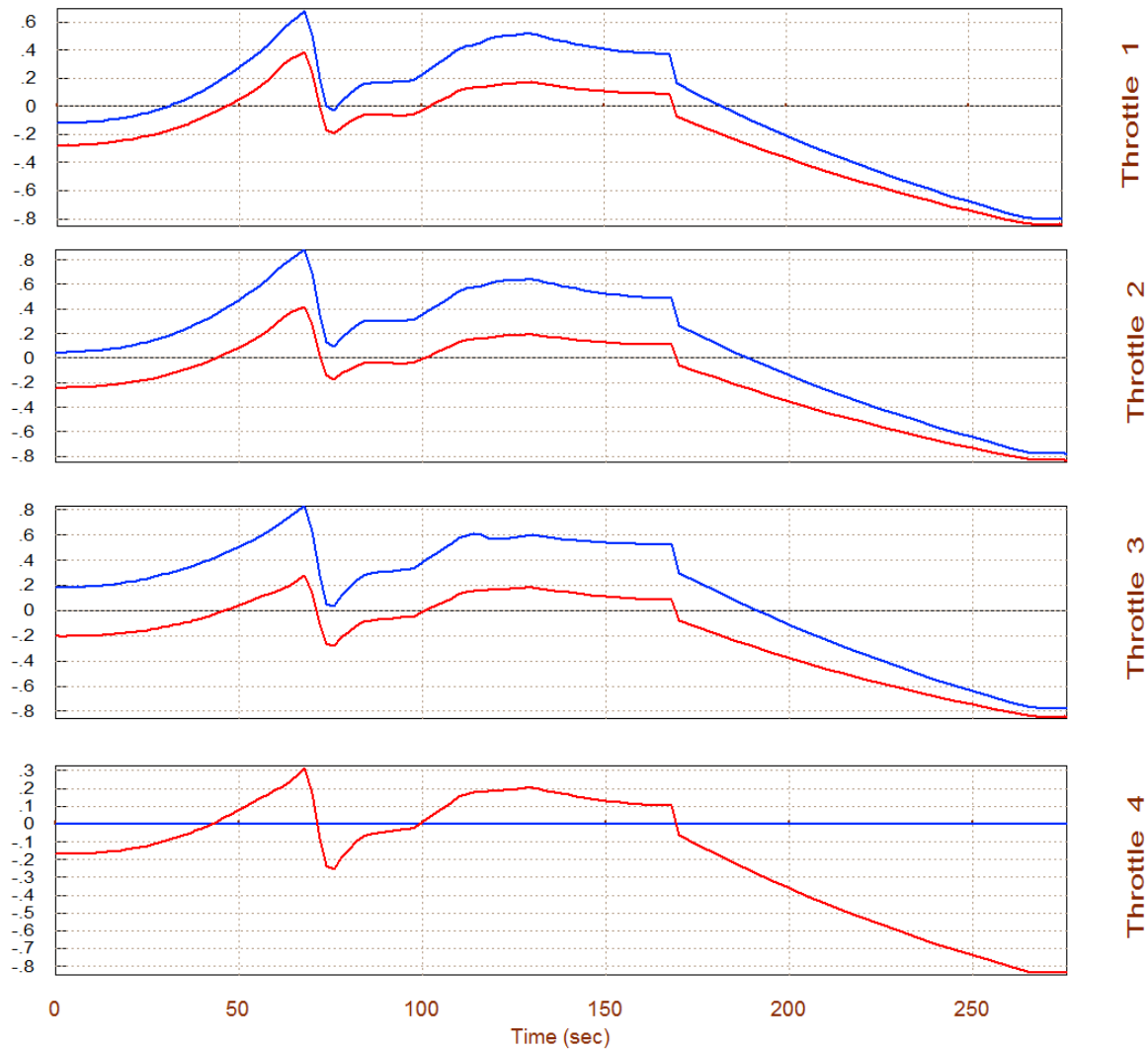
## 2.8 Trimming with a Faulty Effector

The Trim program is also used to evaluate the vehicle's ability to trim in the event of an effector failure, such as an engine or RCS jet thrust, an aerosurface or an actuator hard-over failure. In this example we have a launch vehicle that is controlled by a combination of throttling and gimbaling engines and also by aerosurfaces. Two of the engines are only gimbaling, two of the engines are only throttling, and two engines are both: gimbaling and throttling. The CG in this vehicle is off-centered in the Y direction. We will use the Trim program to trim the three moments and the x-axis acceleration, using all engines and aerosurfaces. After trimming with all engines, we would also like to know if we can still trim it if we lose thrust from one of the engines.



The plot above shows the angles of attack and sideslip after trimming. Beta is not zero, as it is in the trajectory, but slightly positive and varying with time. This is necessary in order to provide the yawing moment required to offset the moment due to the  $Y_{CG}$  displacement which also varies. To fail Engine #6 we set its thrust to zero and also its throttling parameter to zero in the Engine data file (\*.Engn) below.

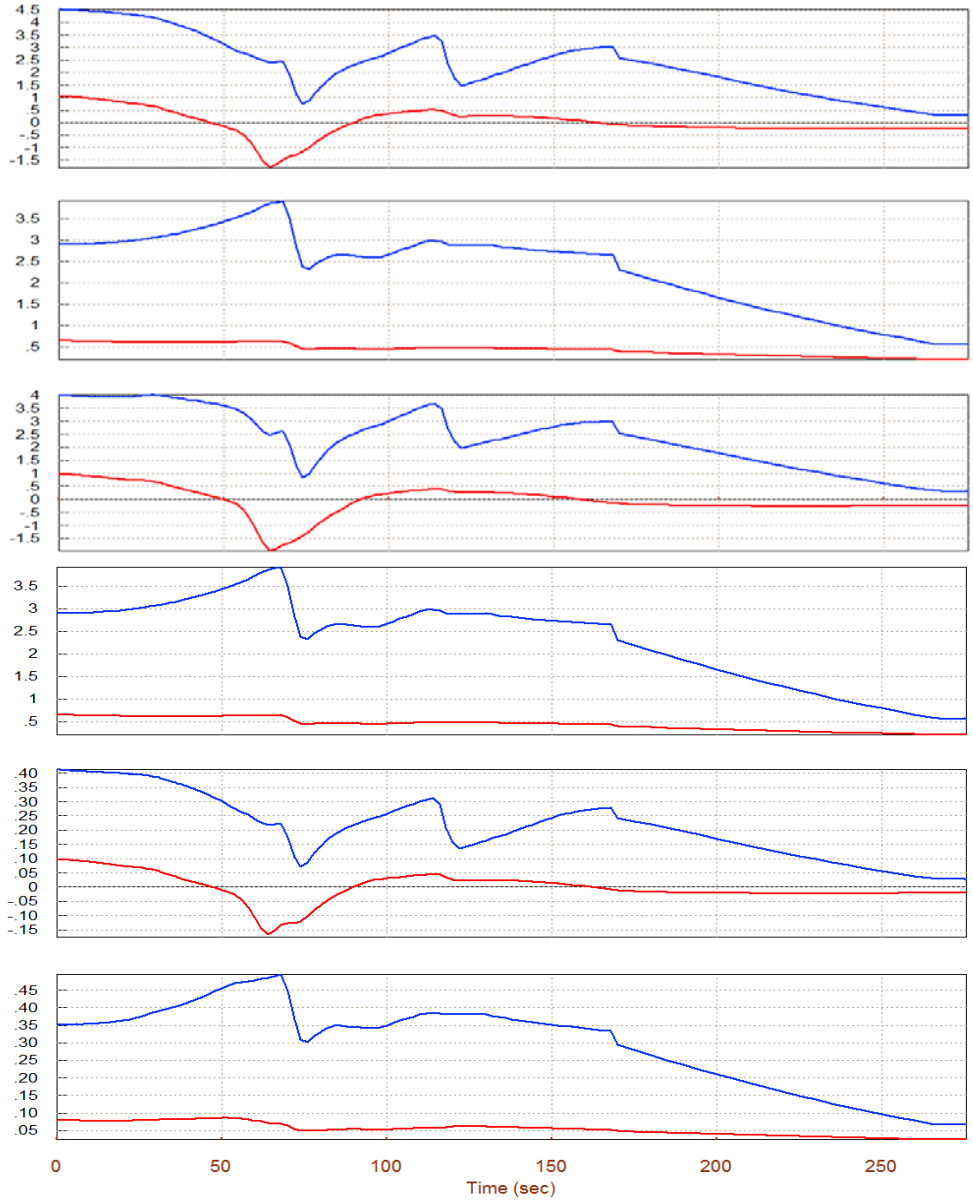
Engine Description	Thrust (lb)	Mass (slug)	Ieng (slug-ft <sup>2</sup> )	Mom Arm (ft)	Gimbaling Location (x,y,z) (feet)	Mounting Angles (Dy, Dz) Elevat, Azimuth (degr)	Max Deflection Dym,Dzm (deg)	Max Throttling (0-1)
Main Engine#1	70000.0	100.0	1500.0	2.8	-89.0 -4.8 0.0	-2.0 0.0	14.0 12.0	0.0
Main Engine#2	70000.0	100.0	1500.0	2.8	-89.0 +4.8 0.0	-2.0 0.0	14.0 12.0	0.0
Main Engine#3	52000.0	100.0	1500.0	2.8	-89.0 -2.25 +3.9	-2.0 0.0	5.0 5.0	0.95
Main Engine#4	52000.0	100.0	1500.0	2.8	-89.0 +2.25 +3.9	-2.0 0.0	5.0 5.0	0.95
Main Engine#5	52000.0	100.0	1500.0	2.8	-89.0 -2.25 -3.9	-2.0 0.0	0.0 0.0	0.95
Main Engine#6	0.01	100.0	1500.0	2.8	-89.0 +2.25 -3.9	-2.0 0.0	0.0 0.0	0.01



This figure above shows the throttling functions of the four throttling engines, before the engine failure (shown in red), and after the engine failure (shown in blue). Note, that the Thrusts in the remaining 3 Throttling Engines are increased as they try to achieve the axial acceleration that is required in the trajectory. That's because they are compensating for the fourth throttling engine (Engine #6) that has lost its thrust and throttling ability.

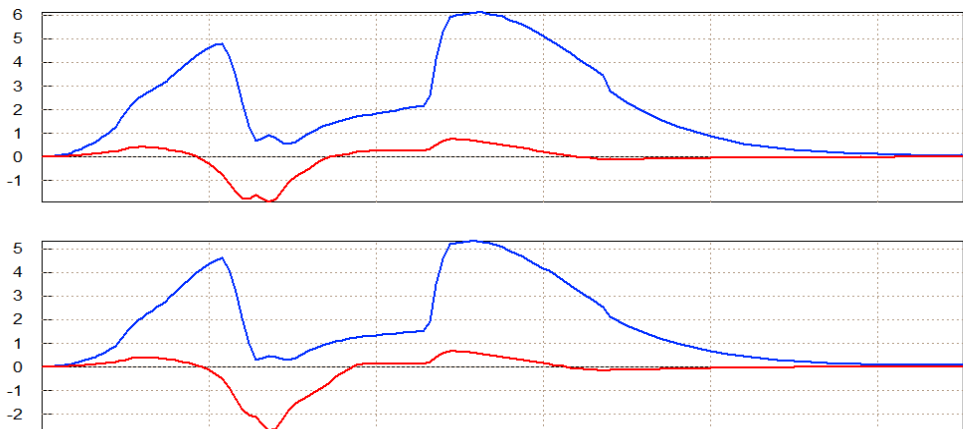
The figure below shows the pitch and yaw gimbal deflections of the four gimbaling engines, before the engine failure (shown in red), and after the engine failure (shown in blue). The yaw deflections ( $\delta_{z1}$  to  $\delta_{z4}$ ) of the four gimbaling engines are increased after the failure, in order to provide a negative yawing moment and to compensate against the positive yawing moment that is produced by the absence of engine #6 thrust. The pitch deflections ( $\delta_{y1}$  to  $\delta_{y4}$ ) in the four TVC engines are also increased in order to make up for the lack of symmetry due to the thrust failure. The flap deflections are increased in comparison with the nominal trim, and also the difference between left and right flaps is also increased in order to counteract the rolling moment caused due to the lack of lateral symmetry.

Surface & Engine Deflections/ Throttle, Reusable Space-Plane Ascent Trajectory-2



Dy\_Engine 1  
Dz\_Engine 1  
Dy\_Engine 2  
Dz\_Engine 2  
Dy\_Engine 3  
Dz\_Engine 3

Surface & Engine Deflections/ Throttle, Reusable Space-Plane Ascent Trajectory-2



Left Flap  
Right Flap

## 9.3 Static Performance Analysis Along a Trajectory

---

Before analyzing the dynamic characteristics of a flight vehicle the designer must first evaluate if the airframe satisfies certain performance characteristics along the mission trajectory. Characteristics such as control authority, maneuverability and stability along the estimated trajectories are important in determining if the vehicle will be able to achieve the planned missions. Low airspeed and gusts place the greatest demands on control authority. In addition, agile maneuvers accomplished by frequent excursions into high angle-of-attack regimes and high roll performance can result in critical control power conditions, including adverse coupling effects. To achieve a successful design, it is important to assess the control power of a proposed design concept against the anticipated performance requirements early in the conceptual stage. The static and dynamic performance of the flight vehicle is captured in the data, and its flying performance must be evaluated along the expected trajectory or trajectories, prior to any control analysis and simulations. The proposed trajectory defines the environment, the performance requirements, and the vehicle stability and maneuverability qualities, which also depend on the vehicle configuration, its mass properties, aerodynamic characteristics, mixing logic and the effector controllability.

In this section we will define some important parameters that should allow the analyst to evaluate in a static sense the overall performance quality of a generic flight vehicle by processing the flight vehicle data along the trajectory, as a function of time. This analysis is not only for aircraft but it may include all types of flight vehicles controlled by aero-surfaces, TVC, throttling engines, and RCS jets. The performance parameters are calculated at each trajectory point as a function of the trajectory data, mass properties, aerodynamic coefficients for the basic vehicle and for the control surfaces, hinge moment coefficients, engine data, reaction control jets (RCS), vehicle geometry, and the control effector combination logic matrix, which defines the control allocation among the effectors. That is, how the flight control system demands are converted to effector deflection commands and, therefore, it plays an important role in evaluating performance. The aerosurface and TVC engine trim angles and the throttle values are also needed in the calculation of the performance parameters. The effectors must, therefore, be trimmed prior to assessing the vehicle performance. The parameters that will be used in the evaluation of static performance are: Static Stability (percent), Center of Pressure, location of the Aerodynamic Center along the x-axis, time-to-double amplitude in (sec), Short Period and Dutch-roll frequencies in (rad/sec),  $C_n\beta$ -dynamic, the control authority of the effectors to maneuver the vehicle as a system against wind disturbances, the lateral control departure parameter (LCDP) which affects roll controllability, inertial cross-coupling moments between axes generated due to fast maneuvering, hinge moments at the control surfaces which are needed for sizing the actuators, the bank  $\phi$  and sideslip  $\beta$  angles due to cross-wind which are important near landing, and also the maximum accelerations generated by the effectors along the control axes.

The Trim program provides the capability to temporarily modify some of the input data by including dispersions and biases in the performance analysis process. This is for checking the system's robustness and sensitivity to changes, by re-evaluating the performance parameters using modified values in the mass properties, trajectory variables, CG location, angles of attack and sideslip, aero coefficients, etc.

### 3.1 Transforming the Aero Moment Coefficients

The basic aero moment coefficients  $C_L$ ,  $C_M$ , and  $C_N$ , the aerosurface coefficients, and their derivatives, are not necessarily calculated about the vehicle CG because the mass properties and the CG position usually vary during flight as the propellant is depleted. The moment coefficients are calculated instead with respect to a fixed point on the vehicle called the Moment Reference Center (MRC). The aerodynamic coefficients must, therefore, be transformed from the MRC to the instantaneous vehicle CG at each trajectory point, and the performance parameters are calculated relative to the CG. The location of the MRC ( $X_{MRC}$ ,  $Y_{MRC}$ ,  $Z_{MRC}$ ) in vehicle coordinates is usually included in the basic aero data file. Equation 3.1 is used to transform the aero moment coefficients from the MRC to the vehicle CG, where  $l_{ch}$  and  $l_{sp}$  are the reference length and span. The aerosurface coefficients and their derivatives are transformed similarly.

$$C_{L_{CG}} = C_{L_{MRC}} + C_Y \frac{Z_{CG} - Z_{MRC}}{l_{sp}} - C_Z \frac{Y_{CG} - Y_{MRC}}{l_{sp}}$$

$$C_{M_{CG}} = C_{M_{MRC}} + C_Z \frac{X_{CG} - X_{MRC}}{l_{ch}} + C_A \frac{Z_{CG} - Z_{MRC}}{l_{ch}}$$

$$C_{N_{CG}} = C_{N_{MRC}} - C_Y \frac{X_{CG} - X_{MRC}}{l_{sp}} - C_A \frac{Y_{CG} - Y_{MRC}}{l_{sp}}$$

Equation 3.1 Aero Moment Transformation Equations from MRC to CG

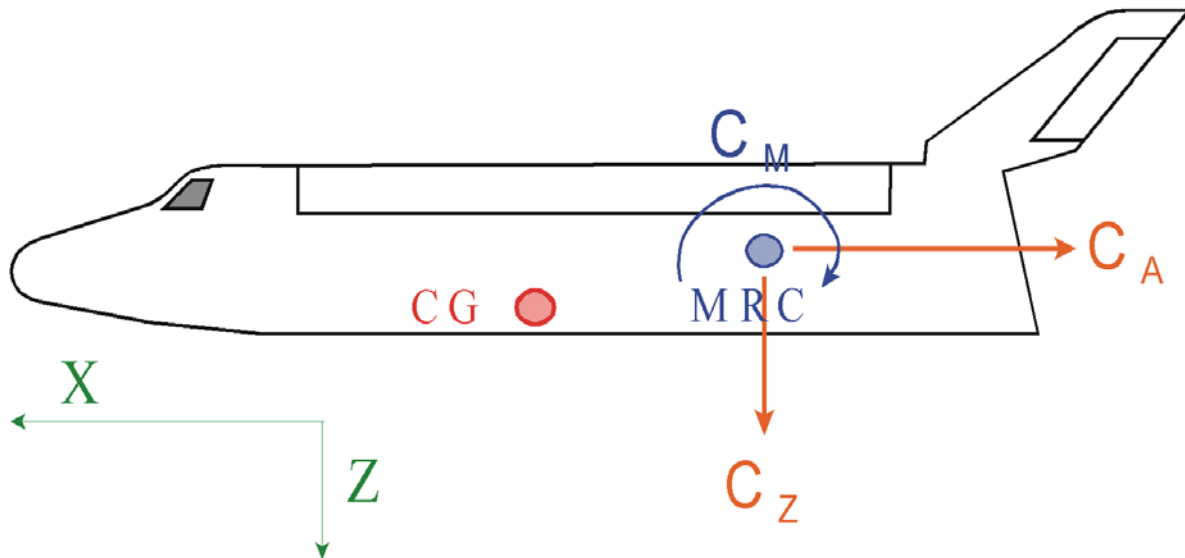


Figure 3.1 Visualization of the Pitch Moment Transformation from MRC to CG

### 3.2 Converting FCS Demands to Vehicle Moments and Forces

Figure 3.2 shows the interconnection of the subsystems which are participating in the flight control loop and they determine the vehicle static performance. The vehicle subsystem receives the control moments and forces ( $M_\delta$ ) and generates responses which are compared with the flight control commands and generate the error signals. The flight control system calculates the rotational and translational acceleration demands ( $\delta_{FCS}$ ) as a function of errors in vehicle response. The flight control demands are defined in the control directions, which are a minimum of 3 rotational accelerations (roll, pitch, and yaw) plus some optional translational accelerations along x, y, and z. Direct translational control should only be included if the vehicle has translational control requirements and the effectors capability for linear acceleration control, otherwise, they may degrade the control authority of the moments.

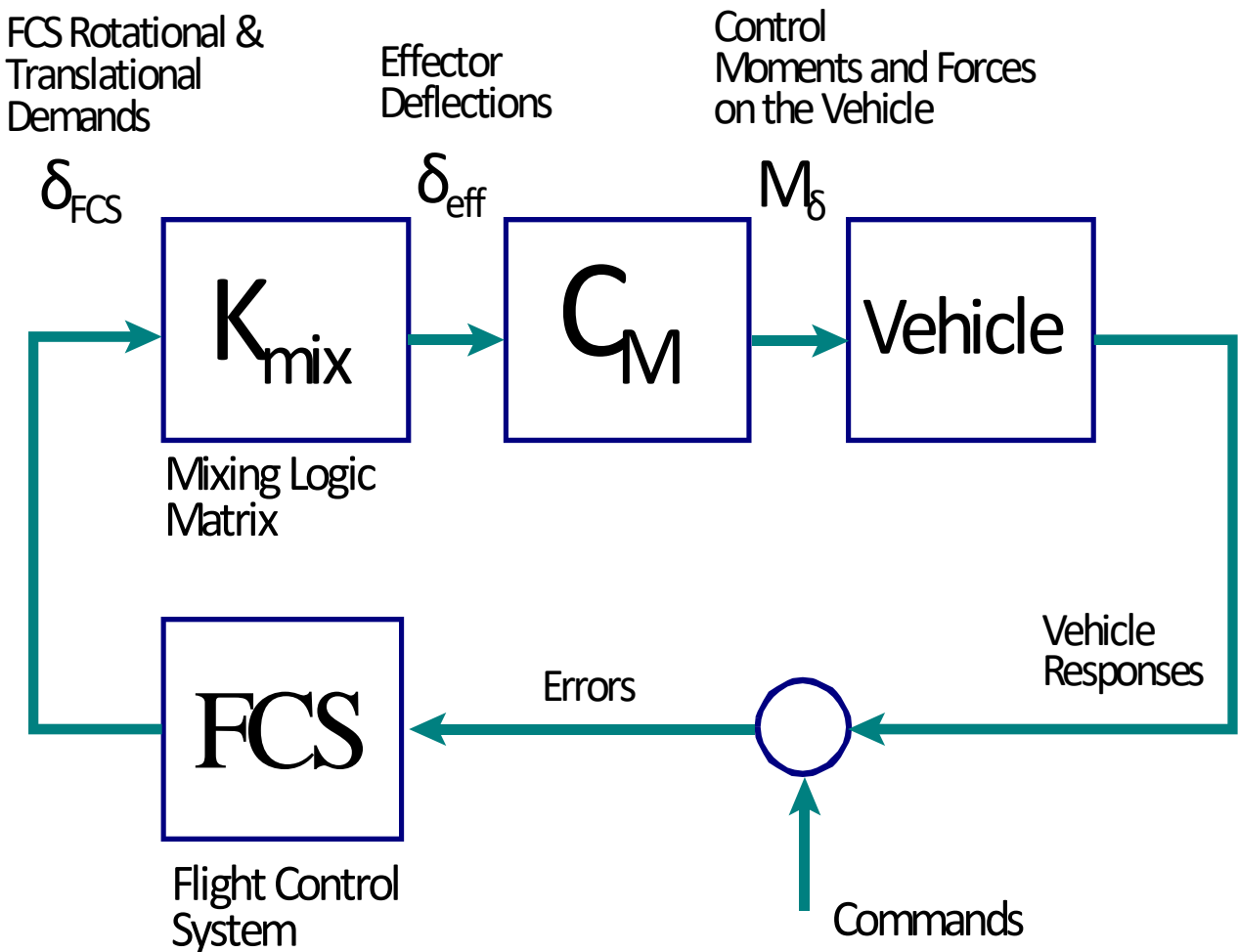
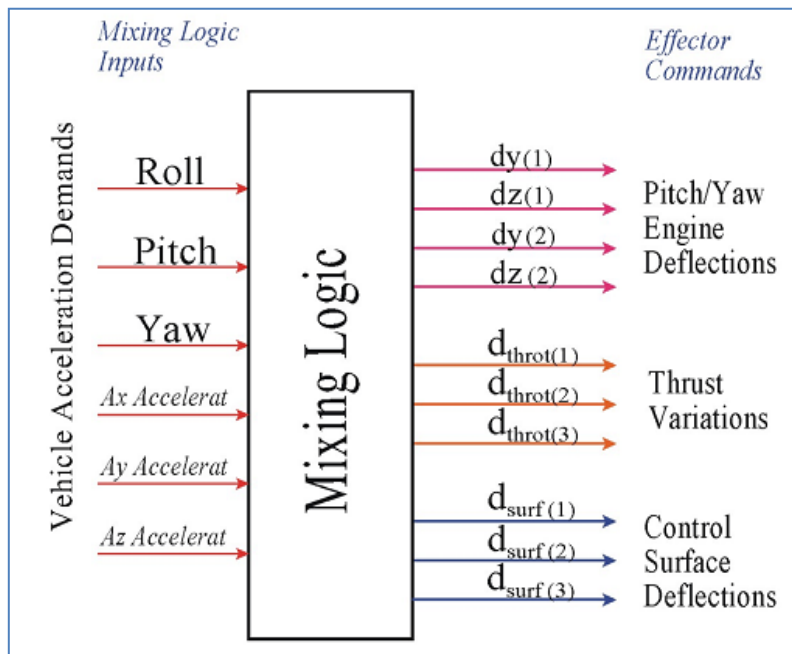


Figure 3.2 Flight Control Loop Showing the Mixing Logic Matrix, the FCS, and Matrix  $C_M$

We must develop equations that convert the FCS demands to moments and forces  $M_\delta$  applied on the vehicle. This relationship requires a mixing logic matrix  $K_{mix}$  that connects between the flight control system outputs and the vehicle effectors  $\delta_{eff}$ , as shown in Figure 3.2. The mixing logic matrix combines all the vehicle effectors together as a system and becomes an integral part of the



flight control system. It receives the acceleration demands  $\delta_{FCS}$ , which are mainly: roll, pitch, and yaw rotational accelerations and may include some linear acceleration demands, and generates the effector deflections and throttle commands vector  $\delta_{eff}$ . These are inputs to the effector system ( $C_M$ ) and consist of: gimbaling engines, throttling engines, RCS jets, and aerosurfaces.  $C_M$  generates the moments and forces vector  $M_\delta$ . The effector mixing matrix  $K_{mix}$  is calculated from the vehicle mass properties, geometry, engines and aero data which depend on the flight conditions. Its derivation is presented in a separate section and it is based on pseudo-inversion of the moment matrix. In the event of an effector failure it is the mixing logic matrix that must be changed and not the FCS gains.



The combined matrix ( $C_T = C_M K_{mix}$ ) is essential in the calculation of the performance parameters because its elements consist of moment and force partials per control acceleration demands. Let us assume that the vehicle is controlled by multiple types of effectors, such as: gimbaling engines, throttling engines, RCS jets, and aero surfaces. It is evident that if the vehicle has multiple control effectors that influence many directions the vehicle becomes more controllable and it can be guided in multiple directions. Launch vehicles, for example, use thrust vector control (TVC) engines to provide control forces and moments and sometimes in combination with engine throttling and RCS jets for linear acceleration control. In most aircraft the FCS controls three rotational axes using aileron, elevator, and rudder. Velocity along the x axis is also controlled by varying the engine thrust or by modulating drag using the speed-brake. The z acceleration is usually controlled indirectly through pitching but some aircraft have the capability to control normal acceleration directly and independently from pitching, by using flaps or jets. It is also possible, although not as frequent, to control lateral translation along the y axis independently from other axes using jets.

In addition to  $K_{mix}$  in our performance calculations we also need to derive the matrix  $C_M$  in Figure 3.2. This matrix relates the effector deflections to the combined moments and forces applied on the vehicle. The two matrices are then combined together to obtain the partials matrix ( $C_T = C_M K_{mix}$ ) that relates the FCS output demands ( $\delta_{FCS}$ ) to the moments and forces applied to the vehicle ( $M_\delta$ ), which is important in the calculation of the performance parameters. The matrix  $C_M$  is derived by combining the forces and moments from each individual type of effectors, as shown below.

### 3.3 Vehicle Moments and Forces Generated by a Double-Gimbaling Engine

Equation 3.2 calculates the three moments and three forces acting on the vehicle from a single engine (i) that is gimbaling in pitch ( $\delta y$ ) and yaw ( $\delta z$ ) directions relative to the trim positions ( $\Delta_E$ ,  $\Delta_Z$ ), see Figure 2.5. This equation is also written in matrix form at the bottom.

$$\begin{aligned}
 \begin{bmatrix} L_{G2} \\ M_{G2} \\ N_{G2} \\ F_{XG2} \\ F_{YG2} \\ F_{ZG2} \end{bmatrix}_{(i)} &= T_e(i) \left\{ \begin{bmatrix} 0 & -l_{zei} & l_{yei} \\ l_{zei} & 0 & -l_{xei} \\ -l_{yei} & l_{xei} & 0 \end{bmatrix} \begin{bmatrix} -\cos(\Delta_Z) \sin(\Delta_E) & -\cos(\Delta_E) \sin(\Delta_Z) \\ -\sin(\Delta_Z) \sin(\Delta_E) & \cos(\Delta_E) \cos(\Delta_Z) \\ -\cos(\Delta_E) & 0 \end{bmatrix}_{(i)} \right\} \begin{Bmatrix} \delta_{Y(i)} \\ \delta_{Z(i)} \end{Bmatrix} \\
 &= \{V_{G2Y} \quad V_{G2Z}\} \begin{Bmatrix} \delta_{Y(i)} \\ \delta_{Z(i)} \end{Bmatrix}
 \end{aligned} \tag{3.2}$$

The total moments and forces on the vehicle generated by N number of engines (N=3 in this case) which are gimbaling in pitch and yaw directions ( $\delta z_i$ ,  $\delta y_i$ ) can be written in the compact matrix form as shown in Equation 3.3 with the 6 deflection inputs combined in a single vector (3-pitch and 3-yaw). Where,  $V_{G2yi}$  and  $V_{G2zi}$  are column vectors for engine (i) obtained from Equation 3.2.

$$\begin{aligned}
 \begin{bmatrix} L_{G2} \\ M_{G2} \\ N_{G2} \\ F_{XG2} \\ F_{YG2} \\ F_{ZG2} \end{bmatrix}_{(T)} &= \begin{bmatrix} \uparrow & \uparrow & \uparrow & \uparrow & \uparrow & \uparrow \\ V_{G2y1} & V_{G2z1} & V_{G2y2} & V_{G2z2} & V_{G2y3} & V_{G2z3} \\ \downarrow & \downarrow & \downarrow & \downarrow & \downarrow & \downarrow \end{bmatrix} \begin{Bmatrix} \delta_{Y1} \\ \delta_{Z1} \\ \delta_{Y2} \\ \delta_{Z2} \\ \delta_{Y3} \\ \delta_{Z3} \end{Bmatrix}
 \end{aligned} \tag{3.3}$$

### 3.4 Vehicle Moments and Forces Generated by an Engine Gimballing in Single Direction

We can also calculate the moments and forces vector for a vehicle with TVC engines that gimbal only in one direction ( $\gamma_{ei}$ ). The gimballing direction ( $\gamma_{ei}$ ) is defined by the max pitch and yaw deflections ( $\delta_{Y_{max}}, \delta_{Z_{max}}$ ), where:  $\gamma_{ei} = \tan^{-1}(\delta_{Z_{max}} / \delta_{Y_{max}})$ .

The moments and forces on the vehicle generated by an engine (i) that is gimballing in a single direction ( $\gamma_{ei}$ ), and deflects at an angle ( $\delta\gamma_{ei}$ ) along ( $\gamma_{ei}$ ), are obtained from equation 3.4.

$$\begin{bmatrix} L_{SG} \\ M_{SG} \\ N_{SG} \\ F_{XSG} \\ F_{YSG} \\ F_{ZSG} \end{bmatrix}_{(i)} = T_e(i) \left\{ \begin{array}{l} \begin{bmatrix} 0 & -l_{zei} & l_{yei} \\ l_{zei} & 0 & -l_{xei} \\ -l_{yei} & l_{xei} & 0 \end{bmatrix} \begin{bmatrix} -\cos(\Delta_Z) \sin(\Delta_E) \cos(\gamma_i) - \cos(\Delta_E) \sin(\Delta_Z) \sin(\gamma_i) \\ -\sin(\Delta_Z) \sin(\Delta_E) \cos(\gamma_i) + \cos(\Delta_E) \cos(\Delta_Z) \sin(\gamma_i) \\ -\cos(\Delta_E) \cos(\gamma_i) \end{bmatrix}_{(i)} \\ \begin{bmatrix} -\cos(\Delta_Z) \sin(\Delta_E) \cos(\gamma_i) - \cos(\Delta_E) \sin(\Delta_Z) \sin(\gamma_i) \\ -\sin(\Delta_Z) \sin(\Delta_E) \cos(\gamma_i) + \cos(\Delta_E) \cos(\Delta_Z) \sin(\gamma_i) \\ -\cos(\Delta_E) \cos(\gamma_i) \end{bmatrix}_{(i)} \end{array} \right\} \left\{ \delta_{\gamma(i)} \right\}$$

The total moments and forces on the vehicle generated by (N=3) single gimballing engines which are gimballing along some skewed direction ( $\gamma_{ei}$ ) and deflecting at an angle ( $\delta\gamma_{ei}$ ) can be obtained from equation 3.5, where  $V_{SGi}$  are the column vectors for each engine (i) as defined in equation 3.4 above.

$$\begin{bmatrix} L_{SG} \\ M_{SG} \\ N_{SG} \\ F_{XSG} \\ F_{YSG} \\ F_{ZSG} \end{bmatrix}_{(T)} = [V_{SG1} \quad V_{SG2} \quad V_{SG3}] \left\{ \begin{array}{l} \delta_{\gamma 1} \\ \delta_{\gamma 2} \\ \delta_{\gamma 3} \end{array} \right\} \quad (3.5)$$

### 3.5 Vehicle Moments and Forces Generated by a Throttling Engine

The moment and force variations on the vehicle generated by the thrust variation of a single throttling engine (i) are:

$$\begin{bmatrix} L_{TH} \\ M_{TH} \\ N_{TH} \\ F_{XTH} \\ F_{YTH} \\ F_{ZTH} \end{bmatrix}_{(i)} = T_e(i) \left\{ \begin{array}{l} \begin{bmatrix} 0 & -l_{zei} & l_{yei} \\ l_{zei} & 0 & -l_{xei} \\ -l_{yei} & l_{xei} & 0 \end{bmatrix} \begin{bmatrix} \cos(\Delta_E) \cos(\Delta_Z) \\ \cos(\Delta_E) \sin(\Delta_Z) \\ -\sin(\Delta_E) \end{bmatrix}_{(i)} \\ \begin{bmatrix} \cos(\Delta_E) \cos(\Delta_Z) \\ \cos(\Delta_E) \sin(\Delta_Z) \\ -\sin(\Delta_E) \end{bmatrix}_{(i)} \end{array} \right\} \left\{ \delta_{Thr(i)} \right\} \quad (3.6)$$

Where:  $\delta_{Thr(i)}$  is the throttle control that varies from 0 to  $\pm\delta_{ThrMax}$ , (where  $\delta_{ThrMax} < 1$ ), and  $T_{e(i)}$  is the nominal engine thrust.

The actual thrust of the  $i^{th}$  engine  $T_{(i)}$  is equal to  $T_{e(i)} * (1 + \delta_{Thr(i)})$ . The force and moment variations are due to the thrust variation  $T_{e(i)} \delta_{Thr(i)}$ . For an RCS jet the force variation equation is the same, except that in this case  $T_{e(i)}$  represents the maximum jet thrust because its nominal thrust is zero. The moment and force variations on the vehicle generated by (N=3) throttling engines are shown in equation 3.7, where:  $\delta_{Thr_i}$  is the throttle control of engine (i), and  $V_{TH_i}$  are column vectors for engine (i) obtained from equation 3.6 above

$$\begin{bmatrix} L_{TH} \\ M_{TH} \\ N_{TH} \\ F_{XTH} \\ F_{YTH} \\ F_{ZTH} \end{bmatrix}_{(T)} = \begin{bmatrix} \uparrow & \uparrow & \uparrow \\ V_{TH1} & V_{TH2} & V_{TH3} \\ \downarrow & \downarrow & \downarrow \end{bmatrix} \left\{ \begin{array}{l} \delta_{Thr1} \\ \delta_{Thr2} \\ \delta_{Thr3} \end{array} \right\} \quad (3.7)$$

### 3.6 Vehicle Moments and Forces Generated by Control Surfaces

Similarly, we can calculate the moment and force variations from each aero-surface. We are assuming that the coefficients for each aerosurface correspond to separate rotating panels and they do not represent a combination of surfaces, such as an aileron, for example, which is defined to be the differential rotation of two aerosurfaces. An individual panel often excites multiple directions, and by defining the aero coefficients for each surface separately it allows us to combine the surfaces more efficiently by means of the surface combination logic. The control moments and forces on the vehicle generated by a single aero-surface panel (i) rotating at an angle ( $\delta_{asi}$ ) is shown in equation 3.8a. Equation 3.8b shows the control moments and forces in matrix form generated by multiple surfaces.

$$\begin{bmatrix} L_{AS} \\ M_{AS} \\ N_{AS} \\ F_{XAS} \\ F_{YAS} \\ F_{ZAS} \end{bmatrix}_{\delta(i)} = \overline{QS}_{ref} \begin{bmatrix} bC_{l\delta i} \\ cC_{m\delta i} \\ bC_{n\delta i} \\ -C_{A\delta i} \\ C_{Y\delta i} \\ C_{Z\delta i} \end{bmatrix} \{ \delta_{asi} \}; \quad \begin{bmatrix} L_{AS} \\ M_{AS} \\ N_{AS} \\ F_{XAS} \\ F_{YAS} \\ F_{ZAS} \end{bmatrix}_{(T)} = \begin{bmatrix} \uparrow & \uparrow & \uparrow \\ V_{AS1} & V_{AS2} & V_{AS3} \\ \downarrow & \downarrow & \downarrow \end{bmatrix} \begin{Bmatrix} \delta_{as1} \\ \delta_{as2} \\ \delta_{as3} \end{Bmatrix} \quad (3.8)$$

### 3.7 Total Vehicle Moments and Forces due to All Effectors Combined

We will now combine the equations (3.3, 3.7, & 3.8) together and present them in a form that relates the total moments and forces on the vehicle due to the combined effectors consisting of: gimbaling engines, throttling engines (or RCS), and aerosurfaces. Equation 3.9 is an example showing how the moments and forces from individual effector deflections or throttles are combined together in a matrix equation to calculate the combined effectors moments and forces  $M_{\delta}$ . The effector control inputs are lined up as a column vector on the right side, and the moment and force contribution vectors from each individual effector are stacked together to form the matrix  $C_M$ . The equation is also written in compact matrix form below.

$$\begin{bmatrix} L_X \\ M_Y \\ N_Z \\ F_X \\ F_Y \\ F_Z \end{bmatrix}_{(Tot)} = \begin{bmatrix} \uparrow & \uparrow & \uparrow & \uparrow & \uparrow & \uparrow & \uparrow & \uparrow & \uparrow & \uparrow \\ V_{GY1} & V_{GZ1} & V_{GY2} & V_{GZ2} & V_{G\gamma 1} & V_{G\gamma 2} & V_{TH1} & V_{TH2} & V_{AS1} & V_{AS2} \\ \downarrow & \downarrow & \downarrow & \downarrow & \downarrow & \downarrow & \downarrow & \downarrow & \downarrow & \downarrow \end{bmatrix} \begin{Bmatrix} \delta_{y1} \\ \delta_{z1} \\ \delta_{y2} \\ \delta_{z2} \\ \delta_{\gamma 1} \\ \delta_{\gamma 2} \\ \delta_{Th1} \\ \delta_{Th2} \\ \delta_{as1} \\ \delta_{as2} \end{Bmatrix}$$

or  $\underline{M}_{\delta} = (C_M) \underline{\delta}_{eff}$  where  $\underline{\delta}_{eff} = (K_{Mix}) \underline{\delta}_{FCS}$  (3.9)

The vector  $\underline{\delta}_{eff}$  may consist of all three types of effectors. It is the product of the FCS output vector  $\underline{\delta}_{FCS}$  multiplied with the mixing logic matrix  $K_{mix}$ , see Figure 3.2. The FCS output vector  $\underline{\delta}_{FCS}$  consists of the acceleration demands along the control directions, which are a minimum three rotations: roll, pitch, and yaw, plus some optional translations along: x, y, and z axes. Translational demands in the FCS and in the mixing logic should only be included when the effector system has the control authority to perform translations along those directions without degrading the moments controllability.

By multiplying the two matrices together we obtain the demands partial matrix ( $C_T = C_M K_{mix}$ ), shown in equation 3.10, which converts the FCS output demands  $\underline{\delta}_{FCS}$  to vehicle control moments and forces  $M_\delta$ . The FCS vector  $\delta_{FCS}$  consist of at least 3 rotations, plus optionally up to 3 translations. In equation 3.10  $\delta_{FCS}$  is shown with all 6 direction demands included.

$$M_\delta = C_T \delta_{FCS} \quad \text{where}$$

$$\begin{bmatrix} L_X \\ M_Y \\ N_Z \\ F_X \\ F_Y \\ F_Z \end{bmatrix}_{(Tot)} = \begin{bmatrix} L_{\delta P} & 0 & L_{\delta R} & 0 & L_{\delta Y} & 0 \\ 0 & M_{\delta Q} & 0 & M_{\delta X} & 0 & M_{\delta Z} \\ N_{\delta P} & 0 & N_{\delta R} & 0 & N_{\delta Y} & 0 \\ 0 & F_{X\delta Q} & 0 & F_{X\delta X} & 0 & F_{X\delta Z} \\ F_{Y\delta P} & 0 & F_{Y\delta R} & 0 & F_{Y\delta Y} & 0 \\ 0 & F_{Z\delta Q} & 0 & F_{Z\delta X} & 0 & F_{Z\delta Z} \end{bmatrix} \begin{bmatrix} \delta_P \\ \delta_Q \\ \delta_R \\ \delta_X \\ \delta_Y \\ \delta_Z \end{bmatrix}_{FCS}$$

(3.10)

The partial matrix  $C_T$  in equation 3.10 is very useful in the calculations of the performance parameters, as we shall see in Section 3.3, because its elements consist of moment and force partials per FCS demands. The diagonal elements of  $C_T$  measure the effector system's ability to maneuver the vehicle along the controllable directions, which are: three rotations and optionally up to three translations. The size of matrix  $C_T$  is  $(6 \times N_{dof})$ . The number of columns is equal to the number of controllable degrees of freedom  $N_{dof}$ , which is 3 rotations plus some translations. We exclude of course the non-controllable directions by removing the corresponding rows from the equation and  $C_T$  becomes a diagonal matrix that is also diagonally dominant, as it should be if the mixing logic matrix is properly designed. For example, the (2,2) element of  $C_T$  is  $M_{\delta Q}$ . That is, the pitch moment partial per pitch FCS demand  $\delta_{QFCS}$ .

By introducing the demands partial matrix representation  $C_T$  we are essentially replacing the classical  $Cm\delta_{elevator}$ ,  $Cl\delta_{aileron}$ , and  $Cn\delta_{rudder}$  partials, which are the classical aircraft controls, with a more generic form that it is applicable to multiple types of effectors and in more than three directions. Instead of aileron, elevator and rudder deflections we now have the rotational acceleration demands  $(\delta_{PFCS}, \delta_{QFCS}, \delta_{RFCS})$ . The x-axis translational acceleration demand is  $\delta_{XFCS}$  instead of throttle or speed-brake command, etc. The first three inputs  $\delta_{PFCS}$ ,  $\delta_{QFCS}$ , and  $\delta_{RFCS}$  on the right side of equation (3.10) are the rotational FCS acceleration demands, and the last three inputs  $\delta_{XFCS}$ ,  $\delta_{YFCS}$ ,  $\delta_{ZFC}$  are translational acceleration demands which are optional. Translation controls are introduced in the demands vector only when there is a requirement for direct translational control and controllability along those directions is available. Otherwise, translations are performed indirectly by means of rotational maneuvering. The individual effector deflections (or thrust variations)  $\delta_{eff}$  become transparent in this formulation, since they are combined together by the mixing logic matrix towards a common purpose, which is to provide the required acceleration in the demanded direction. The mixing logic matrix takes care of the control distribution among the effectors and it must avoid saturating the controls.

The most commonly used translation demands are:  $\delta_{XFCS}$  and  $\delta_{ZFC}$  for controlling the axial and normal accelerations. They are included when the flight vehicle has the necessary effectors to maneuver and to perform translational motion along those directions, such as: throttling

capability, reaction control jets, body flap, or speed brake. The y direction  $\delta_{yFCS}$  is rarely controlled directly by the FCS. The Harrier aircraft has such a feature when hovering.

### 3.8 Performance Parameters

The following parameters are used by the Trim program to evaluate the vehicle performance in a static sense along a predefined trajectory.

#### Aerodynamic Center

The aerodynamic center is defined to be the point in the x-axis where the partial of pitch moment with respect to angle of attack is zero, that is:  $(\partial C_m / \partial \alpha) = 0$

$$\frac{\partial C_{m_{AC}}}{\partial \alpha} = \frac{\partial C_{m_{MRC}}}{\partial \alpha} + \frac{\partial C_z}{\partial \alpha} \left[ \frac{x_{AC} - x_{MRC}}{\bar{c}} \right] = 0 \quad (3.11)$$

$$x_{AC} = x_{MRC} - \frac{C_{m_{\alpha_{MRC}}}}{C_{z_{\alpha}}} \bar{c}$$

Where  $\bar{c}$  is the vehicle "reference length." The location of the  $x_{AC}$  with respect to the  $x_{CG}$  determines the static stability of the vehicle. If the CG is ahead of the AC then the vehicle is stable and it has a negative  $C_{m\alpha}$ .

#### Static Margin

The Static Margin is defined to be the ratio of:

$$SM = \left[ \frac{x_{CG} - x_{AC}}{\text{Vehicle Length}} \right] 100 \quad (3.12)$$

#### Center of Pressure

The center of pressure is defined to be the point about which the pitch aerodynamic moment is zero.

$$C_{m_{CP}} = C_{m_{MRC}} + C_z \left[ \frac{x_{CP} - x_{MRC}}{\bar{c}} \right] = 0 \quad (3.13)$$

$$x_{CP} = x_{MRC} - \frac{C_{m_{MRC}}}{C_z} \bar{c}$$

The location of the CP with respect to the  $x_{CG}$  determines how much surface deflection is required to trim the vehicle. If the CP and the CG are co-located then the vehicle can be trimmed with zero surface deflection.

## Pitch Static Stability/ Time to Double Amplitude (T2) Parameter

*Static stability* refers to the tendency of a flight vehicle under static conditions to return to its trimmed attitude. The transfer function in equation 3.14 is an approximate relationship (ignoring damping) between pitch control demand  $\delta_{Q_{FCS}}$  and the vehicle angle of attack  $\alpha$ . The coefficient  $M_{\delta Q}$  is the pitch control moment partial per pitch demand  $\delta_{Q_{FCS}}$ . It is the second diagonal element in the partials demands matrix  $C_T(2,2)$ , in equation 3.10, as we have already shown.

$$\frac{\alpha(s)}{\delta_{Q_{FCS}}(s)} = \left\{ \frac{M_{\delta Q} / I_{YY}}{s^2 + \omega_p^2} \right\} \text{ where: } \omega_p^2 = \left[ -\frac{M_\alpha}{I_{YY}} \right] \text{ and } M_\alpha = \bar{Q} S_{ref} \bar{c} C_{m\alpha} \quad (3.14)$$

Static stability is determined by the sign of the pitch moment derivative coefficient  $C_{m\alpha}$ . When  $C_{m\alpha}$  is negative,  $\omega_p^2 > 0$ , the vehicle is statically stable and it has a short period resonance  $\omega_p$  (rad/sec). Otherwise, when  $C_{m\alpha}$  is positive,  $\omega_p^2 < 0$ , the solution of the transfer function is divergent, and the vehicle is open-loop unstable. We typically like the vehicle to be statically stable, but not too stable, because when it is too stable it becomes less maneuverable and bigger aerosurfaces and also deflections are needed to control it. If on the other hand  $C_{m\alpha}$  is a little positive (slightly unstable) the vehicle becomes more maneuverable and it can be trimmed and controlled with smaller effectors. The flight control system is usually able to tolerate a certain amount of instability, but not too much. The actuators must be fast enough to respond when the angle of attack diverges due to instability and latency. The amount of static instability in a vehicle that is open-loop unstable is measured by the time it takes to double its amplitude or  $\alpha$ . The time to double amplitude (T2) is obtained from the equation 3.15, and as a rule of thumb it should be greater than 0.4 seconds, depending on the vehicle size and its actuator bandwidth.

$$T2 = \ln(2) / |\omega_p| \quad (3.15)$$

The T2 requirement on an unstable flight vehicle depends on its size and the capability of its actuators, in terms of: bandwidth, delay, maximum deflections, rate, and acceleration characteristics. Obviously, the T2 requirement must be greater than the time it takes for its effectors to travel from trim to maximum deflection, plus some extra time margin to account for any latency in the system, such as computational delay. When the vehicle is statically stable, on the other hand, and  $C_{m\alpha}$  is negative, static-stability is measured by the frequency of the short-period resonance  $\omega_p$ . A useful parameter for analyzing the pitch static stability or instability of a flight vehicle along the trajectory is to plot the inverse of T2 as a function of time when the vehicle is unstable and the frequency of the short period resonance with a negative sign,  $(-\omega_p)$  in (rad/sec) in the regions where it is stable, see Figure 3.3. This makes it easy to differentiate between stable and unstable regions along the trajectory without plotting T2 which diverges to infinity when static stability fluctuates between stable and unstable regions. In fact, for a vehicle that is marginally stable, as it should be ideally, the "T2-inverse/ Short-Period" stability parameter is close to zero, either a little positive or a little negative.



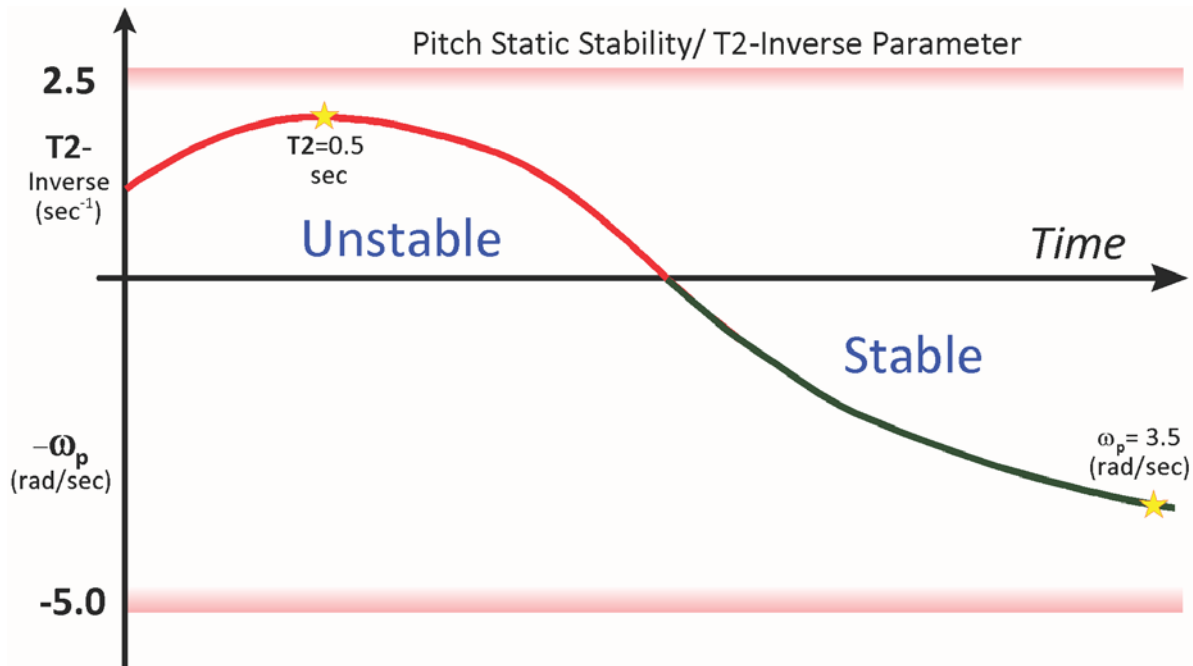


**Figure 3.3 Example of: Pitch Stability/ T2-Inverse Parameter versus Time Showing the Stable and Unstable Regions**

The vehicle is more maneuverable when the T2-inverse parameter is a little positive, slightly unstable, and typically it should not exceed  $2.5 \text{ sec}^{-1}$ . When the parameter is negative the vehicle is stable, and as a rule of thumb the short period frequency  $\omega_p$  should not exceed  $5 \text{ (rad/sec)}$ , otherwise, it becomes difficult to maneuver and requires bigger effectors and a wider control bandwidth. In Figure 3.3 we have a stability parameter that is transitioning between unstable and stable regions. When unstable, it has a maximum time to double amplitude  $T2= 0.5$  seconds, and when it is stable, the largest short-period resonance is  $3.5$  radians per second near the end of the trajectory. The static stability parameter does not exceed the upper and lower limits throughout the trajectory, and therefore, the vehicle stability is acceptable.

### Directional Stability ( $C_{n\beta\_dynamic}$ )

Static stability in the lateral directions is measured by the  $C_{n\beta\_dynamic}$  parameter which is used for predicting directional stability at high angles of attack. In general, the vehicle will be directionally stable when the parameter  $C_{n\beta\_dynamic}$  is greater than zero. Otherwise, it may experience yaw departure and Dutch-Roll mode instability. Aircraft with  $C_{n\beta\_dynamic}$  greater than  $0.004 \text{ deg}^{-1}$  have very little tendency for yaw departure.

$$C_{n\beta\_dynamic} = C_{n\beta} \cos \alpha_o - \frac{I_{zz}}{I_{xx}} C_{l\beta} \sin \alpha_o \quad (3.16)$$

Increasing the wing dihedral improves yaw departure. Too much dihedral, however, makes the vehicle sensitive to gusts and to lateral control inputs, see the Lifting-Body aircraft example. When the aircraft is directionally stable, the roll/ yaw frequency  $\omega_D$  otherwise also known as “Dutch-Roll” mode is obtained from the following equation:

$$\omega_D^2 = \bar{Q} S_{ref} b \left[ C_{n\beta} \frac{\cos \alpha_o}{I_{zz}} - C_{l\beta} \frac{\sin \alpha_o}{I_{xx}} \right] \quad (3.17)$$

## Lateral Time to Double Amplitude/ Stability Parameter (T2)

When the lateral directions are unstable (which happens when  $C_n\beta_{dynamic} < 0$ ), the time to double sideslip  $\beta$  amplitude should typically be greater than 0.5 second. The time to double amplitude in the lateral direction is defined by an equation similar to the pitch T2. Notice that the square of Dutch-Roll frequency is negative when unstable.

$$T2 = \ln(2)/|\omega_D| \quad (3.18)$$

The lateral stability parameter is evaluated similar to the pitch stability, by plotting the T2-inverse when the vehicle is directionally unstable. Otherwise, when the vehicle is directionally stable we plot the Dutch-Roll frequency with a negative sign ( $-\omega_D$ ). When the lateral stability parameter is positive (unstable), the T2-inverse should not exceed  $2 \text{ sec}^{-1}$ , and when the vehicle is stable,  $\omega_D$  should not exceed 5 (rad/sec).

## Control Authority of Effectors

Our next objective is to examine the efficiency of the control effectors in maneuvering the vehicle in various directions. The demands vector  $\underline{\delta}_{FCS}$  comes from the flight control system and consists of acceleration commands in 3 to 6 directions. The effectors are operating as a system and their authority in the control directions is evaluated by their ability to maneuver the vehicle in the commanded directions and to achieve the expected accelerations without saturating the effectors. The control distribution among the effectors is accomplished by the mixing logic matrix which optimizes the control efficiency. It attempts to provide the expected accelerations in the commanded directions while minimizing their activity and also reducing the cross-coupling interaction between the control directions. An acceleration demand from the flight control system will in general activate multiple effectors. Each effector has its saturation limit and for the maneuver to be executed efficiently, none of the effector deflections or throttles should reach their limits. The control authority of the effector system can be measured by the maximum angles of attack  $\pm\alpha_{max}$  and sideslip  $\pm\beta_{max}$  dispersions from trim ( $\alpha_0, \beta_0$ ) that can be achieved due to maneuvering, or tolerated due to cross-winds, before saturating at least one of the effectors. It is also evaluated by the maximum accelerations that can be achieved along the control directions when the FCS demands are maximized.

We must now derive equations that impose saturation limits on the acceleration demands. So far we have not discussed about any hard limits in the flight control demands  $\underline{\delta}_{FCS}$ . We know that the acceleration demand is a software input to the mixing logic and the mixing logic generates deflection and throttle commands to the effectors that have physical limits. So we need a relationship that translates the effector  $\underline{\delta}_{eff}$  physical limits back to demands  $\underline{\delta}_{FCS}$  software limits. The question is: what is the maximum FCS demand  $\underline{\delta}_{FCSmax}$  that the mixing logic matrix can accept along the 3 to 6 controlled directions before it saturates at least one of the vehicle effectors?

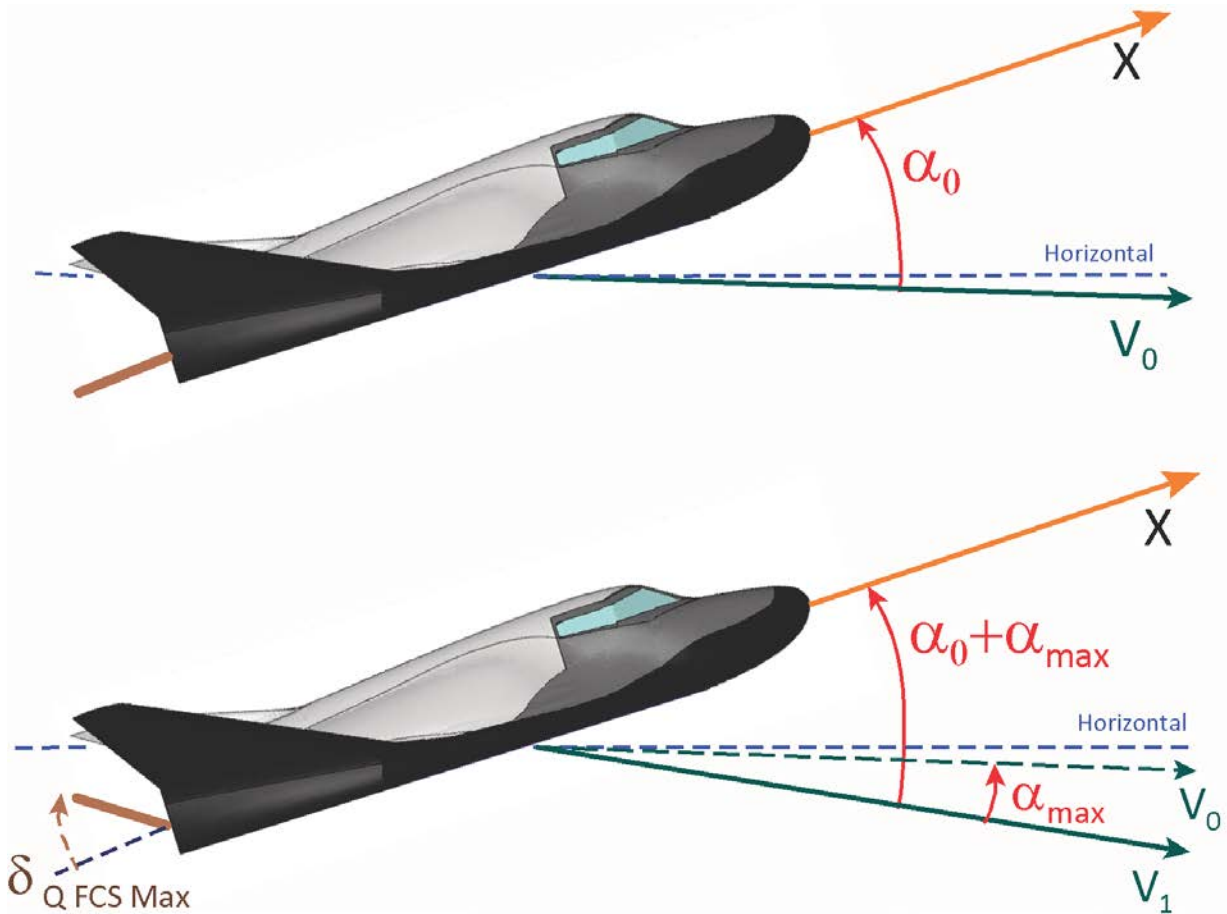


**Figure 3.4 Pitch Effector Deflection is  $\delta_{Q \text{ FCS Max}}$  from trim in order to Balance the Moment produced due to an Increase in the Angle of Attack  $\alpha_{\text{max}}$  from trim  $\alpha_0$**

The mixing logic matrix  $K_{\text{mix}}$  plays an important role in control authority calculation because ideally it should be distributing the control authority evenly among the effectors, so they should all be reaching to their saturation limits simultaneously when the acceleration demand begins to exceed the capability of the effector system. The control distribution should be allocated optimally according to the capability of each individual effector, and thus preventing the weaker guy from saturating when others have additional capability. The size of the effector mixing matrix is  $(N_{\text{eff}} \times N_{\text{dof}})$ , where  $N_{\text{eff}}$  is the number of effectors, and  $N_{\text{dof}}$  is the number of controllable degrees of freedom. Now let us try to place some limits on the FCS demands. The mixing logic matrix equation that calculates the effector deflections from the demands can be normalized by dividing each row with the maximum deflection  $\delta_{i\text{max}}$  of the corresponding effector, as shown in equation 3.19, which now relates the demands  $\underline{\delta}_{\text{FCS}}$  to the normalized effector deflections  $(\delta_i/\delta_{i\text{max}})$ . The magnitudes of the normalized effector deflection outputs on the left side must never exceed one, in order to prevent the effectors from reaching their hard limits. Note that  $\delta_{i\text{max}}$  represents the maximum effector deflection from trim to saturation due to positive FCS demand which is not necessarily a positive effector deflection. It may be a negative deflection resulting from positive FCS demand.

$$\begin{pmatrix} \delta_1/\delta_{1\max} \\ \delta_2/\delta_{2\max} \\ \vdots \\ \delta_n/\delta_{n\max} \end{pmatrix} = \begin{bmatrix} \uparrow & \uparrow & \uparrow & \uparrow & \uparrow & \uparrow \\ \underline{U}_P & \underline{U}_Q & \underline{U}_R & \underline{U}_X & \underline{U}_Y & \underline{U}_Z \\ \downarrow & \downarrow & \downarrow & \downarrow & \downarrow & \downarrow \end{bmatrix} \begin{bmatrix} \delta_P \\ \delta_Q \\ \delta_R \\ \delta_X \\ \delta_Y \\ \delta_Z \end{bmatrix}_{FCS} \quad (3.19)$$

Each of the column vectors:  $\{\underline{U}_P, \underline{U}_Q, \underline{U}_R, \underline{U}_X, \underline{U}_Y, \underline{U}_Z\}$  in the normalized mixing-logic matrix equation 3.19, determines the normalized deflections of the effectors vector resulting from 1 unit of FCS acceleration demand in one of the corresponding directions  $\{\delta_{PFCS}, \delta_{QFCS}, \delta_{RFCS}, \delta_{XFCS}, \delta_{YFCS}, \delta_{ZFCs}\}$ . Let us assume that the elements with the largest magnitude in each of these normalized vectors are:  $(U_{P\max}, U_{Q\max}, U_{R\max}, U_{X\max}, U_{Y\max}, U_{Z\max})$  respectively. They determine which effector (i) produces the largest deflection from one unit of FCS demand in the corresponding direction:  $\delta_{PFCS}, \delta_{QFCS}, \delta_{RFCS}, \delta_{XFCS}, \delta_{YFCS},$  or  $\delta_{ZFCs}$ . In pitch, for example, the deflection  $\delta_i$  of the most active effector (i) due to a pitch demand  $\delta_{QFCS}$  is

$$\delta_i = U_{Q\max} \delta_{i\max} \delta_{QFCS} \quad (3.20)$$

Let us assume that the most active effector (i) produces the largest normalized deflection magnitude  $(\delta_i/\delta_{i\max})$  coming from a pitch demand  $\delta_{QFCS}$ . The element in vector  $\underline{U}_Q$  that corresponds to the largest deflection is  $U_{Q\max}$ . From equation 3.20 we conclude that the most active effector in pitch reaches its limit when the FCS command  $\delta_{QFCS}$  is maximized at:

$$\delta_{+QFCS\ MAX} = \frac{1}{U_{Q\ MAX}} \quad (3.21)$$

Now that we have calculated the maximum control demand let us calculate the maximum steady-state alpha dispersion that the FCS can achieve. Let us consider the transfer function in equation 3.14 which is an approximate relationship between the pitch FCS control demand  $\delta_{QFCS}$  and the vehicle angle of attack response  $\alpha$ . When the aircraft is statically stable the parameter  $M_\alpha$  is negative which implies that  $\omega_p^2$  is positive. The partial derivative  $M_{\delta Q}$  represents the pitch moment on the vehicle due to a pitch FCS demand  $\delta_{QFCS}$  and it is defined in equation 3.10. The vehicle control authority can be measured by the amount of steady alpha variation from trim  $\alpha_{+\max}$  that can be achieved (or tolerated) when the pitch control demand is maximized at  $\delta_{+QFCS\ MAX}$ . This occurs when the most active effector reaches its limit, i.e.  $(\delta_i = \delta_{i\max})$ , due to maximizing the pitch demand, as shown in equation 3.23, where  $U_{Q\max}$  is the largest element in the column vector  $U_Q$ .

$$\alpha_{+\max} = \frac{M_{\delta Q}/I_{YY}}{\omega_p^2} \delta_{+QFCS\ MAX} = -\frac{M_{\delta Q}}{U_{Q\max} M_\alpha} \quad (3.23)$$

## Biased Effectors

In equation 3.19 we initially assumed that the effectors are centered, and the maximum peak deflections  $\delta_{imax}$  between trim position and the upper or the lower limits are the same, either due to a positive or a negative FCS demand  $\delta_{FCS}$ . In reality, however, the trim position of the effectors are not centered, and some effectors may be biased either in the positive or the negative direction and the peak displacements from trim  $\delta_{imax}$  due to a positive demand  $\delta_{+FCSMax}$  may be different than the peak displacement  $\delta_{imin}$  from trim in the opposite direction due to a negative demand  $\delta_{-FCSMax}$ . If we assume that the normalized mixing-logic matrix equation 3.19 is written for positive FCS demands  $\delta_{+FCSMax}$ , we can rewrite the normalized matrix equation for negative acceleration demands  $\delta_{-FCSMax}$ , as follows:

$$\begin{pmatrix} \delta_1/\delta_{1min} \\ \delta_2/\delta_{2min} \\ \vdots \\ \delta_n/\delta_{nmin} \end{pmatrix} = \begin{bmatrix} \uparrow & \uparrow & \uparrow & \uparrow & \uparrow & \uparrow \\ U_P & U_Q & U_R & U_X & U_Y & U_Z \\ \downarrow & \downarrow & \downarrow & \downarrow & \downarrow & \downarrow \end{bmatrix} \begin{bmatrix} \delta_{-P} \\ \delta_{-Q} \\ \delta_{-R} \\ \delta_{-X} \\ \delta_{-Y} \\ \delta_{-Z} \end{bmatrix}_{FCS} \quad (3.19b)$$

Where:  $\delta_{imin}$  in this case are the peak deflections of the effectors in the opposite direction due to a negative demand  $\delta_{-FCSMax}$ , that is, between the trim position and the opposite saturation limit. This  $\delta_{imin}$  is not necessarily a negative effector deflection and not the same magnitude as  $\delta_{imax}$  but it is in the opposite direction to the deflection resulting from a positive FCS demand  $\delta_{+FCSMax}$ . The column vectors in equation (3.19b) are now normalized differently  $\{U'_P, U'_Q, U'_R, U'_X, U'_Y, U'_Z\}$  because their corresponding rows are divided by  $\delta_{imin}$  instead of  $\delta_{imax}$ . The largest element of each of these normalized vectors:  $(U_{Pmin}, U_{Qmin}, U_{Rmin}, U_{Xmin}, U_{Ymin}, U_{Zmin})$  are different from those obtained using positive demands:  $(U_{Pmax}, U_{Qmax}, U_{Rmax}, U_{Xmax}, U_{Ymax}, U_{Zmax})$ .

Based on this result we can calculate the peak FCS demand in the negative direction, and also the maximum alpha dispersion in the opposite direction from trim, as a result of this maximum negative pitch demand  $\delta_{-FCSMax}$ , see equation 3.23b.

$$\delta_{-QFCSMAX} = \frac{1}{U_{QMin}}; \quad \alpha_{-max} = -\frac{M_{\delta Q}}{U_{QMin} M_{\alpha}} \quad (3.23b)$$

## Control to Disturbance Partial (M<sub>α</sub>/M<sub>δ</sub>)

A flight vehicle must be designed to be able to counteract a certain amount of wind-shear, gusts and other disturbances by using its controls. The aerodynamic environment is typically characterized in terms of  $\alpha$  and  $\beta$  disturbances which are introduced in simulations as gusts and wind-shear. The gusts are short period disturbances applied in the dynamic model for analyzing the dynamic behavior of the flight vehicle. In static analysis the aero disturbance is defined as a steady wind-shear. A wind-shear causes steady-state variations in the angles of attack and sideslip. This  $\alpha$  and  $\beta$  variation generates additional forces and moments applied to the aircraft which must

be counteracted by further deflections of the control surfaces or engines. The ratio of the disturbance moment per alpha divided by the control moment per control deflection ( $M_\alpha/M_\delta$ ) is a parameter that is typically used for assessing controllability and in general this parameter should be less than one. This controllability parameter, however, does not take into account the maximum values of both parameters: the angle of attack (or sideslip in the lateral case) and the maximum control authority of the FCS, and we shall derive better criteria.

Note, when the vehicle is statically unstable, that is CG is behind the CP, the smallest control system bandwidth for achieving a minimum of 6 dB gain margin occurs when the attitude feedback gain is  $K_p = 2 M_\alpha/M_{\delta Q}$ , assuming a PD type controller  $\delta_{QFCS} = -K_p\theta - K_r\dot{\theta}$ . With this controller gain the control system bandwidth is  $\omega_b = \sqrt{M_\alpha/I_{YY}}$ . Increasing the attitude feedback gain  $K_p$  and bandwidth further improves rigid-body stability margin and also the system performance to attitude commands. However, you cannot increase it too much without exciting structure flexibility. In general there should be a separation factor of 10, between the control system bandwidth and the first structural mode.

#### **Pitch Control Authority against an Angle of Attack Variation: $\alpha_{\max}$**

We will now define a parameter for measuring the control authority of the effectors system in different directions. Consider the controllability in the pitch axis. An aircraft should have sufficient control authority to be able to tolerate a certain amount of  $\alpha$  variation, let's say  $\alpha_{\max} = \pm 5^\circ$ , without affecting its attitude and flight path and without saturating the pitch control, which is limited to  $\delta_{\pm Q_{\max}}$ . The authority of the pitch control system can be defined by the amount of pitch moment produced towards maximizing the angle of attack variation from trim against the total pitch control availability. For an acceptable pitch controllability we should expect the pitching moment produced when the pitch demand is maximized to  $\delta_{+Q_{\max}}$  from trim condition, to be considerably greater (at least twice as big) than the moment produced due to the dispersion  $\alpha_{\max}$  from trim.

$$\left| C_{m\delta Q} \delta_{Q_{\max}} \right| > 2 \left| C_{m\alpha} \alpha_{\max} \right|$$

We introduce a factor of 2 to allow some control authority for maneuvering and responding to gust disturbances. If we take into consideration that the max control demand is:  $\delta_{Q_{\max}} = 1/U_{Q_{\max}}$  the pitch control authority criterion becomes:

$$\text{Pitch Control Effort} : \left( \frac{\delta_{Q_{FCS}}}{\delta_{+Q_{\max FCS}}} \right) = \left| \frac{C_{m\alpha} U_{Q_{\max}} \alpha_{\max}}{C_{m\delta Q}} \right| < 0.5 \quad (3.24)$$

In other words, the control authority is defined by the amount of effort used by the effectors, which is the ratio of the pitch control used against the dispersion  $\alpha_{\max}$  divided by the maximum pitch control capability and it should be less than 1. In fact less than 0.5 is better for margin.

When the vehicle has multiple control effectors that can provide translational control in the x and z directions we may extend the control authority criterion along those directions. Let's say that the effectors system can provide control in the x and z directions and we would like the vehicle to

have the control authority to counteract disturbance forces due to  $\alpha_{\max}$  variations in those directions. This may obviously require the use of throttle control, RCS jets, or a speed-brake in the x direction to provide forces along those directions and to regulate speed in the presence of winds. The control authority definition in equation 3.24 can be extended to translational control for assessing the amount of effort it takes to control the vehicle against  $\alpha_{\max}$  dispersions from trim in the x and z directions.

$$\begin{aligned}
 X \text{ acceler. Control Effort} : \left( \frac{\delta_{X_{FCS}}}{\delta_{+X \max_{FCS}}} \right) &= \left| \frac{C_{A\alpha} U_{X \max} \alpha_{\max}}{C_{X\delta X}} \right| < 0.5 \\
 Z \text{ acceler. Control Effort} : \left( \frac{\delta_{Z_{FCS}}}{\delta_{+Z \max_{FCS}}} \right) &= \left| \frac{C_{Z\alpha} U_{Z \max} \alpha_{\max}}{C_{Z\delta Z}} \right| < 0.5
 \end{aligned} \tag{3.24b}$$

The coefficients:  $C_{m\delta Q}$ ,  $C_{Z\delta Z}$  and  $C_{X\delta X}$  are non-dimensional moment and force partials per FCS acceleration demands in pitch, z and x directions respectively. They are obtained from the demands partial matrix  $C_T$  in equation 3.10. They include contributions not only from aerosurfaces but from all vehicle effectors which are combined together by the mixing matrix. The parameters  $U_{Q\max}$ ,  $U_{Z\max}$ , and  $U_{X\max}$ , are the biggest elements of the column vectors  $\underline{U}_Q$ ,  $\underline{U}_z$  and  $\underline{U}_x$  in the normalized mixing matrix, equation 3.19.

When the dispersion is in the opposite direction  $-\alpha_{\max}$  the control authorities are determined by the control availability in the opposite direction  $\{U_{Q\min}, U_{X\min}, U_{Z\min}\}$  which may be different than  $+\alpha_{\max}$ .

$$\begin{aligned}
 Pitch \text{ Control Effort} : \left( \frac{\delta_{Q_{FCS}}}{\delta_{-Q \max_{FCS}}} \right) &= \left| \frac{C_{m\alpha} U_{Q \min} \alpha_{\max}}{C_{m\delta Q}} \right| < 0.5 \\
 X \text{ acceler. Control Effort} : \left( \frac{\delta_{X_{FCS}}}{\delta_{-X \max_{FCS}}} \right) &= \left| \frac{C_{A\alpha} U_{X \min} \alpha_{\max}}{C_{X\delta X}} \right| < 0.5 \\
 Z \text{ acceler. Control Effort} : \left( \frac{\delta_{Z_{FCS}}}{\delta_{-Z \max_{FCS}}} \right) &= \left| \frac{C_{Z\alpha} U_{Z \min} \alpha_{\max}}{C_{Z\delta Z}} \right| < 0.5
 \end{aligned} \tag{3.24c}$$

### Pitch Control Authority against Velocity Variation: $v_{\max}$

Similarly, the control authority of the effectors system can be evaluated by its capability to react against maximum velocity variations  $\pm v_{\max}$  from trim airspeed  $V_0$ . When the vehicle has an axial force control capability by means of thrust variation, RCS jets, or speed-brake, the axial force produced due to maximum axial control  $\delta_{X\max}$  should be at least twice as big as the axial force generated by the expected variation in velocity  $\pm v_{\max}$ . Also, the pitch moment produced due to maximum pitch control  $\delta_{Q\max}$  should be at least twice as big as the pitch moment generated by the velocity variation  $\pm v_{\max}$ .

$$\left| C_{X\delta X} \delta_{X\max_{FCS}} \right| > 2 \left| C_{XV} v_{\max} \right|$$

$$\left| C_{m\delta Q} \delta_{Q\max_{FCS}} \right| > 2 \left| C_{mV} v_{\max} \right|$$

The control authority against airspeed variation in the pitch axis is defined to be the ratio of the pitch control used against  $v_{\max}$  divided by the maximum available pitch control, and it should be less than 0.5 including margin. Similarly, if the vehicle has throttle control or a speed-brake, the control authority against  $v_{\max}$  dispersions in the x axis is defined to be the ratio of the axial force necessary against  $v_{\max}$  divided by the maximum available axial control capability, and it should be less than 0.5. The control authority criterion against  $v_{\max}$  can also be extended in the z direction, assuming of course, that the effectors system is able to control the z axis.

$$\begin{aligned} \text{Pitch Control Effort :} & \quad \left( \frac{\delta_{Q_{FCS}}}{\delta_{+Q\max_{FCS}}} \right) = \left| \frac{C_{m\delta V} U_{Q\max} v_{\max}}{C_{m\delta Q}} \right| < 0.5 \\ \text{X acceler. Control Effort :} & \quad \left( \frac{\delta_{X_{FCS}}}{\delta_{+X\max_{FCS}}} \right) = \left| \frac{C_{X\delta V} U_{X\max} v_{\max}}{C_{X\delta X}} \right| < 0.5 \\ \text{Z acceler. Control Effort :} & \quad \left( \frac{\delta_{Z_{FCS}}}{\delta_{+Z\max_{FCS}}} \right) = \left| \frac{C_{Z\delta V} U_{Z\max} v_{\max}}{C_{Z\delta Z}} \right| < 0.5 \end{aligned} \quad (3.24d)$$

When the airspeed variation is in the opposite direction  $-v_{\max}$  the control authorities are affected by the control availabilities in the opposite directions  $\{U_{Q\min}, U_{X\min}, U_{Z\min}\}$ .

$$\begin{aligned} \text{Pitch Control Effort :} & \quad \left( \frac{\delta_{Q_{FCS}}}{\delta_{-Q\max_{FCS}}} \right) = \left| \frac{C_{m\delta V} U_{Q\min} v_{\max}}{C_{m\delta Q}} \right| < 0.5 \\ \text{X acceler. Control Effort :} & \quad \left( \frac{\delta_{X_{FCS}}}{\delta_{-X\max_{FCS}}} \right) = \left| \frac{C_{X\delta V} U_{X\min} v_{\max}}{C_{X\delta X}} \right| < 0.5 \\ \text{Z acceler. Control Effort :} & \quad \left( \frac{\delta_{Z_{FCS}}}{\delta_{-Z\max_{FCS}}} \right) = \left| \frac{C_{Z\delta V} U_{Z\min} v_{\max}}{C_{Z\delta Z}} \right| < 0.5 \end{aligned}$$



The partials of the aerodynamic pitch moment and the X and Z forces per velocity variations are defined as a function of aerodynamic coefficients.

$$C_{mV} = \left( \frac{2C_{m0}}{V_0} + \frac{\partial C_m}{\partial V} \right); C_{xV} = - \left( \frac{2C_{A0}}{V_0} + \frac{\partial C_A}{\partial V} \right); C_{zV} = \left( \frac{2C_{z0}}{V_0} + \frac{\partial C_z}{\partial V} \right)$$

### Lateral Control Authority against Angle of Sideslip Dispersions: $\beta_{\max}$

An important requirement for the lateral effector design is to have sufficient control authority to execute a steady sideslip maneuver during turning or to be able to react against cross-winds near landing. When an aircraft is near landing with cross-wind, the side-force creates a sideslip angle, and the aircraft has to bank towards the wind in order to balance the side-force. For an aircraft to maintain a steady angle of sideslip  $\beta$ , the net side-force and also the rolling and yawing moments must be equal to zero. In order for the aircraft to maintain a constant sideslip, both: roll and yaw FCS controls  $\delta_{PFCS}$  and  $\delta_{RFCS}$  are used. The designer must evaluate if the effector deflections due to the roll and yaw FCS demands are within range and if the vehicle bank angle ( $\phi$ ) is acceptable, especially near landing. From the roll and yaw moment balance equations the amount of roll and yaw FCS control required to achieve a constant angle of sideslip  $\beta_{ss}$  are obtained from equations 3.25.

$$\delta_{PFCS} = \frac{(L_\beta N_{\delta R} - N_\beta L_{\delta R})}{(L_{\delta R} N_{\delta P} - N_{\delta R} L_{\delta P})} \beta_{ss}; \delta_{RFCS} = \frac{(N_\beta L_{\delta P} - L_\beta N_{\delta P})}{(L_{\delta R} N_{\delta P} - N_{\delta R} L_{\delta P})} \beta_{ss} \quad (3.25)$$

The partial derivatives  $N_{\delta R}$  and  $L_{\delta R}$  are the vehicle yaw and roll moments per yaw flight control acceleration demand  $\delta_{RFCS}$ . Similarly, the partial derivatives  $N_{\delta P}$  and  $L_{\delta P}$  are the vehicle yaw and roll moments per roll demand  $\delta_{PFCS}$ . They are obtained directly from the demands partial matrix  $C_T$  in equation 3.10. The roll and yaw control authority is measured by the magnitude of steady state angle of sideslip  $\beta_{\max}$  produced when the effector is at full deflection or by the amount of  $\beta$  dispersion they can tolerate. They should be able to handle at least 5 degrees of steady sideslip  $\beta_{\max}$ . After dividing the equations 3.25 with the maximum roll and yaw FCS demands,  $\delta_{P\max}$  and  $\delta_{R\max}$ , we obtain equations 3.26 that express the roll and yaw control authority as follows.

$$\begin{aligned} \text{Roll Control Effort: } & \left( \frac{\delta_{PFCS}}{\delta_{+P\max FCS}} \right) = \left| \frac{(L_\beta N_{\delta R} - N_\beta L_{\delta R}) U_{P\max} \beta_{\max}}{(L_{\delta R} N_{\delta P} - N_{\delta R} L_{\delta P})} \right| < 0.5 \\ \text{Yaw Control Effort: } & \left( \frac{\delta_{RFCS}}{\delta_{+R\max FCS}} \right) = \left| \frac{(N_\beta L_{\delta P} - L_\beta N_{\delta P}) U_{R\max} \beta_{\max}}{(L_{\delta R} N_{\delta P} - N_{\delta R} L_{\delta P})} \right| < 0.5 \end{aligned} \quad (3.26)$$

The control effort ratios ( $\delta_{PFCS}/\delta_{PMax}$ ) and ( $\delta_{RFCS}/\delta_{RMax}$ ) required to trim the roll and yaw moments against  $\beta_{max}$  should obviously be less than 1. In fact, they should be less than 0.5 to allow some margin for dynamic control. Similarly, when the vehicle has control authority such as RCS jets to accelerate in the y direction and to counteract  $\beta$  disturbances due to winds, we can extend the control authority definition in the y direction as follows:

$$Y \text{ acceler. Control Effort} : \left( \frac{\delta_{Y_{FCS}}}{\delta_{+Y \max_{FCS}}} \right) = \left| \frac{C_{Y\beta} U_{Y \max} \beta_{\max}}{C_{Y\delta Y}} \right| < 0.5 \quad (3.26b)$$

Where:  $U_{Pmax}$ ,  $U_{Rmax}$  and  $U_{Ymax}$  are the largest elements in the column vectors  $\underline{U}_P$ ,  $\underline{U}_R$  and  $\underline{U}_Y$  in the normalized mixing logic equation 3.19. When the dispersion is in the opposite direction  $-\beta_{max}$  the control authorities are affected by the availabilities in the opposite direction:  $U_{Pmin}$ ,  $U_{Rmin}$ ,  $U_{Ymin}$ .

$$Roll \text{ Control Effort} : \left( \frac{\delta_{P_{FCS}}}{\delta_{-P \max_{FCS}}} \right) = \left| \frac{(L_{\beta} N_{\delta R} - N_{\beta} L_{\delta R}) U_{P \min} \beta_{\max}}{(L_{\delta R} N_{\delta P} - N_{\delta R} L_{\delta P})} \right| < 0.5$$

$$Yaw \text{ Control Effort} : \left( \frac{\delta_{R_{FCS}}}{\delta_{-R \max_{FCS}}} \right) = \left| \frac{(N_{\beta} L_{\delta P} - L_{\beta} N_{\delta P}) U_{R \min} \beta_{\max}}{(L_{\delta R} N_{\delta P} - N_{\delta R} L_{\delta P})} \right| < 0.5$$

$$Y \text{ acceler. Control Effort} : \left( \frac{\delta_{Y_{FCS}}}{\delta_{-Y \max_{FCS}}} \right) = \left| \frac{C_{Y\beta} U_{Y \min} \beta_{\max}}{C_{Y\delta Y}} \right| < 0.5$$

#### **Lateral Control Authority against Velocity Variations: $\pm v_{max}$**

Similarly, when the vehicle is flying with a steady sideslip  $\beta_0$  due to  $Y_{CG}$  offset or thrust mismatch, the roll and yaw control deflections from trim produced by a constant airspeed variation  $v_{ss}$  relative to  $V_0$  are:

$$\delta_{P_{FCS}} = \frac{(L_{\delta V} N_{\delta R} - N_{\delta V} L_{\delta R})}{(L_{\delta R} N_{\delta P} - N_{\delta R} L_{\delta P})} v_{ss} ; \quad \delta_{R_{FCS}} = \frac{(N_{\delta V} L_{\delta P} - L_{\delta V} N_{\delta P})}{(L_{\delta R} N_{\delta P} - N_{\delta R} L_{\delta P})} v_{ss}$$

The control authority of the roll and yaw effectors system against maximum velocity variations  $\pm v_{max}$  from trim airspeed  $V_0$  can be evaluated by control effort ratios ( $\delta_{PFCS}/\delta_{PMax}$ ) and ( $\delta_{RFCS}/\delta_{RMax}$ ) required to trim the roll and yaw moments against  $v_{max}$  and naturally it should be less than 0.5.

$$Roll \text{ Control Effort} : \left( \frac{\delta_{P_{FCS}}}{\delta_{+P \max_{FCS}}} \right) = \left| \frac{(L_{\delta V} N_{\delta R} - N_{\delta V} L_{\delta R}) U_{P \max} v_{\max}}{(L_{\delta R} N_{\delta P} - N_{\delta R} L_{\delta P})} \right| < 0.5$$

$$Yaw \text{ Control Effort} : \left( \frac{\delta_{R_{FCS}}}{\delta_{+R \max_{FCS}}} \right) = \left| \frac{(N_{\delta V} L_{\delta P} - L_{\delta V} N_{\delta P}) U_{R \max} v_{\max}}{(L_{\delta R} N_{\delta P} - N_{\delta R} L_{\delta P})} \right| < 0.5$$

When the vehicle has side-force control capability by means of RCS thrust variation, in order to maintain steady lateral flight, the side-force produced due to maximum axial control  $\delta_{Y_{\max}}$  should be at least twice as big as the side-force generated by the expected variation in velocity  $\pm v_{\max}$ .

$$|C_{Y\delta Y} \delta_{Y_{\max_{FCS}}}| > 2|C_{YV} v_{\max}|$$

$$Y \text{ acceler. Control Effort: } \left( \frac{\delta_{Y_{FCS}}}{\delta_{+Y_{\max_{FCS}}}} \right) = \left| \frac{C_{Y\delta V} U_{Y_{\max}} v_{\max}}{C_{Y\delta Y}} \right| < 0.5$$

The controllability must also be analyzed when the airspeed variation along  $V_0$  is in the opposite direction  $-v_{\max}$ . The control authorities are determined by the effector availabilities in the opposite directions:  $\{U_{P_{\min}}, U_{R_{\min}}, U_{Y_{\min}}\}$ .

$$Roll \text{ Control Effort: } \left( \frac{\delta_{P_{FCS}}}{\delta_{-P_{\max_{FCS}}}} \right) = \left| \frac{(L_{\delta V} N_{\delta R} - N_{\delta V} L_{\delta R}) U_{P_{\min}} v_{\max}}{(L_{\delta R} N_{\delta P} - N_{\delta R} L_{\delta P})} \right| < 0.5$$

$$Yaw \text{ Control Effort: } \left( \frac{\delta_{R_{FCS}}}{\delta_{-R_{\max_{FCS}}}} \right) = \left| \frac{(N_{\delta V} L_{\delta P} - L_{\delta V} N_{\delta P}) U_{R_{\min}} v_{\max}}{(L_{\delta R} N_{\delta P} - N_{\delta R} L_{\delta P})} \right| < 0.5$$

$$Y \text{ acceler. Control Effort: } \left( \frac{\delta_{Y_{FCS}}}{\delta_{-Y_{\max_{FCS}}}} \right) = \left| \frac{C_{Y\delta V} U_{Y_{\min}} v_{\max}}{C_{Y\delta Y}} \right| < 0.5$$

Where the partials of the lateral aerodynamic coefficients per velocity variations are:

$$C_{l\delta V} = \frac{2C_{l0}}{V_0}; \quad C_{n\delta V} = \frac{2C_{n0}}{V_0}; \quad C_{Y\delta V} = \frac{2C_{Y0}}{V_0}$$

### Normal and Lateral Loads

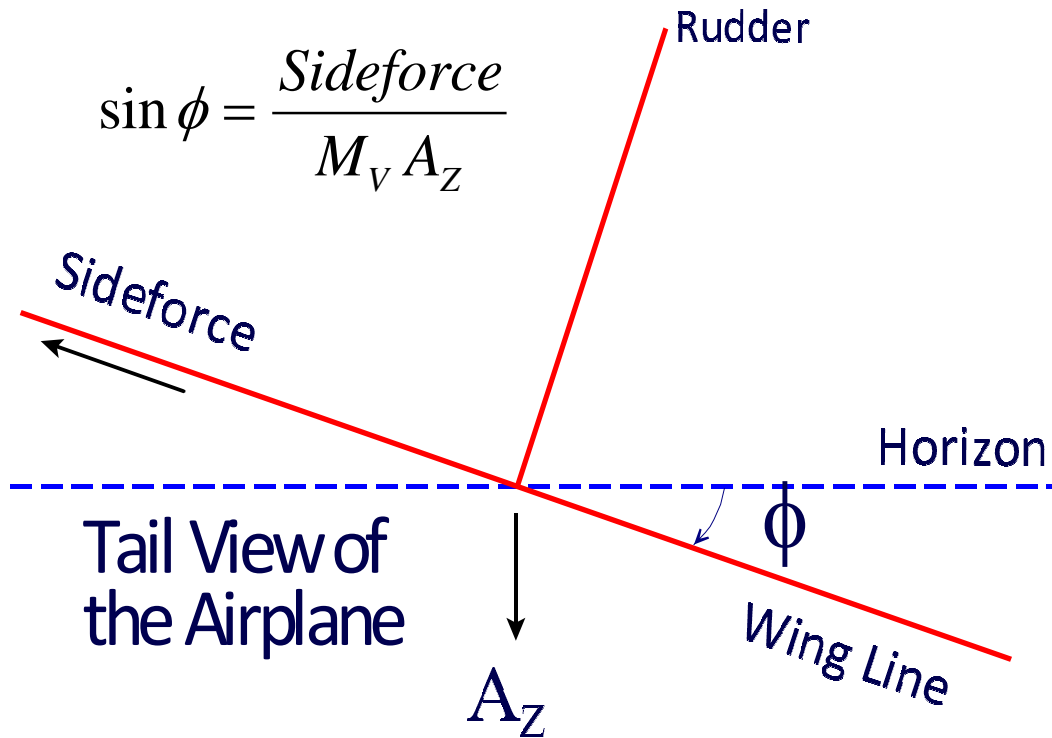
The normal and lateral load parameters ( $Q\alpha$  and  $Q\beta$ ) are used for analyzing the flight vehicle capability to endure structural loads produced by the angles of attack and sideslip. These loads increase during periods of high dynamic pressure and for this reason some vehicles have a load-relief system that reduces the angles of attack and sideslip by steering the vehicle towards the airflow and sometimes contrary to guidance commands. The flight vehicle normal and lateral loads are measured by the product of dynamic pressure and alpha or beta and they should be limited to between 3,000 and 4,000 (lb-deg/ft<sup>2</sup>) or (PSF-deg).

$$Q_{\alpha} = \bar{Q}\alpha; \quad Q_{\beta} = \bar{Q}\beta$$

### Bank Angle and Side-Force during a Steady Sideslip

Another set of parameters which are important to calculate when the aircraft is under constant sideslip, is the side-force and the bank angle. This is particularly important near landing. The aerodynamic side-force due to a steady cross-wind from the starboard side is balanced with a gravity component by banking the aircraft at a small angle  $\phi$  towards the wind, in order to maintain a zero force along the body y-axis, as shown in the Figure below. After solving equations 3.25 for the roll and yaw controls  $\delta_{PFCS}$  and  $\delta_{RFCS}$  which are needed for maintaining a steady sideslip, let's say  $\beta_{ss} = 5$  (deg), from equation 3.27 we calculate the aerodynamic side-force and then the bank angle  $\phi$  required to balance it.

Typically, near landing the bank angle  $\phi$  should be less than 5 degrees. In level flight and near landing the normal acceleration  $A_z$  is approximately 1-g. The partials  $F_{Y\delta R}$  and  $F_{Y\delta P}$  are the forces along the y axis per yaw and roll FCS demands and they are calculated from the partials demands matrix  $C_T$  in equation 3.10. In general, it is sufficient to demonstrate that no more than 75% of the roll and yaw control authority be devoted to maintaining a steady sideslip. Typically the bank angle due to cross-wind should not exceed  $5^\circ$  during landing.



$$\sin \phi = \frac{\text{Sideforce}}{M_V A_Z}$$

$$\text{Side Force} = \bar{Q} S_{ref} C_{Y\beta} \beta_{ss} + F_{Y\delta R} \delta_{RFCS} + F_{Y\delta P} \delta_{PFCS}$$

$$\text{Bank Angle: } \sin \phi = \frac{\text{Side Force}}{M_V A_Z \cos \gamma} \quad (3.27)$$

## Engine-Out or Y<sub>CG</sub> Offset Situations

The lateral control authority analysis can be extended to include asymmetric situations caused due to uneven aerodynamic forces, thrust mismatch due to engine or actuator failures, and Ycg offset as a result of an unbalanced payload. The roll and yaw effectors must have sufficient control authority to counteract the forces and moments generated due to the absence of lateral symmetry. This requirement is more demanding when operating at very low speeds. To maintain steady straight flight, the roll and yaw effectors must be able to offset the asymmetric moments and forces or an asymmetric CG, and to produce zero side-force and zero rolling and yawing moments. The following three equations must be solved simultaneously.

$$\begin{aligned} \bar{Q} S_{ref} C_{Y\beta} \beta + F_{Y\delta R} \delta_{R_{FCS}} + F_{Y\delta P} \delta_{P_{FCS}} + M_V A_Z \cos \gamma \sin \phi + \Delta F_Y &= 0 \\ L_{\beta} \beta + L_{\delta R} \delta_{R_{FCS}} + L_{\delta P} \delta_{P_{FCS}} + \Delta L &= 0 \\ N_{\beta} \beta + N_{\delta R} \delta_{R_{FCS}} + N_{\delta P} \delta_{P_{FCS}} + \Delta N &= 0 \end{aligned} \quad (3.27a)$$

Where:  $\Delta F_Y$ , is the sideforce, and  $\Delta L$  and  $\Delta N$ , are the roll and yaw moments generated due to the thrust mismatch and the Ycg offset. The Ycg offset will only produce moments and no side-force. When the vehicle is trimmed and  $\underline{\delta}_{Tr}$  is the vector consisting of the controls, then equation 3.27a becomes.

$$\begin{aligned} \bar{Q} S_{ref} C_{Y\beta} \beta + F_{Y\delta} \underline{\delta}_{Tr} + M_V A_Z \cos \gamma \sin \phi + \Delta F_Y &= 0 \\ L_{\beta} \beta + L_{\delta} \underline{\delta}_{Tr} + \Delta L &= 0 \\ N_{\beta} \beta + N_{\delta} \underline{\delta}_{Tr} + \Delta N &= 0 \end{aligned} \quad (3.27b)$$

## Lateral Control Departure Parameter (LCDP)

At high angles of attack the effectiveness of the control surfaces in roll is sometimes reduced or lost, plus at high alpha the roll effectors may produce significant adverse yaw that may lead to "Roll-Reversal". As a result, the aircraft rolls in the direction opposite to the roll command. The LCDP ratio is a good indicator of the roll axis dynamic controllability and it is defined in equation 3.28, which is the ratio of the lateral departure parameter ( $\omega_0^2$ ) divided by the Dutch-roll frequency ( $\omega_D^2$ ). This parameter is a good indicator of roll dynamic controllability and the flight vehicle susceptibility to departure during high angle of attack operation. It is usually positive, but it changes sign as a function of flight conditions and mainly the angle of attack. When it is different from one it indicates that there is dynamic coupling between the roll and yaw axes. Values greater than one, are good for yaw control, but when they are too high, it has a tendency to induce beta oscillations. When the LCDP ratio is near zero the aircraft response to roll commands is sluggish. When it becomes negative it causes reversal in the roll (aileron) control which can be disastrous if unaccounted. The flight control system should, therefore, be able to detect this situation and take an appropriate action when it happens.

$$LCDP \text{ Ratio} = \left( \frac{\omega_0^2}{\omega_D^2} \right) = \frac{N_\beta - L_\beta \frac{N_{\delta P}}{L_{\delta P}}}{N_\beta - L_\beta \frac{I_{ZZ}}{I_{XX}} \tan \alpha_0} \quad (3.28)$$

For a re-entry vehicle, such as the Space Shuttle, entering the atmosphere at high angles of attack there are periods where directional stability is poor because the vertical stabilizer is ineffective since the wake from the wings is preventing it from operating in a clean air flow. During this period the rudder flight control gain is phased-out and the aileron is used for roll and directional control and often in combination with yaw RCS jets. The vehicle must, therefore, have an acceptable LCDP ratio in order to be stabilizable with the ailerons. When the angle of attack is reduced the rudder becomes more effective to provide directional stability and the gain in the rudder control loop is increased accordingly. At high angles of attack the LCDP ratio may be negative which implies that the roll gain must be reversed. This is not a problem, however, as long as the LCDP is not too close to zero which implies uncertain and sluggish roll controllability. As the angle of attack decreases further there is a period during which the LCDP ratio is transitioning from negative to positive, and its magnitude becomes very small before it changes sign to positive. During this period the aileron is ineffective and unreliable for lateral control. The yaw control may also be insufficient, and the vehicle has to rely fully on the RCS jets.

The transfer function in equation 3.29 approximates the roll acceleration due to a roll FCS command. The coefficients  $N_\beta$  and  $L_\beta$  represent the vehicle yaw and roll moment partials per sideslip angle sideslip  $\beta$ . The partials  $N_{\delta p}$  and  $L_{\delta p}$  represent the yaw and roll vehicle moments due to variations in roll flight control demand  $\delta_{pFCS}$ , and they are obtained from the partials demands matrix  $C_T$ . Notice that the Dutch-Roll frequency ( $\omega_D^2$ ) is only a function of the vehicle aerodynamics and inertias, but ( $\omega_\phi^2$ ) also depends on the effector partials. This makes the LCDP ratio to depend on the effector characteristics, and also on the mixing logic matrix, which is software.

$$\frac{\dot{p}(s)}{\delta_{pFCS}(s)} = \frac{L_{\delta p}}{I_{XX}} \left\{ \frac{s^2 + \omega_\phi^2}{s^2 + \omega_D^2} \right\} \quad \text{where}$$

$$\omega_\phi^2 = \frac{\cos \alpha_o}{I_{ZZ} L_{\delta p}} [N_\beta L_{\delta p} - L_\beta N_{\delta p}] \quad \text{and} \quad \omega_D^2 = \left[ \frac{N_\beta \cos \alpha_o}{I_{ZZ}} - \frac{L_\beta \sin \alpha_o}{I_{XX}} \right] \quad (3.29)$$

$$N_\beta = \bar{Q} S_{ref} b C_{n\beta} \quad L_\beta = \bar{Q} S_{ref} b C_{l\beta}$$

$$N_{\delta p} = \frac{\partial N}{\partial \delta_{pFCS}} \quad L_{\delta p} = \frac{\partial L_x}{\partial \delta_{pFCS}}$$

Notice that the roll transfer function equation 3.29 has two terms: a gain term that includes the roll effector partial  $L_{\delta p}$ , and a dynamic term consisting of pairs of poles and zeros. The dynamic term in parenthesis is a function of the aerodynamic moments. It introduces an oscillatory or divergent transient in the transfer function response. When the aerodynamics is weak the vehicle must be controlled with TVC or RCS jets, and the dynamic term in the parenthesis becomes small in comparison with the gain term, and in this case the transfer function simplifies to a gain.

$$\frac{\dot{p}(s)}{\delta_{P_{FCS}}(s)} = \frac{L_{\delta p}}{I_{XX}}$$

The LCDP to Dutch-roll frequency ratio is important for analyzing the condition when the  $L_{\delta p}$  partial is weak, and the dynamic term in parenthesis dominates the transfer function in comparison with the gain term. In this case you would like to have directional stability ( $\omega_D^2 > 0$ ), and the LCDP ratio sufficiently far away from zero, otherwise it will not respond to roll commands. Pole and Zero cancellations occur when LCDP=1. In this situation the vehicle response to a roll command becomes ideal, producing a perfectly coordinated turn with zero sideslip angle  $\beta$ . An acceptable range for the LCDP magnitude is:  $15 > |\text{LCDP}| > 0.2$ . This range provides a satisfactory compromise between performance and robustness against aerodynamic uncertainties. Negative LCDP ratios are also acceptable as long as they are not near zero. They cause, however, reversal in roll control gain because it changes the sign of the transfer function 3.29 and the roll control system must be able to predict the reversal in order to compensate it.

When the magnitude of the LCDP ratio becomes small or negative at high angles of attack, the mixing matrix can be adjusted to include contributions from the yaw effectors. This may improve the value of the LCDP at high alphas, sometimes at the expense of control authority. The weakness in the LCDP ratio, however, can always be improved through the use of propulsion that will strengthen the  $L_{\delta p}$  gain in the transfer-function. In order for the roll control loop to be reliable and robust against instability due to aerodynamic uncertainties, the magnitude of the LCDP ratio should be sufficiently greater than zero (either positive or negative), especially, during periods of poor yaw controllability. Reaction control jets are often required to control the vehicle in roll and yaw during LCDP transitioning. It is not sufficient to control only the roll axis, but both roll and yaw are commanded because the vehicle is maneuvering about the velocity vector at high angles of attack. This type of maneuvering minimizes sideslip and lateral loads. During the transitioning period the RCS torques must be properly sized in order to be able to overcome the uncertain aerodynamic moments and should be able to provide at least 1.5 (deg/sec<sup>2</sup>) angular acceleration in roll and yaw.

Figure 3.3 is a plot of  $(\omega_0^2)$  in the vertical axis, against  $(\omega_D^2)$  in the horizontal axis. It shows the acceptable regions of the LCDP ratio. At high angles of attack a Shuttle type of reentry vehicle operates in the regions of negative  $(\omega_0^2)$ , where the roll control gain is reversed. As the angle of attack decreases the operation shifts in the positive  $(\omega_0^2)$  region. The aileron and in general roll control is unreliable when the LCDP ratio is small and near the horizontal shaded region of Figure 3.3. It should not be very large either because it causes large sideslip transients. The region where  $(\omega_D^2 < 0)$  is statically unstable and unreliable when operating very close to the vertical axis. It is not recommended to operate there without powerful RCS.

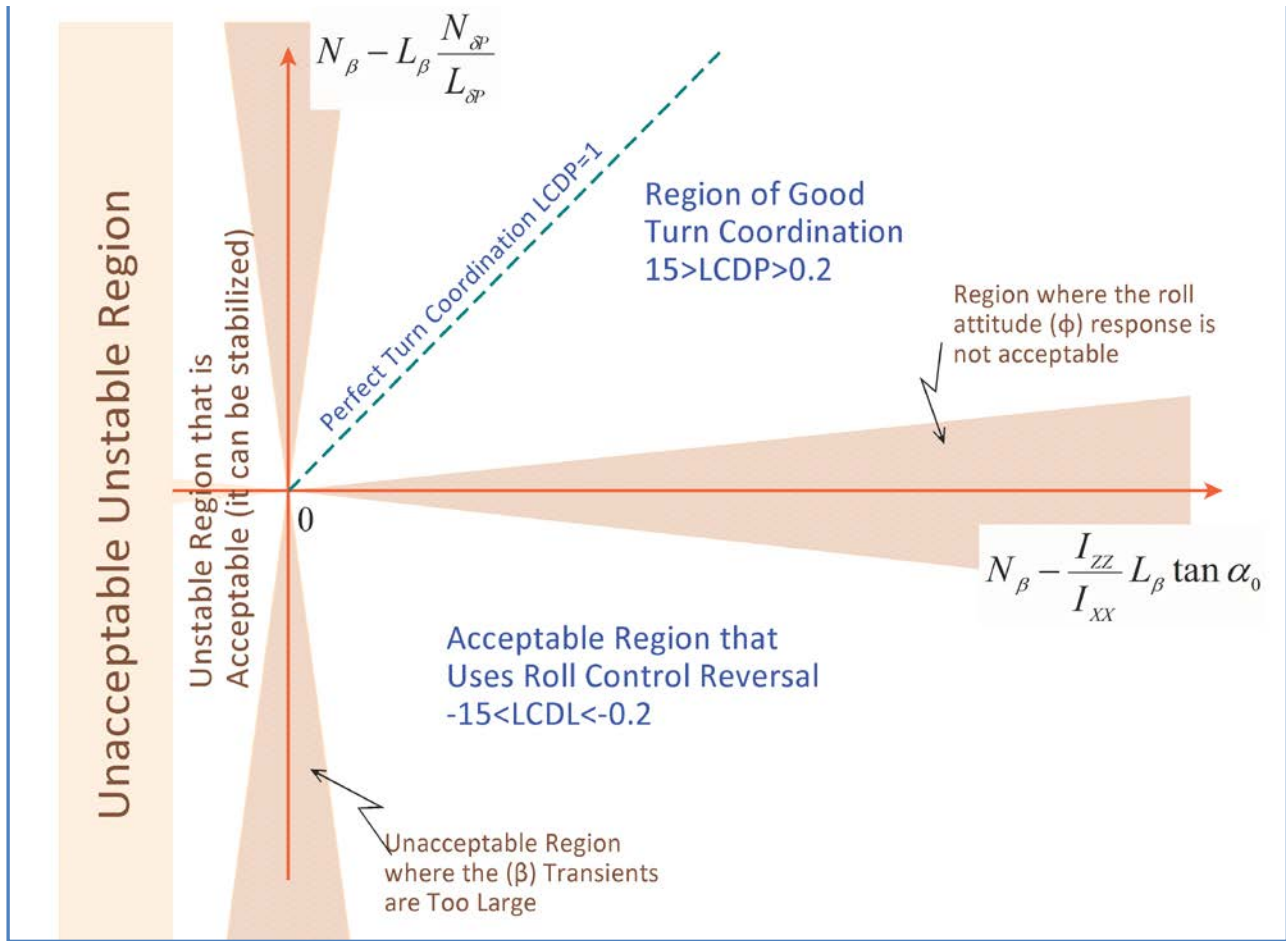


**Figure (3.3) Plot of  $(\omega_0^2)$  versus  $(\omega_D^2)$ , Showing the Acceptable Regions of the LCDP Ratio**

The dashed line shows the ideal value of the LCDP ratio, which is 1. It produces a perfectly coordinated turn in response to a roll command with zero angle of sideslip  $\beta$ , and it happens when the following equation 3.30 is satisfied.

$$\frac{N_{\delta P}}{L_{\delta P}} = \frac{I_{ZZ}}{I_{XX}} \tan \alpha \quad (3.30)$$

In general, it is desirable to have the value of LCDP ratio as close to 1.0 as possible and to avoid sign reversals but this is impossible to achieve in most cases because the vehicle parameters change significantly with flight conditions. With RCS, however, it is possible to operate in the marginally stable and the somewhat unstable regions and also in the region where the LCDP ratio is small. An acceptable range of positive LCDP ratio is:  $15 > |LCDP| > 0.2$ . This range of values provides sufficient performance and robustness against aerodynamic uncertainties.



### Examples Showing the Effects of LCDP Sign Reversal on Stability

The effects of the LCDP and  $C_n\beta$ -dynamic variations on lateral stability and on the control feedback gains are better illustrated with an example. Let us consider a lateral vehicle model that is controlled by aileron and rudder inputs and its states consisting of: roll and yaw rates ( $p, r$ ), roll attitude ( $\phi$ ), plus angle of sideslip ( $\beta$ ). This system is controlled by a (2x4) state-feedback matrix (KSpr1) and the roll angle is controlled by a command ( $\phi_{cmd}$ ). This system is open-loop statically stable with a Dutch-roll resonance of 2 (rad/sec),  $C_{nb}$ -dynamic $>0$ , and it has a negative LCDP ratio,  $\omega_0^2/\omega_D^2 = -0.334$ . It corresponds to the region in Figure (3.3) where ( $\omega_0^2 < 0$ ; reverse roll) and ( $\omega_D^2 > 0$ ; statically stable). This system is shown in Figure (3.3.1) responding to a  $\phi_{cmd}=1$  (rad). The state-feedback matrix is also included in the figure.

A parameter of this system was modified which causes the LCDP to change sign. Figure (3.3.2) is almost an identical system with a different  $C_n \delta_{ail}$ . The yawing moment due to aileron was changed from negative to positive value. The system is still stable with the same Dutch-roll resonance but the LCDP ratio is now +0.302, almost the opposite of the previous system. It corresponds to the region in Figure (3.3) where ( $\omega_0^2 > 0$ ) and ( $\omega_D^2 > 0$ ; statically stable). This system is no longer stabilizable with the previous state-feedback matrix and a new feedback (KSpr2) was designed in order to stabilize it and respond to a  $\phi_{cmd}=1$  (rad) with a similar performance. Notice how the signs of most of the elements in this new state-feedback matrix are reversed.

This example, therefore, demonstrates that an unexpected reversal in the LCDP sign can have destabilizing effect on the vehicle, even though the vehicle was identically stable in both cases. The exact time of sign reversal in the parameter is not known due to the uncertainties in the aerodynamics so there is a transitioning period where we cannot rely on the aileron for control. A solution when the LCDP ratio is small and it transitions between positive and negative is to introduce some rudder control in roll which can increase the magnitude of the LCDP, either positive or negative, but not less than 0.02. An even better solution is to use RCS jets for roll control during this type of transitioning period.

LCDP sign reversal may require reversal in the control law gains

```

a =      p      r      beta
p -0.02415  0.01042 -6.535
r  0.001779 -0.009517 -0.269
bet 0.6088  -0.7934  0.0001326

b =      d_ail  d_rud
p  0.9451    2.748
r -0.1828   -0.03653
bet 7.875e-005 -9.45e-005

c =      p      r      beta
p  1  0  0
r  0  1  0
bet 0  0  1

d =      d_ail  d_rud
p  0  0
r  0  0
bet 0  0
    
```

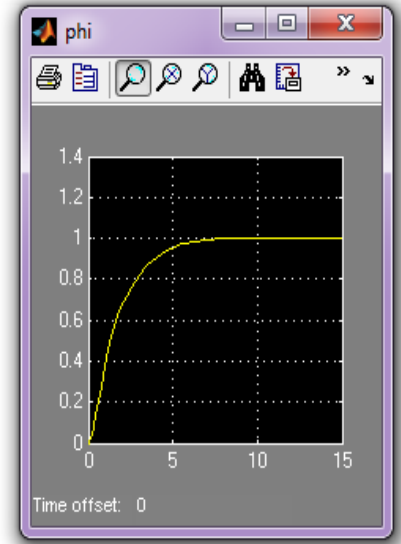
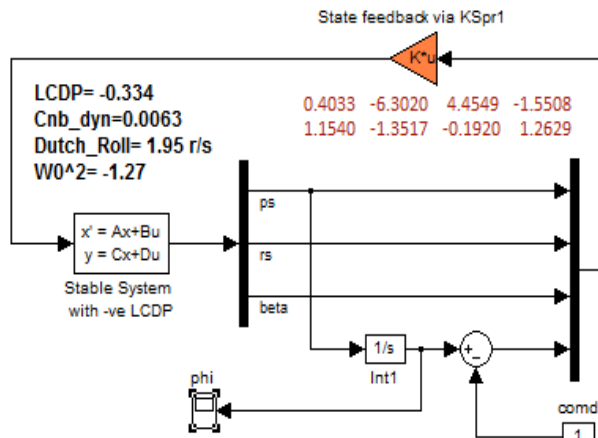


Figure 3.3.1 Closed-Loop System with Negative LCDP Ratio and Cnb Dynamic>0

LCDP sign reversal may require reversal in the control law gains

```

a =      p      r      beta
p -0.02415  0.01042 -6.535
r  0.001779 -0.009517 -0.269
bet 0.6088  -0.7934  0.0001326

b =      d_ail  d_rud
p  0.9451    2.748
r  0.250    -0.03653
bet 7.875e-005 -9.45e-005

c =      p      r      beta
p  1  0  0
r  0  1  0
bet 0  0  1

d =      d_ail  d_rud
p  0  0
r  0  0
bet 0  0
    
```

Change in Cn\_daileron causes reversal in LCDP and control gain reversal

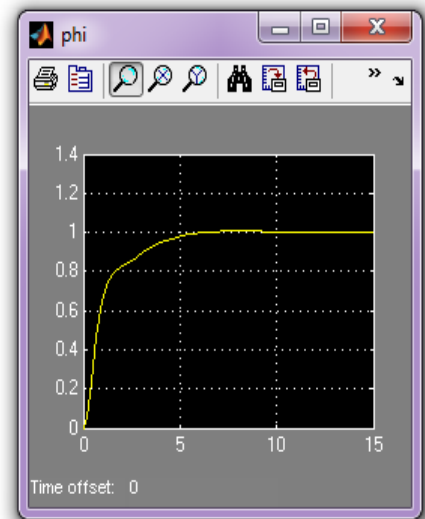
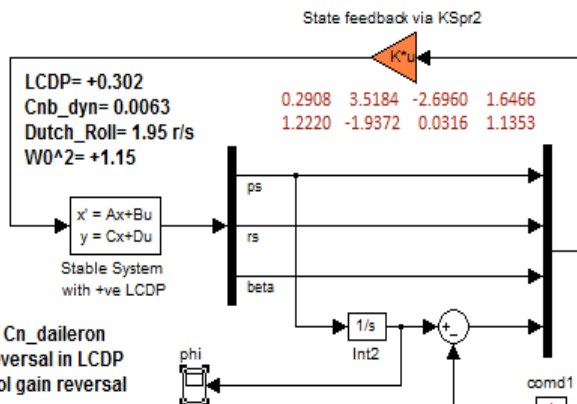


Figure 3.3.2 Closed-Loop System with Positive LCDP Ratio and Cnb-Dynamic>0

LCDP ratio reversal can also be caused by a change in the sign of  $Cn\beta$ -dynamic. This is when the vehicle transitions let's say from a statically stable to a statically unstable region where  $Cn\beta$ -dynamic  $< 0$ . This corresponds to the statically unstable region in Figure (3.3) where  $(\omega_D^2 < 0)$ . This change in sign also requires a change in the state-feedback control law in order to avoid a lateral instability, as shown in Figure (3.3.3). In this example, which is similar to Figure (3.3.1), the sign of  $Cn\beta$ -dynamic was changed to negative by a modification in the aero coefficients  $Cn\beta$  and  $Cl\beta$ . The new state-feedback control law ( $KSpr3$ ) that stabilizes the modified system and enables it to respond to a  $\phi_{cmd}=1$  (rad) is also significantly different from the original state-feedback matrix ( $KSpr1$ ). Notice how some of the rudder gains are now reversed. Notice also how the  $(\phi)$  response is not monotonic as in the previous two cases but it first responds towards the opposite direction and then it reverses. This is also an unreliable situation and one cannot rely on the aero-surfaces for lateral control during this type of transitioning period and, therefore, RCS is the only reliable solution during periods of uncertainty in the LCDP.

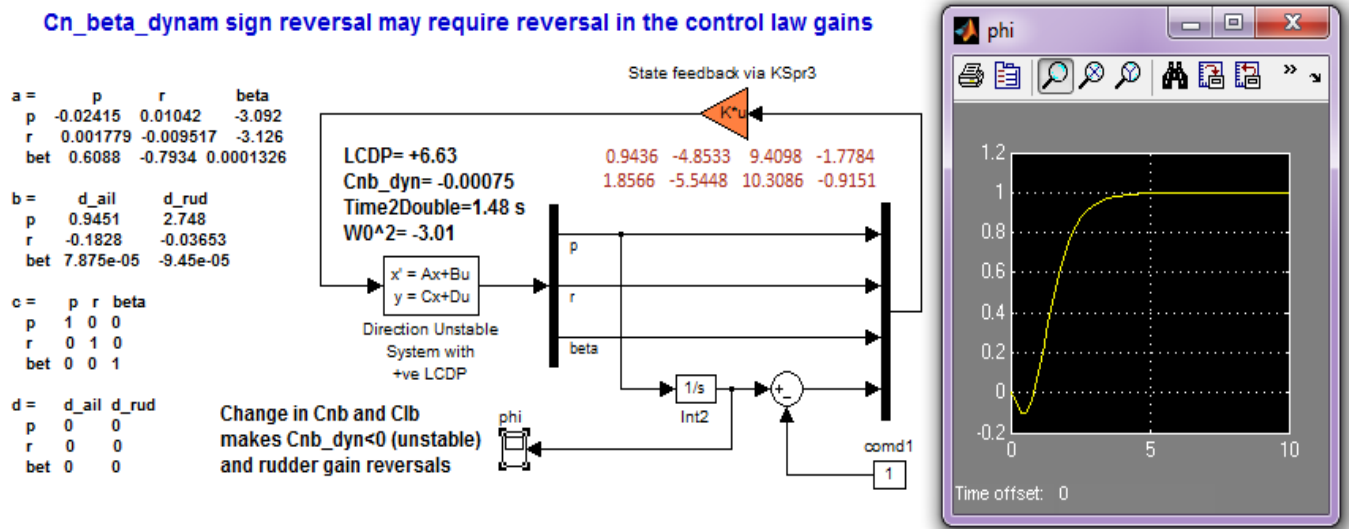


Figure 3.3.3 Closed-Loop System with Positive LCDP Ratio and  $Cn\beta$ -Dynamic  $< 0$  (unstable)

## Effector Capability to Provide Rotational and Translational Accelerations

The capability of the control effectors system to provide rotational acceleration in roll, pitch and yaw is also measured in terms of the largest rotational accelerations that can be attained in the corresponding direction without saturating any effectors. From the moment equations we can calculate the following accelerations, as a function of the rotational acceleration demands from the FCS:  $\delta_{PFCS}$ ,  $\delta_{QFCS}$ ,  $\delta_{RFCS}$ .

$$\dot{p} = \frac{L_{\delta P}}{I_{XX}} \delta_{PFCS} \quad \dot{q} = \frac{M_{\delta Q}}{I_{YY}} \delta_{QFCS} \quad \dot{r} = \frac{N_{\delta R}}{I_{ZZ}} \delta_{RFCS} \quad (3.31)$$

The rotational accelerations in roll, pitch, or yaw are maximized when the demands in the corresponding directions are also maximized, and this happens when the deflection of the most active effector (i) reaches saturation limit  $\delta_{iMax}$ . By substituting equation 3.21 for the maximum pitch demand we obtain the maximum pitch acceleration in (rad/sec<sup>2</sup>) from equation 3.33, similarly we can obtain the maximum accelerations in roll and yaw.

$$\dot{p}_{Max} = \frac{L_{\delta P}}{I_{XX} U_{P Max}} \quad \dot{q}_{Max} = \frac{M_{\delta Q}}{I_{YY} U_{Q Max}} \quad \dot{r}_{Max} = \frac{N_{\delta R}}{I_{ZZ} U_{R Max}} \quad (3.33)$$

Where:  $U_{Qmax}$  is the element that has the largest magnitude in the column vector  $\underline{U}_Q$  in the normalized Mixing Logic matrix equation 3.19 that corresponds to the pitch demand  $\delta_{QFCS}$ . The dimension of  $\underline{U}_Q$  is equal to the number of control effectors, similarly for  $U_{Pmax}$  and  $U_{Rmax}$ .

Similarly, the capability of the effectors system to perform translations along the x, y, and z body axes can be measured in terms of the largest translational accelerations that can be produced along those directions, before the effectors reach saturation limits. The acceleration along a linear direction is maximized when the deflection of the most active effector (i) reaches saturation limit  $\delta_{iMax}$ . The maximum linear accelerations in (feet/sec<sup>2</sup>) along x, y, and z are:

$$\dot{u}_{Max} = \frac{F_{X\delta X}}{M_V U_{X Max}} \quad \dot{v}_{Max} = \frac{F_{Y\delta Y}}{M_V U_{Y Max}} \quad \dot{w}_{Max} = \frac{F_{Z\delta Z}}{M_V U_{Z Max}} \quad (3.34)$$

Where:  $U_{Xmax}$  is the element that has the largest magnitude in the column vector ( $\underline{U}_X$ ) in the normalized mixing logic matrix equation 3.19 that corresponds to the axial acceleration FCS demand  $\delta_{XFCS}$ , similarly for  $U_{Ymax}$  and  $U_{Zmax}$ .

### Steady Pull-Up Maneuverability

Another important parameter which is applicable mainly to aircraft is the amount of pitch FCS command and the angle of attack required to hold the vehicle in a steady pull-up maneuver with a load factor  $n_z$ . When the vehicle performs a circular pull-up maneuver at constant speed  $V$ , see Figure 3.4, at the point where the flight path tangent is horizontal, the normal force is vertically upward, and the increment in Lift, which is  $\Delta L = L - W = (n_z - 1)W$ . The normal acceleration, therefore, is  $(n_z - 1)g$ , and the vehicle angular pitch rate is:

$$q = \frac{(n_z - 1)g}{V} \quad (3.35)$$

The increment in lift above what is required for 1g level flight is  $\Delta L = (n_z - 1)W$  or in coefficient form it is:

$$\Delta C_L = \frac{\Delta L}{\bar{q}S} = \frac{(n_z - 1)W}{\bar{q}S} \quad (3.36)$$

The increment in lift and moment  $\{\Delta C_L \& \Delta C_m\}$  during the pull-up maneuver generated by increments in pitch demand and in angle of attack from level trim, are reduced to two equations with two unknowns: change in angle of attack ( $\Delta\alpha$ ), and change in pitch control ( $\Delta\delta_{QFCS}$ ).

$$\begin{aligned} \Delta C_L &= C_{L_\alpha} \Delta\alpha + C_{L_q} \hat{q} + C_{L_{\delta Q}} \Delta\delta_{QFCS} \\ \Delta C_m &= C_{m_\alpha} \Delta\alpha + C_{m_q} \hat{q} + C_{m_{\delta Q}} \Delta\delta_{QFCS} = 0 \quad ; \text{ Where: } \hat{q} = \frac{(n_z - 1)cg}{2V^2} \end{aligned} \quad (3.37)$$

This is reduced to two equations with two unknowns: change in alpha ( $\Delta\alpha$ ) and change in pitch control ( $\Delta\delta_{QFCS}$ ) that must be solved to obtain the required load factor  $n_z$ .

$$\begin{aligned} C_{L_\alpha} \Delta\alpha + C_{L_{\delta Q}} \Delta\delta_{QFCS} &= (n_z - 1) \left[ \frac{W}{\bar{q}S} - C_{L_q} \frac{g\bar{c}}{2V^2} \right] \\ C_{m_\alpha} \Delta\alpha + C_{m_{\delta Q}} \Delta\delta_{QFCS} &= -(n_z - 1) C_{m_q} \frac{g\bar{c}}{2V^2} \end{aligned} \quad (3.38)$$

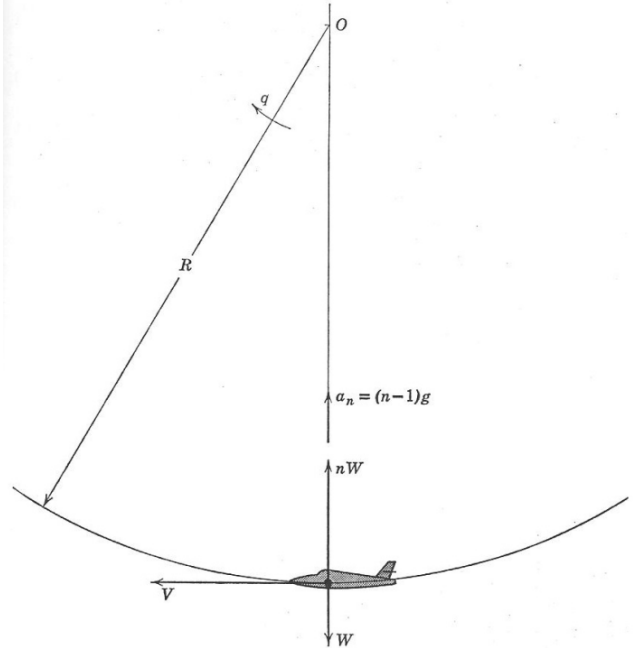


Figure 3.4 Steady Pull-Up Maneuver

Notice that if the required load factor is one, which is equivalent to a steady level flight, the right side of the lift increment equation 3.38 becomes zero, and the increments in alpha and pitch control  $\delta_{QFCS}$  must also be zero. From equations 3.38 we can solve for the change in pitch control per g, and the change in angle of attack per g.

$$\left[ \frac{\Delta \delta_{QFCS}}{n_z - 1} \right] = -\frac{1}{D} \left\{ \left( C_{m_q} \frac{g\bar{c}}{2V^2} \right) C_{L\alpha} + \left( \frac{W}{\bar{q}S} - C_{L_q} \frac{g\bar{c}}{2V^2} \right) C_{m\alpha} \right\} \quad (3.39a)$$

$$\left[ \frac{\Delta \alpha}{n_z - 1} \right] = \frac{1}{D} \left\{ \left( C_{m_q} \frac{g\bar{c}}{2V^2} \right) C_{L\delta Q} + \left( \frac{W}{\bar{q}S} - C_{L_q} \frac{g\bar{c}}{2V^2} \right) C_{m\delta Q} \right\} \quad (3.39b)$$

Where:  $D = C_{L\alpha} C_{m\delta Q} - C_{m\alpha} C_{L\delta Q}$  and:  $\frac{W}{\bar{q}S} = C_L$  which is the lift coefficient at level flight

The issue here is to evaluate vehicle maneuverability by analyzing if it has enough control authority to achieve its maximum loading specifications during a pull-up maneuver. Another way of solving these equations is to calculate what would the increase in the pitch FCS command,  $\Delta\delta_{QFCS}$  be, in order to raise the load factor ( $n_z-1$ ) to its maximum specification limit. An even better measure of steady Pull-Up maneuverability is to calculate the control effort, which is the ratio ( $\Delta\delta_{QFCS} / \Delta\delta_{QFCS \text{ Max}}$ ), required to reach the expected load factor, where  $\Delta\delta_{QFCS \text{ Max}}$  is the max FCS demand before it saturates the effectors. From equation 3.21 the maximum pitch command increment is:

$$\Delta\delta_{QFCS \text{ Max}} = \frac{1}{U_{Q \text{ Max}}} \quad (3.40)$$

Assuming a constant speed V and pitch rate q and that the angle of attack is small, from equation 3.39a we can calculate the controllability as the ratio of increment to achieve maximum load divided by the maximum control available before effector saturation. This ratio should be less than 1, but we should be aiming towards a smaller number ( $f=0.7$ ) because the aircraft is already using some pitch control to trim at level flight.

$$\left[ \frac{\Delta \delta_{QFCS}}{\Delta \delta_{QFCS \text{ Max}}} \right] = (n_z - 1) \frac{U_{Q \text{ Max}}}{D} \left\{ \left( C_{m_q} \frac{g\bar{c}}{2V^2} \right) C_{Z\alpha} + \left( C_{Z0} - C_{Z_q} \frac{g\bar{c}}{2V^2} \right) C_{m\alpha} \right\} < f \quad (3.41)$$

From equation 3.39b we calculate the change in angle of attack required to reach maximum load.

$$\left[ \frac{\Delta \alpha}{n_z - 1} \right] = -\frac{1}{D} \left\{ \left( C_{m_q} \frac{g\bar{c}}{2V^2} \right) C_{Z\delta Q} + \left( C_{Z0} - C_{Z_q} \frac{g\bar{c}}{2V^2} \right) C_{m\delta Q} \right\} \quad (3.42)$$

Where:  $D = -C_{Z\alpha} C_{m\delta Q} + C_{m\alpha} C_{Z\delta Q}$

Where:  $C_{m\delta Q} = M_{\delta Q} / \bar{q}S\bar{c}$ , is the pitch control moment derivative, and the normal control force derivative is  $C_{Z\delta Q} = Z_{\delta Q} / \bar{q}S$ , where the partials  $M_{\delta Q}$  and  $Z_{\delta Q}$  are the pitch moment and the normal force (along +z) variations with respect to the pitch FCS command ( $\delta_{QFCS}$ ), obtained from equation (3.10).

### Pitch Inertial Coupling due to Stability Roll

When a maneuvering vehicle is rolling about the velocity vector  $V$ , at constant flight path, it generates a pitching moment due to inertial coupling, and therefore, it must possess sufficient nose down pitch control authority to overcome the nose up moment produced as a result of inertial cross-coupling during stability axis roll maneuvers at high angles of attack. The pitching moment ( $M$ ) is obtained from equation 3.43, as a function of the roll and yaw body rates.

$$M = I_Y \dot{q} - I_{XZ}(r^2 - p^2) - (I_Z - I_X)rp \quad (3.43)$$

The stability axis roll rate ( $p_{stab}$ ), which is rotation about the velocity vector, is a function of the body rates ( $p$  and  $r$ ). After some equation manipulations, the pitching moment ( $M_{IC}$ ) due to the inertial coupling with the stability axis rate  $p_{stab}$  is obtained from equation 3.44, which demonstrates how the induced pitching moment  $M_{IC}$  is dramatically increased with stability roll rate.

$$M_{IC} = [I_{XZ} \cos(2\alpha) - 0.5(I_Z - I_X) \sin(2\alpha)] p_{stab}^2 \quad (3.44)$$

This nose up moment due to coupling with roll reaches its maximum magnitude when  $\alpha = 45^\circ$ , so the vehicle must have sufficient pitch control authority to counteract this coupling moment. By combining equations (3.44) with (3.10) and (3.21), we can calculate the maximum acceptable stability rate as a function of pitch controllability. The maximum roll rate must be less than:

$$p_{stab}^2 < \frac{M_{\delta Q}}{[I_{XZ} \cos(2\alpha) - 0.5(I_Z - I_X) \sin(2\alpha)] U_{Q Max}} \quad (3.45)$$

Actually, it should be significantly less than what is shown in the inequality 3.45 because we should allow some margin for flight control, because some pitch control is needed only to trim at zero roll rate.

### Yaw Inertial Coupling due to Loaded Roll

The yaw control system must possess sufficient control authority to counteract the yaw inertial coupling moment produced during a roll pullout maneuver, which simultaneously produces roll and pitch rates. The adverse yawing moment  $N_{IC}$  during a roll pullout maneuver, also known as “loaded roll” is

$$N_{IC} = (I_X - I_Y)pq \cos(\alpha) \quad (3.46)$$

The maximum pitch rate  $q$  is determined by the bank angle and the normal load factor ( $n_z$ ) applied to the airframe. The adverse yawing moment is most severe when the loading occurs while the airplane is inverted, because it results to highest pitch rate, due to additional loading from gravity. The pitch rate of the aircraft ( $q$ ) while inverted at maximum loading is

$$q = \frac{(n_z+1)g}{V} \quad (3.47)$$

The yaw FCS control ( $\delta_{RFCS}$ ) needed to counteract this adverse yawing moment at maximum pitch rate is obtained from this equation

$$N_{\delta R} \delta_{RFCS} = (I_Y - I_X)p \cos(\alpha) \frac{(n_z+1)g}{V} \quad (3.48)$$

After taking into consideration the maximum yaw control authority  $\delta_{RFCS \text{ MAX}} = \frac{1}{U_{R \text{ Max}}}$

We can solve for the maximum roll rate that the yaw FCS can tolerate before it saturates the yaw effectors, assuming of course maximum pitch rate from equation 3.47.

$$p_{max} < \frac{VN_{\delta R}}{U_{R \text{ Max}}(I_Y - I_X)\cos(\alpha)(n_z+1)g} \quad (3.49)$$



## Moments at the Hinges of the Control Surfaces

Control surfaces rotate about a hinge line that is parallel to the wings and tails, and powered by electro-mechanical or hydraulic actuators. The torque supplied by the actuators must be greater than the aerodynamic moments generated at the aerosurface hinges, and therefore, the aerosurfaces hinge moments are used for sizing the actuator torques.

Equation 3.50 calculates the moment at the hinge of an aerosurface. It is a function of the dynamic pressure, reference area of the aerosurface, the chord which is the distance between the surface center of pressure and the hinge line, the deflection angle, and the hinge moment coefficient that varies as a function of  $\alpha$ ,  $\beta$ , Mach number and aerosurface deflection ( $\delta_{so}$ ).

$$M_{HSi} = \bar{Q} S_{rsi} \bar{c}_{hsi} \left\{ C_{hmc}(i, M, \alpha, \beta, \delta_{so}) + \left( \frac{\partial C_{hmc}(i, M, \alpha, \beta, \delta_{so})}{\partial \delta_{si}} \right) \Big|_{so} \{ \delta_{si} - \delta_{so} \} \right\} \quad (3.50)$$

Where:

$\delta_{si}$	is the control surface (i) deflection	(deg)
$\delta_{so}$	is the nearest deflection with available data	(deg)
$C_{hsi}$	is the chord of the control surface (i)	(feet)
Q-bar	is the aerodynamic pressure	(PSF)
$S_{Rsi}$	is the Reference Area of the Control Surface (i)	(feet <sup>2</sup> )
$C_{hmc}(i, m, \alpha, \beta, \delta)$	is the Hinge Moment Coefficient of Surface (i)	(-)

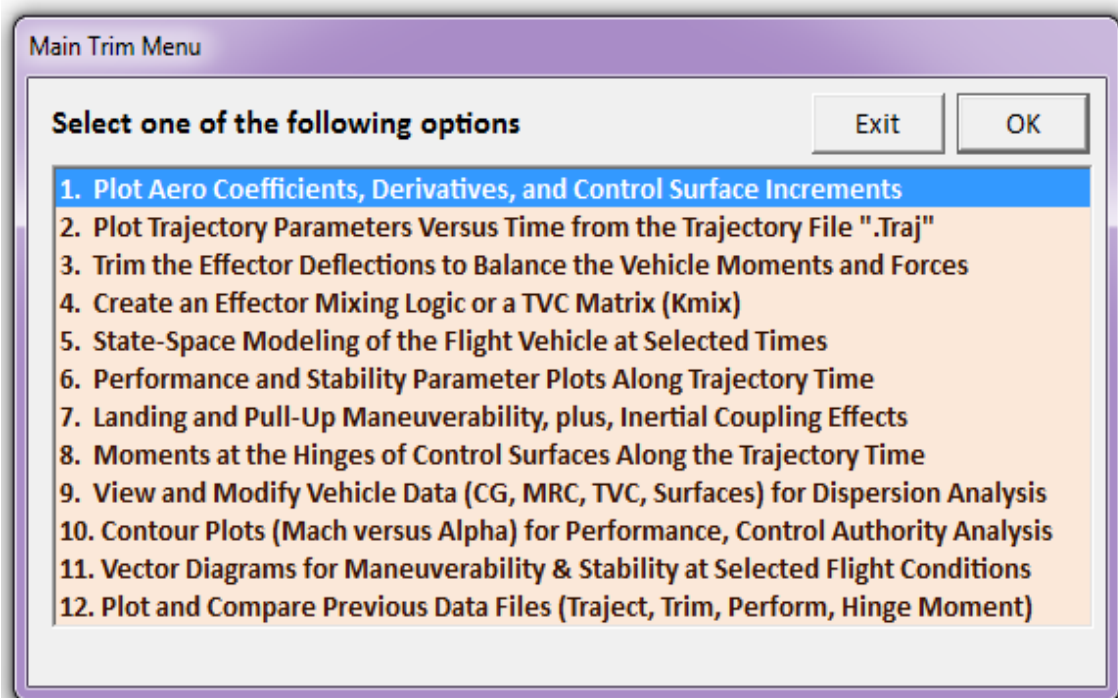
Equation 3.50 consists of two terms. The first term calculates the hinge moment of the  $i^{\text{th}}$  aerosurface at an increment ( $\delta_{so}$ ) which is the nearest to the actual aerosurface deflection ( $\delta_{si}$ ). The equation includes a second interpolation term to smooth out the hinge moment calculations. It uses the derivative coefficients of hinge moment per aerosurface deflection to interpolate the hinge moments between increments, as a function of difference in deflection ( $\delta_{si} - \delta_{so}$ ). The hinge moment coefficients and their derivatives are generated by aerodynamics specialists.

In Trim the hinge moment coefficients of all vehicle surfaces are included in a single file that has an extension ".HMCO". This file must contain as many sets of HM coefficients as the number of aerosurfaces included in the surface coefficients file (\*.Delt). The hinge moment coefficients array of the  $i^{\text{th}}$  aerosurface  $C_{hmc}(i, m, \alpha, \beta, \delta)$  is a function of four variables: the Mach number (M), the angles of attack and sideslip ( $\alpha$ ,  $\beta$ ), and the control surface deflection ( $\delta_{si}$ ). The number of increments for each aerosurface in the aerosurface hinge-moments data file is fixed.

## 9.4 Aero Data, Trajectory Analysis and Plotting

---

The Trim program also includes various types of graphic utilities for viewing and plotting vehicle data for presentation and analysis purposes. Some of the graphic utilities are interactive allowing the user to modify some of the data for dispersion analysis purposes, using windows, dialogs, and plots that can be modified using the mouse. The Trim program performs several functions/ utilities that can be accessed from a main menu shown below.



### 4.1 Plotting the Aero Data

The first option in the menu is used for plotting the aero data. The user selects option (1) and clicks "OK". The utility plots the basic aero-dynamic coefficients or their derivatives versus alpha or beta at different flight conditions. It also plots the control surface coefficients or their derivatives versus surface deflection. A flight condition must be selected from the following dialog that contains four menus. It is defined by the vehicle mass, the Mach number, and the angles of attack and sideslip. The user must select them from the menus, and click on "Select" button. The mass is needed for transforming the aero moments from the moments reference center (MRC) to the vehicle CG.

Select the following parameters

Select a Vehicle Mass, Mach Number, Alpha, and Beta from the lists below and click "Select"

Vehicle Mass (slug)	Mach Number	Angle of Attack (deg)	Angle of Sideslip (deg)
450.00	0.8000	-2.00	0.00
827.00	0.3000	-6.00	-5.00
777.00	0.6000	-4.00	0.00
726.90	0.8000	-2.00	5.00
676.90	0.9000	0.00	
626.90	1.200	2.00	
576.80	1.500	4.00	
526.80	2.000	6.00	
522.40	3.000	8.00	
450.00	4.000	10.0	

Select

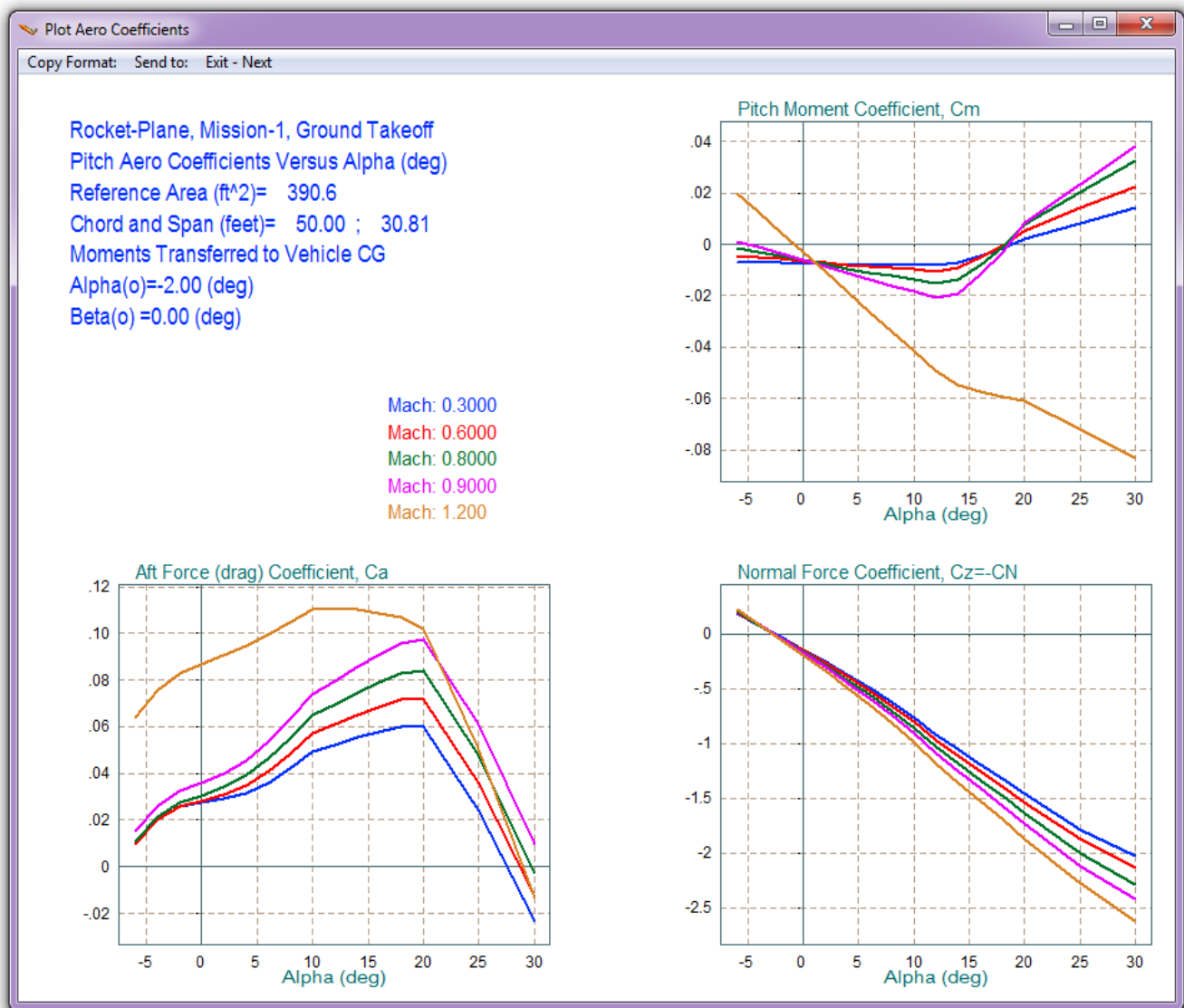
The menu that follows has eight options for plotting the aero data. The first four options are used for plotting the basic aero coefficients and their derivatives versus alpha or beta. The data are obtained from the basic aero data file ".Aero". The last four options are used for plotting the aero-surface coefficients or their derivatives versus surface deflection. The data are read from the surface aero data file ".Delt". From this menu the user may select one option, for example, to plot the basic pitch aero coefficients, and click "OK". The following figure shows plots of the pitching moment  $C_m$ , the normal force  $C_z$ , and the aft force  $C_A$  aero coefficients, as a function of (Mach and  $\alpha$ ). Five curves at corresponding to different Mach numbers are shown for comparison. More detail descriptions of the aero data plotting utility can be found in the examples, in Section 10.

Plot Aero Coefficients and Derivatives

Plot the Pitch or Lateral Aero Coefficients and Derivatives Versus the Angles of Attack, Sideslip, or Surface Deflection in (degrees)

OK Exit

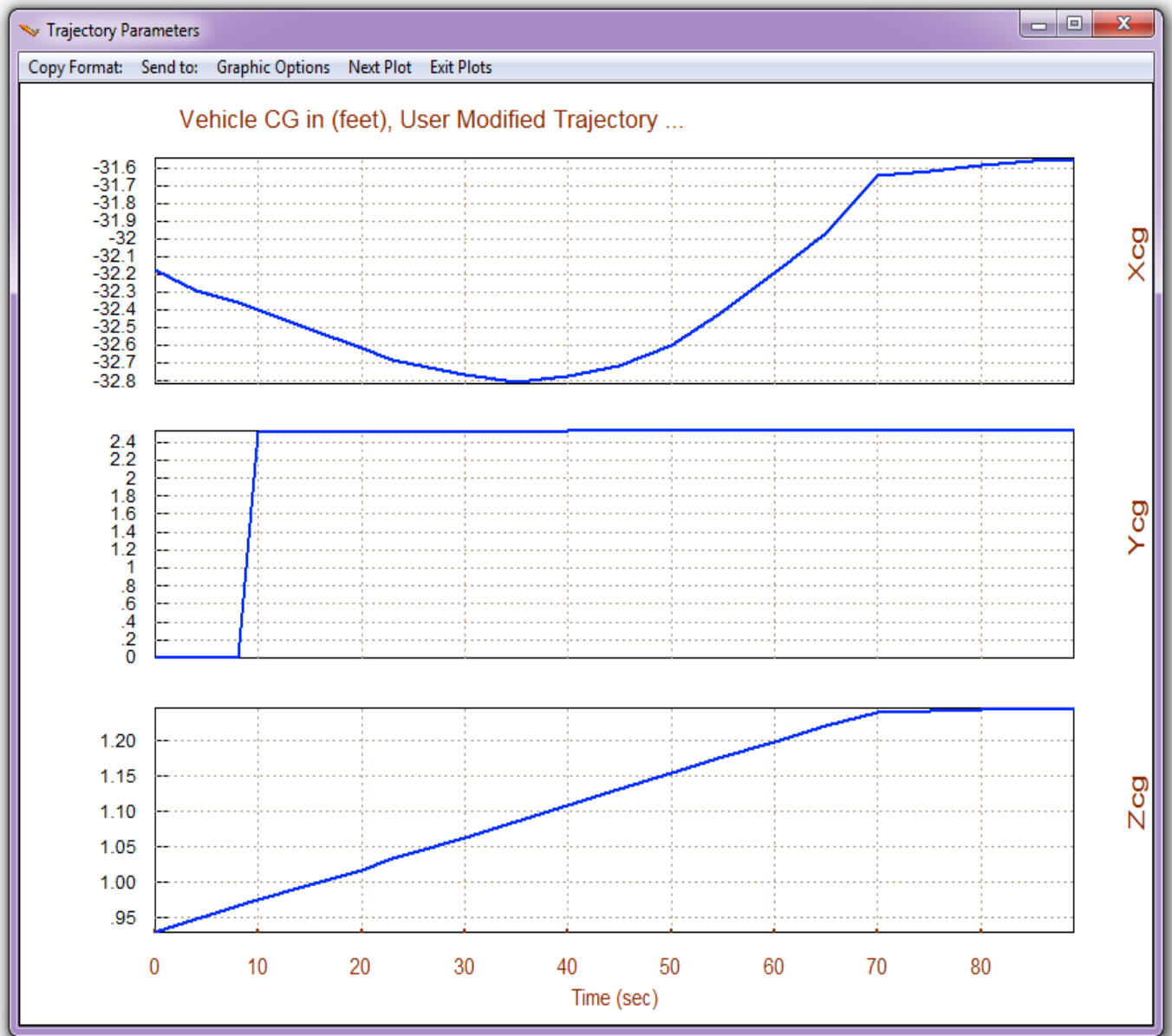
- Basic Pitch Aero Coefficients Versus Alpha
- Basic Lateral Aero Coefficients Versus Beta
- Basic Pitch Aero Derivatives Versus Alpha
- Basic Lateral Aero Derivatives Versus Beta
- Pitch Control Surface Coefficients versus Surface Deflection
- Lateral Control Surface Coefficients versus Surface Deflection
- Pitch Control Surface Derivatives versus Surface Deflection
- Lateral Control Surface Derivatives versus Surface Deflection



## 4.2 Plotting the Trajectory Data

Plots of the selected trajectory variables versus time can be obtained by choosing the second option from Trim main menu. The trajectory files have an extension (.Traj) and they are described in detail in Section 9. Some of the trajectory variables are: the ( $\alpha$ ,  $\beta$ ) angles in (deg), the flight path ( $\gamma$ ) in (deg), the relative velocity ( $V_0$ ) in (ft/sec), Mach number, dynamic pressure (lb/ft<sup>2</sup>), vehicle mass in (slugs), bank angle ( $\phi$ ) in (deg), altitude (h) in (ft), the measured accelerations ( $A_x$ ,  $A_y$ ,  $A_z$ ) in (ft/sec<sup>2</sup>), the body rates ( $p$ ,  $q$ ,  $r$ ) in (deg/sec), the rotational accelerations which are usually zero in (deg/sec<sup>2</sup>), the engine thrust ( $T_e$ ) in (lb), Lift and Drag forces in (lb), the CG location ( $x$ ,  $y$ ,  $z$ ) in (ft), and optionally, user supplied external forces (lb) and moments (ft-lb) which initially they are zero, and the user may add them later by creating a modified version of the trajectory. Some of the trajectory variables, such as the lift and drag forces, are not used by the Trim program and they are only included for reference. A typical trajectory plot is presented inside a window/ dialog

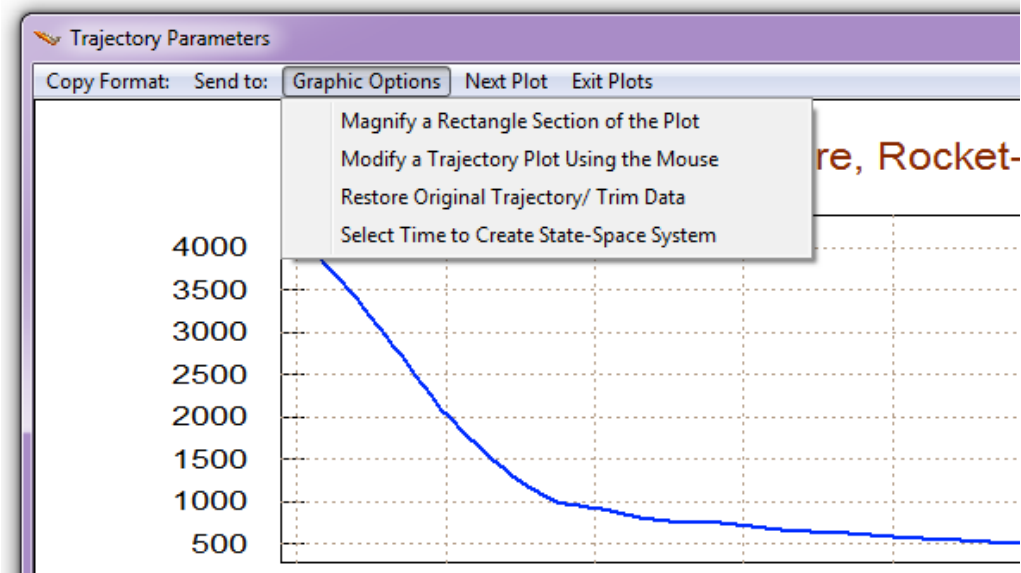
that has a horizontal menu bar on the top. Each plot includes 3 variables, as shown below. From the top menu bar the user may either exit the trajectory plotting by clicking on "Exit Plots", or plot the next set of variables by clicking on "Next Plot". The two options on the left are for sending the plot to a printer or saving it in a standard file format. The "Graphic Options" are mainly used for modifying trajectory variables using the mouse, and for selecting a time to create a linear dynamic model.



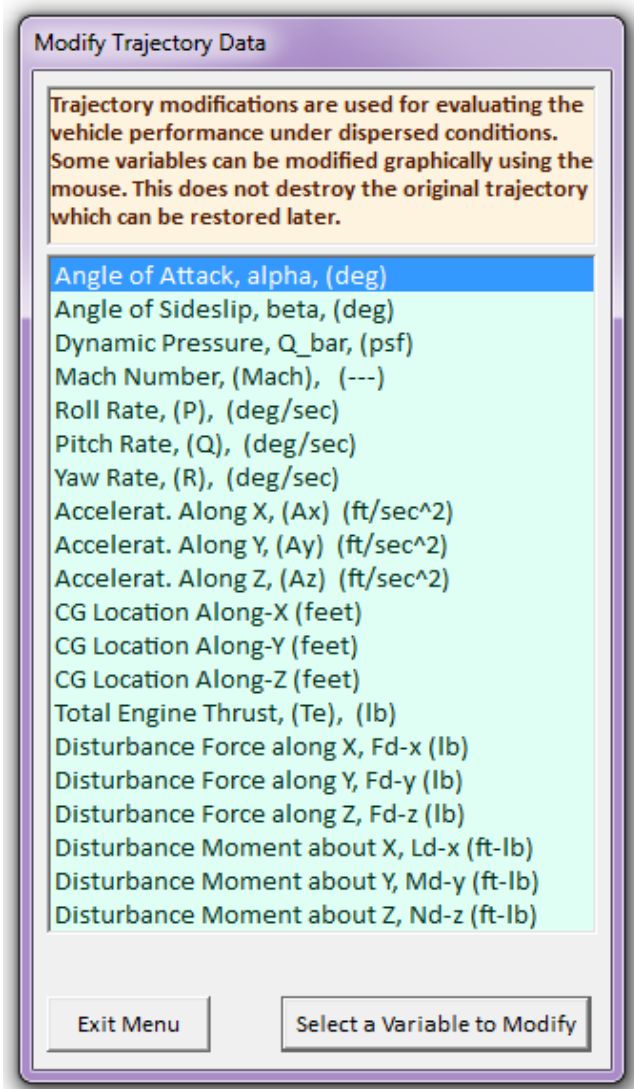
### 4.3 Modifying the Trajectory Data for Dispersion Analysis

Dispersion analysis is used for analyzing the vehicle performance by creating conditions which are different from those defined in the trajectory. It is possible that the vehicle may sometimes deviate from its expected trajectory due to winds, failures or other environmental disturbances. It should, therefore, be robust enough, capable to trim and meet its performance requirements with some variations of its trajectory parameters. We should, therefore, have the capability to temporarily modify the trajectory and to evaluate performance when some of the parameters are not exactly what we expect them to be. For example, we may vary some of the trajectory parameters, such as:  $\alpha$ ,  $\beta$ , the CG, the dynamic pressure, fail an engine, or introduce some external disturbances. Then we reevaluate how well the vehicle trims and performs under these adverse conditions and if it has the necessary controllability to maneuver. In other words, if by some unexpected event the vehicle deviates from its nominal trajectory to a different path, we would like to make sure that it will maintain a satisfactory performance and that it will have the control capability to converge back towards its course. The Trim program provides this capability by allowing the user to graphically modify the time histories of some of the trajectory parameters, such as:  $\alpha$ ,  $\beta$ , the CG, the dynamic pressure, the Mach number, body rates, vehicle accelerations, and to introduce time histories of external forces and moments. The modified trajectory is saved in a temporary filename with a title "*Temporary Trajectory*", and the effectors are re-trimmed using the modified trajectory. The user may then analyze vehicle performance and maneuverability using the modified trajectory and compare results. The original trajectory is not lost, but it can be retrieved later by selecting "*Restore Original Trajectory*" from the "*Graphic Options*".

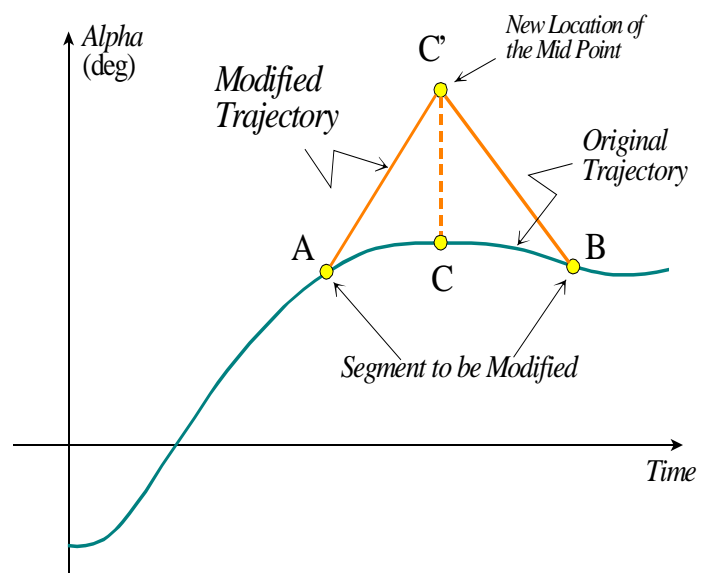
The trajectory modification option can be selected from one of the trajectory plots, as shown below. From the horizontal menu bar on the top, click on "*Graphic Options*", and then from the vertical pop-up menu select the option "*Modify a Trajectory Plot Using the Mouse*", as shown below.

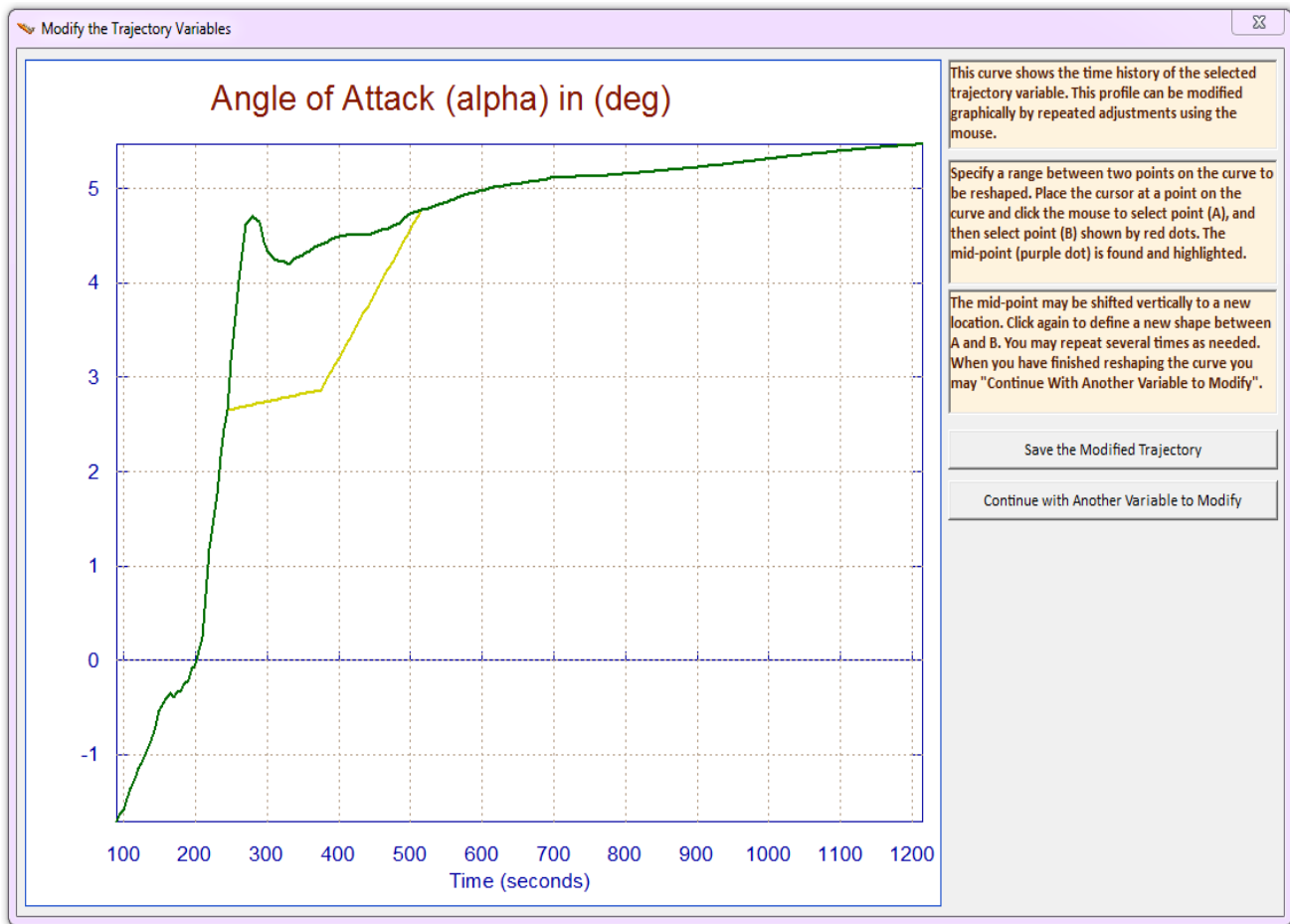


A menu of trajectory parameters comes up and from that menu the user may select some of the variables to be modified, one at a time, the angle of attack, for example, and click on "Select a Variable to Modify". A window dialog appears showing the original time history of alpha. The shape of this variable versus time can be modified by using the mouse, one segment at a time. First, a section of the variable to be modified is defined between two points by clicking at the two points (A) and (B), see figure below. The points are highlighted by two red dots. The program finds the mid-point (C) between points (A) and (B). It highlights it with a purple dot and places the mouse cursor on C. The user may now move the mid-point (C) up and down by shifting the cursor vertically using the mouse. The mid-point can now be moved to a new location (C'), as shown in figure, and after clicking the mouse again the new mid-point (C') becomes fixed and it is joined to the two extreme points A and B by straight lines (AC') and (BC'). The modified section is drawn in yellow. The original shape of the section is also shown in green. The user may continue modifying this trajectory variable many times, one section at a time, until the final shape of the modified yellow curve appears acceptable.



The user may now press on "Continue with Another Variable to Modify" and select another variable from the menu. Notice, that when you select either the first point or the last point of the curve to be modified, the adjustable point (C) becomes either the first point (A), or the last point (B) of the segment to be modified. When you select both the first and the last points of the curve then the entire curve can be shifted up or down. Notice also that if you want to shift the mid-point C to the new location C' by a big amount, such as an order of magnitude, you must shift the cursor vertically from the original point C to a new location outside the margins of the plot. If the shift happens to be more than expected you can adjust it again.





You may select other trajectory variables to modify by clicking on "*Continue with Another Variable to Modify*". When you finish modifying them you must click on "*Save the Modified Trajectory*" to save it. The modified trajectory will be saved by the program under a different filename, for example, if the original trajectory is "Shuttle.Traj" the modified trajectory becomes "Shuttle1.Traj". The modified trajectory file can be selected and loaded later for further analysis and modifications. After saving the trajectory, from the variable selection menu, click on "Exit Menu", and it will return to the trajectory plots which they should now be modified. Exit again and return to the Trim main menu. The modified "*Temporary Trajectory*" will remain in memory and it may be used for further analysis, such as, performance, controllability, etc, using contour plots and vector diagrams. It will remain in memory until you exit Trim or restore the original. The original trajectory can be restored in Trim by returning to the trajectory plots, and from the top menu click on "*Graphic Options*", and then from the vertical pop-up menu select the option "*Restore the Original Trajectory*".

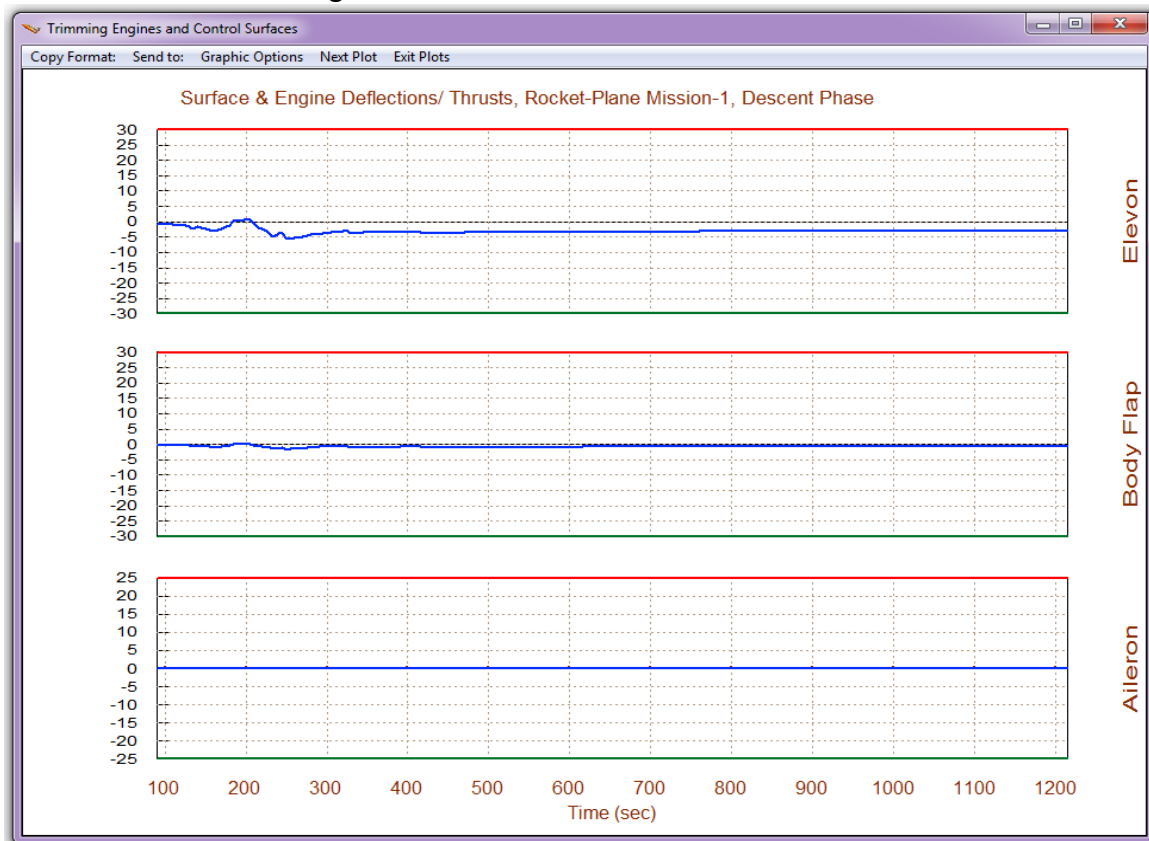
With the modified trajectory active in memory you may now re-trim the effectors to calculate their new positions (or throttles). Return to the Trim main menu and choose the third option: "*Trim the Effector Deflections*" to calculate the new trim positions based on the modified trajectory. Then you may select option (12) to compare the recent trim histories of the effectors against the trim data (.Trim) obtained from the original trajectory and analyze the effects of the trajectory modifications.



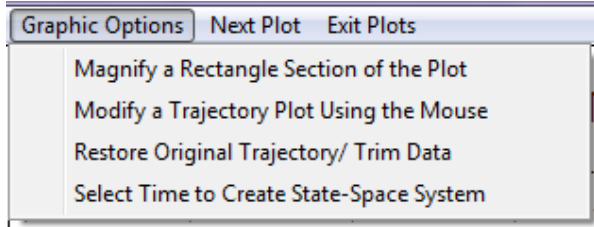
## 4.4 Adjusting the Effector Trim Data

Note that, not only the trajectory data can be modified interactively by the user. It is also the effector trim positions against time which are generated by Trim that can also be modified using similar graphic methods. This option is used when the analyst wants to modify the trimming conditions generated by the Trim program and to trade usage of some effectors against others. As it was already described in Section 2, the Trim program initially calculates the effector trim positions along the trajectory by taking into consideration the control capability of each individual effector. It allocates greater authority to the effectors that have bigger control capability in certain directions than to those who are less capable. The control capability is determined by the effector characteristics and also the maximum deflection or throttling ability.

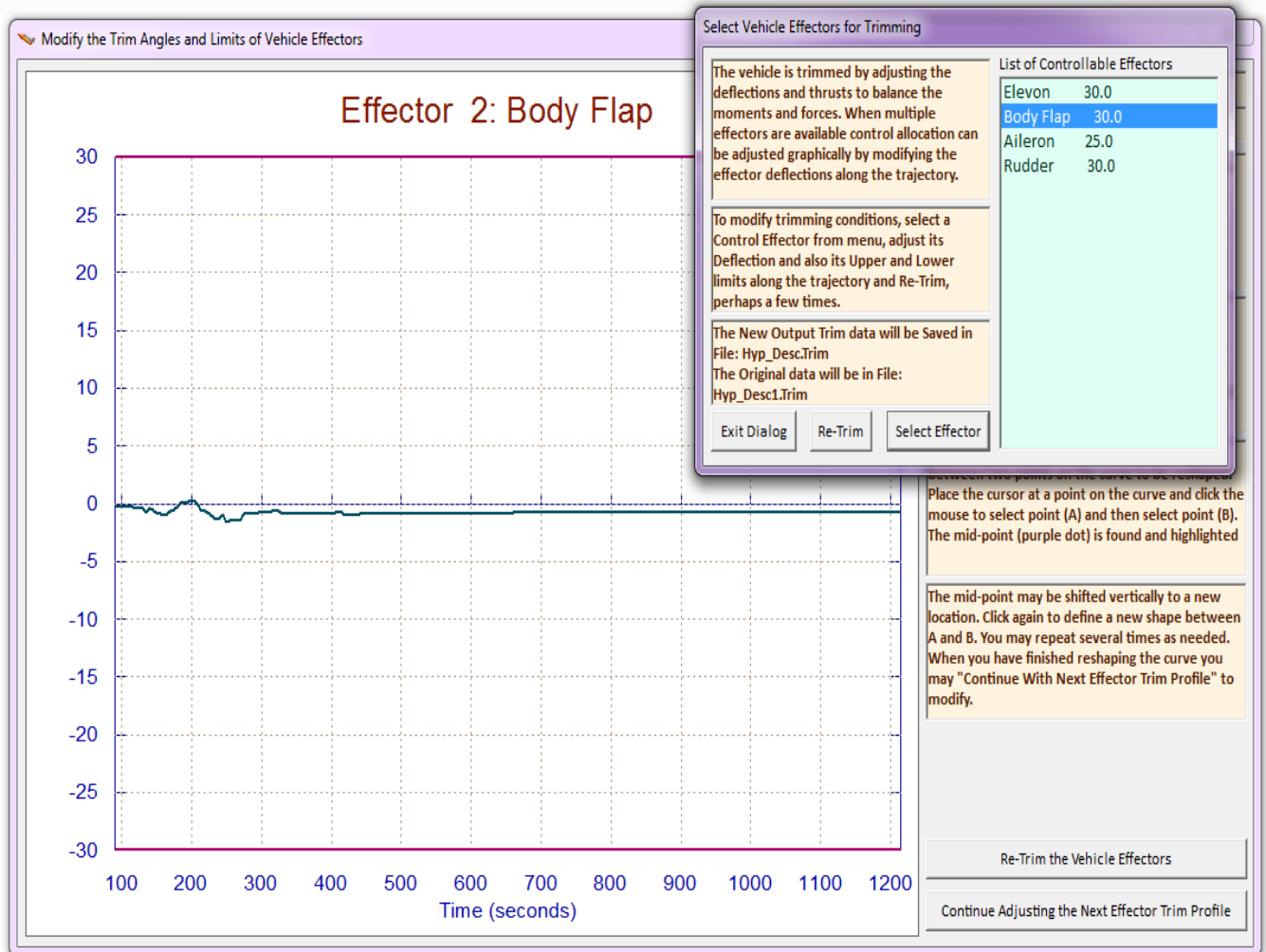
When the vehicle has multiple effectors controlling the same directions, this increases the possibility that usage of some effectors may be traded-off against others and the analyst may wish to explore this option. In the longitudinal direction, for example, the effector system may consist of: an elevon, a body-flap, a speed-brake, and TVC engine. It may be possible to eliminate or to reduce activity of some effectors, for example the body-flap, by keeping it at a fixed position or at a scheduled path, and re-trimming with the other effectors. This of course is only possible when the vehicle is equipped with other effectors that can provide sufficient controllability in the trim directions. However, if the effectors system is deficient or barely able to provide control in all directions the program will not allow the user to make any adjustments in the effector trim positions or will permit very small adjustments. In the following example the elevon trims with a negative bias. We will re-schedule the body-flap by biasing it negative. This will remove the bias from the elevon and bring it closer to zero.



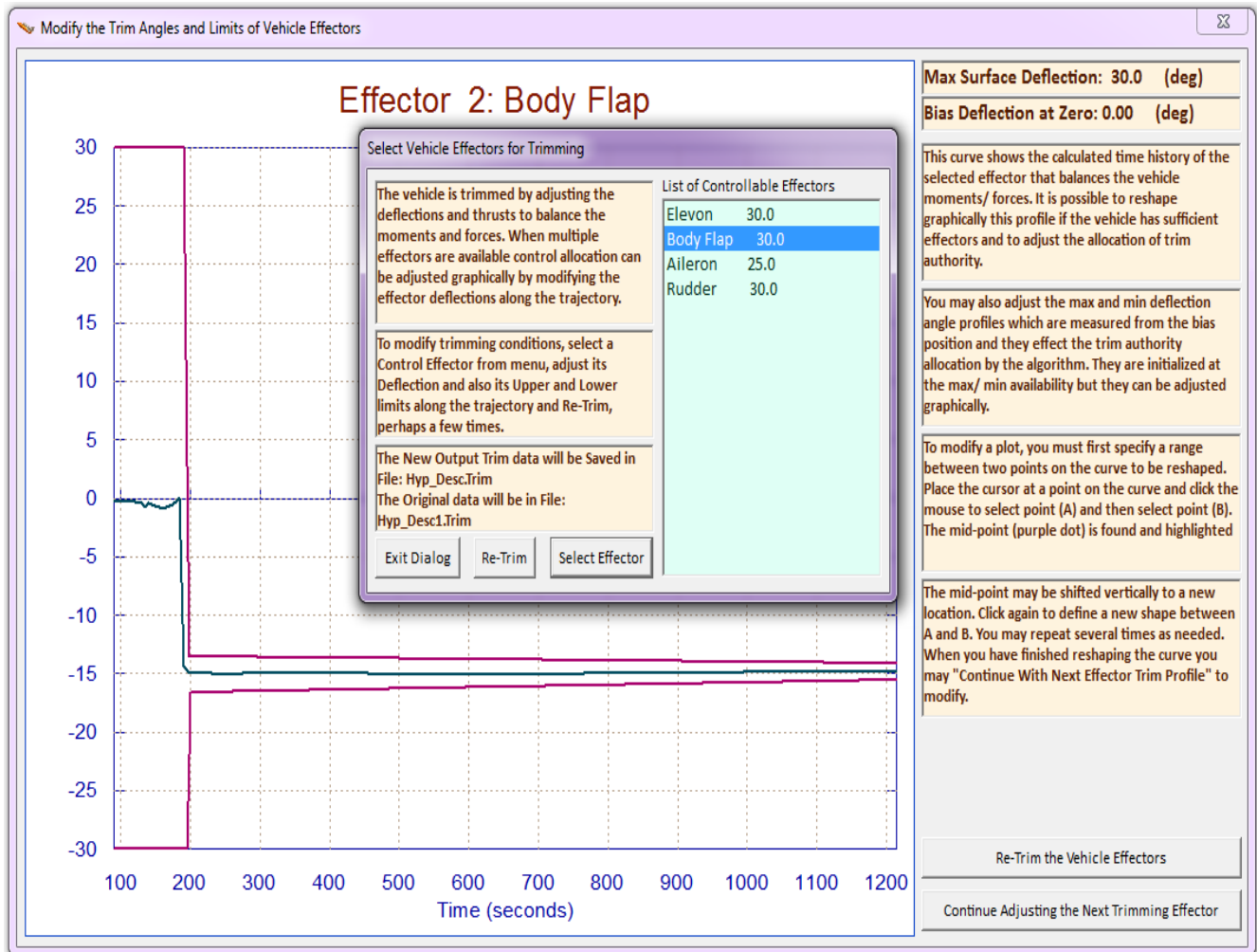
When the initial trim is completed, and before returning to the main menu, go to the horizontal menu bar located above the effector plots versus time. Click on "Graphic Options", and from the vertical pop-up menu select "Modify a Trajectory Plot Using the Mouse", as shown below.



A dialog/menu comes up showing a list of the vehicle effectors. Four aerosurfaces are used in this example. We may select one of the surfaces to modify, for example the Body-Flap, and then click on "Select Effector" button. The plot below shows the original trim route of the Body-Flap (green) which was generated by the initial trim. It also shows its upper and lower deflection limits (magenta lines) which are  $\pm 30^\circ$  (as defined in the aero-surfaces data file). It shows that very little Body-Flap was used. It was mostly the Elevon that did the trimming.



We will now modify the Body-Flap trim curve and re-schedule it by making it more negative as we attempt to shift the Elevon trim position closer to zero. The plot below shows the modified Body-Flap trim position versus time (green line) which was set at  $-14^\circ$  starting at  $t=200$  seconds. They were modified by the user using mouse driven interactive graphics. Notice that the upper and lower limits (magenta lines) were also reduced because reducing the limits de-emphasizes the effector authority during trim and prevents it from changing much in the next trim. The limit lines also restrain the deflection during trimming. When the user modifications are complete, click on the "Re-Trim" button, in either dialog, and the program will generate a new trim history, as shown in the next figure.



The plot below shows the effector positions after re-trimming. As you can see, the user modified body-flap trim position versus time is more negative now as adjusted by the user. The elevon deflection is now reduced to zero, as expected. In essence we replaced the elevon usage for trimming with body-flap. This will provide more elevon deflection capability for flight-control by allowing it to use its full range. The elevon is also faster and has higher bandwidth than the BF.

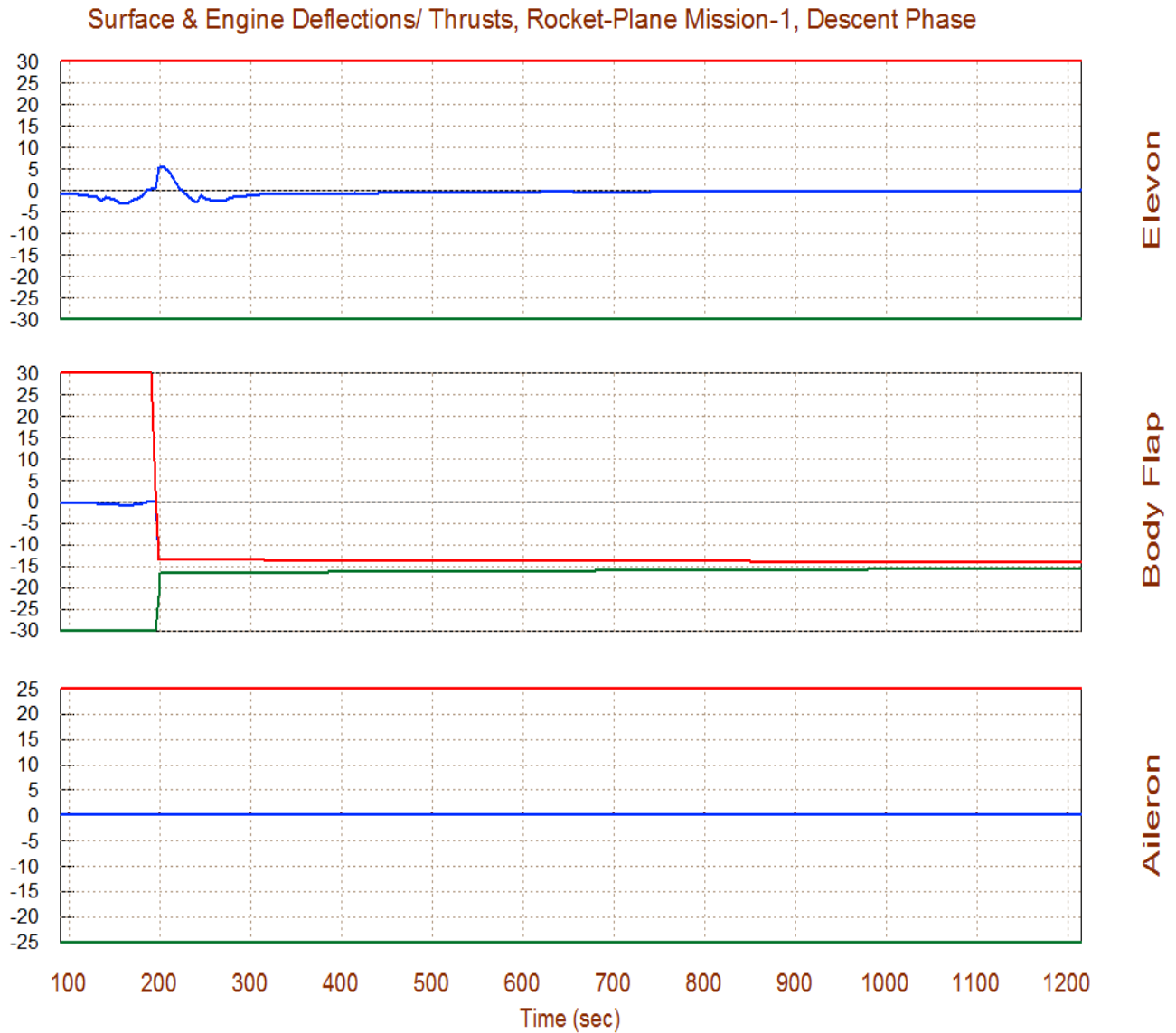
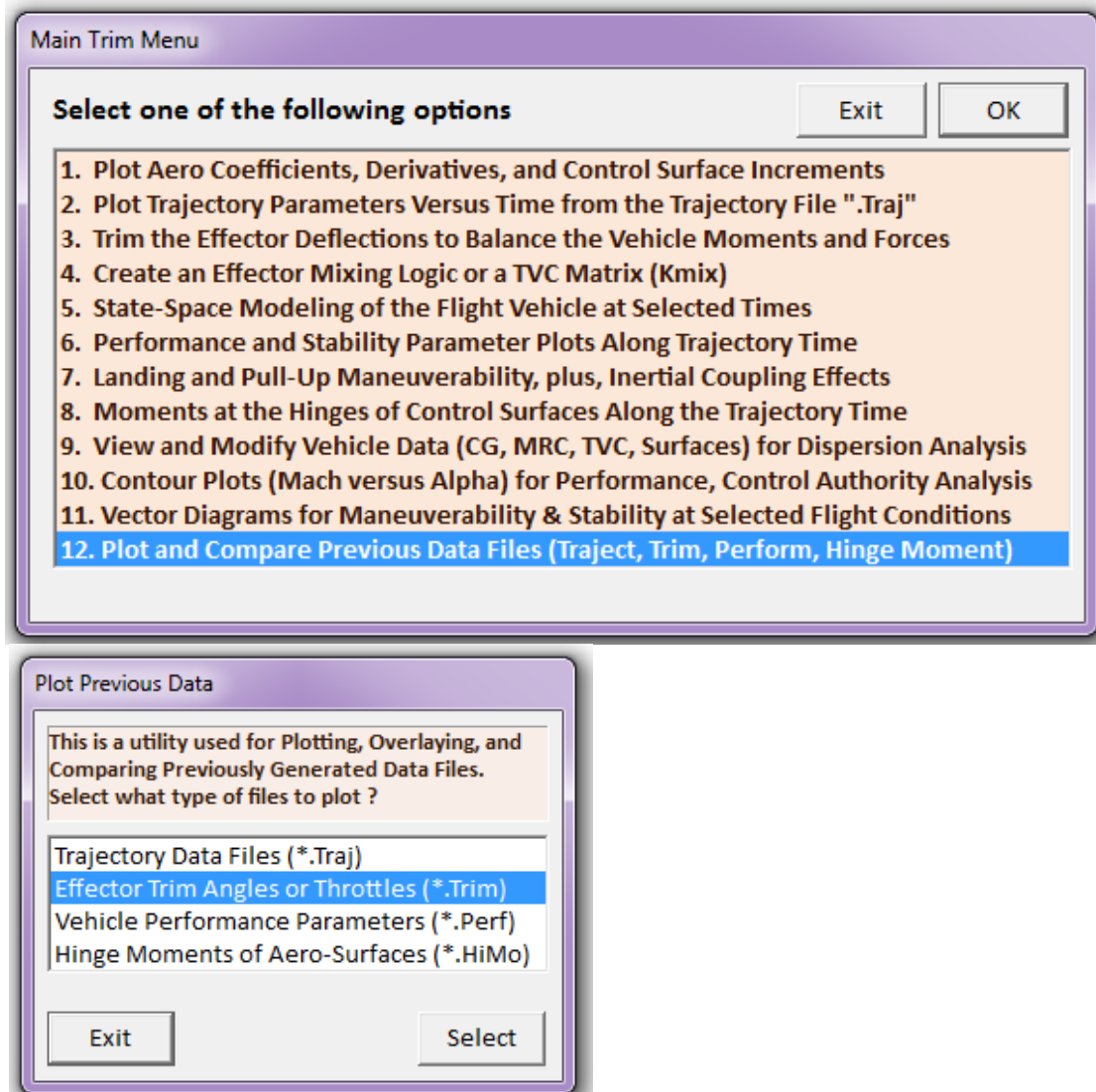


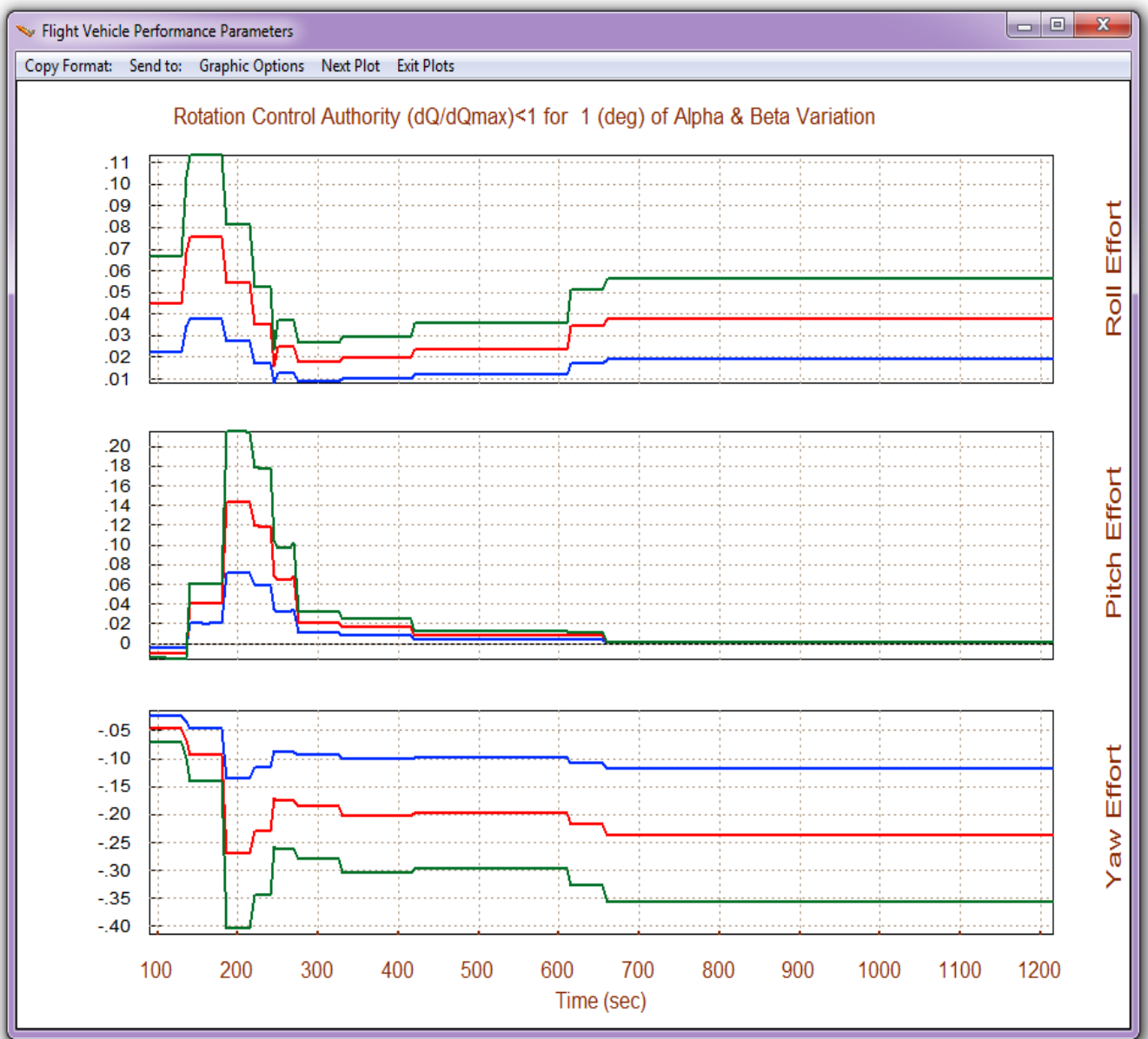
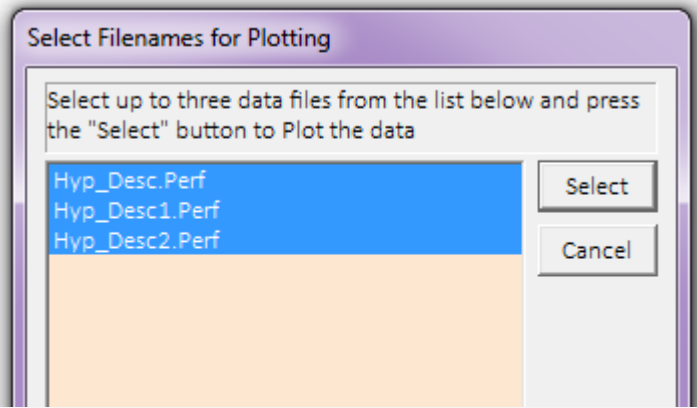
**Figure 4.1 The Body-Flap Deflection was Re-Scheduled more Negative to remove the Elevon Bias**

## 4.5 Plotting and Comparing Data

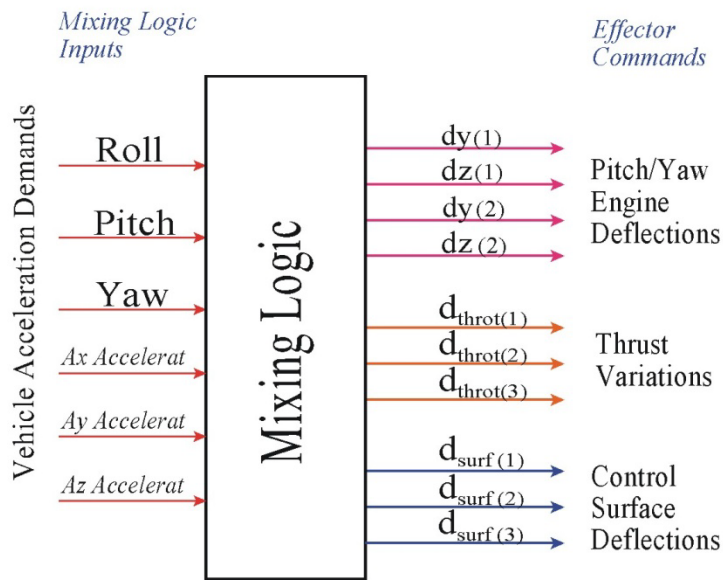
Option (12) in the Trim main menu is used for plotting and comparing previously generated data files. Select option (12), click "OK", and then from the next menu the user may select the type of data files to plot. There are four different types of data files to choose from: (a) trajectory data files (.Traj), (b) effector trim position files (.Trim), (c) performance parameters (.Perf), and (d) control surface hinge moment files (.HiMo).



This option is also used to overlay data and to compare results obtained from similar vehicles or variations. From the following menu the user selects the filenames to be plotted together. The program will overlay up to 3 files in the same plot. For example, if we selected to plot performance parameter files, the program searches the project directory to find all filenames with extension (.Perf) and places them in the following menu. In this example there are 3 performance data files. The user may select either: one, two, or three filenames and click on "Select" to plot them. The following example plots the control effort of the effectors obtained from 3 separate analysis/ runs. The first file is shown in blue, the second one in red, and the third one in green.



# 9.5 Effector Combination Logic



Flight vehicles are usually controlled by multiple effectors and effector types that produce moments and forces in 3 or more directions. Mainly 3 rotations and optionally some translations. The effectors provide the "muscle" power that maneuvers the vehicle. The effector sizing is based on requirements defined by mission goals. Some of the mission goals are captured in the trajectory. The effectors must be capable of providing the required accelerations for maneuverability and for counteracting disturbances along the controlled directions which are at minimum, 3 rotations, plus some

translations. The mixing logic in its simplest form is a gain matrix ( $K_{mix}$ ) that combines the effectors to operate as a system and interconnects between the actuators and the flight control system. It converts the acceleration demands coming from the FCS to effector deflection (or throttle variations) commands. The commands are optimized by  $K_{mix}$  for the purpose of maximizing the vehicle response in the directions demanded by the FCS and at the same time producing a small amount of cross-coupling in other directions. In a typical flight vehicle the FCS generates 3 rotational acceleration demands which control the vehicle rotations and attitude. X-acceleration is also included to control velocity and range. Translations along y and z are often controlled indirectly by rotating the vehicle. There are cases, however, like during vehicle separation or when hovering at low speeds where direct translation control along x, y and z independently from rotations is also necessary. This is possible, of course, when the vehicle has the effector capability to independently control translations, such as, a throttling engine, jets, body-flap, or a speed-brake to provide linear control in those directions.

An efficient mixing logic should be time-varying because the control authority of the effectors changes as a function of geometry, dynamic pressure, thrust, and CG location. The derivation of a mixing logic matrix for a vehicle that is controlled by gimbaling engines, throttling engines or jets, and control surfaces is presented in a separate section. The Trim program uses a dedicated utility for calculating the mixing logic matrix. It provides the option to either calculate it and save it at discrete/ selected time points or it generates a time-varying mixing logic internally when evaluating the performance along the trajectory. There is also a third option of reading a user supplied mixing matrix from a systems file (.Qdr) instead of creating it. For example, when a fixed matrix is already selected to combine the effectors along the entire trajectory. Also, when the aero-surfaces data are defined as aileron, elevon, and rudder, instead of separate surface panels, in which case a user supplied identity matrix can be used as a mixing logic in the trimming analysis.

## 5.1 Input Data

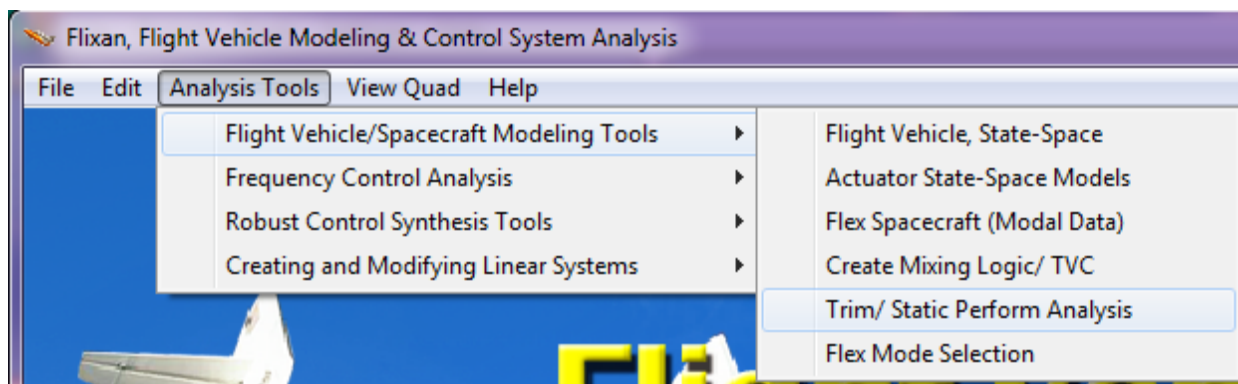
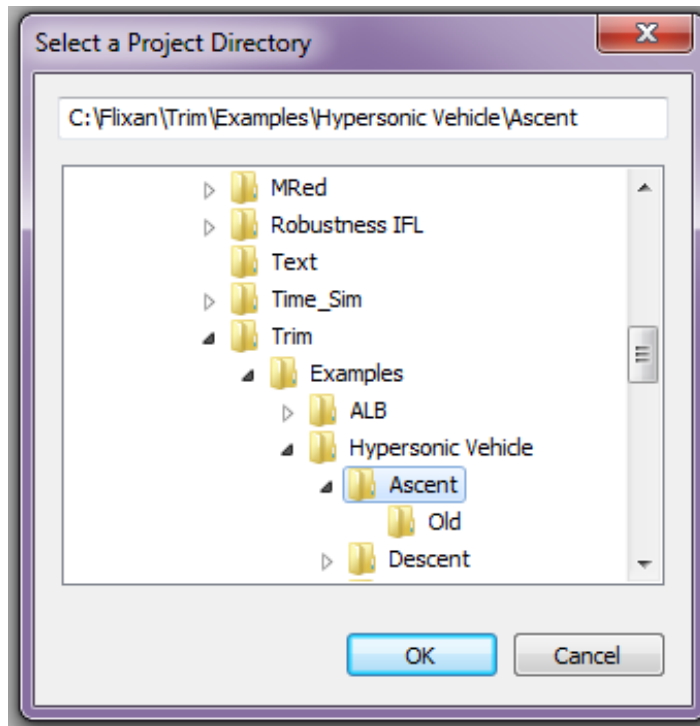
The Mixing Logic program in Trim combines four types of effectors: (a) thrust vector control (TVC) engines that pivot in pitch and yaw, (b) variable thrust engines (throttling), (c) reaction control jets (RCS), and (d) aero-surfaces. The inputs to the mixing logic program are the engine and aero-surface data, mass properties, and also trim angles or throttles (from files with extension ".Trim"). Since the trim positions are required prior to calculating the mixing matrix, the mixing logic program will request for the trimming function to be performed first. The engine or RCS jet parameters are defined in the propulsion data file that has an extension (.Engn). An engine is defined as gimbaling when the max deflection pitch and yaw angles in the engine data file are non-zero. A throttling engine is usually a fixed engine that has a nominal thrust ( $T_0$ ) and it provides control forces on the vehicle by varying its thrust. The maximum thrust variation above and below nominal ( $T_0$ ) is defined in the input data by a throttle parameter ( $T_h$ ) which must be greater than zero and less than one. During trimming the program calculates the throttle control  $\delta T_{hr}(t)$  that defines the actual thrust for each engine at each time step along the trajectory. The throttle control is time variable and it can vary between zero and  $\pm T_h$ , i.e. ( $+T_h > \delta T_{hr}(t) > -T_h$ ). The actual engine thrust is:  $T(t) = T_0 [1 + \delta T_{hr}(t)]$ . So the thrust is at its nominal value ( $T_0$ ) when the throttle control is zero and the thrust remains always positive even at minimum throttle. An engine may also be defined to be both, gimbaling and throttling. The RCS jets in Trim are also continuous throttling engines but they are defined slightly different. Each thruster represents a pair of opposite firing jets (back-to-back). Their nominal thrust is zero and they can apply a positive or negative (throttle) force at a location on the vehicle along a specified direction. The maximum jet thrust magnitude ( $T_{jet}$ ) is defined in the data file. The actual jet thrust can vary between ( $\pm T_{jet}$ ). The Trim program calculates the throttle control  $\delta T_{hr}(t)$  that defines the actual thrust:  $T(t) = T_{jet} \delta T_{hr}(t)$  at each time point. The throttle control  $\delta T_{hr}(t)$  varies between  $\pm 1$ . So the thrust is zero when the throttle control is zero and the thrust magnitude cannot exceed  $\pm T_{jet}$ . The parameter that separates between a throttling engine and an RCS jet in the input data file (.Engn) is the throttle parameter ( $T_h$ ). When the throttle parameter is exactly 1, the thruster is interpreted by the Trim program as a pair of back-to-back firing jets, and the thrust defined in file (.Engn) represents the max jet thrust. Otherwise, when the throttle parameter is between zero and less than 1, it is interpreted as a propulsion engine of nominal thrust ( $T_0$ ) and the throttle control  $\delta T_{hr}(t)$  defines thrust variations above and below  $T_0$ . A propulsion engine can be defined as both, gimbaling and throttling. The orientation of a thruster, and hence its force direction, is defined in terms of two angles (pitch and yaw) relative to the -x vehicle direction.

The aero data for the control surfaces are in file (\*.Delt). This file includes force and moment increment coefficients, which are increments in addition to the forces and moments defined in the base aero-data file (.Aero). The coefficients are functions of: Mach number, alpha, beta, and the control surface deflections. The program calculates the mixing logic matrix based on the moments and forces created from each effector.



## 5.2 Creating a Mixing Logic Matrix from "Trim"

The following example demonstrates how to calculate a mixing logic matrix from the Trim program. Note that the mixing logic can also be calculated from Flixan using the flight vehicle input data. Start the Flixan program, select the project folder that contains the analysis files, such as: trajectory, mass, engine, and control surface aero data. The files must be properly formatted for the program to be able to read them. From the Flixan main menu select "Analysis Tools". From the drop-down menu select "Flight Vehicle/ Spacecraft Modeling Tools", and from the menu on the right: "Trim/ Static Performance Analysis".



From the following filename selection menu you can select the files to be used in the Trim analysis. Also from the input/ output filename menu select or enter an input data file (.Inp) and a systems file (.Qdr). The mixing matrix will be saved in the systems file.

Select One Data File from Each Menu Category

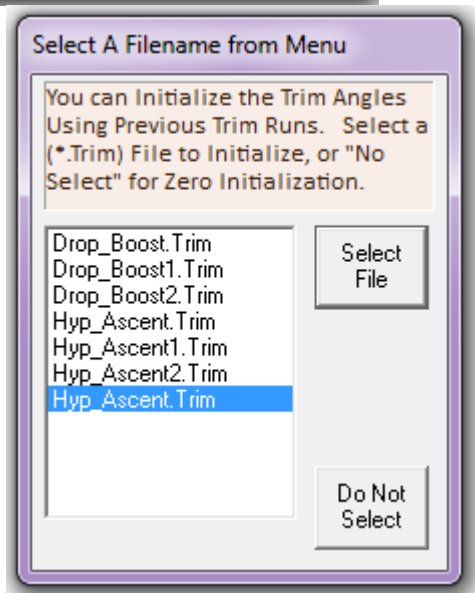
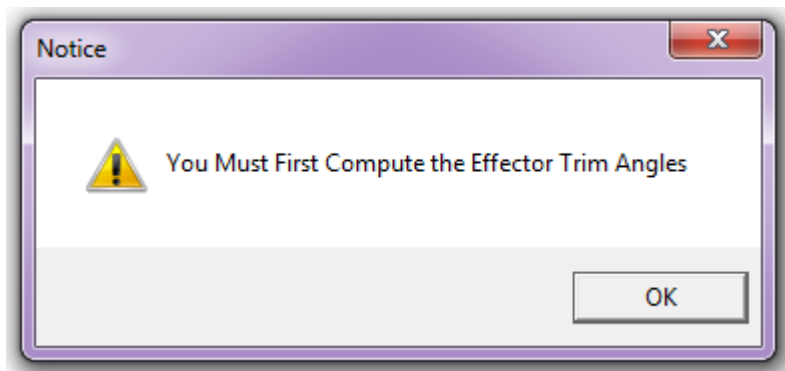
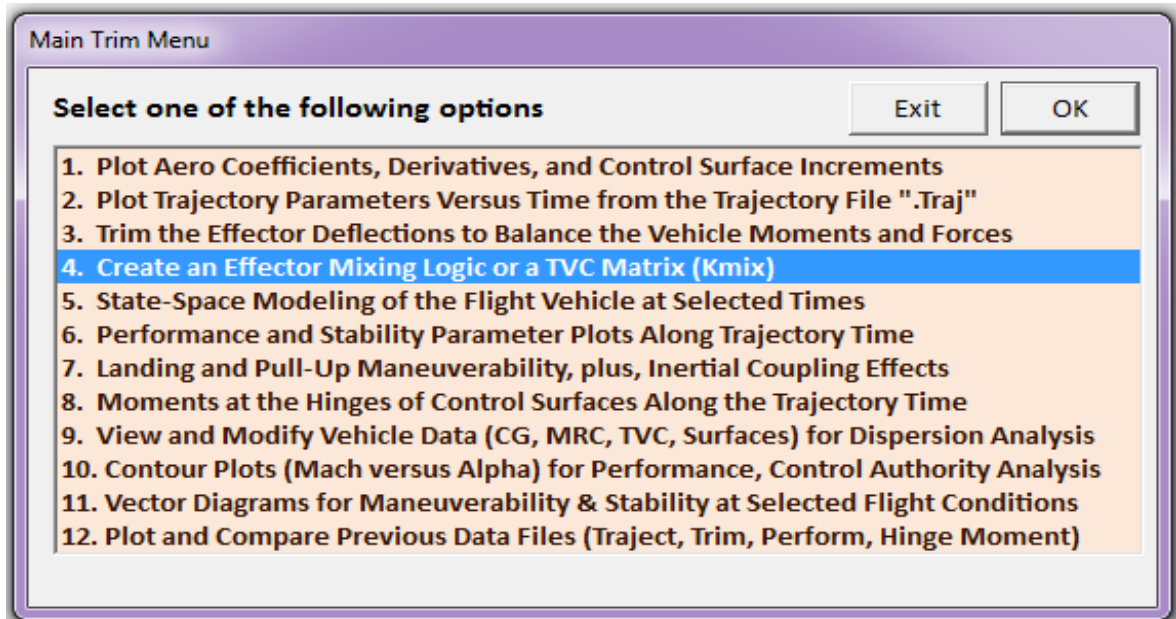
The following analysis requires some data files to be selected from the current project directory. Select one data file for each category, (some of the categories are optional).

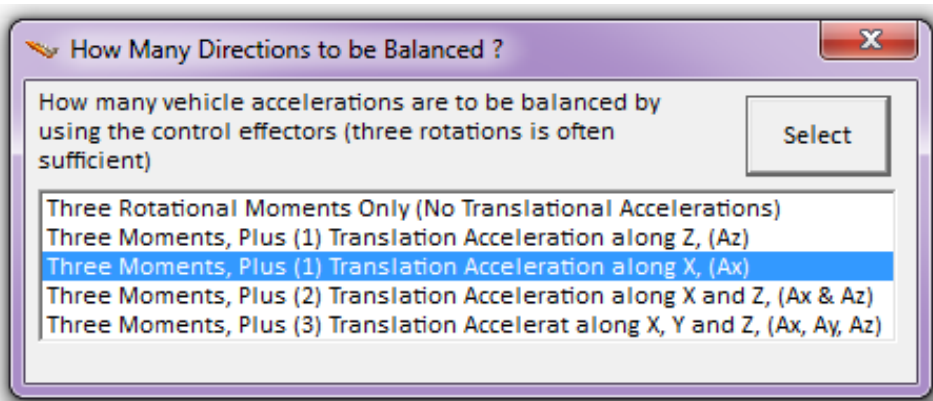
<b>Mass Properties</b> Hyper.Mass	<b>Surface Hinge Moments</b> Hyper.HMco
<b>Trajectory Data</b> Hyp_Ascent.Traj	<b>Aero Damping Derivat</b> NO DATA FILE
<b>Basic Aero Data</b> Hyp_Ascent.Aero	<b>Engine Parameters</b> Hyper.Engn
<b>Contr Surface Aero Coeff</b> Hyp_Ascent.Delt	<b>Aero Uncertainties</b> Hyp_Desc.Unce
<b>Slosh Parameters</b> NO DATA FILE NO DATA FILE	OK

Enter Filenames

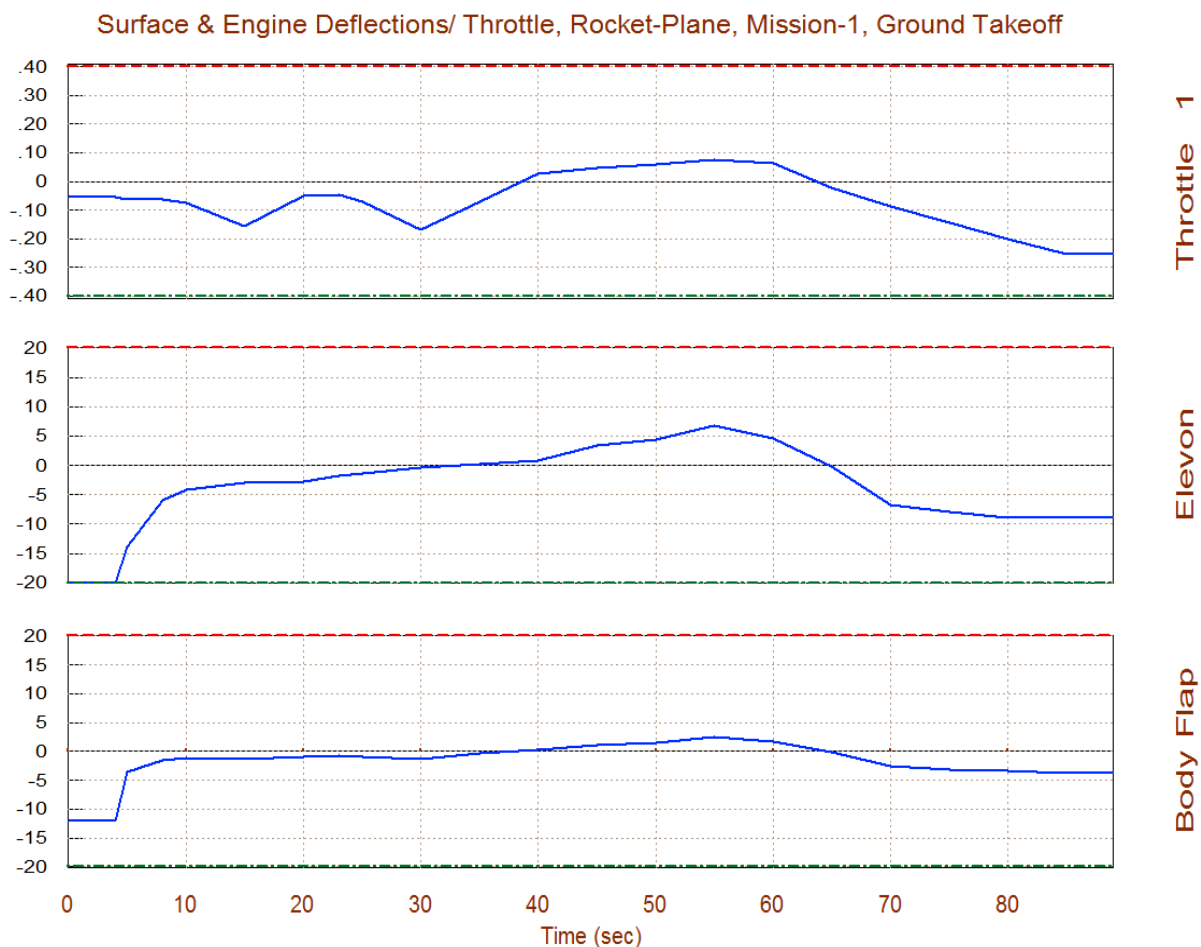
Enter a File Name containing the Input Data (xxx.Inp)	Enter a File Name containing the Quadruple Data (xxx.Qdr)
NewFile.Inp Hyp_Ascent.inp NewFile.Inp	Matrix.Qdr Matrix.Qdr NewFile.qdr Shuttle_Stg1_T55.Qdr System.Qdr NewFile.Qdr
Create New Input Set	Exit Program    Select Files

From the Main Trim menu select option (4) "Create an Effector Mixing Logic". This option requires the effector trimming process to be performed prior to calculating the mixing logic. It will check for the existence of a trim data file (.Trim) and if it does not find one it will initiate a trim, as demonstrated in the following example. It will ask for a (\*.Trim) file to initialize Trim. Assuming that we do not have one and click on "Do Not Select" an initialization file. In the following menu we must select the trimming directions, assuming of course that they are the same as the control directions used in the calculation of the mixing logic matrix. In this example we include the x translational direction in addition to the three rotational directions, and click "Select". This is achievable because our main engine is defined as throttling and it can provide control in the x-direction. Otherwise, it would not have been possible to control or trim in the x direction.



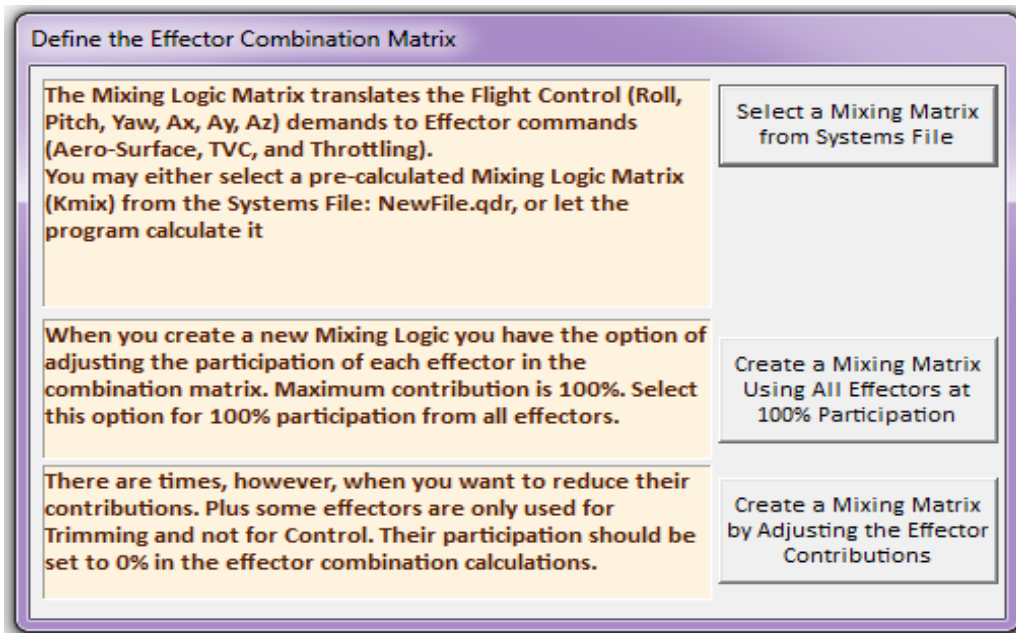


Copy Format Send to Graphic Options Next Plot Exit Plots

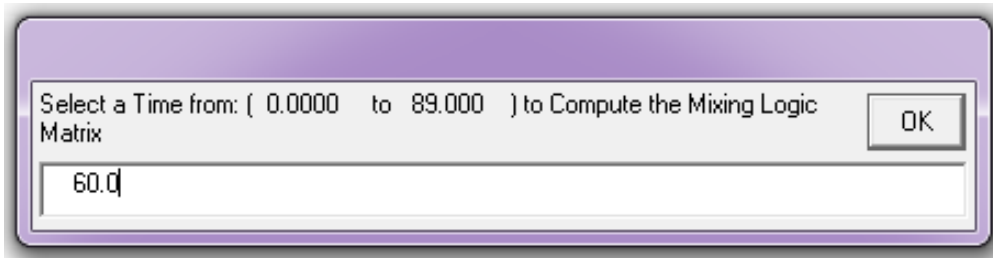


The Trim program calculates the trim positions of the 5 effectors (engine throttle control, elevon, body-flap, aileron, and rudder) as a function of the trajectory time as shown in the plot above. These positions are used to balance the 3 rotational moments and the acceleration force along the x axis along the input trajectory. The figure shows the Elevon and Body-Flap deflections in (deg) and also the throttle control variation versus time. In this case the throttle control can vary between zero and  $\pm 0.4$ , but it uses less than 0.25. The aileron and rudder are not shown because they are zero.

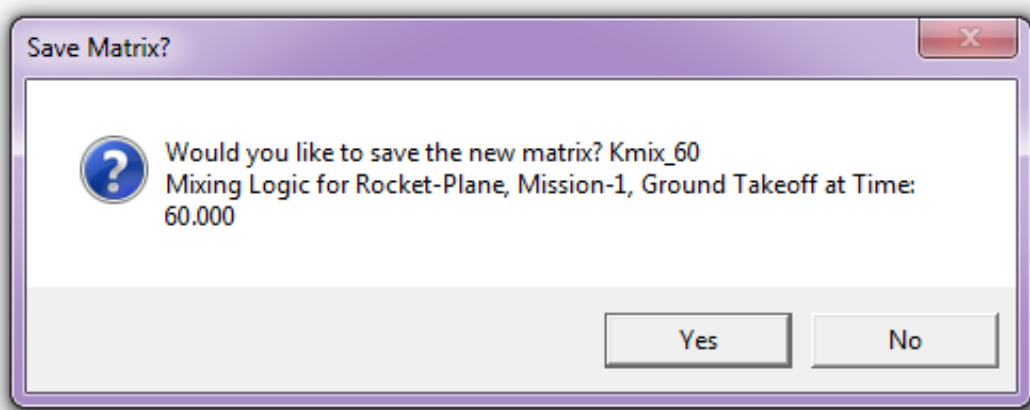
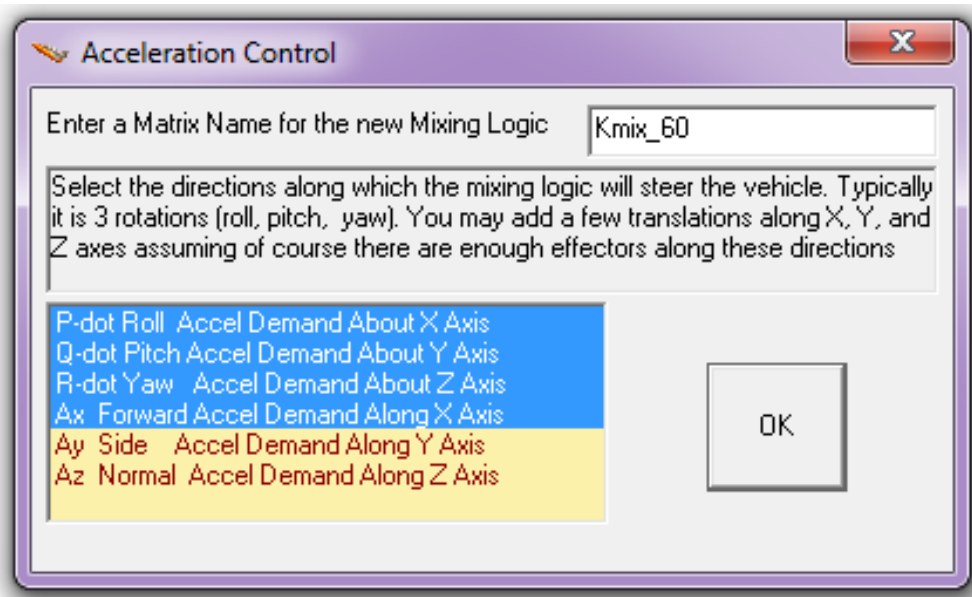
The trim is now complete and we are back in the mixing-logic calculation process. The following effector combination dialog is used for defining the amount of participation of each effector in the Kmix calculation. The top option, obviously, does not apply here because we are not interested to read an already existing mixing matrix from file. The choice is between the bottom two options. In this case we select the second option which creates a mixing matrix with 100% participation from all effectors. The third option can be used to define the percentage of participation contributed from each effector in the Kmix calculation.



In the next dialog we must enter a trajectory time, which in this case it is  $t=60$  sec. Kmix will be calculated using the vehicle data in this flight condition. It means that the mixing matrix will perfectly diagonalize the dynamic model at this time.



In the following dialog we select the directions along which we expect to achieve acceleration control. We must select 3 rotations plus the x-axis accelerations. We must also enter a short name "Kmix\_60" that will identify the matrix, and click "OK". In this case, the mixing logic matrix receives 3 rotational acceleration demands (roll, pitch, yaw) and one translation acceleration demand along x, from the FCS, and it converts them to 4 control surface deflection commands and to a thrust variation command for the main engine.



If you answer "Yes" in the above question, the program will save the newly created matrix in the selected systems file, which is "Matrix.Qdr".

### 5.3 Derivation of an Effector Combination Matrix

Flight vehicles are controlled by various types of effectors that produce the forces and moments which are required to guide them. They provide the "muscle" power to maneuver the vehicle around by changing its attitude or providing linear acceleration. The effectors are either gimbaling engines known as thrust vector control (TVC), thrust varying engines (throttling), reaction control jets (RCS), and rotating aero-surfaces. The deflections and thrust variations are commanded by the flight control system. The mixing logic is a matrix that interconnects between the flight control system outputs and the vehicle effectors. The FCS outputs are mainly rotational acceleration demands in (roll, pitch, yaw), and it may sometimes include linear acceleration demands ( $A_x$ ,  $A_y$ ,  $A_z$ ). The mixing logic matrix combines the vehicle effectors together and uses them as a system. It translates the flight control demands into effector commands, such as, engine or control surface deflections, main engine thrust variations, or RCS jet thrust commands, and it becomes an integral part of the flight control system. In the event of an effector failure it is the mixing logic matrix that must be changed and not the FCS gains.

The effectors as a system must be capable of providing maneuverability against disturbances along the controlled directions which are at least 3 rotations, plus some translations. The deflections must be combined efficiently in order to maximize the vehicle acceleration in the direction commanded by the FCS with as minimal coupling as possible in other directions. The Flixan program has a special utility for calculating the mixing logic matrix as a function of the vehicle geometry, thrusts, alpha, mass properties, and surface coefficients. The algorithm uses pseudo-inversion to determine an optimal combination of the controls to achieve the demanded change in vehicle rates while minimizing the coupling between the control axes. When the matrix is connected open-loop in front of the vehicle model (as shown in fig. 5-2) it attempts to diagonalize the plant, which means, that the vehicle accelerations approach the commanded accelerations. Ignoring, of course, the basic aero-dynamics and other high order dynamics.

The FCS generates at least 3 rotational acceleration demands which control the vehicle attitude. Translations along y and z are controlled indirectly by rotating the vehicle. In some cases direct acceleration control along x and z independently from attitude is also a requirement, assuming of course that the vehicle has the effector capability to independently control translations, such as, throttling engines, jets, body-flap, or a speed-brake to provide control along those directions. An efficient mixing logic should be time-varying because the vehicle parameters and the control authority of the effectors change as a function of geometry, dynamic pressure, thrust, and CG location, etc. The derivation of a mixing logic matrix for a vehicle that is controlled by gimbaling engines, throttling engines or jets, and control surfaces is presented in the following section.

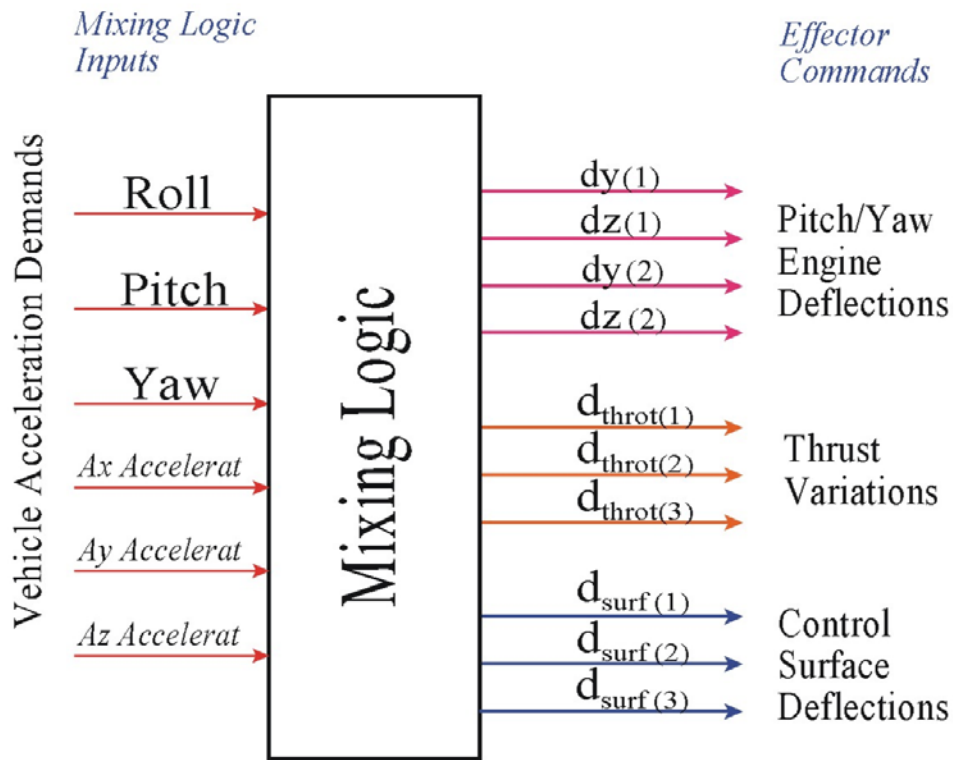


Figure 5.1 Effector Combination or Mixing Logic Matrix

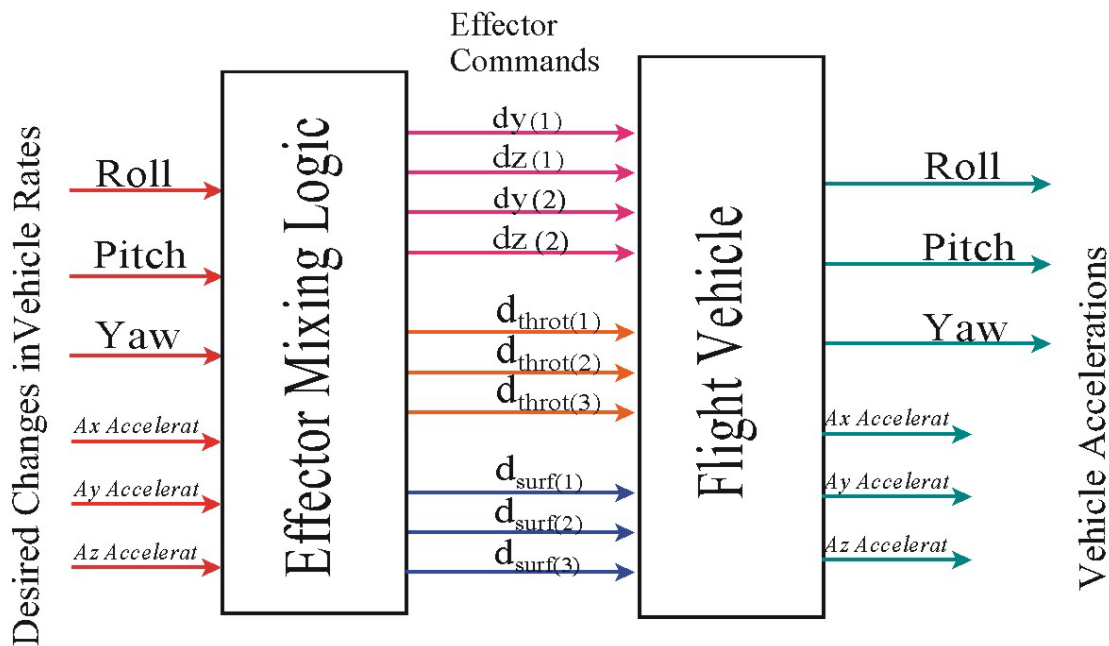


Figure 5.2 When the Mixing Logic Matrix is Connected in Series with the Vehicle Model (Open-Loop), the Vehicle Accelerations should be Approximately Equal to the Demanded Accelerations coming from the FCS



### 5.3.1 Forces and Moments Generated By a Single Engine

The following equation calculates the forces generated by a single thruster engine (i) mounted on a vehicle at fixed orientation angles (or trimmed at those angles):  $\Delta y$  in pitch (elevation angle with respect to the x y plane), and  $\Delta z$  in yaw (azimuth angle about the body z axis), see Figure 5-3. The forces along the body x, y, and z axes are:

$$\begin{aligned} F_{Xe(i)} &= T_{e(i)} \cos(\Delta_E) \cos(\Delta_Z) \\ F_{Ye(i)} &= T_{e(i)} \cos(\Delta_E) \sin(\Delta_Z) \\ F_{Ze(i)} &= -T_{e(i)} \sin(\Delta_E) \end{aligned} \quad (5.1.1)$$

Let us define the throttle control  $D_{th(i)}$  for engine (i) to be the ratio of thrust variation divided by the nominal engine thrust.

$$D_{th(i)} = \frac{\delta T_{e(i)}}{T_{e(i)}} \text{ where: } \delta T_{e(i)} \text{ is the Thrust Variation} \quad (5.1.2)$$

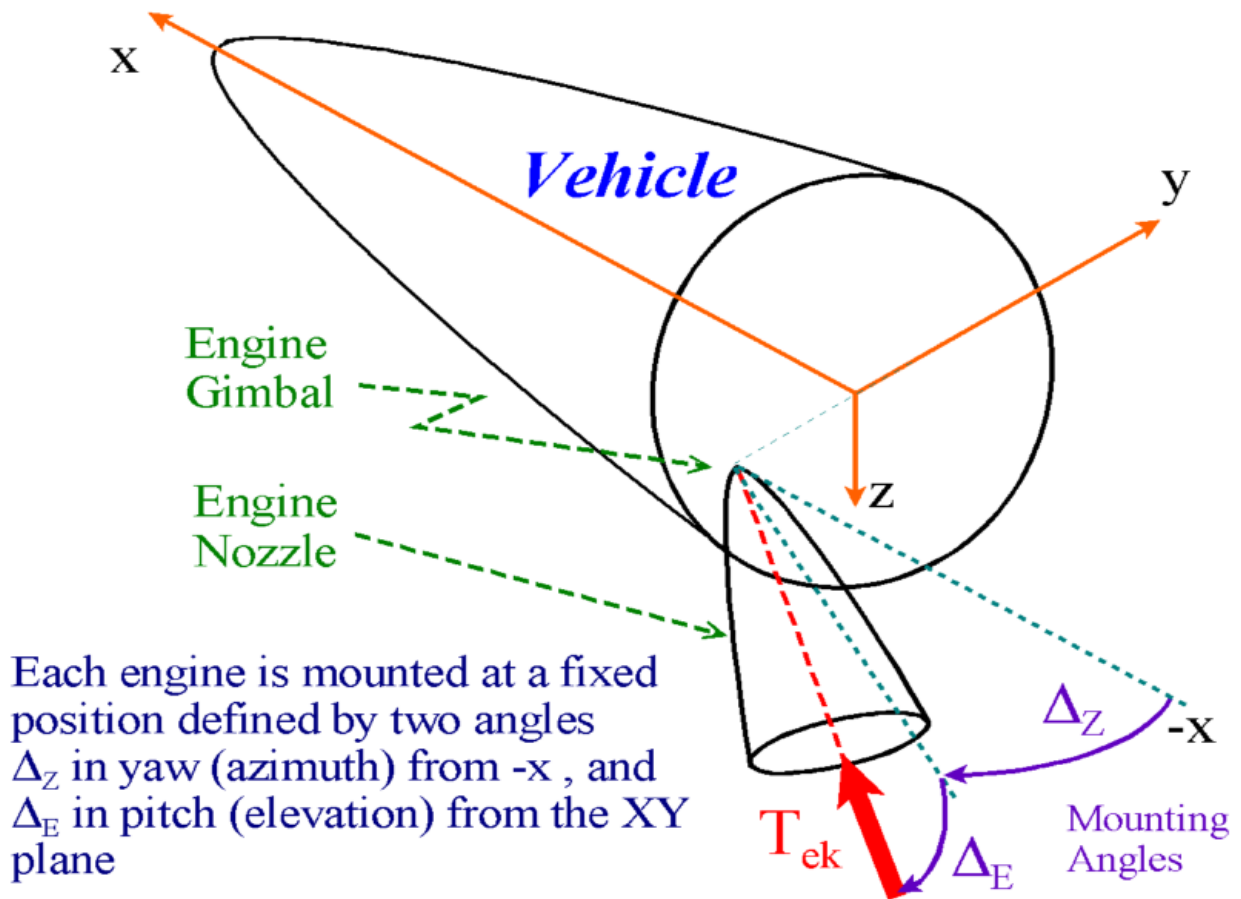


Figure 5.3 Engine Orientation Angles ( $\Delta y$  and  $\Delta z$ ) with respect to the Vehicle Body Axis

The product  $Dth(i) * T_{e(i)} = \delta T_{e(i)}$  is the variation of engine thrust force above or below its nominal thrust value  $T_{e(i)}$ . The following equation calculates the force variation at the gimbal of an engine (i) due to the combined effects of gimbaling and throttling, resolved along the vehicle x, y, and z axes.

$$\begin{aligned}
 F_{xe(i)} &= T_{e(i)} \left[ -s(\Delta_E) c(\Delta_Z) \delta y_{(i)} - c(\Delta_E) s(\Delta_Z) \delta z_{(i)} + c(\Delta_E) c(\Delta_Z) Dth_{(i)} \right] \\
 F_{ye(i)} &= T_{e(i)} \left[ -s(\Delta_E) s(\Delta_Z) \delta y_{(i)} + c(\Delta_E) c(\Delta_Z) \delta z_{(i)} + c(\Delta_E) s(\Delta_Z) Dth_{(i)} \right] \\
 F_{ze(i)} &= T_{e(i)} \left[ -c(\Delta_E) \delta y_{(i)} - s(\Delta_E) Dth_{(i)} \right]
 \end{aligned} \tag{5.1.3}$$

Let us define the distances between the engine (i) gimbal to the vehicle CG,  $\{l_{xe(i)}, l_{ye(i)}, l_{ze(i)}\}$  as follows

$$l_{xe(i)} = X_{e(i)} - X_{CG} \quad l_{ye(i)} = Y_{e(i)} - Y_{CG} \quad l_{ze(i)} = Z_{e(i)} - Z_{CG} \tag{5.1.4}$$

The roll, pitch, and yaw moments on the vehicle resulting from the forces generated by a single engine (i) are obtained from the following matrix equation

$$\begin{bmatrix} L_{e(i)} \\ M_{e(i)} \\ N_{e(i)} \end{bmatrix} = \begin{bmatrix} 0 & -l_{zei} & l_{yei} \\ l_{zei} & 0 & -l_{xei} \\ -l_{yei} & l_{xei} & 0 \end{bmatrix} \begin{bmatrix} F_{xe(i)} \\ F_{ye(i)} \\ F_{ze(i)} \end{bmatrix} \tag{5.1.5}$$

We will now calculate the force and moment variations in the vehicle body axes produced by each effector independently. That is, due to gimbaling, throttling, and also due to a control surface deflection. The effect of each effector will be added up to derive an expression for the total vehicle moment due to the contributions from all vehicle effectors. One further detail that will be considered in the mixing logic calculations is the maximum effectiveness of each effector. This consideration is important because the various engines or aero surfaces may have different max gimbaling angles or throttling capabilities. We must derive, therefore, a mixing law that will utilize the effector contributions according to their effectiveness, by spreading the control authority evenly among the effectors proportionally according to their capabilities. This type of mixing logic maximizes the control effectiveness by allowing all the effectors to reach saturation simultaneously. For example, if two engines have equal thrust but different gimbaling capabilities, the engine with the larger rotational capability should be allowed to deflect at a larger angle than the engine with the smaller rotation range.

### 5.3.2 Moments and Forces Generated by a Single Engine Gimbaling in Pitch and Yaw

Consider an engine (i) which is mounted at fixed elevation and yaw angles  $D_Y(i)$  and  $D_E(i)$  respectively, see figure (5.3). The engine is further gimbaling at small angles  $\delta y(i)$  and  $\delta z(i)$  in pitch and yaw directions with respect to the fixed orientation. The moment variations on the vehicle are obtained from the equation (5.2.1).

$$\begin{pmatrix} L_{g(i)} \\ M_{g(i)} \\ N_{g(i)} \end{pmatrix} = T_{e(i)} \begin{pmatrix} 0 & -l_{zei} & l_{yei} \\ l_{zei} & 0 & -l_{xei} \\ -l_{yei} & l_{xei} & 0 \end{pmatrix} \begin{pmatrix} -c(\Delta_Z)s(\Delta_E) & -c(\Delta_E)s(\Delta_Z) \\ -s(\Delta_Z)s(\Delta_E) & +c(\Delta_E)c(\Delta_Z) \\ -c(\Delta_E) & 0 \end{pmatrix} \begin{pmatrix} \delta_{y(i)} \\ \delta_{z(i)} \end{pmatrix} \quad (5.2.1)$$

This equation can be normalized by dividing the pitch and yaw engine deflections with the max deflection capabilities in both directions, so that the normalized inputs can vary between  $\{0$  and  $\pm 1\}$  as follows:

$$\begin{pmatrix} L_{g(i)} \\ M_{g(i)} \\ N_{g(i)} \end{pmatrix} = T_{e(i)} \begin{pmatrix} 0 & -l_{zei} & l_{yei} \\ l_{zei} & 0 & -l_{xei} \\ -l_{yei} & l_{xei} & 0 \end{pmatrix} \begin{pmatrix} -c(\Delta_Z)s(\Delta_E)\delta_{y\max} & -c(\Delta_E)s(\Delta_Z)\delta_{z\max} \\ -s(\Delta_Z)s(\Delta_E)\delta_{y\max} & +c(\Delta_E)c(\Delta_Z)\delta_{z\max} \\ -c(\Delta_E)\delta_{y\max} & 0 \end{pmatrix} \begin{pmatrix} \delta_{y(i)}/\delta_{y\max} \\ \delta_{z(i)}/\delta_{z\max} \end{pmatrix}$$

By multiplying out the matrices in the above equation, it be expressed in a simplified form as follows:

$$\begin{pmatrix} L_{g(i)} \\ M_{g(i)} \\ N_{g(i)} \end{pmatrix} = \begin{pmatrix} | & | \\ V_{gyi} & V_{gzi} \\ | & | \end{pmatrix} \begin{pmatrix} \delta_{y(i)}/\delta_{y\max} \\ \delta_{z(i)}/\delta_{z\max} \end{pmatrix} \quad (5.2.3)$$

where:  $V_{gy(i)}$  and  $V_{gz(i)}$  are column vectors that correspond to the pitch and yaw engine deflections respectively.

### Forces of an Engine Gimbaling in Pitch and Yaw Directions

Similarly, the forces applied at the gimbal due to an engine (i) gimbaling in pitch and yaw can be resolved along the body x, y, and z axes and normalized by dividing the pitch and yaw deflections with the max deflections as shown in the following equation, written also in column vector form:

$$\begin{pmatrix} F_{X(i)} \\ F_{Y(i)} \\ F_{Z(i)} \end{pmatrix} = T_{e(i)} \begin{pmatrix} -c(D_Z)s(D_Y)\delta_{y\max} & -c(D_Y)s(D_Z)\delta_{z\max} \\ -s(D_Z)s(D_Y)\delta_{y\max} & +c(D_Y)c(D_Z)\delta_{z\max} \\ -c(D_Y)\delta_{y\max} & 0 \end{pmatrix} \begin{pmatrix} \delta_{y(i)}/\delta_{y\max} \\ \delta_{z(i)}/\delta_{z\max} \end{pmatrix}$$

$$\begin{pmatrix} F_{X(i)} \\ F_{Y(i)} \\ F_{Z(i)} \end{pmatrix} = \begin{pmatrix} | & | \\ U_{gyi} & U_{gzi} \\ | & | \end{pmatrix} \begin{pmatrix} \delta_{y(i)}/\delta_{y\max} \\ \delta_{z(i)}/\delta_{z\max} \end{pmatrix} \quad (5.2.4)$$

where:  $U_{gy(i)}$  and  $U_{gz(i)}$  are column vectors that correspond to the pitch and yaw engine deflections respectively.

### 5.3.3 Moments and Forces of an Engine Gimbaling in a Single Skewed Direction

A vehicle with multiple engines may have sufficient degrees of freedom to be maneuvered by gimbaling some of the engines in a single direction instead of two (pitch and yaw). Single axis engine gimbaling requires fewer actuators and saves on weight and cost. Figure (5.4) shows a single gimbaling engine that rotates only about an axis that is skewed at an angle  $\gamma(i)$ . The engine is mounted at fixed  $D_Y(i)$  and  $D_E(i)$  orientation (or trim) angles and it can gimbal in a direction defined by an angle  $\gamma(i)$  from its mounting position. The roll, pitch, and yaw moments on the vehicle generated by a single gimbaling engine (i) that is gimbaling at a skewed direction  $\gamma(i)$  are shown in equation (5.3.2). In the mixing logic program the gimbaling direction angle  $\gamma_{e(i)}$  of a single gimbaling TVC engine is defined by the maximum pitch and yaw deflection angles  $\delta y_{\max}$  and  $\delta z_{\max}$  which are included in the input data.

$$\gamma_{e(i)} = \tan^{-1} \left\{ \frac{\delta z_{\max}}{\delta y_{\max}} \right\} \quad (5.3.1)$$

The deflection angle ( $\delta_\gamma$ ) is in the direction  $\gamma_{e(i)}$ , and it can be resolved in pitch and yaw components.

$$\delta_{y(i)} = \delta\gamma_{(i)} \cos(\gamma_{e(i)}) \quad \delta_{z(i)} = \delta\gamma_{(i)} \sin(\gamma_{e(i)})$$

Engine Gimbaling in a Single Skewed Direction ( $\gamma_{ei}$ )

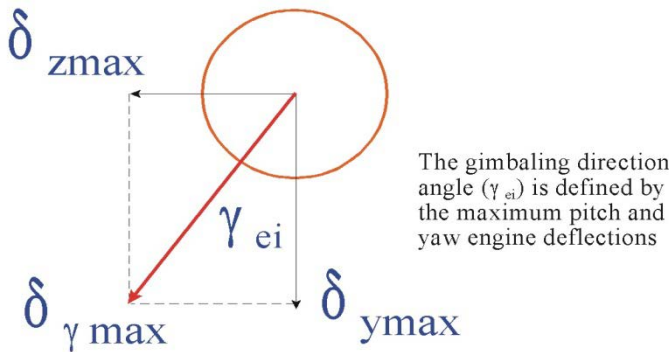


Fig. (5.4)

The roll, pitch, and yaw moments on the vehicle generated by a single gimbaling engine (i) are obtained from the following normalized equation, written also in column vector form

$$\begin{pmatrix} L_{g(i)} \\ M_{g(i)} \\ N_{g(i)} \end{pmatrix} = \delta\gamma_{\max} T_{e(i)} \begin{pmatrix} 0 & -l_{zei} & l_{yei} \\ l_{zei} & 0 & -l_{xei} \\ -l_{yei} & l_{xei} & 0 \end{pmatrix} \begin{pmatrix} -c(\Delta_Z)s(\Delta_E)c(\gamma_{ei}) - c(\Delta_E)s(\Delta_Z)s(\gamma_{ei}) \\ -s(\Delta_Z)s(\Delta_E)c(\gamma_{ei}) + c(\Delta_E)c(\Delta_Z)s(\gamma_{ei}) \\ -c(\Delta_E)\cos(\gamma_{ei}) \end{pmatrix} \left( \delta\gamma_{(i)} / \delta\gamma_{\max} \right)$$

$$\begin{pmatrix} L_{g(i)} \\ M_{g(i)} \\ N_{g(i)} \end{pmatrix} = \begin{pmatrix} | \\ V_{g\gamma(i)} \\ | \end{pmatrix} \left( \delta\gamma_{(i)} / \delta\gamma_{\max} \right)$$

(5.3.2)

where:  $V_{g\gamma(i)}$  is a column vector, and the normalized input  $\{\delta\gamma / \delta\gamma_{\max}\}$  varies from  $\{0$  to  $\pm 1\}$ . The forces in the x, y and z directions are also obtained from a similar equation (5.3.3).

$$\begin{pmatrix} F_{X(i)} \\ F_{Y(i)} \\ F_{Z(i)} \end{pmatrix} = \delta\gamma_{\max} T_{e(i)} \begin{pmatrix} -c(\Delta_Z)s(\Delta_E)c(\gamma_{ei}) - c(\Delta_E)s(\Delta_Z)s(\gamma_{ei}) \\ -s(\Delta_Z)s(\Delta_E)c(\gamma_{ei}) + c(\Delta_E)c(\Delta_Z)s(\gamma_{ei}) \\ -c(\Delta_E)\cos(\gamma_{ei}) \end{pmatrix} \left( \delta\gamma_{(i)} / \delta\gamma_{\max} \right)$$

$$\begin{pmatrix} F_{X(i)} \\ F_{Y(i)} \\ F_{Z(i)} \end{pmatrix} = \begin{pmatrix} | \\ U_{g\gamma(i)} \\ | \end{pmatrix} \left( \delta\gamma_{(i)} / \delta\gamma_{\max} \right) \quad (5.3.3)$$

### 5.3.4 Moments and Forces Generated by a Throttling Engine or an RCS Jet

Similarly, the change in moments on the vehicle generated by throttling an engine (j) or by an RCS jet which is mounted at fixed orientation angles  $D_Y(i)$  and  $D_E(i)$  with respect to the vehicle -x axis, can be obtained from the following equation

$$\begin{pmatrix} L_{T(i)} \\ M_{T(i)} \\ N_{T(i)} \end{pmatrix} = T_{R(i)} \begin{pmatrix} 0 & -l_{zei} & l_{yei} \\ l_{zei} & 0 & -l_{xei} \\ -l_{yei} & l_{xei} & 0 \end{pmatrix} \begin{pmatrix} c(\Delta_E)c(\Delta_Z) \\ c(\Delta_E)s(\Delta_Z) \\ -s(\Delta_E) \end{pmatrix} \left( D_{Th(i)} \right)$$

Where  $T_{R(j)}$  is the nominal engine thrust and  $D_{Th(j)}$  is the throttle control input. The throttle input can vary between  $\{0 \text{ and } \pm D_{Th\max}\}$ , where the maximum throttle input  $|D_{Th\max}| < 1$ . The product  $(T_{R(j)} * D_{Th(j)})$  represents the thrust force variation, above or below the nominal thrust value  $T_{R(j)}$ . The throttle input can be normalized in a similar fashion as in the TVC equation so that the normalized throttle input  $(D_{Th(j)} / D_{th\max})$  varies from:  $\{0 \text{ to } \pm 1\}$ . The roll, pitch, and yaw moment variations due to a throttling engine or an RCS jet are:

$$\begin{pmatrix} L_{T(i)} \\ M_{T(i)} \\ N_{T(i)} \end{pmatrix} = D_{Th\max} T_{R(i)} \begin{pmatrix} 0 & -l_{zei} & l_{yei} \\ l_{zei} & 0 & -l_{xei} \\ -l_{yei} & l_{xei} & 0 \end{pmatrix} \begin{pmatrix} c(\Delta_E)c(\Delta_Z) \\ c(\Delta_E)s(\Delta_Z) \\ -s(\Delta_E) \end{pmatrix} \left( \frac{D_{Th(i)}}{D_{Th\max}} \right)$$

$$\begin{pmatrix} L_{T(i)} \\ M_{T(i)} \\ N_{T(i)} \end{pmatrix} = \begin{pmatrix} | \\ V_{T(i)} \\ | \end{pmatrix} \left( \frac{D_{Th(i)}}{D_{Th\max}} \right) \quad (5.4.1)$$

Similarly the forces in the x, y and z directions are obtained from equation (5.4.2)

$$\begin{pmatrix} F_{X(i)} \\ F_{Y(i)} \\ F_{Z(i)} \end{pmatrix} = D_{Th\max} T_{R(i)} \begin{pmatrix} c(Dy)c(Dz) \\ c(Dy)s(Dz) \\ -s(Dy) \end{pmatrix} \left( \frac{D_{Th(i)}}{D_{Th\max}} \right) = \begin{pmatrix} | \\ U_{T(i)} \\ | \end{pmatrix} \left( \frac{D_{Th(i)}}{D_{Th\max}} \right) \quad (5.4.2)$$

where:  $V_{T(j)}$  and  $U_{T(j)}$  are column vectors.

### 5.3.5 Moments and Forces Generated by a Control Surface Deflection

The change in vehicle moments generated by a control surface (i) that is deflecting at an angle  $\delta_{csi}$  is:

$$\begin{pmatrix} L_{CS(i)} \\ M_{CS(i)} \\ N_{CS(i)} \end{pmatrix} = \bar{Q} S_{ref} \begin{pmatrix} l_{sp} C_{l\delta cs(i)} \\ l_{ch} C_{m\delta cs(i)} \\ l_{sp} C_{nl\delta cs(i)} \end{pmatrix} \delta_{cs(i)}$$

Where  $l_{ch}$  is the mean aerodynamic chord and ( $l_{sp}$ ) is the wing span aero reference lengths. The above equation is normalized using the maximum control surface deflection capability  $\delta_{csi\max}$ , so that the normalized control surface input can vary from: {0 to  $\pm 1$ }. The normalized equations for the moments and forces are:

$$\begin{pmatrix} L_{CS(i)} \\ M_{CS(i)} \\ N_{CS(i)} \end{pmatrix} = \bar{Q} S_{ref} \delta_{csi\max} \begin{pmatrix} l_{sp} C_{l\delta cs(i)} \\ l_{ch} C_{m\delta cs(i)} \\ l_{sp} C_{nl\delta cs(i)} \end{pmatrix} \begin{pmatrix} \delta_{csi} \\ \delta_{csi\max} \end{pmatrix} = \begin{pmatrix} | \\ | \\ | \end{pmatrix} \begin{pmatrix} \delta_{csi} \\ \delta_{csi\max} \end{pmatrix}$$

$$\begin{pmatrix} F_{X(i)} \\ F_{Y(i)} \\ F_{Z(i)} \end{pmatrix} = \bar{Q} S_{ref} \delta_{csi\max} \begin{pmatrix} -C_{A\delta as1} \\ C_{Y\delta as1} \\ C_{Z\delta as1} \end{pmatrix} \begin{pmatrix} \delta_{csi} \\ \delta_{csi\max} \end{pmatrix} = \begin{pmatrix} | \\ | \\ | \end{pmatrix} \begin{pmatrix} \delta_{csi} \\ \delta_{csi\max} \end{pmatrix} \quad (5.4.3)$$

where:  $V_{AS(j)}$  and  $U_{AS(j)}$  are column vectors.

### 5.3.6 Change in Vehicle Rate due to the Combined Effect from All Actuators

The total moment and forces on the vehicle are obtained by the superposition of the individual moments and forces from each effector. That is, the TVC engines, the throttling engines, the RCS jets, and the control surface deflections. The combined effectors moment matrix is obtained by stacking up the column vectors  $\{V_{X(i)}\}$  from each individual effector. The following equation (5.4.4) converts the normalized effector deflections to vehicle accelerations or change in rates ( $\delta P$ ,  $\delta Q$ ,  $\delta R$ ). It is also written in matrix form.

$$\begin{pmatrix} \delta P \\ \delta Q \\ \delta R \end{pmatrix} = \begin{pmatrix} I_{XX} & -I_{XY} & -I_{XZ} \\ -I_{XY} & I_{YY} & -I_{YZ} \\ -I_{XZ} & -I_{YZ} & I_{ZZ} \end{pmatrix}^{-1} *$$

$$\left\{ \begin{matrix} V_{gy1} & V_{gz1} & V_{gy2} & V_{gz2} & V_{gy1} & V_{gz2} & V_{T1} & V_{T2} & V_{T3} & V_{AS1} & V_{AS2} \end{matrix} \right\} \begin{bmatrix} \delta_{y1}/\delta_{y1 \max} \\ \delta_{z1}/\delta_{z1 \max} \\ \delta_{y2}/\delta_{y2 \max} \\ \delta_{z2}/\delta_{z2 \max} \\ \delta\gamma_1/\delta\gamma_{1 \max} \\ \delta\gamma_2/\delta\gamma_{2 \max} \\ D_{Th1}/D_{Th1 \max} \\ D_{Th2}/D_{Th2 \max} \\ D_{Th3}/D_{Th3 \max} \\ \delta_{as1}/\delta_{as1 \max} \\ \delta_{as2}/\delta_{as2 \max} \end{bmatrix}$$

$$\text{or } (\delta \underline{R}_o) = I_n^{-1} [V] (\underline{\delta}/\underline{\delta}_{\max}) \quad (5.6.1)$$

Similarly, the translational accelerations due to the normalized effector deflections are obtained from the following F=m\*a equation:

$$\begin{pmatrix} A_x \\ A_y \\ A_z \end{pmatrix} = \left( \frac{1}{m_v} \right) *$$

$$\left\{ \begin{matrix} U_{gy1} & U_{gz1} & U_{gy2} & U_{gz2} & U_{gy1} & U_{gz2} & U_{T1} & U_{T2} & U_{T3} & U_{AS1} & U_{AS2} \end{matrix} \right\} \begin{bmatrix} \delta_{y1}/\delta_{y1 \max} \\ \delta_{z1}/\delta_{z1 \max} \\ \delta_{y2}/\delta_{y2 \max} \\ \delta_{z2}/\delta_{z2 \max} \\ \delta\gamma_1/\delta\gamma_{1 \max} \\ \delta\gamma_2/\delta\gamma_{2 \max} \\ D_{Th1}/D_{Th1 \max} \\ D_{Th2}/D_{Th2 \max} \\ D_{Th3}/D_{Th3 \max} \\ \delta_{as1}/\delta_{as1 \max} \\ \delta_{as2}/\delta_{as2 \max} \end{bmatrix}$$

$$\text{or } (\delta \underline{A}_c) = m_v^{-1} [U] (\underline{\delta}/\underline{\delta}_{\max}) \quad (5.6.2)$$

By combining the two previous equations together we obtain the matrix equation (5.6.3)

$$\begin{pmatrix} \underline{\delta R_o} \\ \underline{\delta A_c} \end{pmatrix} = [A] \left( \underline{\delta} / \underline{\delta_{\max}} \right) \quad \text{where: } [A] = \begin{bmatrix} I_n^{-1} V \\ m_v^{-1} U \end{bmatrix} \quad (5.6.3)$$

The above equation calculates the change in vehicle accelerations resulting due to the normalized effector deflections input vector  $\{\underline{d}/\underline{d_{\max}}\}$ , where each input varies from  $\{0 \text{ to } \pm 1\}$ . The elements of the following diagonal matrix  $[D_{\max}]$  consist of the maximum deflections of each effector, as follows:

$$D_{\max} = \text{diag} \left\{ \delta_{y1\max} \quad \delta_{z1\max} \quad \delta_{y2\max} \quad \delta_{z2\max} \quad \delta_{y3\max} \quad \delta_{z3\max} \quad \delta_{\gamma 1\max} \cdots D_{th1\max} \quad D_{th2\max} \cdots \delta_{cs1\max} \quad \delta_{cs2\max} \right\}$$

The mixing logic matrix is obtained by solving the pseudo-inverse of the above matrix equation, as shown below. A solution exists when the number of effectors are greater than or equal to the number of degrees of freedom to be controlled (the number of rotations plus the number of translations). That is, when all control directions are spanned by the effectors, and the mixing logic matrix has full rank. After solving the pseudo inverse a typical mixing logic matrix has the following form and it translates the demanded changes in vehicle rates ( $\delta R_o$ ) and accelerations ( $\delta A_c$ ) to effector commands  $\delta_{com}$ .

$$\delta_{com} = D_{\max} A^T [A A^T]^{-1} \begin{pmatrix} \underline{DR} \\ \underline{DAc} \end{pmatrix} \quad \text{or} \quad \begin{bmatrix} \delta_{y1} \\ \delta_{z1} \\ \delta_{y2} \\ \delta_{z2} \\ \delta_{\gamma 1} \\ \delta_{\gamma 2} \\ D_{Th1} \\ D_{Th2} \\ D_{Th3} \\ \delta_{as1} \\ \delta_{as2} \end{bmatrix} = \begin{bmatrix} X & X & X & X & X & X \\ X & X & X & X & X & X \\ X & X & X & X & X & X \\ X & X & X & X & X & X \\ X & X & X & X & X & X \\ X & X & X & X & X & X \\ X & X & X & X & X & X \\ X & X & X & X & X & X \\ X & X & X & X & X & X \\ X & X & X & X & X & X \\ X & X & X & X & X & X \end{bmatrix} \begin{pmatrix} DP \\ DQ \\ DR \\ DA_x \\ DA_y \\ DA_z \end{pmatrix}$$

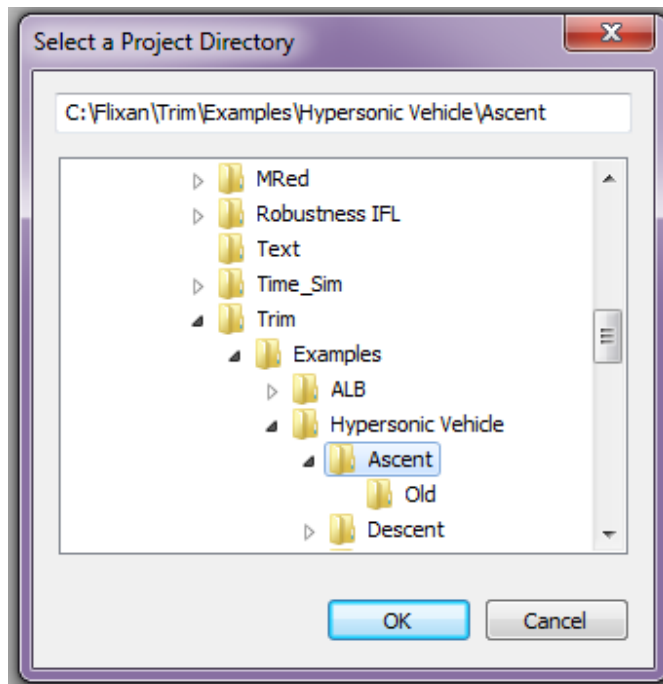


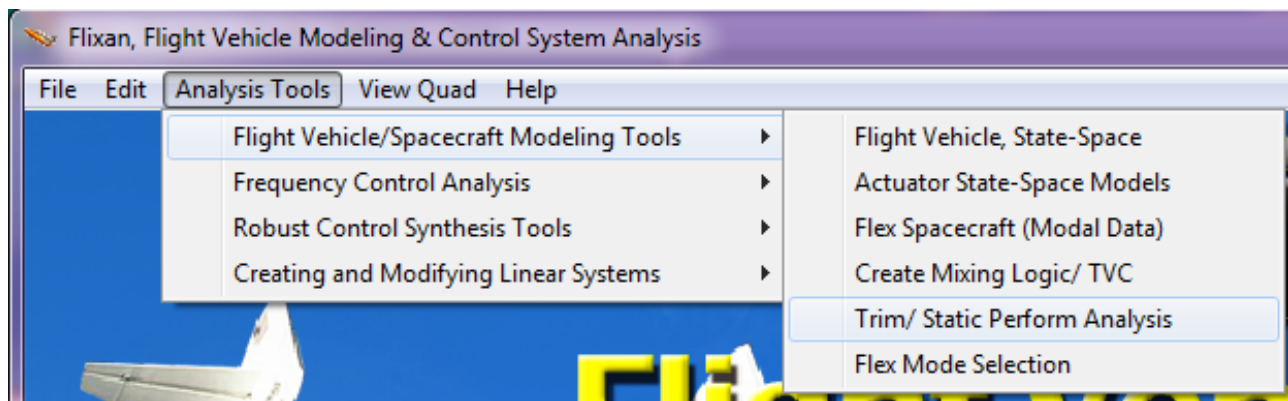
# 9.6 Generating State-Space Models for Linear Control Analysis

---

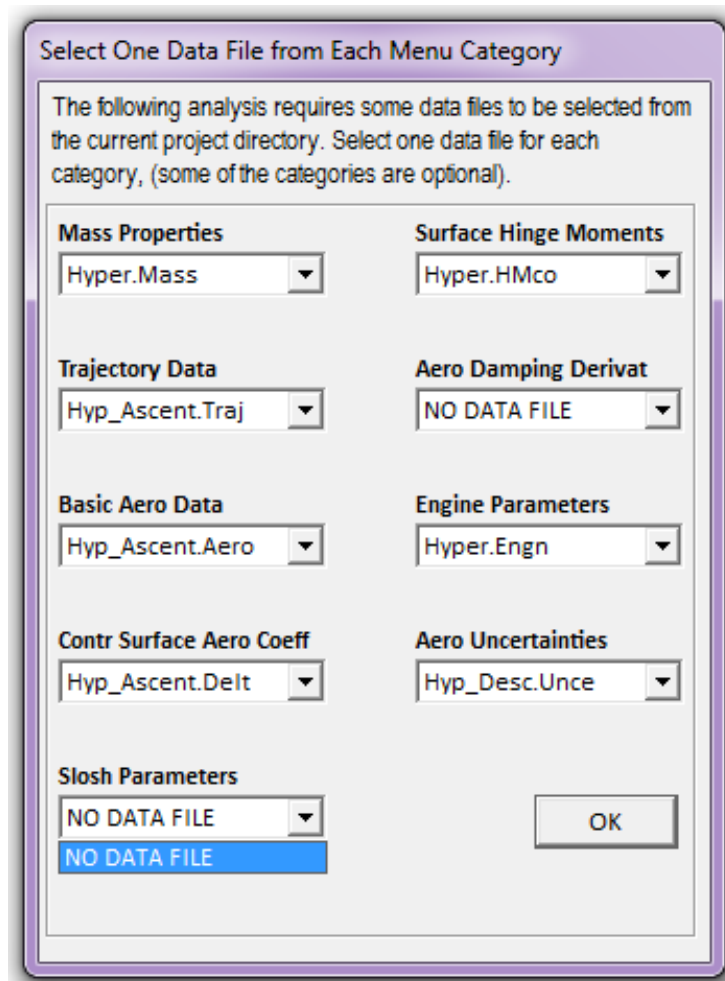
One of the most important functions of the Trim program is its capability of generating input data for the "Flight Vehicle Modeling Program". The FVMP is a Flixan program that calculates linear dynamic models for flight control analysis, simulation and design. After trimming the effectors the analyst can select some critical flight condition points along the trajectory and create dynamic models for those flight cases. The state-space modeling option can either be selected from the Trim main menu or from the menu bar on the top of a trajectory plot. The user is prompted to select a flight time along the trajectory and the program collects the vehicle data that correspond to this flight time from various file sources. The vehicle data are saved as a data-set in standard Flixan input file (.Inp) format and the FVMP reads them, processes them, creates the required dynamic systems in state-space form, and it saves them in a Flixan systems file (.Qdr). To run this program from a trajectory plot, go to the top menu bar of the trajectory window, click on "*Graphic Options*" and then "*Select Time to Create a State-Space System*". So let's take a look at the following example.

From Flixan you must select the project folder that contains the analysis files, such as: trajectory, mass, engine, and control surface aero data. The files must be in the proper format for the program to be able to read them. From the Flixan main menu select "*Analysis Tools*", then "*Flight Vehicle/ Spacecraft Modeling Tools*", and "*Trim/ Static Performance Analysis*".

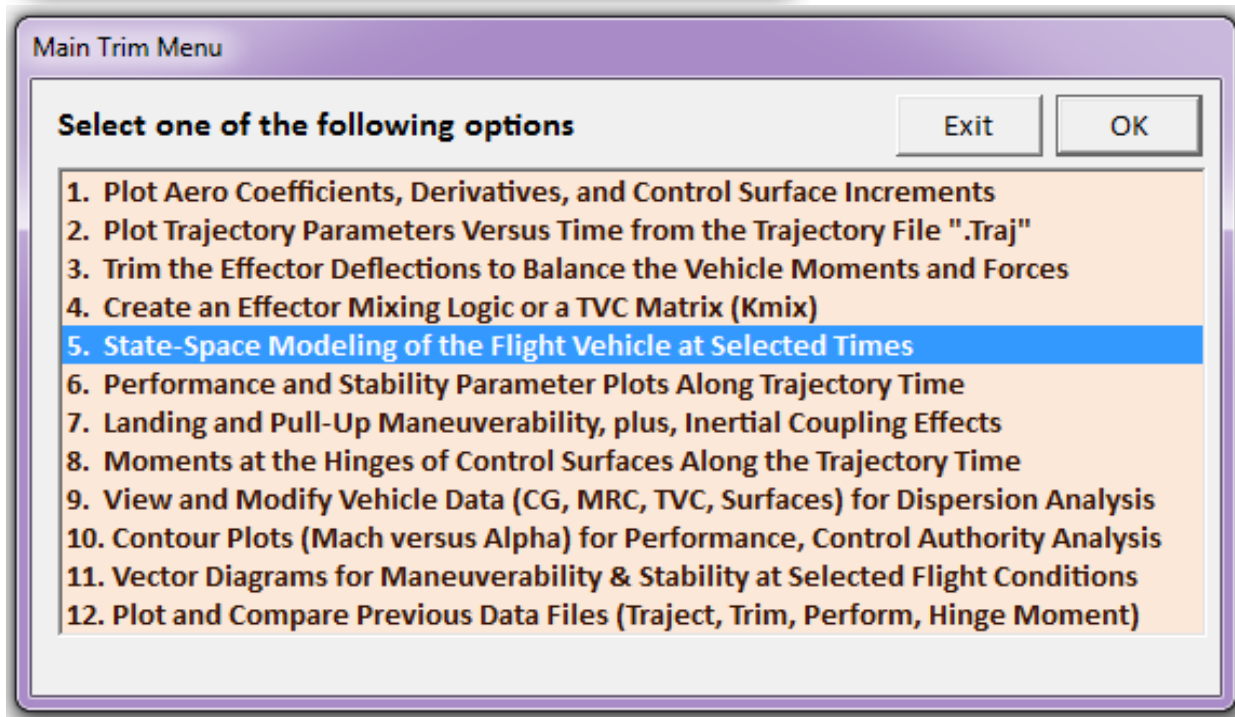
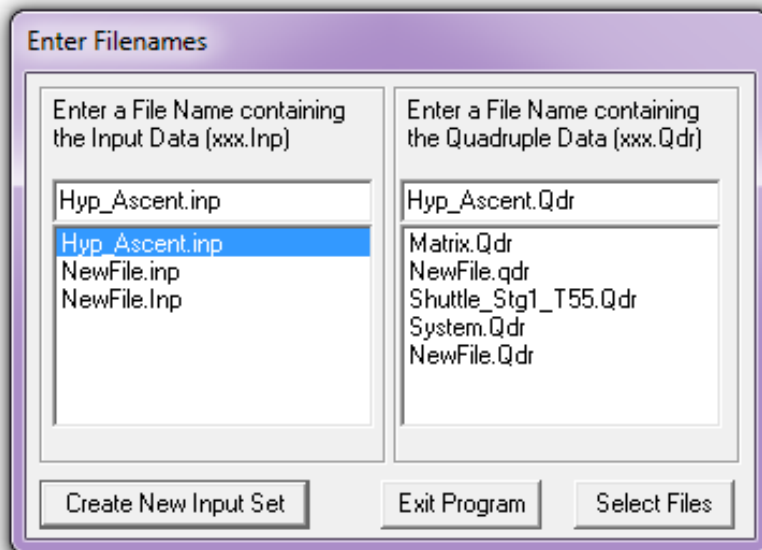




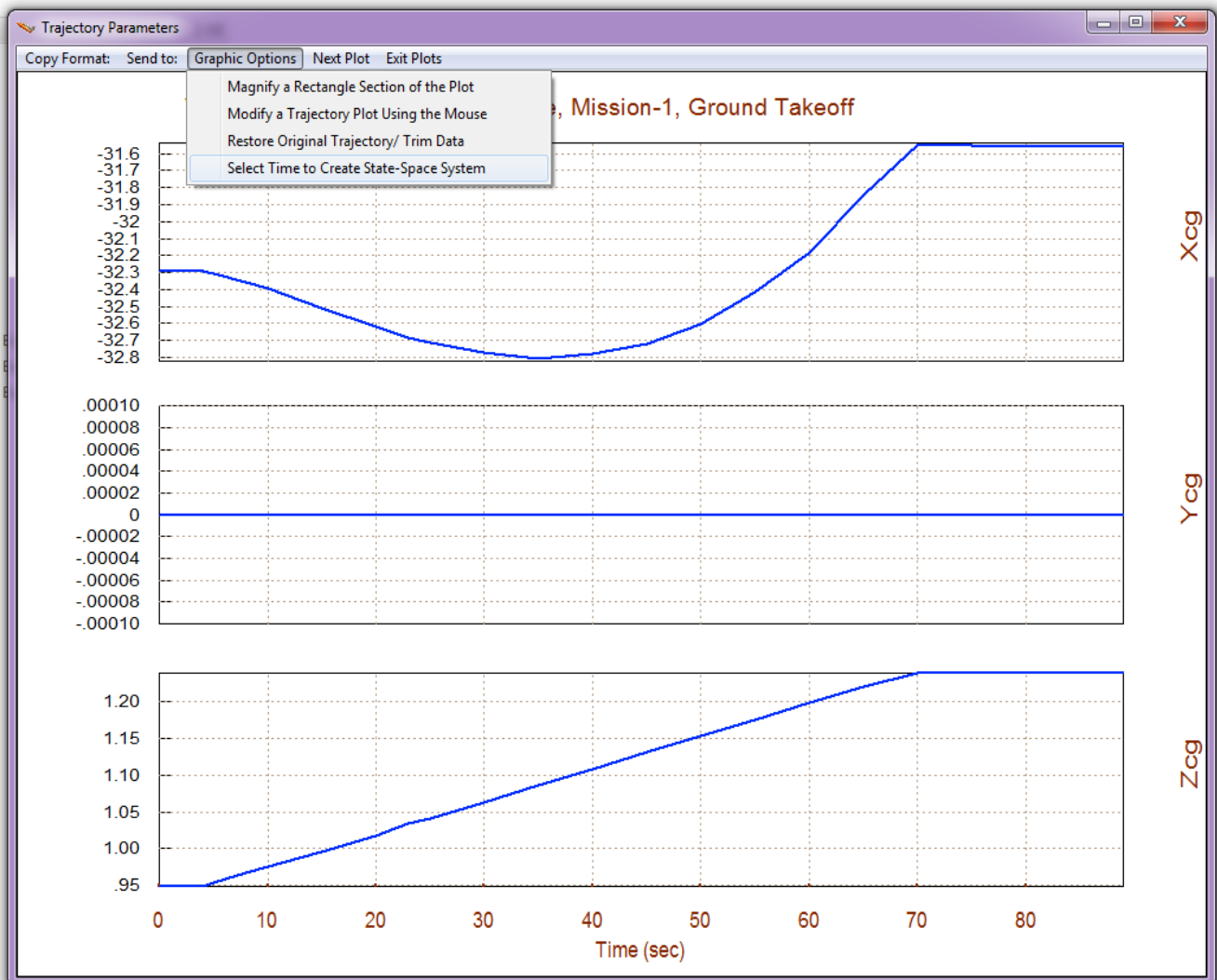
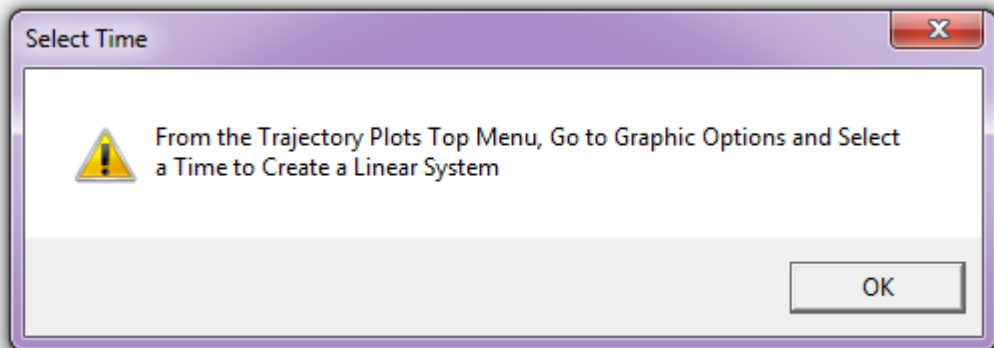
From the following file selection menu select the files that will be used by the Trim program. Some of the files like the slos parameters, hinge moment coefficients, aero uncertainties, and damping derivatives are optional. If they are missing you will not be able to perform some analysis, like for example, uncertainties evaluation or to calculate the hinge moments. The slos parameters are only used by Trim for the creation of linear systems by the FVMP.



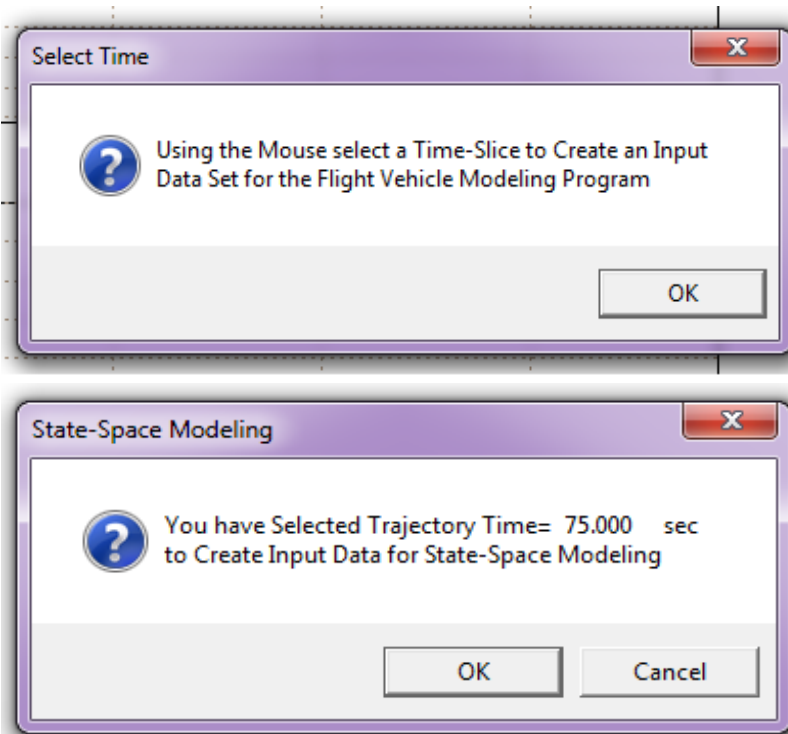
Also from the input/ output filename menu, select an input data file and systems file. In this case, the input data file "*Hyp\_Ascent.Inp*" will receive the vehicle data to be processed by the FVMP, and the state-space models will be saved in the systems file "*Hyp\_Ascent.Qdr*". Then from the Trim main menu select the option (5) which generates state-space models, and click "OK".



It is important to have the effectors trimmed before starting this option. The program searches for a (.Trim) file and if it does not find one it trims the effectors as already described. The user must select a time point at which time the program will generate the vehicle input data. The flight condition time point is selected from one of the trajectory plots as described in the instructions below. To select a time point, go to the horizontal menu bar on top of the trajectory plot and select "Graphic Options". From the vertical pop-up menu select the last option which is "Select Time to Create a State-Space System".



Then place the mouse cursor at a point along the horizontal time scale that corresponds to the time where you want to create a linear system. In this example we pick a time  $t=75$  sec, and click the mouse. The following dialog confirms your selection time and it also allows you to cancel and select another time, in case you picked the wrong time.



At this point the "Flight Vehicle Modeling Program" dialog comes up showing the flight vehicle input data corresponding to our selected flight condition. The data have been collected from various vehicle data files but they are not yet saved to a Flixan input file. This dialog allows us to take a look at the data first before saving and processing them by FVMP. The user may update some of the numbers and titles. Remember to click on the "Update Data" button after every modification. The input data file can also be edited directly by clicking on "Edit Input File". When the modifications are complete and ready to save the vehicle data you must click on "Save in File" button and the vehicle input data will be saved in the selected file, which is "Hyp\_Ascent.Inp". If you click on "Run", the "Flight Vehicle Modeling Program" will generate the state-space system at the selected flight condition and it will save it in the selected file "Hyp\_Ascent.Qdr".

In the examples section we will also demonstrate how to use some of the Flixan utilities to perform other related functions, such as: combining the vehicle model with the effector mixing matrix or actuators, creating effector combination matrices directly from vehicle data, modifying existing dynamic models, creating pitch and lateral design models and synthesizing LQR flight control laws, creating models for frequency domain analysis and simulations, performing stability analysis (gain, phase margins, etc), creating uncertainty models for  $\mu$ -analysis, and converting dynamic models and matrices to Matlab functions that can be loaded into Matlab for further analysis.

Flight Vehicle Parameters

**Vehicle System Title**  
 Rocket-Plane, Mission-1, Ground Takeoff/ T= 75.0 sec

**Number of Vehicle Effectors**  
 Gimbal Engines or Jets. Include Tail-Wags-Dog? 1    
 Rotating Control Surfaces. Include Tail-Wags-Dog? 4    
 Reaction Wheels? 0  
 Single Gimbal CMGs? 0  
**Momentum Control Devices**  
 Include a 3-axes Stabilized Double Gimbal CMG System?

**Number of Sensors**  
 Gyros 0  
 Acceleromet 3  
 Aero Vanes 0  
 External Torques 0

**Modeling Options (Flags)**  
 Output Rates in:    
 Turn Coordination?:    
 Aero-Elasticity Options:    
 Attitude Angles:

**Number of Modes**  
 Structure Bending 0  
 Fuel Sloshing 0

Reaction Wheels | Single Gimbal CMGs | Double Gimbal CMG System | Slewing Appendages | Gyros | Accelerometer | Aero Sensors | Fuel Slosh | Flex Modes | User Notes  
 Mass Properties | Trajectory Data | Gust/ Aero Paramet. | Aero Force Coeffs | Aero Moment Coeffs | Control Surfaces | Gimbal Engines/ RCS | External Torques

**This Vehicle has 4 Control Surfaces** | **Control Surface No: 1 Elevon** | Surface Definition |

**Surface Rotation Angles**  
 Surface Trim Position (deg) -7.869500  
 Largest Positive Deflection from Trim (deg) 20.00000  
 Largest Negative Deflection from Trim (deg) -20.00000

**Surface Location (ft) and Hinge Orientation Angles (deg)**  
 Xcs -41.40000  
 Ycs 0.000000  
 Zcs 2.000000  
 Phi\_cs 0.000000  
 Lambda\_cs 0.000000

**Control Surface Mass Properties**  
 Control Surface Mass in (Slugs) 10.00000  
 Moment of Inertia about Hinge (slug-ft<sup>2</sup>) 100.0000  
 Moment Arm (feet), Surface CG to Hinge 2.000000  
 Control Surface Chord (feet) 2.360000  
 Control Surface Reference Area (ft<sup>2</sup>) 11.81000

**Aero Force Derivatives**  
 Ca\_delta -0.2808500E-03  
 Cy\_delta 0.000000  
 Cz\_delta -0.2655500E-02  
 Ca\_delta\_dot 0.000000  
 Cy\_delta\_dot 0.000000  
 Cz\_delta\_dot 0.000000  
 Control Force Derivatives due to Surface Deflection (1/deg) and Control Force Derivatives due to Surface Rate (1/deg/sec)

**Aero Moment Derivatives**  
 Cl\_delta 0.000000  
 Cm\_delta -0.5580000E-03  
 Cn\_delta 0.000000  
 Cl\_delta\_dot 0.000000  
 Cm\_delta\_dot 0.000000  
 Cn\_delta\_dot 0.000000  
 Control Moment Derivatives due to Surface Deflection (1/deg) and Control Moment Derivatives due to Surface Rate (1/deg/sec)

**Hinge Moment Derivatives**  
 Chm\_Alpha -0.1233500E-01  
 Chm\_Beta 0.000000  
 Chm\_Delta -0.1158500E-01  
 Chm\_Mach -0.2095000E-01  
 Hinge Moment Derivatives with respect to Changes in: Alpha, Beta, Surf Deflection (1/deg) and changes in Mach Number

The following table shows the set of flight vehicle input data generated by Trim for our example. The data is in file "Hyp\_Ascent.Inp". Its title is: "Rocket-Plane, Mission-1, Ground Takeoff/ T= 75.0 sec". The first part of the title is copied from the trajectory file. The flight time is also added at the end of the title. The state-space system created is in file "Hyp\_Ascent.Qdr" and it has the same title. Similar dynamic models can be generated by the FVMP for other critical times along the trajectory. These models are used for analysis, control design, and simulations, as it is demonstrated in the examples section 10.

FLIGHT VEHICLE INPUT DATA .....  
 Rocket-Plane, Mission-1, Ground Takeoff/ T= 75.0 sec  
 ! This Flight Vehicle Model is created by the Trim program which combines various types of data  
 ! files such as: trajectory, mass properties, engine, and basic aero and control surface  
 ! coefficients data. A Linear State-Space model of the vehicle is created at a selected trajectory  
 ! flight time. The user may modify the input data or add more options either by editing the input  
 ! file directly or by means of the window dialogs which are available in the Flight Vehicle  
 ! Modeling program.  
 Body Axes Output:Attitude-Euler Angles,No GAFD-Hpar, No Turn Coordination

Vehicle Mass (lb-sec<sup>2</sup>/ft), Gravity Accelerat. (g) (ft/sec<sup>2</sup>), Earth Radius (Re) (ft) : 493.900 : 32.1740 : 0.208960E+08 : 0.00000 : 669.178 : 0.00000  
 Moments and products of Inertias Ixx, Iyy, Izz, -Ixy, -Ixz, -Iyz, in (lb-sec<sup>2</sup>-ft) : 9409.14 : 87306.1 : 52579.4 : 0.00000 : 0.00000 : 0.00000  
 CG location with respect to the Vehicle Reference Point, Xcg, Ycg, Zcg, in (feet) : -31.5539 : 0.00000 : 1.24000 : 0.00000 : 0.00000 : 0.00000  
 Vehicle Mach Number, Velocity Vo (ft/sec), Dynamic Pressure (psf), Altitude (feet) : 3.43000 : 3224.00 : 825.900 : 68550.0 : 0.00000 : 0.00000  
 Inertial Acceleration Vo\_dot, Sensed Body Axes Accelerations Ax,Ay,Az (ft/sec<sup>2</sup>) : 79.00000 : 91.05000 : 31.85000 : 0.00000 : 0.00000 : 0.00000  
 Angles of Attack and Sideslip (deg), alpha, beta rates (deg/sec) : -4.03700 : 0.00000 : -0.266000E-01 : 0.00000 : 0.00000 : 0.00000  
 Vehicle Attitude Euler Angles, Phi\_o,Theta,Psi\_o (deg), Body Rates P,Q,Ro (deg/sec) : 0.00000 : 12.3130 : 0.00000 : 0.00000 : 0.00000 : 0.00000  
 W-Gust Asim & Elev angles (deg), or Torque/Force direction (x,y,z), Force Locat (x,y,z) : Gust : 45.0000 : 90.0000 : 30.0000 : 0.00000 : 0.00000 : 0.00000  
 Surface Reference Area (feet<sup>2</sup>), Mean Aerodynamic Chord (ft), Wing Span in (feet) : 390.640 : 50.0000 : 30.8090 : 0.00000 : 0.00000 : 0.00000  
 Aero Moment Reference Center (Xmrc,Ymrc,Zmrc) Location in (ft), {Partial\_rho/ Partial\_H} : -31.5000 : 0.00000 : 0.00000 : 0.00000 : 0.00000 : 0.00000  
 Aero Force Coef/Deriv (1/deg), Along -X, {Cao,Ca\_alif,PCa/FV,PCa/Ph,Ca\_alifdot,Ca\_g,Ca\_bet} : 0.254182E-01 : 0.102237E-02 : -0.556962E-05 : 0.00000 : 0.00000 : 0.00000  
 Aero Force Coeff/Derivat (1/deg), Along Y, {Cyo,Cy\_bet,Cy\_x,Cy\_alf,Cy\_p,Cy\_betdot,Cy\_V} : 0.00000 : -0.148280E-01 : 0.00000 : 0.00000 : 0.00000 : 0.00000  
 Aero Force Coeff/Deriv (1/deg), Along Z, {Czo,Cz\_alif,Cz\_g,Cz\_bet,PCz/Ph,Cz\_alifdot,PCz/FV} : 0.253852E-01 : -0.305543E-01 : 0.00000 : 0.00000 : 0.00000 : 0.00000  
 Aero Moment Coeff/Derivat (1/deg), Roll: {Clo, Cl\_beta, Cl\_betdot, Cl\_p, Cl\_r, Cl\_alfa} : 0.00000 : 0.474400E-03 : 0.00000 : 0.00000 : 0.00000 : 0.00000  
 Aero Moment Coeff/Deriv (1/deg), Pitch: {Cmo,Cm\_alfa,Cm\_alifdot,Cm\_bet,Cm\_g,PCm/FV,PCm/Ph} : 0.747483E-03 : -0.410636E-03 : 0.00000 : 0.00000 : 0.00000 : 0.00000  
 Aero Moment Coeff/Derivat (1/deg), Yaw : {Cno,Cn\_beta,Cn\_betdot,Cn\_p,Cn\_r,Cn\_alfa} : 0.00000 : 0.563400E-03 : 0.00000 : 0.00000 : 0.00000 : 0.00000

Number of Control Surfaces, With or No TWD (Tail-Wags-Deg and Hinge Moment Dynamics) ? : 4 NO TWD

Control Surface No: 1 Elevon  
 Trim Angle, Max/Min Deflection Angles from Trim, Hinge Line Angles: Phi\_h, Lambda\_h (deg) : -7.86950 : 20.0000 : -20.0000 : 0.00000 : 0.00000 : 0.00000  
 Surface Mass, Inertia about Hinge, Moment Arm (Hinge to Surface CG), Surface Chord, Area : 10.0000 : 100.000 : 2.00000 : 2.36000 : 11.8100 : 0.00000  
 Hinge Moment Derivatives (1/deg), { Chm\_Alpha, Chm\_Beta, Chm\_Delta, Chm\_Mach } : -0.123350E-01 : 0.00000 : -0.115850E-01 : -0.209500E-01 : 0.00000 : 0.00000  
 Location of the Hinge Line Center with respect to Vehicle Reference (feet), {Xcs,Ycs,Zcs} : -41.4000 : 0.00000 : 2.00000 : 0.00000 : 0.00000 : 0.00000  
 Forces (-x,y,z) due to Deflect. and Rates {Ca\_del,Cy\_del,Ca\_del,Ca\_del,Ca\_del,Cy\_del,Ca\_del,Ca\_del} : -0.280850E-03 : 0.00000 : -0.265550E-02 : 0.00000 : 0.00000 : 0.00000  
 Moments due to Deflections and Rates {Cl\_del,Cm\_del,Cn\_del,Cl\_deldot,Cm\_deldot,Cn\_deldot} : 0.00000 : -0.558500E-03 : 0.00000 : 0.00000 : 0.00000 : 0.00000  
 Control Surface No: 2 Body Flap  
 Trim Angle, Max/Min Deflection Angles from Trim, Hinge Line Angles: Phi\_h, Lambda\_h (deg) : -3.12390 : 20.0000 : -20.0000 : 0.00000 : 0.00000 : 0.00000  
 Surface Mass, Inertia about Hinge, Moment Arm (Hinge to Surface CG), Surface Chord, Area : 10.0000 : 100.000 : 2.00000 : 2.41000 : 17.2200 : 0.00000  
 Hinge Moment Derivatives (1/deg), { Chm\_Alpha, Chm\_Beta, Chm\_Delta, Chm\_Mach } : -0.665000E-02 : 0.00000 : -0.315200E-02 : -0.177800E-01 : 0.00000 : 0.00000  
 Location of the Hinge Line Center with respect to Vehicle Reference (feet), {Xcs,Ycs,Zcs} : -50.0000 : 0.00000 : 0.00000 : 0.00000 : 0.00000 : 0.00000  
 Forces (-x,y,z) due to Deflect. and Rates {Ca\_del,Cy\_del,Ca\_del,Ca\_del,Ca\_del,Cy\_del,Ca\_del,Ca\_del} : -0.548950E-04 : 0.00000 : -0.536700E-03 : 0.00000 : 0.00000 : 0.00000  
 Moments due to Deflections and Rates {Cl\_del,Cm\_del,Cn\_del,Cl\_deldot,Cm\_deldot,Cn\_deldot} : 0.00000 : -0.208800E-03 : 0.00000 : 0.00000 : 0.00000 : 0.00000  
 Control Surface No: 3 Aileron  
 Trim Angle, Max/Min Deflection Angles from Trim, Hinge Line Angles: Phi\_h, Lambda\_h (deg) : 0.00000 : 20.0000 : -20.0000 : 0.00000 : 0.00000 : 0.00000  
 Surface Mass, Inertia about Hinge, Moment Arm (Hinge to Surface CG), Surface Chord, Area : 10.0000 : 100.000 : 2.00000 : 2.36000 : 11.8100 : 0.00000  
 Hinge Moment Derivatives (1/deg), { Chm\_Alpha, Chm\_Beta, Chm\_Delta, Chm\_Mach } : -0.110400E-01 : 0.00000 : -0.115940E-01 : 0.232000E-01 : 0.00000 : 0.00000  
 Location of the Hinge Line Center with respect to Vehicle Reference (feet), {Xcs,Ycs,Zcs} : -41.4000 : 0.00000 : 0.00000 : 0.00000 : 0.00000 : 0.00000  
 Forces (-x,y,z) due to Deflect. and Rates {Ca\_del,Cy\_del,Ca\_del,Ca\_del,Ca\_del,Cy\_del,Ca\_del,Ca\_del} : 0.00000 : 0.00000 : 0.00000 : 0.00000 : 0.00000 : 0.00000  
 Moments due to Deflections and Rates {Cl\_del,Cm\_del,Cn\_del,Cl\_deldot,Cm\_deldot,Cn\_deldot} : 0.00000 : -0.159600E-03 : 0.00000 : 0.00000 : 0.00000 : 0.00000  
 Control Surface No: 4 Rudder  
 Trim Angle, Max/Min Deflection Angles from Trim, Hinge Line Angles: Phi\_h, Lambda\_h (deg) : 0.00000 : 30.0000 : -30.0000 : 0.00000 : 0.00000 : 0.00000  
 Surface Mass, Inertia about Hinge, Moment Arm (Hinge to Surface CG), Surface Chord, Area : 10.0000 : 100.000 : 2.00000 : 2.10000 : 13.4400 : 0.00000  
 Hinge Moment Derivatives (1/deg), { Chm\_Alpha, Chm\_Beta, Chm\_Delta, Chm\_Mach } : 0.00000 : 0.00000 : -0.417333E-03 : 0.00000 : 0.00000 : 0.00000  
 Location of the Hinge Line Center with respect to Vehicle Reference (feet), {Xcs,Ycs,Zcs} : -48.8000 : 0.00000 : -3.00000 : 0.00000 : 0.00000 : 0.00000  
 Forces (-x,y,z) due to Deflect. and Rates {Ca\_del,Cy\_del,Ca\_del,Ca\_del,Ca\_del,Cy\_del,Ca\_del,Ca\_del} : 0.00000 : 0.137867E-02 : 0.00000 : 0.00000 : 0.00000 : 0.00000  
 Moments due to Deflections and Rates {Cl\_del,Cm\_del,Cn\_del,Cl\_deldot,Cm\_deldot,Cn\_deldot} : 0.00000 : -0.662333E-03 : 0.00000 : 0.00000 : 0.00000 : 0.00000

Number of Thruster Engines, Include or Not the Tail-Wags-Dog and Load-Torque Dynamics ? : 1 NO TWD

TVC Engine No: 1  
Engine Nominal Thrust, and Maximum Thrust in (lb) (Gimbaling Throttling Single\_Gimbal) : Main Engine Throttling  
Trim Angles (Dym,Dan) wrt Vehicle x-axis, Maxim Deflections (Dymak,Damak) from Trim (deg) : 52987.7 74182.8 0.00000 0.00000  
Eng Mass (slug), Inertia about Gimbal (lb-sec<sup>2</sup>-ft), Moment Arm, engine CG to gimbal (ft) : 0.00000 0.00000 0.00000 0.00000  
Gimbal location with respect to the Vehicle Reference Axes, Xgimb, Ygimb, Zgimb, in (ft) : 160.000 3500.00 3.50000 0.00000  
 : -47.0000 0.00000 -0.492000

Number of Accelerometers, Along Axis: (x,y,z) : 3  
Acceleromet No 1 Axis: (X,Y,Z), (Position, Velocity, Acceleration), Sensor Location (ft) : X-axis Accelerat. -31.5539 0.00000 1.24000  
Acceleromet No 2 Axis: (X,Y,Z), (Position, Velocity, Acceleration), Sensor Location (ft) : Z-axis Accelerat. -31.5539 0.00000 1.24000  
Acceleromet No 3 Axis: (X,Y,Z), (Position, Velocity, Acceleration), Sensor Location (ft) : Z-axis Accelerat. -31.5539 0.00000 1.24000

-----



## 9.7 Contour Plots of Performance Parameters Plotted Against (Mach and Alpha)

---

In Section 3 we described how to calculate some important performance parameters that characterize vehicle static stability, static controllability and performance as a function of the trajectory time. The performance parameters, such as: static stability, time to double amplitude, lateral control departure, control authority, etc. depend on the trajectory variables, the aerodynamic coefficients, engine data, thrusts, and also the trim angles and throttles of the effectors along the trajectory. Now let us suppose that some of the performance parameters do not meet our required criteria and we would like to modify the trajectory in order to improve the vehicle stability or maneuverability, etc. This would be difficult to accomplish because we wouldn't know how to modify the trajectory in order to improve performance. Furthermore, the performance requirements in most aircraft are not defined along a trajectory but over a wider range of speeds, specifically Mach numbers versus angles of attack. This is a good choice of variables along which to examine performance because it strongly depends on the aerodynamic data that vary with Mach number and angle of attack. There is a need, therefore, for an analytic capability that would expand our performance analysis perspective over a wider range of Mach numbers and angles of attack, rather than restricting it in the vicinity of a trajectory. Contour plots are 3-dimensional surface plots that provide a wider depiction on how the performance parameter varies in the entire Mach versus Alpha envelope. The Mach number is plotted in the horizontal x-axis, the angle of attack in the y-axis, and the performance parameter being analyzed is plotted in the z-axis normal to the paper.

Figure 7.1 is a contour plot of the pitch stability parameter ( $T_2$ -inverse) for an unpowered descending vehicle beginning at Mach 18 to landing at Mach 0.25. This parameter was described in equation 3.15. The Mach number is plotted in the horizontal x-axis, the angle of attack in (degrees) is in the vertical y-axis, and the stability performance parameter is plotted in the z-axis which is normal to the screen, except that instead of using a 3-dimensional plot the value of the performance parameter is color-coded. The trajectory is shown as a black line traveling across the Mach versus alpha field. The colors of the regions in the surface plot specify the values of the pitch stability parameter in that region. Initially, at high Mach the vehicle is statically stable with a short-period frequency about 1 (rad/sec). It begins in the upper right-hand corner at Mach 18 and at 40 degrees angle of attack. It crosses through an unstable (divergent) region between Mach (5 to 3.5), where the time-to-double amplitude  $T_2$  is 0.65 (sec). Then it becomes stable again with a short-period frequency 1.5 (rad/sec), and it finishes in the lower left corner at Mach 0.25 and at 10 degrees of alpha.

## Pitch Stability Contour Plot (Mach vs Alpha)

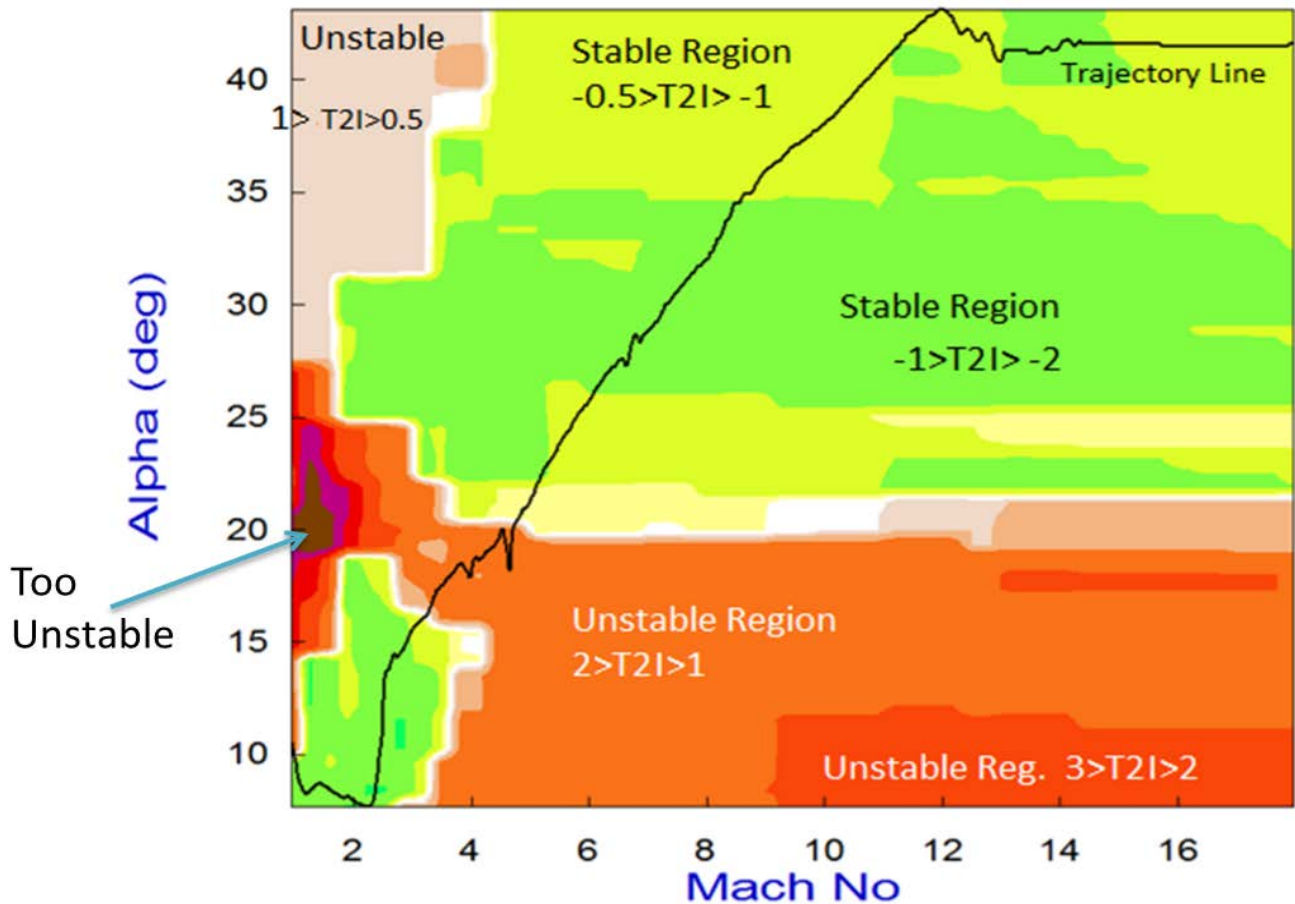


Figure 7.1 Contour Plot showing the Pitch Stability parameter of a hypersonic vehicle along the reentry trajectory as a function of Mach and Alpha. The trajectory begins from a stable region in the upper-right, passes through an unstable region at Mach 4.5, and becomes stable again below Mach 3.3 to landing

This type of presentation helps the analysts to identify any potentially unacceptable regions across the Mach versus alpha field to be avoided in order to reshape the trajectory trail, or to modify the effectors, as needed, in order to achieve an acceptable performance. Trajectory reshaping, however, is not always easy because there are other factors to consider in a trajectory, such as: payload weight maximization, structural loading, aero-heating, etc.

Figure 7.2 shows the control effort necessary to maintain controllability in the pitch direction against 4 degrees variation due to wind in the angle of attack from alpha-trim  $\alpha_0$ . The pitch control effort is defined to be the ratio of the control required against the alpha dispersion divided by the maximum control available in the pitch direction. The colors denote the magnitude of the control effort and also the control direction. The vehicle is neutrally controllable in the white regions where the magnitude of the effort required against the alpha variation is less than 1 percent.

## Pitch Control Effort Contour Plot (Mach vs Alpha)

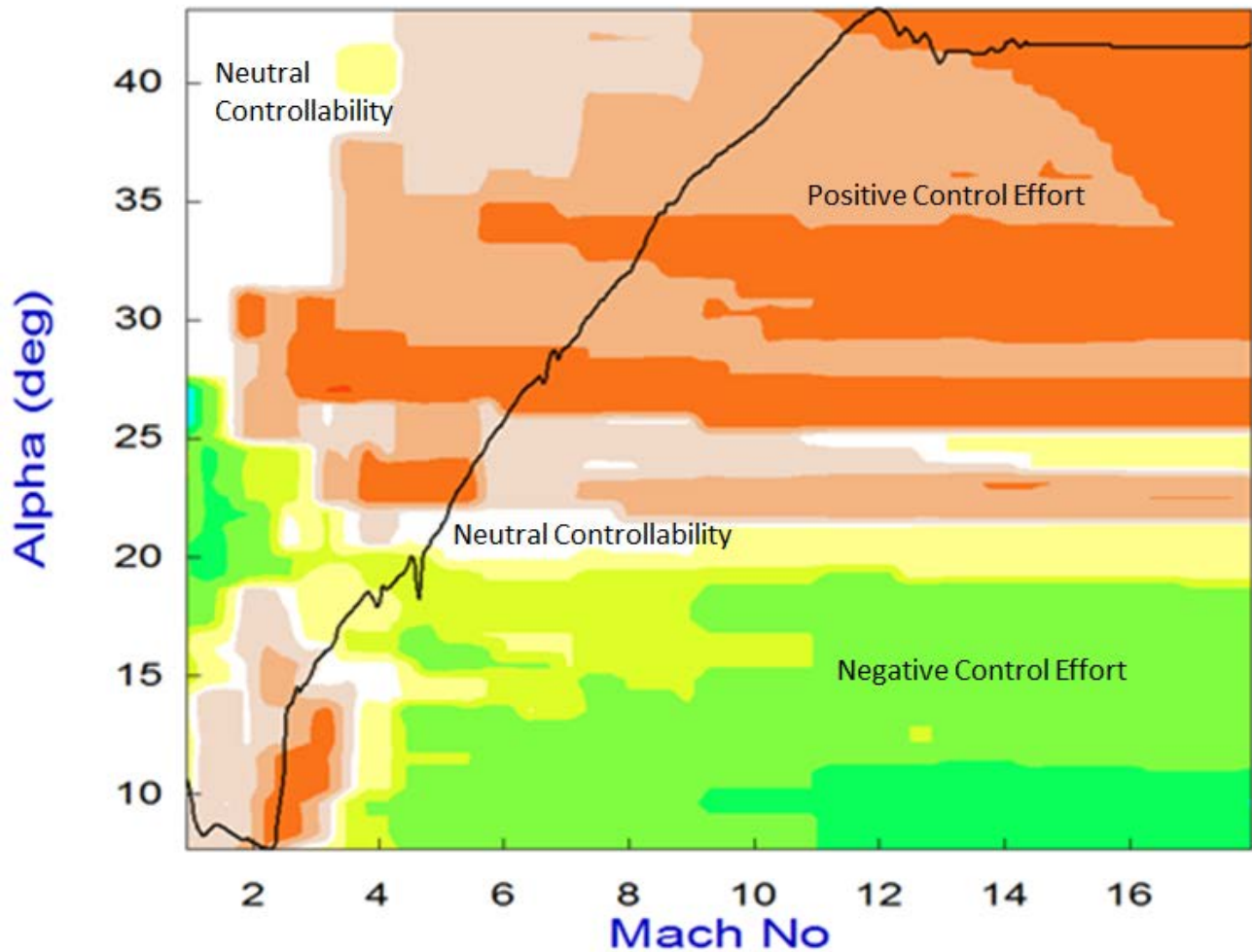


Figure 7.2 Pitch Control Effort Parameter of a Hypersonic Reentry Vehicle, Less than  $\pm 50\%$  Control Effort is required in the entire trajectory, Controllability is transitioning between positive, neutral, and negative regions.

Beige and orange colors correspond to using negative control against a positive alpha dispersion, and green and yellow colors correspond to using positive control. White indicates neutral controllability. We typically like to see the control effort to be less than plus or minus 50 percent, which corresponds to colors between cyan and red. The dark blue color indicates that the control saturates in the negative direction and the dark brown indicates that the control saturates in the positive direction. In this example the pitch control effort along the reentry trajectory begins in the upper right-hand corner at +30% (orange). It reduces to less than  $\pm 1\%$  for a short period in the white region, before it changes to -10% in the light green region, and then it changes back to +5% before landing (light beige).

The Lateral Control Departure (LCDP) ratio is a parameter that indicates roll dynamic controllability and it is described in equation 3.29. We normally want it to be either positive and greater than 0.2 or negative and less than -0.2. But we don't like to see it in the red region which is between -0.2 and +0.2, because roll control performs poorly. The aileron to roll-rate transfer function (3.30) becomes weak, and the aileron would be unreliable for roll control, as described in Section 3. It also becomes sensitive to aerodynamic uncertainties and vulnerable to reverse sign that would cause roll reversals. It would therefore require changes in the sign of the roll control gain.

Figure 7.3 shows the contour plot for the Lateral Control Departure (LCDP) ratio parameter for a rocket-plane vehicle during ascent. The colors below red correspond to positive LCDP, and the colors above red correspond to negative LCDP. The ideal value of the LCDP ratio is +1, but a very good range is between 0.8 and 1.4 denoted in white. Negative values between -0.8 and -1.4 are also good and they are denoted in light gray. Negative LCDP however, requires reversal in the control gains. Large magnitudes greater than 10 should also be avoided because they cause big transients in the sideslip response. That is, magenta for positive and dark purple for negative LCDP.

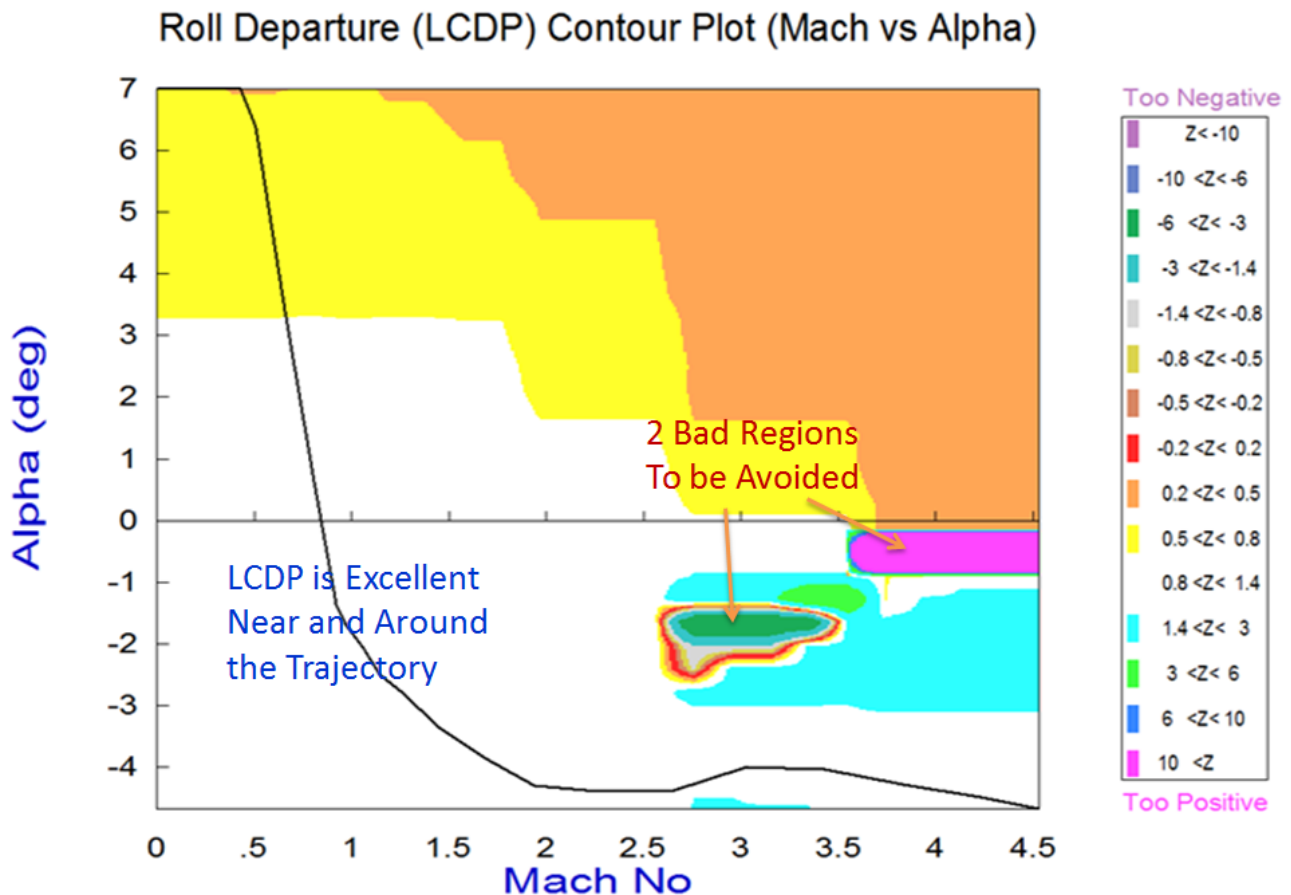
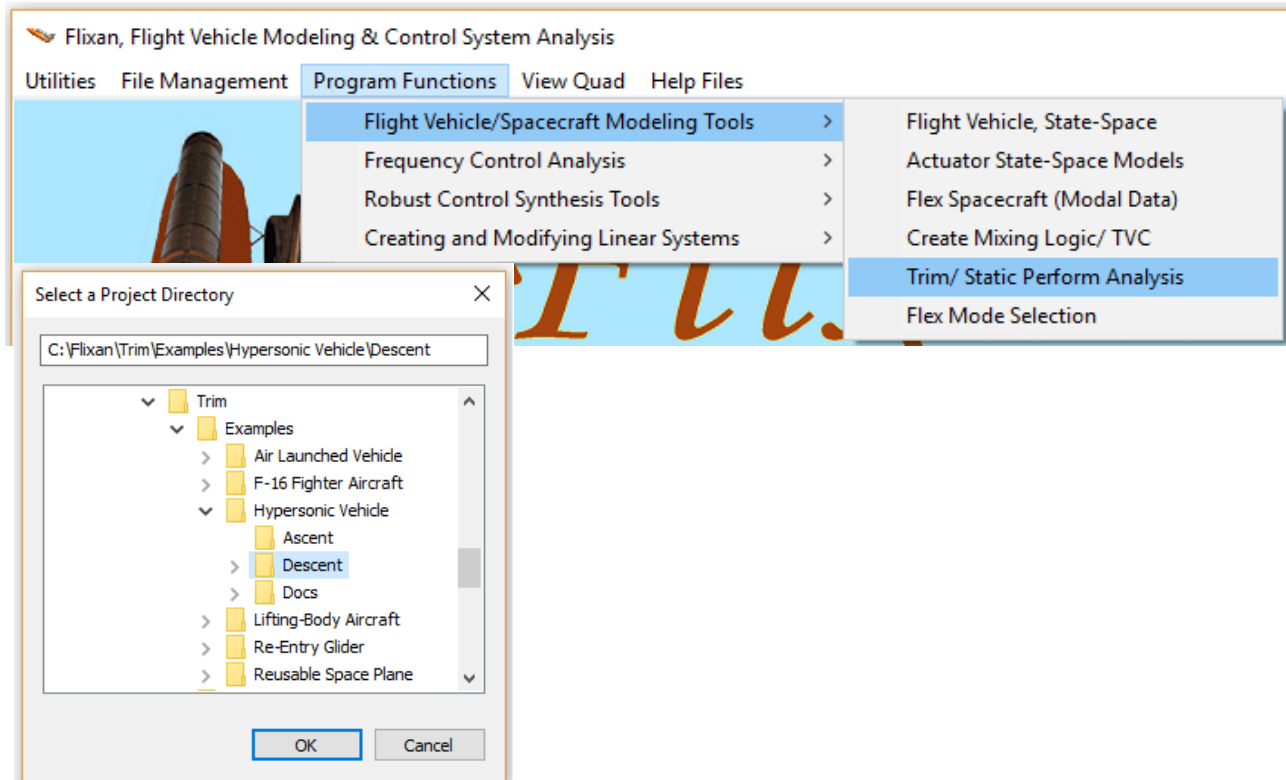


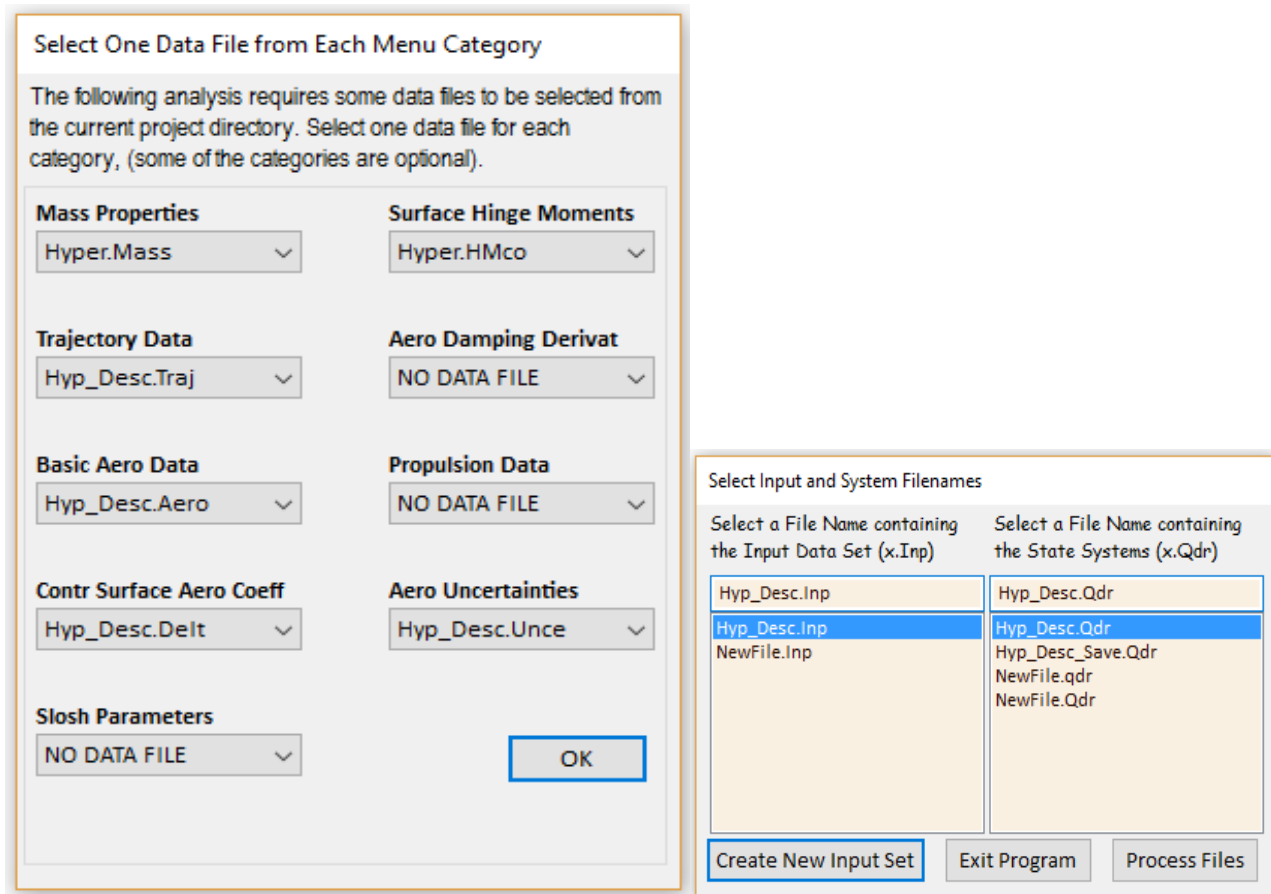
Figure 7.3 LCDP ratio of a Hypersonic Vehicle shows excellent roll performance across the entire Mach versus Alpha region.

In this example we have positive LCDP almost in the entire Mach versus Alpha range. The LCDP magnitude is also very good, especially around the trajectory which begins in the upper left hand corner where alpha is 7 degrees and it finishes in the lower right-hand corner at 4.5 Mach. It indicates that this vehicle has excellent turn coordination. There are two bad regions, however, that must be avoided. A region consists of negative LCDP-ratio denoted by darker colors surrounded by an undesirable red band as it transitions between positive and negative LCDP. If the trajectory would pass through this region it would require reversal in the roll control gain twice, and this would make it vulnerable to aerodynamic uncertainties. The other region to be avoided has very high LCDP ratio exceeding 10. It means that roll maneuvers in this region would induce too much beta transients. Fortunately, those two regions are not near the trajectory. Otherwise, we would have to modify it.

## 7.1 Running the Flixan Contour Plots Program

We can demonstrate the "Contour Plots" option of the Flixan program by choosing an example and running it. In this example we will analyze some of the performance parameters of a hypersonic vehicle, beginning at Mach 4.5 all the way to landing. Start the Flixan program and select the project folder that includes the vehicle data files, such as: trajectory, mass, aero data, aero uncertainties, etc. The files must be in the proper format for the program to be able to read them. Section 9 describes the formatting details of the Trim files. The effectors must be trimmed prior to running the contour plots program because some of the parameters depend on the effector deflections and throttle values. The program reads the effector positions from a previously created trim file that has an extension (.Trim). If it does not find it, it will trim the vehicle and save the trim data as already described in Section 2.





From the Flixan main menu select "Program Functions", "Flight Vehicle/ Spacecraft Modeling Tools", "Trim/ Static Performance Analysis", as shown above, and from the filename selection menu select the files to be used in the analysis. The Trim program consists of many options and from the main menu select option-10, which is: "Contour Plots (Mach versus Alpha) Performance Analysis". You must also enter the  $\alpha_{max}$  and  $\beta_{max}$  dispersion angles in (deg). They define the wind-shear disturbance and the control authority of the effector system is measured against these dispersions. It defines the amount of angle of attack and sideslip variations from trim that the vehicle must be able to counteract by using its control effectors. In this case we enter 4 (deg) for both, and they apply in the entire trajectory.

Vehicle performance also depends on how the effectors combine together to provide control in the demanded directions. A mixing logic matrix is required by the program to convert the flight control demands to effector commands. This matrix is typically supplied by the analyst during the control design and it is read by the program from a systems file. However, if the effector combination matrix is unavailable, such as, during a preliminary analysis, the program provides the capability to create a temporary matrix in order to complete the analysis. It opens a mixing-logic definition dialog that has three options. The first one is for selecting an already existing mixing-logic matrix. In this case, we select the second option that allows the program to create a mixing logic using full participation from all effectors. The third option is similar to the second option but it provides the capability to adjust the amount of participation percentage from each effector.

## Main Trim Menu

Select one of the following options

Exit

OK

1. Plot Aero Coefficients, Derivatives, and Control Surface Increments
2. Plot Trajectory Parameters Versus Time from the Trajectory File ".Traj"
3. Trim the Effector Deflections to Balance the Vehicle Moments and Forces
4. Create an Effector Mixing Logic or a TVC Matrix (Kmix)
5. State-Space Modeling of the Flight Vehicle at Selected Times
6. Performance and Stability Parameter Plots Along Trajectory Time
7. Landing and Pull-Up Maneuverability, plus, Inertial Coupling Effects
8. Moments at the Hinges of Control Surfaces Along the Trajectory Time
9. View and Modify Vehicle Data (CG, MRC, TVC, Surfaces) for Dispersion Analysis
10. Contour Plots (Mach versus Alpha) for Performance, Control Authority Analysis
11. Vector Diagrams for Maneuverability & Stability at Selected Flight Conditions
12. Plot and Compare Previous Data Files (Traject, Trim, Perform, Hinge Moment)

## Maximum Aero Disturbances

The control effectors must be capable of varying the vehicle angles of attack and sideslip (typically 3-5 deg) from their trim values.

Enter the worst expected alpha and beta dispersions in (deg), and also delta-velocity in (ft/sec) from trim that must be controlled by the effectors, and click OK.

Maximum Alpha (deg)

Maximum Beta (deg)

OK

Maximum Change in Velocity due to Wind in (feet/sec)

## Define the Effector Combination Matrix

The Mixing Logic Matrix translates the Flight Control (Roll, Pitch, Yaw, Ax, Ay, Az) demands to Effector commands (Aero-Surface, TVC, and Throttling).

You may either select a pre-calculated Mixing Logic Matrix (Kmix) from the Systems File: Hyp\_Ascent.qdr, or let the program calculate it

Select a Mixing Matrix from Systems File

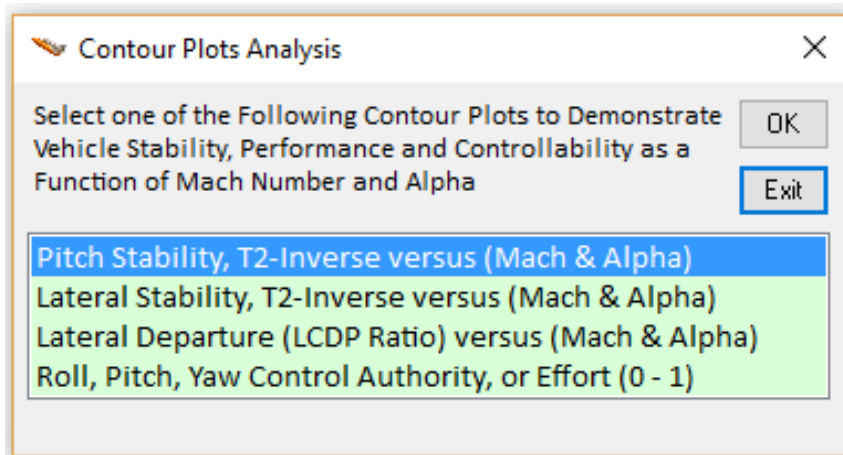
When you create a new Mixing Logic you have the option of adjusting the participation of each effector in the combination matrix. Maximum contribution is 100%. Select this option for 100% participation from all effectors.

Create a Mixing Matrix Using All Effectors at 100% Participation

There are times, however, when you want to reduce their contributions. Plus some effectors are only used for Trimming and not for Control. Their participation should be set to 0% in the effector combination calculations.

Create a Mixing Matrix by Adjusting the Effector Contributions

The program is now ready to generate contour plots for some of the most important performance parameters that were defined in Section 3. The following menu consists of the performance parameters that can be presented in contour plots versus Mach and Alpha. The selection choices are: Pitch and Lateral stability parameters (T2-inverse or short-period resonance) as described in Equations (3.14 through 3.18), the Lateral Control Departure (LCDP) ratio described in Equation 3.28, and the control authority of the effector system in roll, pitch, and yaw directions as described in Equation (3.24 to 3.26).



From the contour plots menu let us select the first option that plots the pitch stability parameter (T2-inverse) across the 2-dimensional, Mach versus alpha array, shown in Figure 7.4. The black line is the trajectory trail along the Mach versus Alpha field. The colors signify the approximate value of the stability parameter at a particular Mach and Alpha. The interpretation of the color coding is shown on the right hand side of the plot. White corresponds to neutral stability which is an ideal condition because the vehicle can be controlled with a very small amount of control effort. Beige corresponds to slight instability which is acceptable. Instability increases as we move towards the orange, reddish, magenta, and brown colors. In the magenta and brown regions the vehicle instability becomes unacceptable because the time-to-double amplitude drops below 0.25 sec, and requires high control bandwidths and fast actuators. On the other side of the color spectrum above white, we have the colors corresponding to statically stable regions. Beginning with light yellow (slightly stable), and moving towards the greenish and cyan colors corresponding to acceptable stability with short-period resonances up to 4 (rad/sec). As we move further up towards the blue and dark blue color regions the vehicle stability increases to unacceptably high levels. Too much stability hurts maneuverability, and requires bigger and more powerful control effectors.

In Figure 7.4 the trajectory begins in the lower right-hand corner where the vehicle is slightly unstable at Mach=4.5, and  $\alpha=-1.7^\circ$ . The color coding in the regions surrounding the trajectory show the value of the pitch stability parameter as a function of Mach and alpha. Initially, at high Mach the trajectory is in a statically unstable (divergent) region with a time-to-double amplitude T2=0.67 (sec). It briefly passes through a neutrally stable region (white) at Mach 3.7 and it crosses



into the stable region (green). The short period oscillations peak to 4 (rad/sec) in the cyan region. It shouldn't be difficult to modify the trajectory to avoid the cyan region but it is not necessary because the stability is acceptable. It remains acceptably stable all the way to landing in the upper-left corner, where  $\alpha=5.3^\circ$ , and Mach=0.2, close to neutrally stable.

### Pitch Stability Contour Plot (Mach vs Alpha)

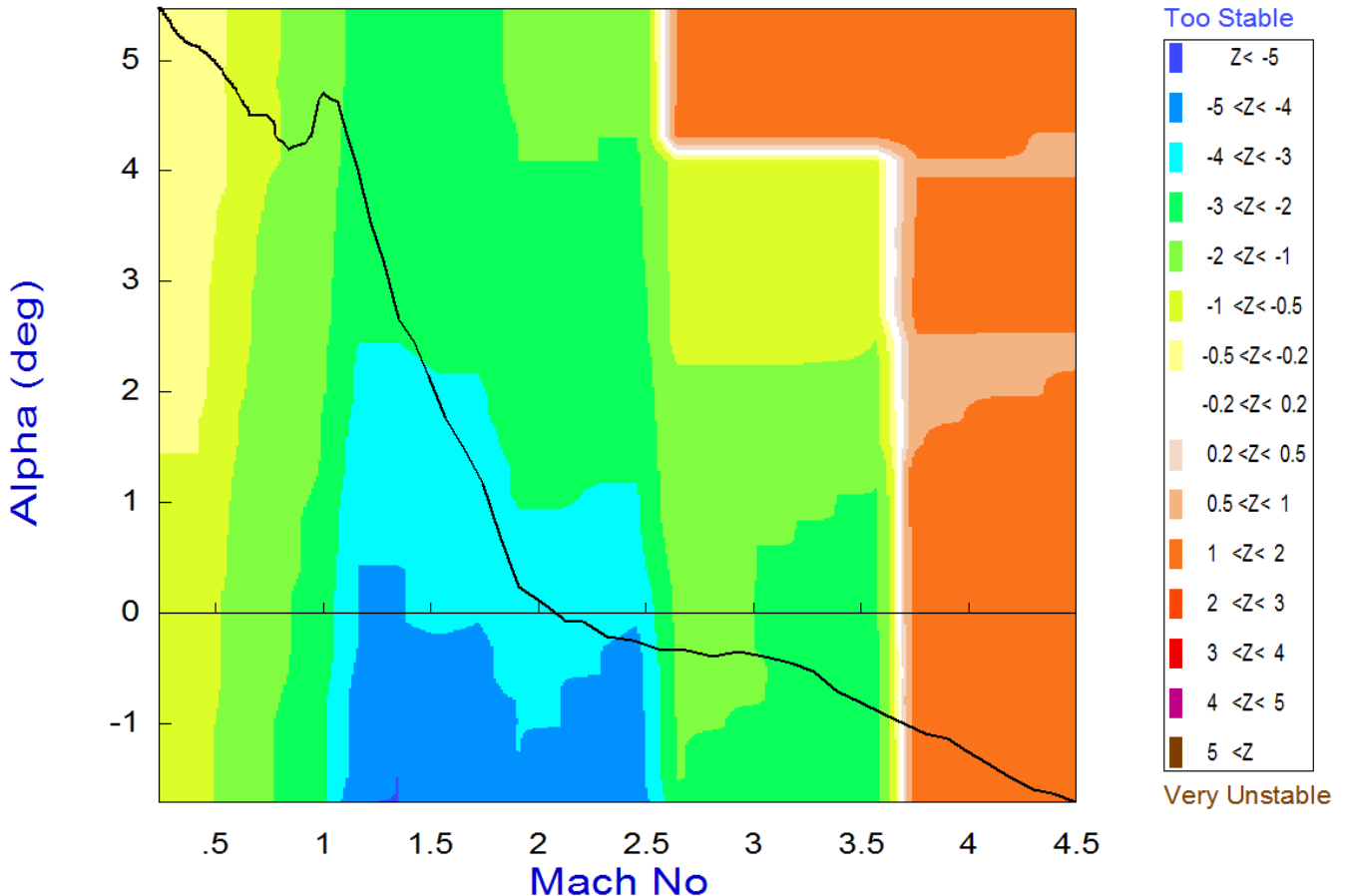


**Figure 7.4** Contour Plot showing the Pitch Stability parameter along the trajectory as a function of Mach and Alpha. The trajectory initially passes through a region of instability and becomes stable below Mach 3.6

From the menu bar located above the plot, click on "Exit Plots" to return to the contour plots menu. From the contour plots menu select the second option to plot the lateral stability parameter T2-inverse as it was defined in Equation 3.18. The color coding is the same as in the pitch stability parameter. The vehicle is more stable in the lateral direction, but it does not exceed the acceptable stability range. The maximum Dutch-roll resonance is at 3.2 (rad/sec). The user may click at a point on the black trajectory curve and a display appears showing some important trajectory parameters that correspond to the selected point. Click on "Exit Plots" to return to the Contour Plots menu.

## Lateral Stability Contour Plot (Mach vs Alpha)

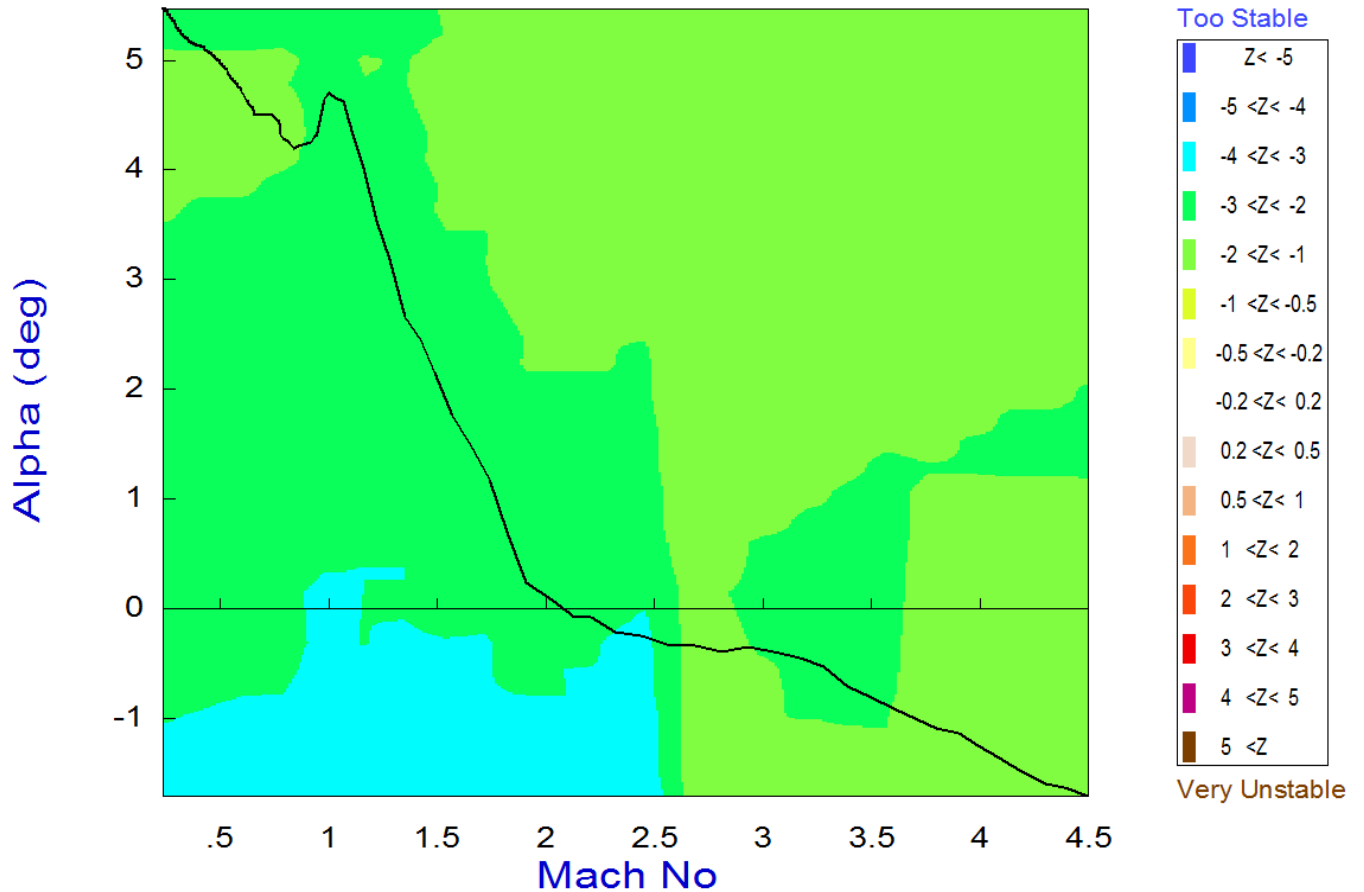


Figure 7.5 Contour Plot showing the Lateral Stability parameter along the trajectory as a function of Mach and Alpha.

From the contour plots menu we may now select the third option which is the "*Lateral Control Departure Ratio (LCDP)*" parameter, shown in Figure 7.6. The LCDP ratio was described in Section 3.3. Figure 3.3 shows the acceptable and unacceptable regions in the LCDP ratio as it was described in Section 3 and it is repeated here. The color coding for the LCDP ratio is different from the coding used in the stability plots. The color coding of the various LCDP regions is defined on the right side of Fig. 7.6 and in Figure 7.7. The unacceptable (red) region is in the middle, and it must be avoided because this is where the aileron to roll-rate transfer function (3.29) becomes weak and the aileron is not reliable for roll control, because it may change sign and reverse control due to aero uncertainties. White is an ideal LCDP value because the roll/ yaw coordination is perfect.

## Roll Departure (LCDP) Contour Plot (Mach vs Alpha)

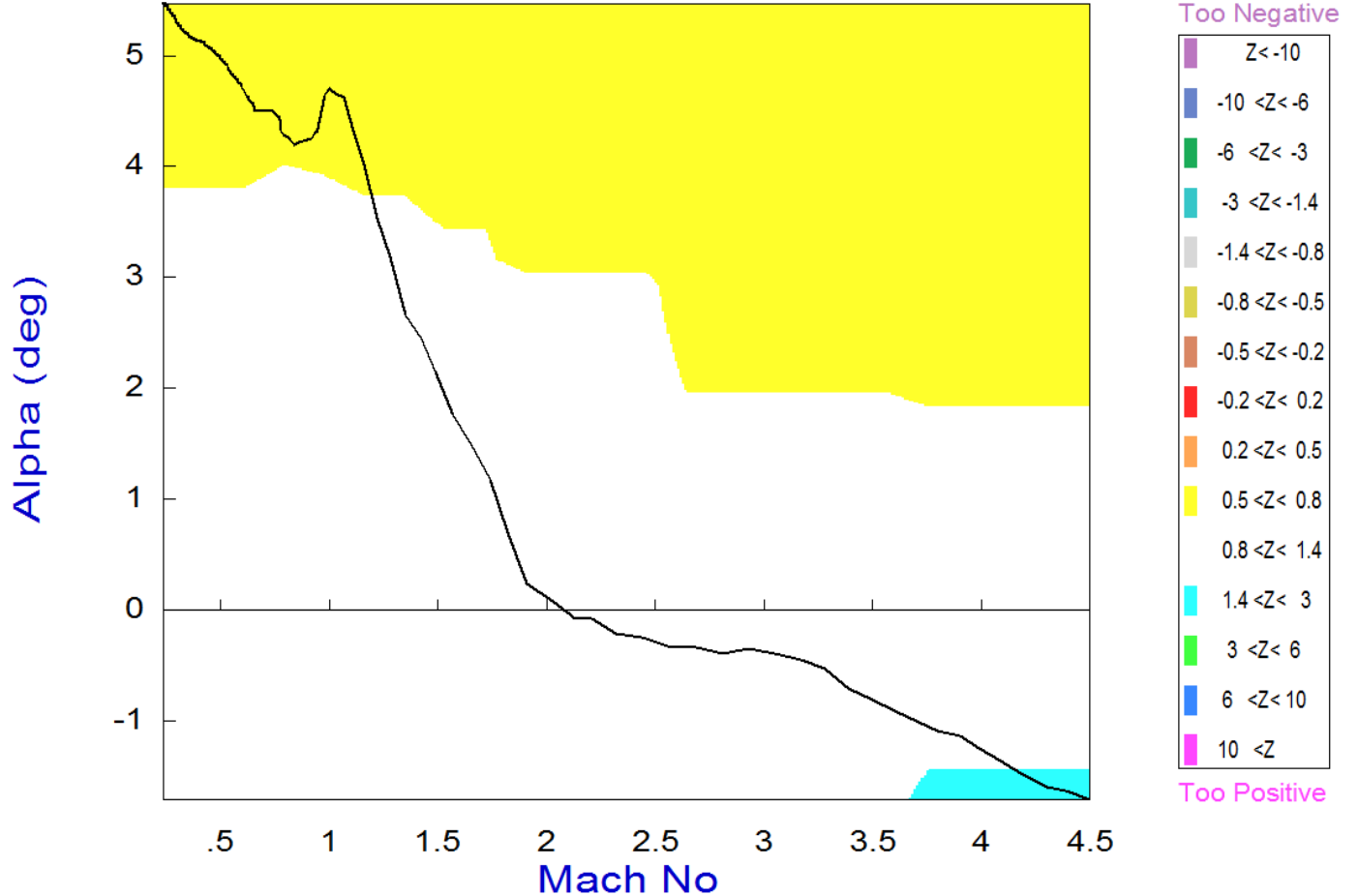


Figure 7.6 The LCDP ratio shows excellent roll performance across the entire Mach versus Alpha region

The vehicle roll performance may also be acceptable in the dark-colored regions (grey, dark-yellow, dark-cyan, and dark-blue) by using reverse roll control. The often transitioning, however, between the light and dark regions is undesirable and requires RCS thrusters. In Figure 3.3, the regions on the left side of the vertical axis demonstrate lateral instability that is usually undesirable, unless the vehicle actuators are exceptionally fast. The purple/ magenta areas near the vertical axis (both dark and light) should also be avoided because the beta transients are too big in those regions. The LCDP ratio contour plot in our hypersonic vehicle example in Figure 7.6 is almost ideal. There are no bad regions, no control reversals (red) across the field and the locus is close to perfect coordination along the entire trajectory.

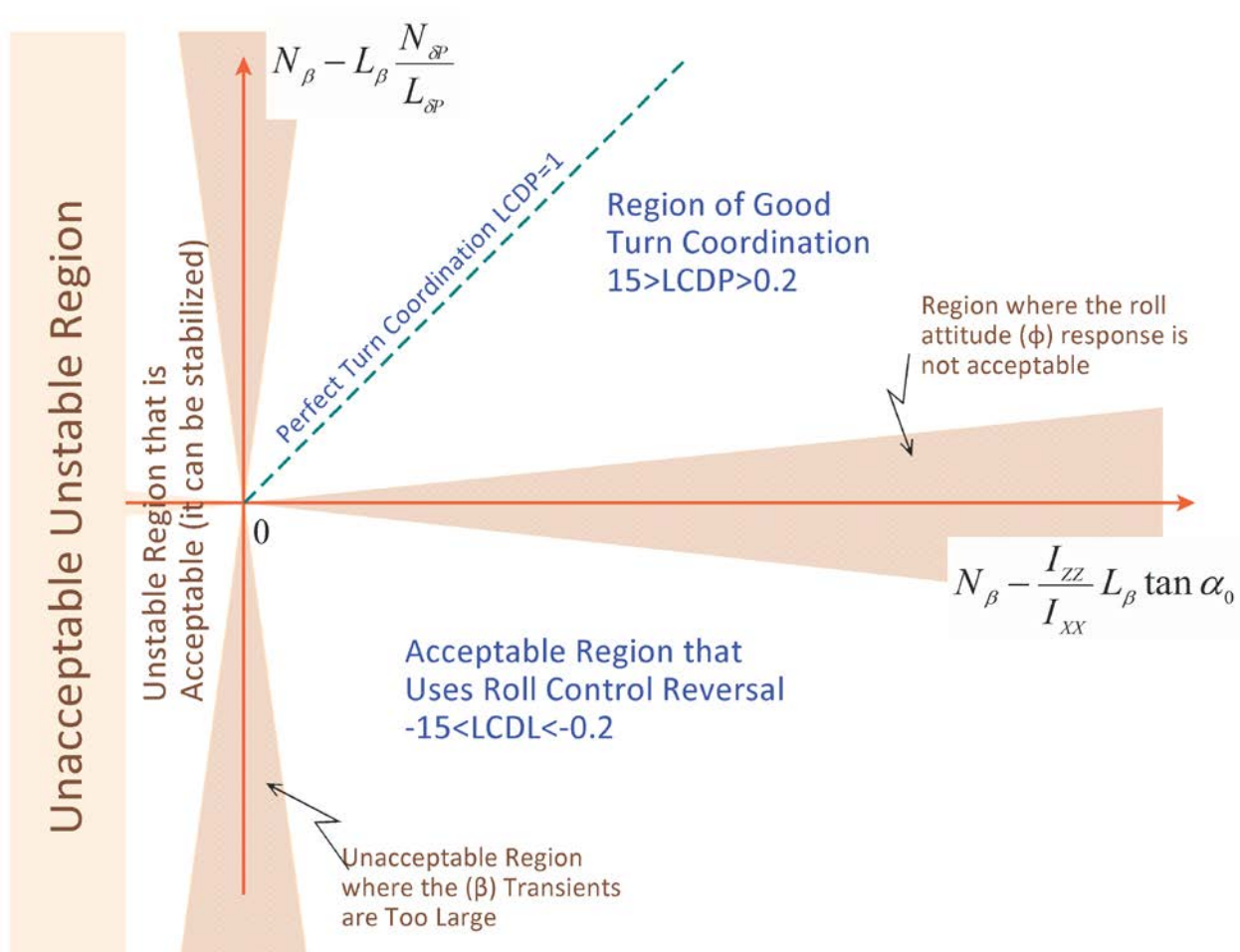


Figure 3.3 Regions of the LCDP Ratio

We now return to the contour plots menu and select the last option that analyzes the effectors authority to control the vehicle against wind disturbances as it was described in equation 3.24. The effectors are evaluated as a system combined together by the mixing-logic matrix. The control authority, therefore, strongly depends on the  $K_{mix}$  selection. In the beginning of the analysis we were asked to define the magnitudes of  $\alpha_{max}$  and  $\beta_{max}$  dispersions from trim. They define the magnitude of the disturbance that the vehicle may experience due to winds or maneuvering. The control authority (or effort) in a certain direction is measured by the ratio of the control used against the dispersion divided by the maximum control authority available in that direction. The magnitude of this ratio should obviously be less than 1, or even better, less than 0.5, to allow some control availability for other functions, such as gusts, commands etc. The color coding used in the control authority plots is different from the previous color codes. There are obviously two control saturation limits, a positive limit of +1, and a negative limit of -1, corresponding to brown and dark blue colors respectively. White corresponds to regions where the control effort is very small and it happens when the vehicle is close to neutral stability.

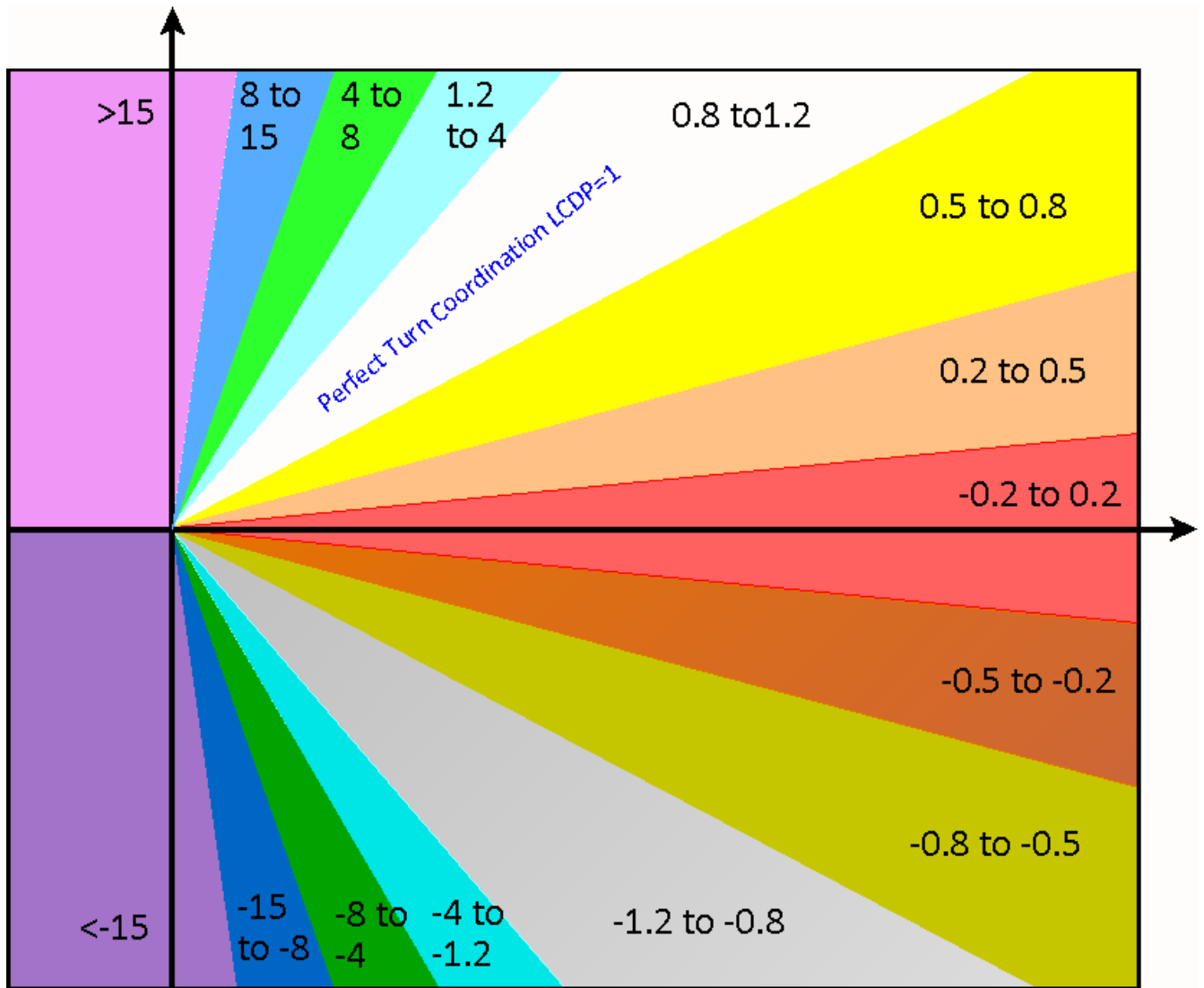
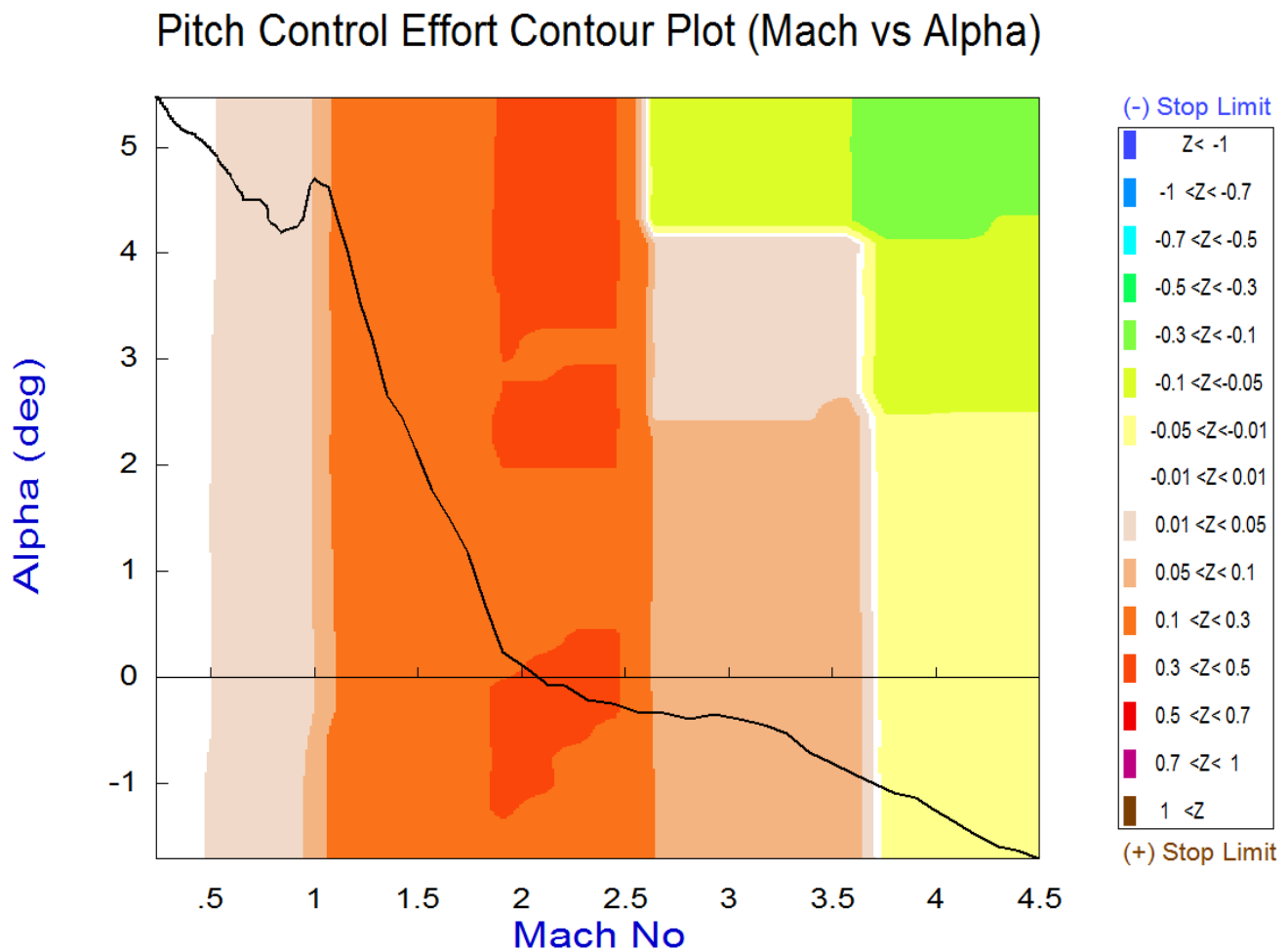


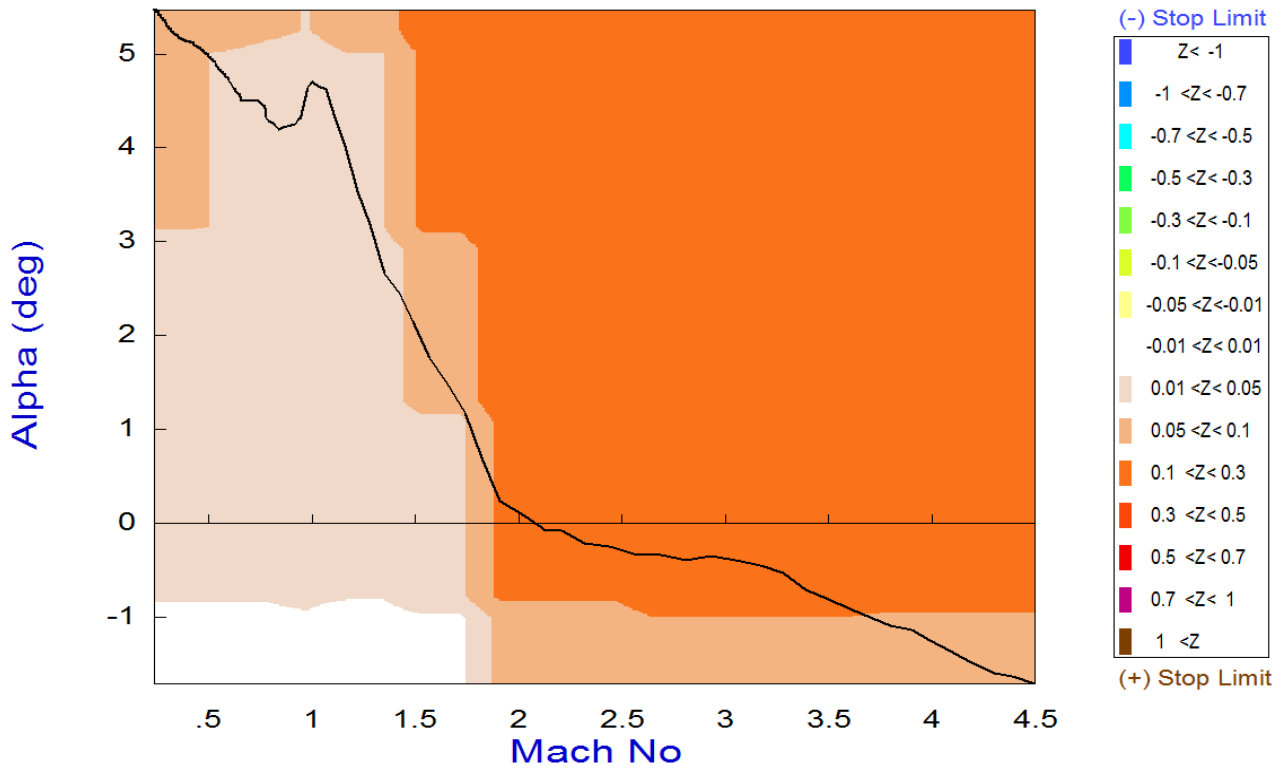
Figure 7.7 Color Coding of the LCDP Contour Plots showing the Acceptable and Unacceptable Regions of the LCDP ratio. The dark color regions below the horizontal axis require Roll-Reversal.

The next 3 contour plots show the pitch, roll, and yaw control effort parameters. When the vehicle is stable, an increase in alpha due to a strong wind shear will have a tendency to deflect the controls in the negative direction towards the yellow, greenish, blue colors and the pitch control will saturate when it reaches the -1 (dark blue) limit. When the vehicle is statically unstable the controls will rotate in the opposite direction towards the orange, red, magenta numbers and it will saturate when it reaches the +1 (brown) limit.

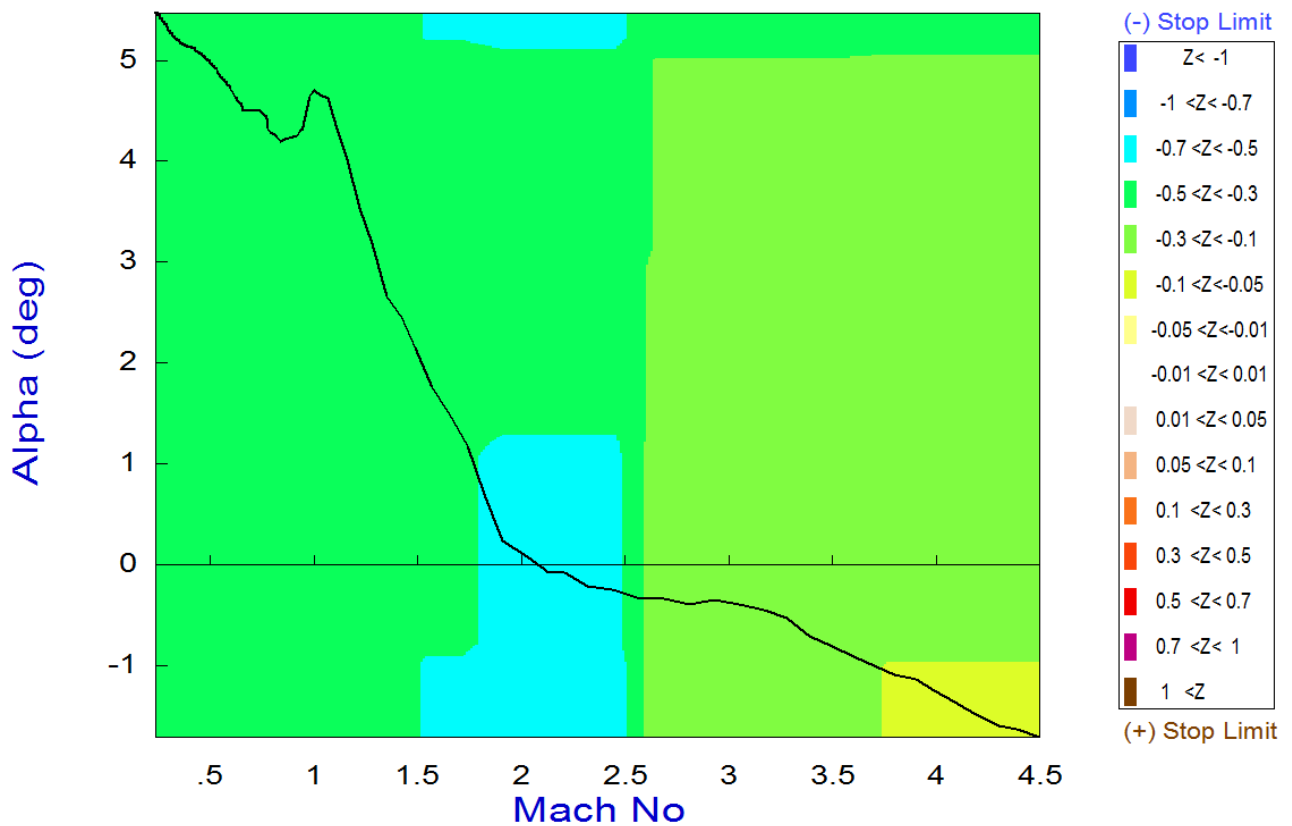
The ideal value of the control effort parameter should be in the white region which indicates that very little control power is needed to oppose the disturbance moments caused by an alpha/ beta wind-shear disturbance. The pitch effort plot shows that since our trajectory is initially stable and close to neutrally stable (in the high Mach and low alpha region) it requires very little negative effort (light yellow) to trim the  $\alpha_{max}$  dispersion. Near the end of the trajectory and before landing (in the low Mach and high alpha region) the control effort is very low (white). In the intermediate Mach range between Mach# (1 to 3) where the vehicle is unstable the control effort against the  $\alpha_{max}$  dispersion is in the positive direction and the pitch control effort reaches 0.3 which is still very good. The roll control effort contour plot is not very different. It shows the amount of effort required to counteract against the  $\beta_{max}$  dispersion. The user must click on the "Next Plot" option at the top menu bar to show the next plot, or click on "Exit Plots" to return to the previous menu. The yaw effort is negative in the entire Mach versus alpha range because the vehicle is always stable. If you click on the trajectory curve (black line), a pop-up display appears showing some of the important trajectory parameters corresponding at the selected point.



### Roll Control Effort Contour Plot (Mach vs Alpha)

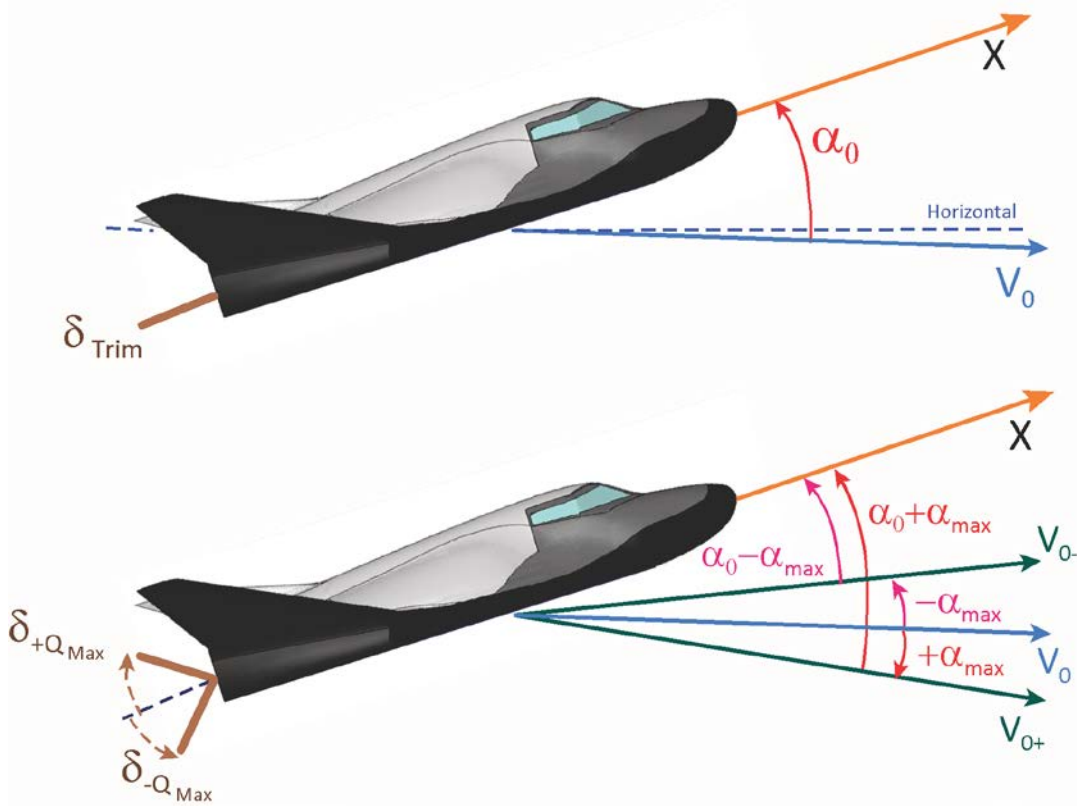


### Yaw Control Effort Contour Plot (Mach vs Alpha)



# 9.8 Static Analysis Using Vector Diagrams

Flight vehicles are usually controlled in 3 rotational directions: roll, pitch, and yaw. In the static sense controllability is interpreted as the ability of the vehicle to respond against environmental disturbances and to maintain a steady attitude. In other words, it is the ability of the effector system to produce enough torque to counteract against the torque produced by the estimated external disturbances. Maneuverability on the other hand is the ability of the effector system to produce sufficient acceleration and fast in order to prevent the vehicle from diverging as a result of a wind disturbance or dispersion in the angle of attack. It is also defined by the vehicle capability to change directions and it is measured by comparing the achievable vehicle acceleration per acceleration demand against the acceleration per alpha or beta dispersions.



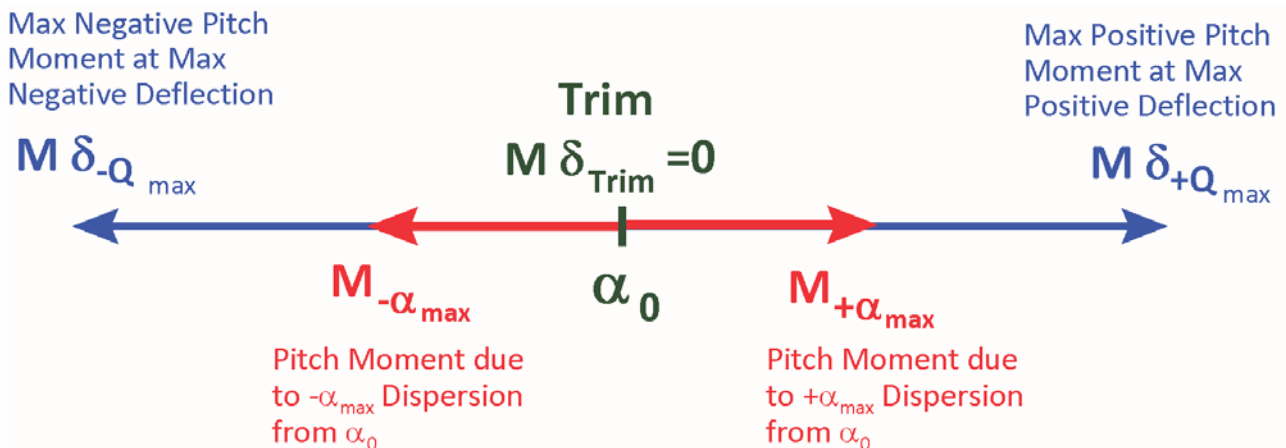
**Figure 8.1 Variation in the Angle of Attack  $\pm\alpha_{\max}$  Requires Variations in Elevon Deflection  $\delta_{\pm Q_{\max}}$  to Trim**

Figure 8.1 shows a statically stable vehicle that is trimmed at an angle of attack  $\alpha_0$ . The aero-surface deflection to balance the pitch moment is at  $\delta_{\text{Trim}}$ . If the magnitude of the velocity  $V_0$  increases or if the direction of the velocity changes to  $(\alpha_0 + \alpha_{\max})$ , in order to maintain the same pitch attitude the Elevon deflection angle must change to  $\delta_{+Q_{\max}}$ . In contrast, if the velocity is reduced or if the direction of the velocity changes in the opposite direction to  $(\alpha_0 - \alpha_{\max})$  the Elevon rotation must also change to  $\delta_{-Q_{\max}}$  in order to balance the pitch moment and to maintain the



same pitch attitude. If a wind disturbance causes a variation in the velocity vector and changes the angle of attack by an amount  $\pm\alpha_{\max}$  from its trim value  $\alpha_0$ , then the vehicle must have enough control authority to counteract the moment variation by rotating the Elevon from  $\delta_{\text{Trim}}$  to  $\delta_{+Q_{\max}}$  or  $\delta_{-Q_{\max}}$ .

To analyze static controllability in one direction, for example in pitch, we compare the maximum moments produced by maximizing the control effectors deflections from trim, against the moment generated by a dispersion  $\alpha_{\max}$  of the angle of attack from trim  $\alpha_0$ . The pitch moment at trim is zero. In Figure 8.2 the blue vector  $M\delta_{+Q_{\max}}$  is the pitch moment generated when the elevon deflection is maximized in the positive direction to  $\delta_{+Q_{\max}}$  from  $\delta_{\text{Trim}}$ , and the vector  $M\delta_{-Q_{\max}}$  is the pitch moment generated in the opposite direction when the elevon deflection is maximized to  $\delta_{-Q_{\max}}$  from  $\delta_{\text{Trim}}$ . The red vector  $M_{+\alpha_{\max}}$  is the moment generated by a positive variation in the angle of attack  $+\alpha_{\max}$ , and the vector  $M_{-\alpha_{\max}}$  in the opposite direction is the moment generated by a negative variation in the angle of attack  $-\alpha_{\max}$  from trim  $\alpha_0$ . In order for the vehicle to maintain its attitude in the presence of alpha variations and to be able to balance the pitch moment we obviously want the blue control vectors to be greater than the red disturbance vectors caused by the  $\alpha_{\max}$  variations.



Partial vector diagrams are used to measure vehicle controllability and its maneuverability in terms of gains per variations rather than comparing maximum magnitudes. They compare the gain of the control partial  $M_\delta$  against the gain of the disturbance partial  $M_\alpha$ . In the pitch case it is the rate of change of the pitch control moment per elevon deflection  $\delta_Q$  against the rate of change of pitch moment per  $\alpha$  variation, and we obviously want the magnitude of the control partial  $M_\delta$  to be greater than the partial of the moment due to alpha  $M_\alpha$ . However, those two partials cannot be compared directly because they are different. One is moment per effector deflection and the other one is moment per angle of attack, and one of them must be scaled. For controllability we want the control torque to be greater than the worst case disturbance torque and we must scale the  $M_\alpha$  partial by multiplying it with the ratio of  $(\alpha_{\max} / \delta_{\max})$  and obviously this vector should be smaller than the control partial.

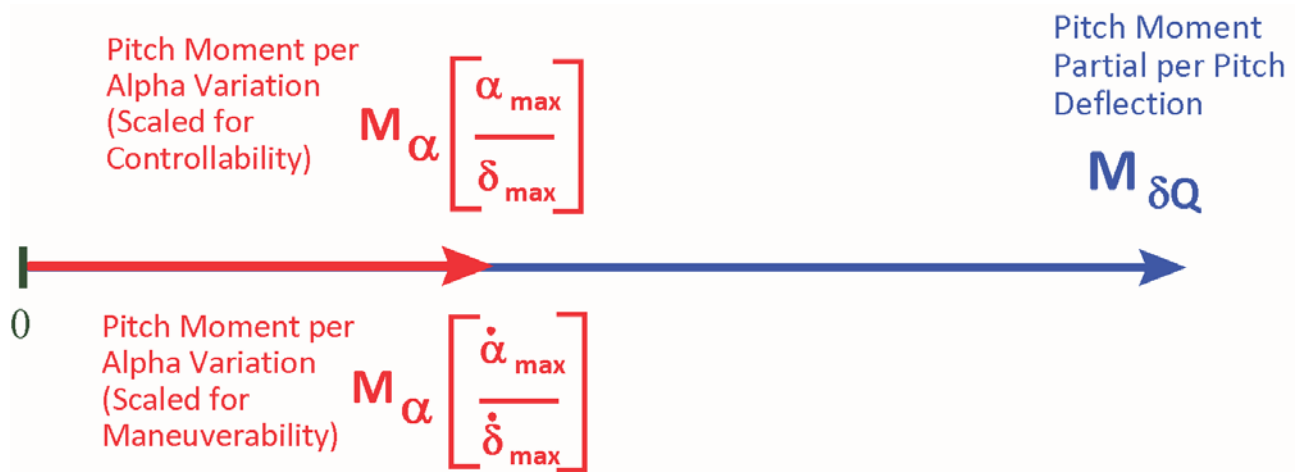
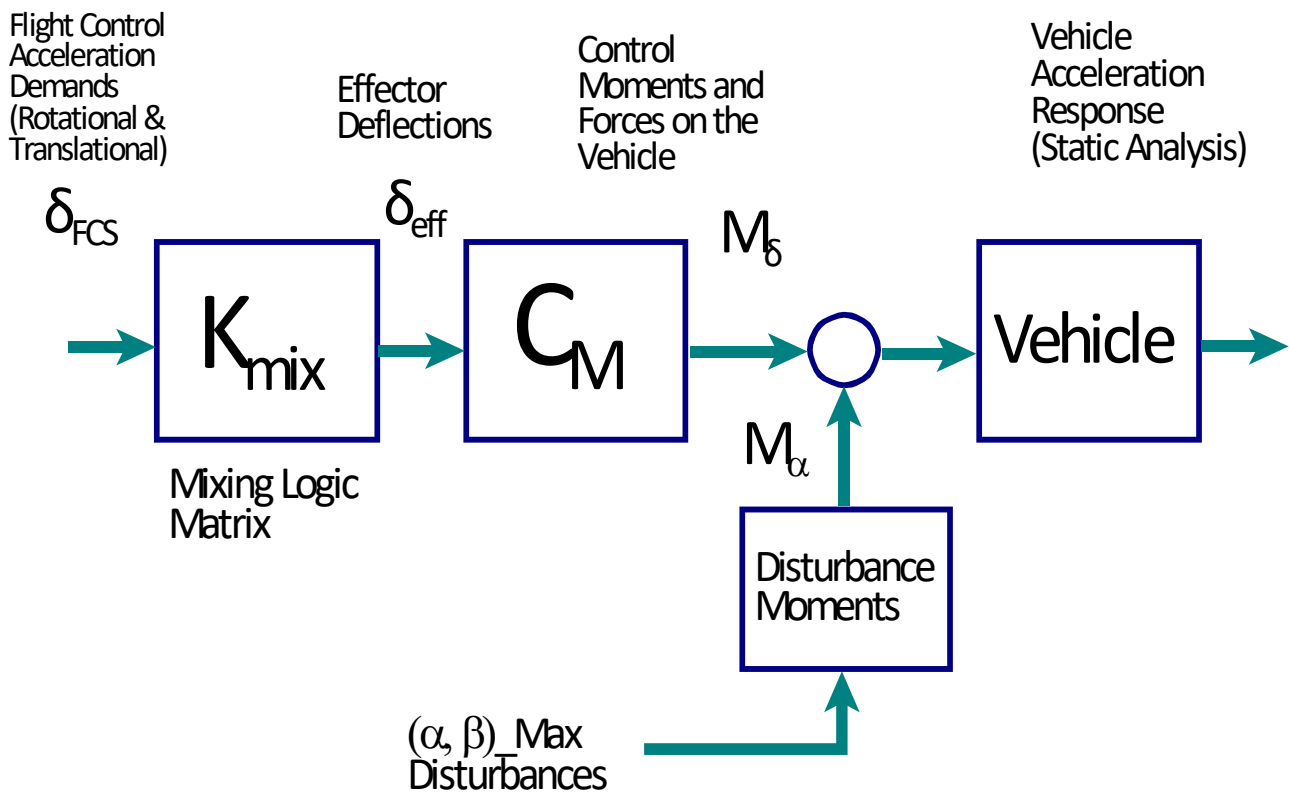


Figure 8.3 Vector Partial in Pitch, Control Moment per Demand against Moment per Alpha Variation

For good maneuverability we want the response of the control system, that is, the rate of change of the control torque  $M_{\delta Q}$ , to be greater than the torque rate of change due to  $\dot{\alpha}$ , and we must therefore scale the  $M_{\alpha}$  partial by multiplying with the ratio of  $(\dot{\alpha}_{\max}/\dot{\delta}_{\max})$  and obviously this vector should be smaller than the control partial in both cases

Vector diagrams are a graphical tool that we use to compare controllability and maneuverability of a flight vehicle at a fixed flight condition against the effects of aerodynamic disturbances. They are two dimensional plots that analyze the vehicle response in two directions by comparing the control moments, forces, and accelerations generated by the effector system, for example, in roll and yaw, or in pitch and normal acceleration, against the moments, forces, and accelerations generated by a wind shear disturbance along the control directions. They examine if the vehicle has enough control authority to oppose the effects of a disturbance along the control directions. The vehicle is trimmed at a certain  $\alpha_0$  and  $\beta_0$  incidence angles and the effectors are at trim positions  $\delta_{\text{Trim}}$ . An aerodynamic disturbance on the vehicle is defined by the maximum dispersions in the angles of attack and sideslip ( $\pm\alpha_{\max}$  and  $\pm\beta_{\max}$ ), relative to the trim alpha and beta positions  $\alpha_0$  and  $\beta_0$  defined in the trajectory and also by variations in the airspeed  $\pm v_{\max}$  relative to  $V_0$ . They also measure maneuverability since the dispersion angles  $\alpha_{\max}$  and  $\beta_{\max}$  may be due to maneuvering. Vector diagrams compare not only magnitudes but they also allow us to examine the direction of the vehicle response to the controls and compare them against the disturbance directions. They helps us analyze the orthogonality of the effector system by comparing the moments, forces, or accelerations of the controls against those generated by the wind disturbance and to determine if the controls are powerful enough and pointing in the proper directions to override the disturbance forces along the control directions.

The vehicle effectors are analyzed as a system consisting of different types of effectors, such as TVC engines, thrust varying engines, aerosurfaces, and reaction control RCS jets, which are combined together by the mixing logic matrix to control certain directions as commanded by the flight control system FCS. Aerodynamic Uncertainties can also be included in the vector diagrams and they are represented by rectangles centered at the vector tips. They help the analyst to determine if the accuracy of the aero-data is sufficient for trim or control design, and perhaps request either more accurate aero data or airframe modifications. Vector diagrams are obviously an open-loop static analysis of the airframe alone at a specific flight conditions and it is not related to control analysis. They are limited to two directions and since there are more than 2 control directions to analyze, we typically need several plots in each study to analyze control authority in multiple directions. For example, roll and yaw moments or accelerations, or pitch moment and axial force, or pitch moment and normal z-force, depending on the controlled axes.



**Figure 8.4 Elements used for Analyzing Vehicle Controllability by means of Vector Diagrams**

Figure 8.4 shows the elements used to calculate the vector diagrams. On the left side we have the control demands  $\delta_{FCS}$  which are generated by the flight control system. They demand vehicle acceleration in certain directions, mainly in roll, pitch, and yaw, and possibly in some of the translational directions. The mixing logic matrix translates the acceleration demands to effector displacements or throttles  $\delta_{effect}$ . These are not the actual displacements but they are increments relative to their trim values  $\delta_{Trim}$  and they are converted to control moment and force variations  $M_\delta$ . The control moment and force vectors generate the vehicle accelerations, hopefully, in the proper directions demanded by the FCS. The disturbances are introduced at the bottom of Figure

8.1 by the maximum expected dispersions  $\pm\alpha_{\max}$  and  $\pm\beta_{\max}$  from trim ( $\alpha_0$  and  $\beta_0$ ). They generate the disturbance moments and forces vector  $M_\alpha$  and disturbance accelerations. The vehicle must have sufficient control authority  $M_\delta$  to overcome  $M_\alpha$  at any given flight condition. In the following sections we shall describe four different types of vector diagrams used to address different aspects of static controllability.

1. **Maximum Moment and Force Vector Diagrams:** They compare the maximum moments and forces produced by maximizing the controls, against the moments and forces generated by aerodynamic dispersions.
2. **Maximum Acceleration Vector Diagrams:** They compare the maximum accelerations produced by maximizing the controls, against the accelerations generated by aerodynamic dispersions.
3. **Moment and Force Vector Partial:** They compare the partials of moments and forces per acceleration demand in the control directions, against the partials of moments and forces per alpha or beta variation.
4. **Acceleration per Acceleration Demand Vector Partial:** They present the partials of vehicle accelerations per acceleration demands in the control directions.

### 8.1 Maximum Moment and Force Vector Diagrams

The first type of vector diagram is the maximum moment and force diagrams. They compare the maximum control authority of the effectors system against the disturbance moments and forces generated by the  $\pm\alpha_{\max}$  and  $\pm\beta_{\max}$  dispersions from trim. We plot the maximum control moments and forces generated by the effectors system in two directions and compare them against the moments and forces generated by the  $\alpha$  and  $\beta$  dispersions. The control moments and forces are calculated by maximizing the flight control demands to their saturation limits in both, positive and in the negative directions relative to  $\delta_{\text{Trim}}$ . The FCS demand in one of the control directions is maximized when at least one of the effectors saturates. It is not sufficient to show only the maximum moment/ force generated when the demand is maximized in the positive direction  $\delta_{+\max}$ , because the efficiency of the effectors is not necessarily symmetric in both directions, plus they are not trimmed exactly at the mid-point between the two saturation limits. We therefore plot the peak moments and forces produced by maximizing the controls in both, positive and negative directions from trim.

In the same diagram, we also plot vectors of the maximum moments and forces produced by the dispersions:  $\pm\alpha_{\max}$  and  $\pm\beta_{\max}$ . They define our design requirements for controllability and maneuverability that the vehicle must be able to withstand. The control vectors are compared against the disturbance vectors in order to analyze the vehicle capability to react against the worst case disturbances.

Equation 8.1 is the same as 3.10, and denotes maximum moments and forces produced when the flight control demands saturate in two opposite directions. That is, when it is maximized in the positive  $\underline{\delta}_{+Max}$  or in the negative  $\underline{\delta}_{-Max}$  directions.

$$\begin{aligned}
 M_{\delta} &= C_M K_{mix} \delta_{FCS} \\
 \begin{bmatrix} L_X \\ M_Y \\ N_Z \\ F_X \\ F_Y \\ F_Z \end{bmatrix}_{+Max} &= \begin{bmatrix} L_{\delta P} & 0 & L_{\delta R} & 0 & L_{\delta Y} & 0 \\ 0 & M_{\delta Q} & 0 & M_{\delta X} & 0 & M_{\delta Z} \\ N_{\delta P} & 0 & N_{\delta R} & 0 & N_{\delta Y} & 0 \\ 0 & F_{X\delta Q} & 0 & F_{X\delta X} & 0 & F_{X\delta Z} \\ F_{Y\delta P} & 0 & F_{Y\delta R} & 0 & F_{Y\delta Y} & 0 \\ 0 & F_{Z\delta Q} & 0 & F_{Z\delta X} & 0 & F_{Z\delta Z} \end{bmatrix} \begin{bmatrix} \delta_P \\ \delta_Q \\ \delta_R \\ \delta_X \\ \delta_Y \\ \delta_Z \end{bmatrix}_{+FCS Max} \quad \text{for max positive demands} \\
 \begin{bmatrix} L_X \\ M_Y \\ N_Z \\ F_X \\ F_Y \\ F_Z \end{bmatrix}_{-Max} &= \begin{bmatrix} L_{\delta P} & 0 & L_{\delta R} & 0 & L_{\delta Y} & 0 \\ 0 & M_{\delta Q} & 0 & M_{\delta X} & 0 & M_{\delta Z} \\ N_{\delta P} & 0 & N_{\delta R} & 0 & N_{\delta Y} & 0 \\ 0 & F_{X\delta Q} & 0 & F_{X\delta X} & 0 & F_{X\delta Z} \\ F_{Y\delta P} & 0 & F_{Y\delta R} & 0 & F_{Y\delta Y} & 0 \\ 0 & F_{Z\delta Q} & 0 & F_{Z\delta X} & 0 & F_{Z\delta Z} \end{bmatrix} \begin{bmatrix} \delta_P \\ \delta_Q \\ \delta_R \\ \delta_X \\ \delta_Y \\ \delta_Z \end{bmatrix}_{-FCS Max} \quad \text{for max negative demands}
 \end{aligned}$$

**Equation 8.1 Maximum Moments and Forces Produced when the Controls are Maximized in two Opposite Directions**

We will illustrate the maximum Moment and Force vector diagrams by two examples, where the moments and forces are represented by non-dimensional coefficients. The vector type is selected from the horizontal menu bar located at the top of the vector diagrams window. You must click on "Select Vector Diagrams" and then from the vertical menu below it, select "Maximum Moment and Force Vector Diagrams".

Figure 8.5 is a  $C_z$  versus  $C_m$  vector diagram. It shows the maximum pitching moment and maximum normal force (non-dimensional) that can be attained by maximizing the pitch control in the positive and also in the negative directions relative to trim positions. This vehicle has only one longitudinal pitch control, and there is no control in the Z-axis. The red vectors also show the maximum moment and force generated by the  $\pm\alpha_{max}$  dispersion from trim. At trim the normal force is negative at  $C_z=-0.45$  because  $\alpha_0>0$ . The solid red vector is when alpha increases to  $(\alpha_0+\alpha_{max})$ . It generates negative pitching moment and force (up). The dashed red vector is when alpha changes to  $(\alpha_0-\alpha_{max})$ . The rectangles centered at the tips of the vectors represent the possible variations of the vectors due to the aerodynamic uncertainties. The control pitch moment is obviously much greater than the maximum dispersion moment in this case.

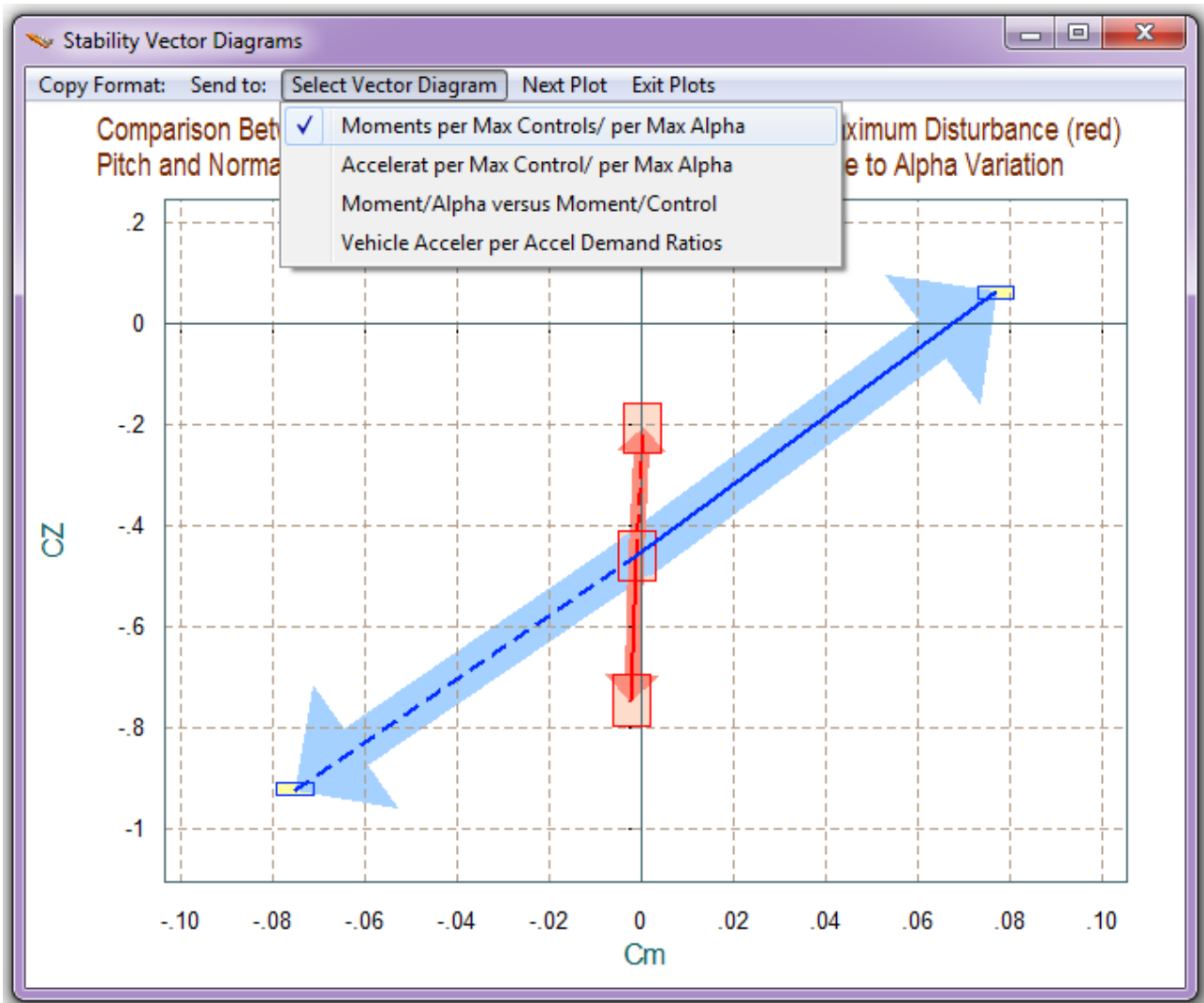


**Figure 8.5 Vector Diagram of Pitch Moment and Normal Force from Maximum Pitch Control against those from  $\pm\alpha_{\max}$  Dispersion**

Figure 8.6 shows a vector diagram of roll and yaw moments where we plot the non-dimensional,  $C_l$  versus  $C_n$  moments. The blue and green vectors are roll and yaw moments produced by maximizing the FCS demands. The solid blue vector corresponds to maximum positive yaw FCS demand  $\delta R_{+FCS_{\max}}$  and the dashed blue vector in the opposite direction corresponds to maximum negative yaw demand  $\delta R_{-FCS_{\max}}$ . Similarly, the green vectors represent the moments generated by maximizing the roll FCS demands in two opposite directions  $\delta P_{+FCS_{\max}}$  and  $\delta P_{-FCS_{\max}}$ .

The control vectors are pointing in the commanded directions but there is some cross-coupling between the axes. The yaw control vector slightly couples into roll but the roll control has a bigger component in the yaw direction. This coupling is intentionally created by the mixing logic matrix which attempts to provide lateral decoupling to compensate against the cross-product of inertia  $I_{xz}$ . For good controllability the two control vectors should be almost orthogonal to each other and their magnitudes exceeding the magnitudes of the disturbance vectors, such as in this illustration.

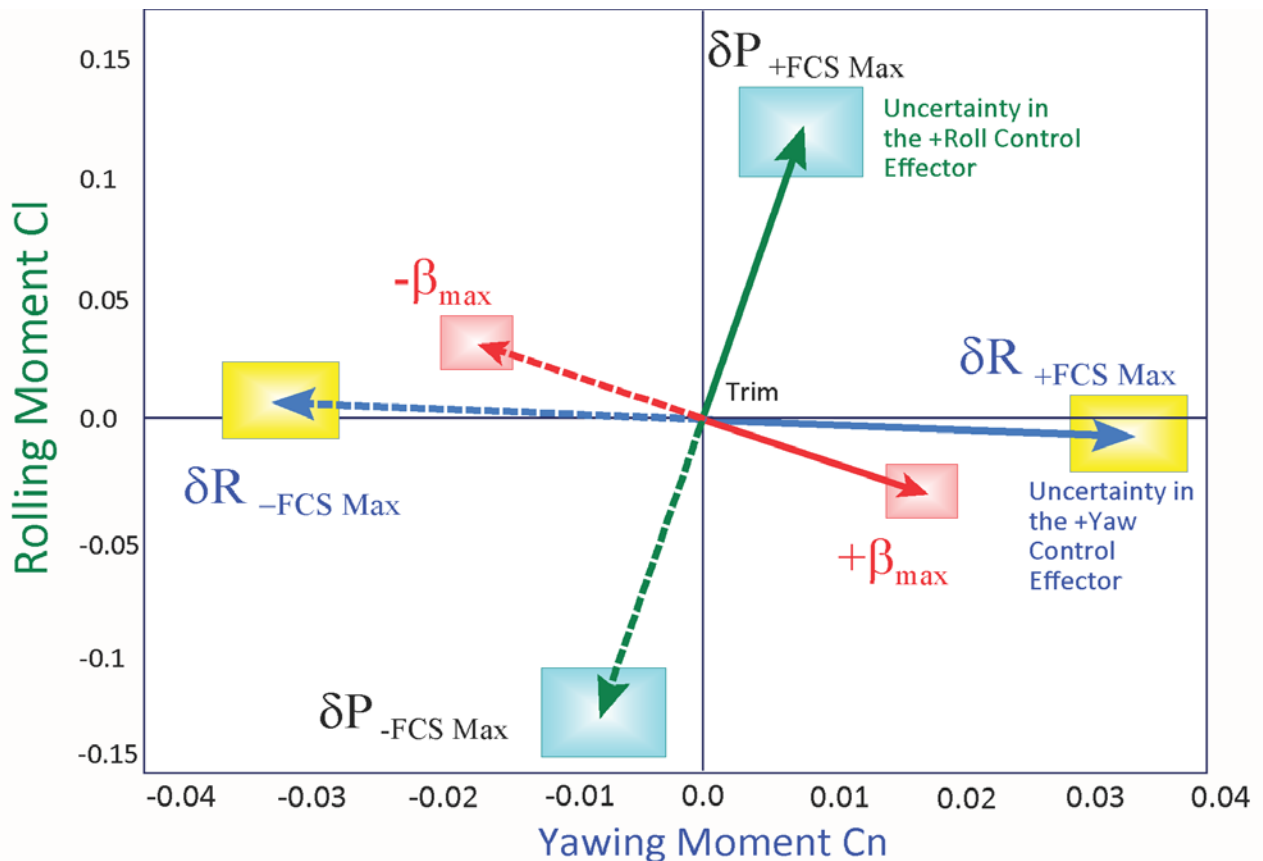


**Figure 8.6 Maximum Roll and Yaw Moment generated by Maximizing the Roll and Yaw Control Demands against the Moments produced by Maximum Sideslip Dispersion  $\pm\beta_{max}$ .**

The two red vectors represent the roll and yaw moments generated by variation in the velocity vector which is defined in terms of dispersions in the angles of attack and sideslip:  $\pm\alpha_{max}$  and  $\pm\beta_{max}$  from their trim positions. The dispersion angles define the worst case wind-shear or maneuverability requirement and they typically vary between  $\pm 2^\circ$  to  $\pm 5^\circ$  from trim, depending on the flight condition. The solid red arrow in Figure 8.6 shows that the yaw moment increases when the angles of attack and sideslip are increased from  $\alpha_0$  to  $(\alpha_0 + \alpha_{max})$ , and from  $\beta_0$  to  $(\beta_0 + \beta_{max})$ . The effect is mainly due to the sideslip and demonstrates that the vehicle is statically stable in yaw because it creates a yawing moment towards the airflow. The dashed red vector shows the moments when the angles of attack and sideslip are reduced from  $\alpha_0$  to  $(\alpha_0 - \alpha_{max})$  and from  $\beta_0$  to  $(\beta_0 - \beta_{max})$ , where  $\beta_{trim}=0$  in this case.

The square rectangles at the tip of the vectors represent the effects of the aerodynamic uncertainties. Their size is proportional to the uncertainty. The uncertainties are read from the uncertainties file that has an extension (.Unce). It is not necessary to provide an uncertainties file, and if this file is not available only the vectors will be shown without the rectangles at their tips. The uncertainty rectangles represent the possible variations of this vector due to the uncertainty in the aero coefficients ( $C_l$  and  $C_n$ ). The yellow rectangles at the tips of the yaw control vectors  $\delta R_{\pm FCS_{Max}}$  represent possible variations due to the uncertainties in the aerosurface derivatives, which are mainly in the rudder  $C_{n\delta rudd}$ , but also the aileron  $C_{n\delta ailr}$  is contributing because they are combined for yaw control. Similarly, the cyan rectangles at the tips of the roll control vectors  $\delta P_{\pm FCS_{Max}}$  represent variations in the roll vector caused by the uncertainties in the aerosurface derivatives, mainly in aileron  $C_{l\delta ailr}$ , but also in the rudder  $C_{l\delta rudd}$  because they are both contributing for roll control. The uncertainty rectangles should be sufficiently small to preclude the possibility that the disturbance moments may be stronger than the control moments in either direction.

The vector diagram in Figure 8.7 analyzes the longitudinal controllability of an accelerating vehicle that possesses pitch and axial acceleration control. The blue vectors show the maximum pitching moment  $C_m$ , axial  $C_x$ , and  $C_z$  forces produced by maximizing the pitch control demand in the positive  $\delta_{+QFCS_{Max}}$  direction (solid blue line) and also in the negative  $\delta_{-QFCS_{Max}}$  direction (dotted blue line). The two green control vectors pointing up and down along the axial force direction are the moment and x-force produced by varying the engine thrust relative to nominal thrust. The solid green line is when the axial acceleration demand is at maximum positive  $\delta_{+XFCS_{Max}}$ , and the dotted green line is when the axial acceleration demand is at maximum negative  $\delta_{-XFCS_{Max}}$ . Notice that the pitch control vectors are pointing mostly toward the  $\pm$ pitch directions and the axial control vectors affect mostly the  $\pm X$  force, and there is minimal amount of cross-coupling between the two control directions. Positive pitch control  $\delta_{QFCS}$  also produces positive Z-force  $C_z$  because of the rotation of the TVC engines. The diagram shows that the vehicle in this flight condition is accelerating under constant thrust and at trim the axial and Z forces are biased at  $C_{x0}=0.128$  and  $C_{z0}=-0.4$ . By throttling  $C_x$  can be varied between 0.09 and 0.20. Notice that the controls are not symmetric relative to trim. The asymmetry in the x-axis control is due to the trimming conditions. There is more force availability when applying a maximum positive throttle  $\delta_{X_{+FCS_{Max}}}$  than a negative force to slow it down when applying max negative throttle  $\delta_{X_{-FCS_{Max}}}$ . There is asymmetry also in the pitch direction. The negative pitch control moment produced when applying max negative pitch demand  $\delta_{-QFCS_{Max}}$  is greater than the moment produced when applying max positive pitch demand  $\delta_{+QFCS_{Max}}$ . This is because the vehicle is statically unstable in this flight condition and it is flying with a negative  $\alpha$  and it is, therefore, easier to rotate and accelerate in the negative direction than to rotate in the positive direction. Figure 8.7 also shows the moment and force produced due to the maximum variations in the angle of attack  $\pm\alpha_{max}$  from trim  $\alpha_0$ . An increase in alpha causes an increase in pitching moment and a further negative normal force (up).



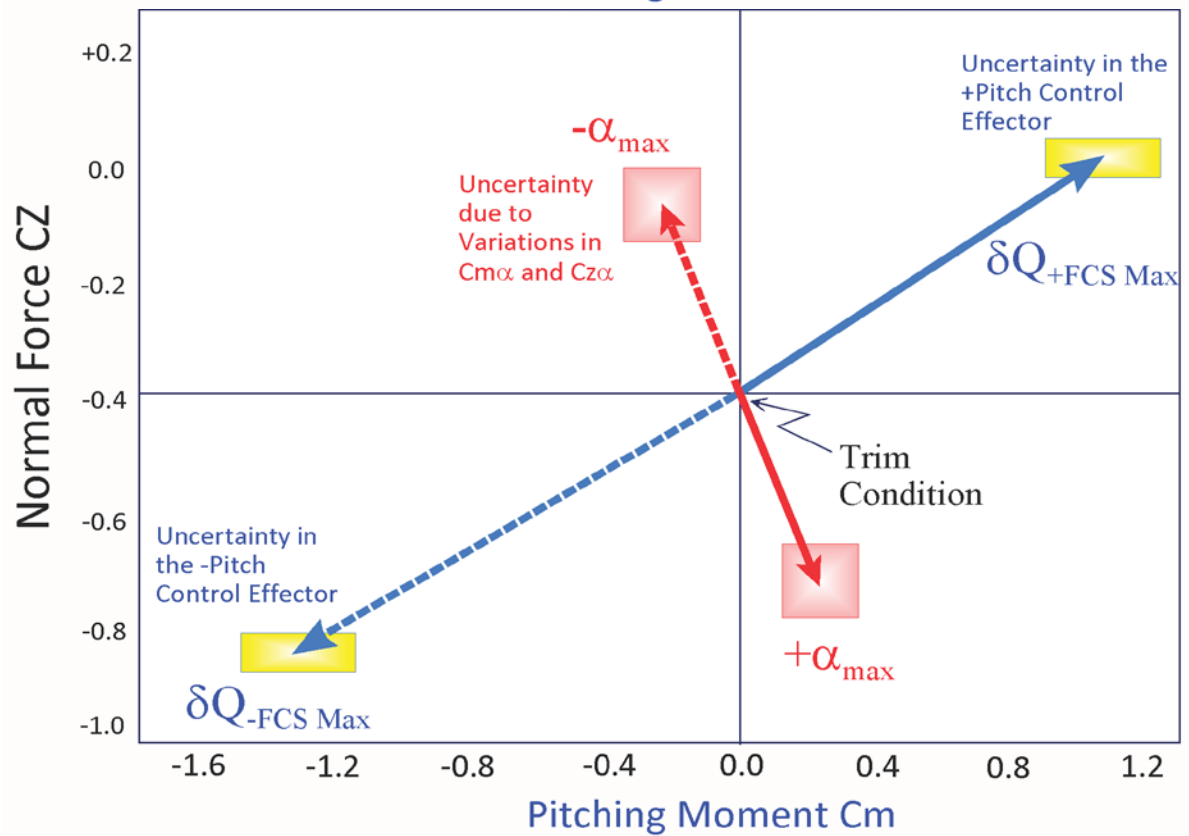
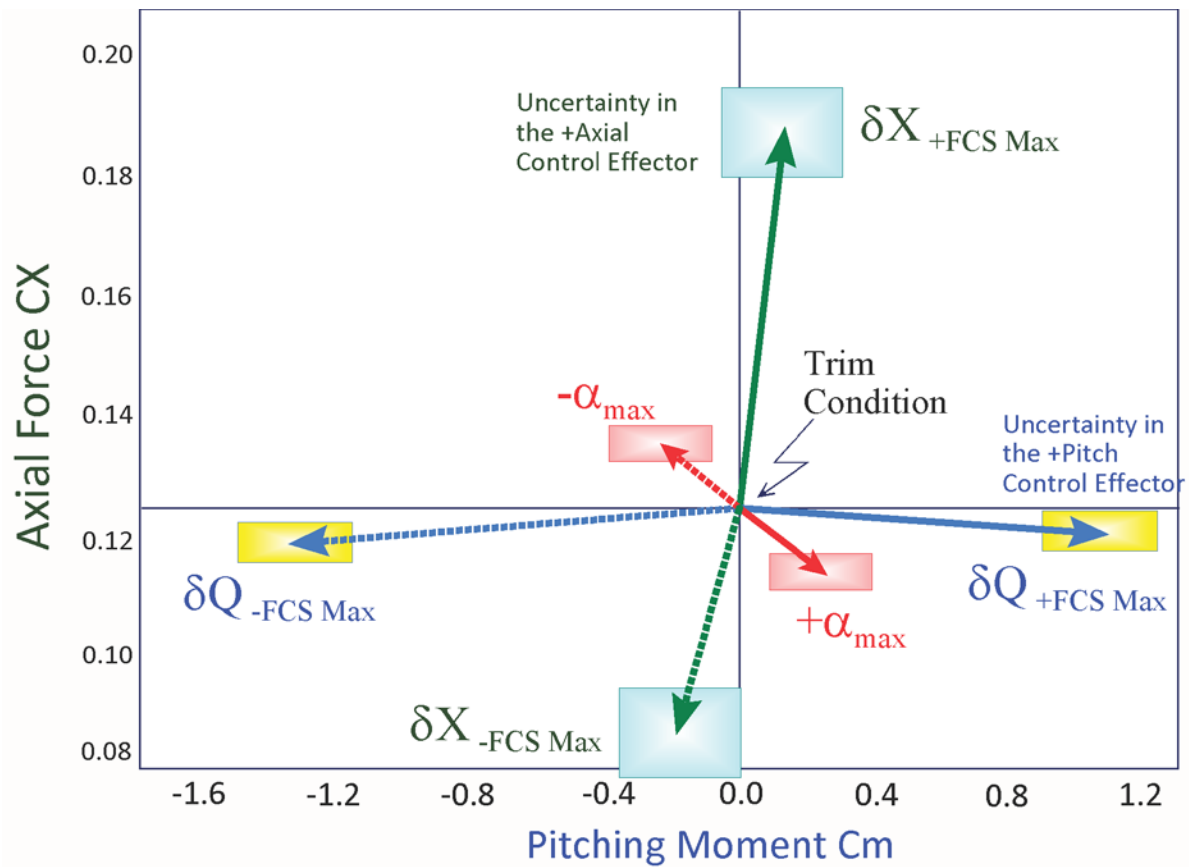


Figure 8.7 Longitudinal Vehicle Controllability Demonstrated in the Maximum Pitch and Maximum Axial and Normal Force Vector Diagram

## 8.2 Maximum Acceleration Vector Diagrams

In some applications it may be more appropriate to plot the accelerations generated by the controls or the dispersions rather than the scaled moments and forces. The maximum acceleration vector diagrams are very similar to the maximum moments and force diagrams. The only difference is that the moment vectors from equation 8.1 are scaled by dividing them with the moments of inertia dyadic matrix and the force vectors are divided by the vehicle mass to be converted to angular and linear accelerations, as shown in equation 8.2.

$$\begin{bmatrix} \dot{p} \\ \dot{q} \\ \dot{r} \\ \ddot{x} \\ \ddot{y} \\ \ddot{z} \end{bmatrix} = \begin{bmatrix} I_{XX} & -I_{XY} & -I_{XZ} & 0 & 0 & 0 \\ -I_{XY} & I_{YY} & -I_{YZ} & 0 & 0 & 0 \\ -I_{XZ} & -I_{YZ} & I_{ZZ} & 0 & 0 & 0 \\ 0 & 0 & 0 & M_V & 0 & 0 \\ 0 & 0 & 0 & 0 & M_V & 0 \\ 0 & 0 & 0 & 0 & 0 & M_V \end{bmatrix}^{-1} \begin{pmatrix} L \\ M \\ N \\ F_x \\ F_y \\ F_z \end{pmatrix}$$

**Equation 8.2 Angular and Linear Accelerations**

The maximum acceleration diagrams are also used in analyzing the effectiveness of the mixing logic matrix against disturbances in multiple directions. The vehicle effectors system may have accessibility to span more than 3 directions, including translational, and in theory, a mixing logic matrix can be designed to provide control in multiple directions. The practicality, however, of this design is evaluated by the capability of the effectors to maneuver and to react against disturbances which are defined by the variations:  $\pm\alpha_{\max}$ ,  $\pm\beta_{\max}$  and in airspeed  $\pm V_{\max}$ . When the effector system attempts to spread its domain and attempts to control multiple directions, in general, it loses its overall effectiveness in some directions against aero disturbances. It may be more efficient when it controls fewer directions.

Figure 8.8 shows a yaw versus  $\ddot{y}$  vector diagram for a vehicle that in addition to roll and yaw control, it also has a side-force effector to compensate against lateral accelerations. The vertical green vectors show the positive and negative accelerations produced in yaw when the yaw control demand  $\delta R_{\pm FCS_{\max}}$  is maximized. The acceleration is entirely in yaw (as it should be) and the vector magnitudes are bigger than the yaw acceleration produced by  $\pm\beta_{\max}$ . The aero uncertainties in yaw are very small, and we should, therefore, expect a very good controllability in yaw. The horizontal blue vectors show the positive and negative accelerations produced when the side-acceleration control demand  $\delta Y_{\pm FCS_{\max}}$  is maximized by throttling the reaction control jets affecting the  $\ddot{y}$  acceleration, as expected.

The red vectors show the effects in yaw acceleration  $\dot{R}$  in ( $\text{rad}/\text{sec}^2$ ) and in side-acceleration  $\dot{y}$  in (g), created when the vehicle is exposed to 2 degrees of  $\pm\beta_{\text{max}}$  variation. Positive  $\beta$  generates positive yaw and a negative  $\dot{y}$  acceleration. The controllability, however, against  $\pm\beta_{\text{max}}$  dispersions in the y direction is not as good as it is in yaw because the disturbance magnitude caused by the  $\pm\beta_{\text{max}}$  variation is almost as big as the side-force control magnitude. It implies that the vehicle requires bigger thrusters in the  $\pm y$  direction.

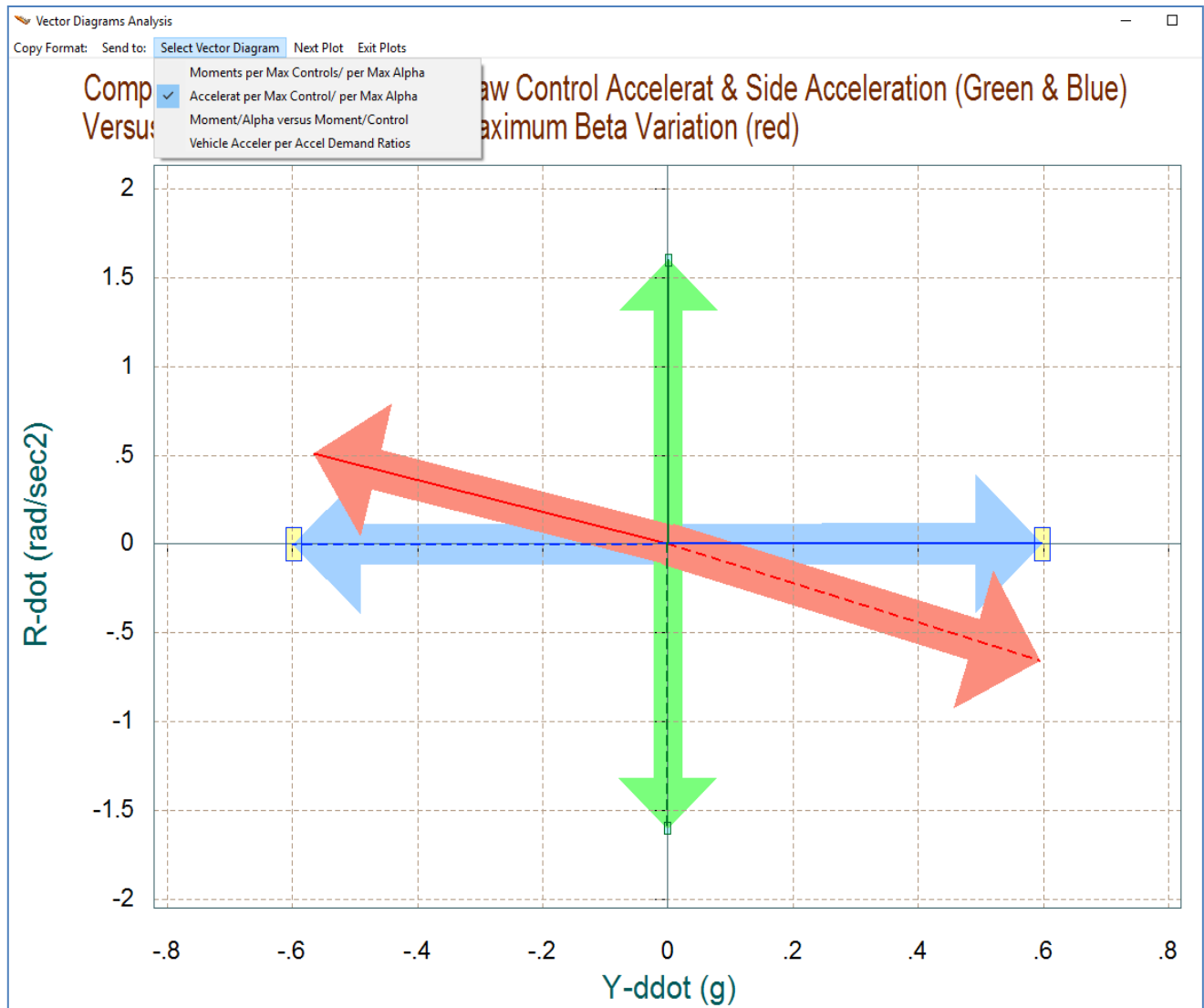
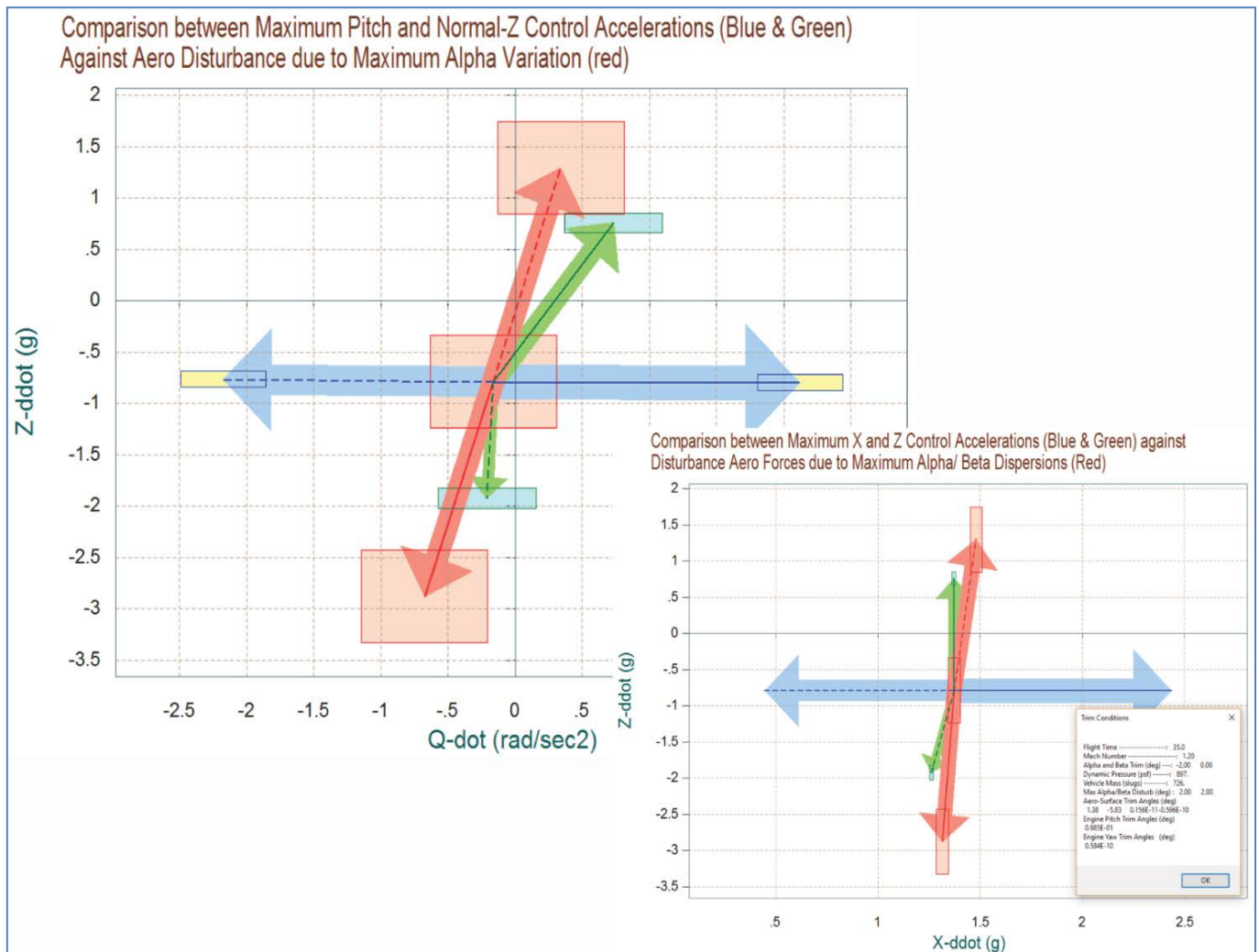


Figure 8.8 Maximum Yaw and Side-Force Accelerations generated by maximizing the Yaw Control and the Lateral Side-Force Throttle Control Demands against the Accelerations produced by Sideslip Dispersion  $\pm\beta_{\text{max}}$ .

Figure 8.9 is a maximum accelerations vector diagram of a launch vehicle in the longitudinal directions. All 3 longitudinal directions: pitch, normal, and axial accelerations are accessible and commanded by the effector system. The pitch acceleration is in ( $\text{rad}/\text{sec}^2$ ). The normal and axial accelerations are in g. The red vectors show the accelerations produced when the vehicle is exposed to  $2^\circ$  of  $\pm\alpha_{\text{max}}$  variation from trim. The horizontal blue vectors in the top diagram show the ( $\ddot{z}$  and  $\dot{Q}$ ) accelerations produced by maximizing the pitch control ( $\delta Q_{\pm\text{FCS Max}}$ ), and it is mainly

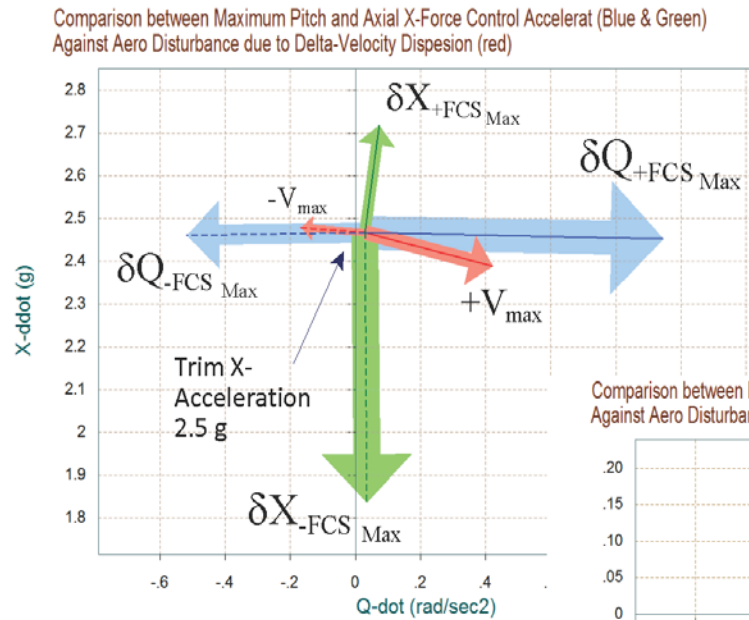
in pitch. Their magnitudes exceed the pitching moment due to  $\pm\alpha_{\max}$  variations, including uncertainties. Also the horizontal blue vectors in the bottom diagram show the ( $\ddot{z}$  and  $\ddot{x}$ ) accelerations produced by maximizing the axial throttle control ( $\delta X_{\pm FCS \text{ Max}}$ ), and it is mainly in the x-axis. Their magnitudes also exceed the acceleration variations due to  $\pm\alpha_{\max}$ . The green vector shows the effects of maximizing the  $\pm z$  acceleration demand ( $\delta Z_{\pm FCS \text{ Max}}$ ) by firing the RCS jets in the  $\pm z$  direction. The RCS throttle control provides some acceleration in z but its controllability is insufficient to overcome the  $\pm\alpha_{\max}$  dispersion red vector. The uncertainty rectangles centered at the tips of the vectors denote the possible spread of this vector due to the aerodynamic uncertainties.



**Figure 8.9 Maximum Pitch, Normal, and Axial Accelerations produced by Max Controls in all 3 Directions against Accelerations produced by Alpha Dispersion  $\pm\alpha_{\max}$**

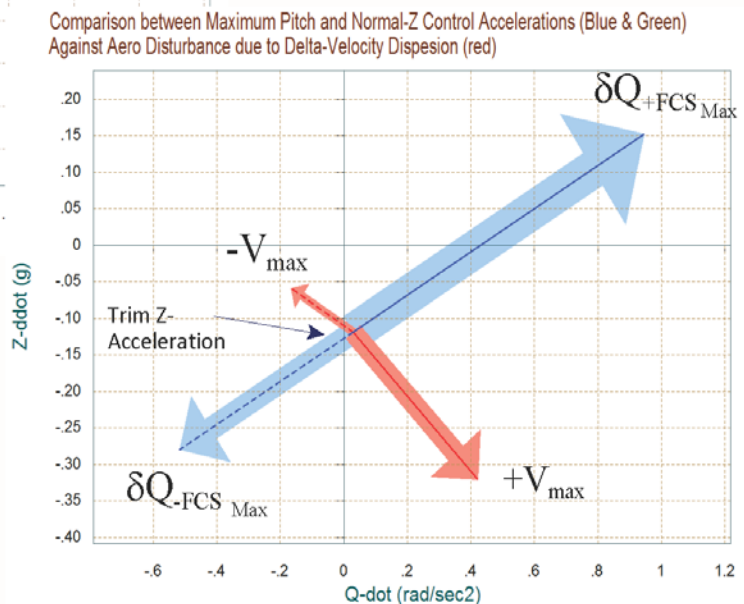
### 8.2.1 Maximum Accelerations due to Air-Speed Variation $v_{max}$

Similar to analyzing the effectors control capability against  $\alpha_{max}$  and  $\beta_{max}$  dispersions, we can also compare the capability of the effector system against disturbances generated by air-speed variations relative to  $V_0$ . Flinxan calculates the maximum moments, forces or accelerations generated by the maximum air-speed variation  $\pm v_{max}$  and plots them against the controls. The figure below is from a launch vehicle example that has pitch TVC control and axial acceleration control by varying the thrust. It is trimmed at 2.45 g acceleration due to the main engine thrusting and it can change its acceleration from  $\delta X_{-FCS_{Max}}=1.85$  g to  $\delta X_{+FCS_{Max}}=2.72$  g by throttling the engines (green vectors). It can also change its pitch acceleration by gimbaling the TVC engines from  $\delta Q_{-FCS_{Max}}$  to  $\delta Q_{+FCS_{Max}}$  (blue vectors). The diagram below compares the control accelerations against the accelerations generated by the airspeed variations. The red vectors show the pitch, axial, and normal accelerations generated by positive and negative airspeed variations  $\pm v_{max}$  relative to  $V_0$ . This vehicle is statically unstable and it is flying with a positive  $\alpha_0$ . An increase in the airflow due to wind  $+v_{max}$ , therefore, produces a positive pitching moment, a negative z-acceleration (upwards), and a negative x-acceleration (more drag). In this example, the pitch and axial controls are more powerful than the disturbance and they can compensate against the  $\pm v_{max}$  variation.



Comparison on a Launch Vehicle Accelerations produced by maximizing the controls from Trim, and also by air-speed variations due to wind disturbances.

Blue and Green Vectors show the variations in Pitch, Axial, and Normal Accelerations produced by the maximization of the Pitch and Axial controls. The Red Vectors show the acceleration variations generated by the air-speed variation  $\pm V_{max}$  from  $V_0$



### 8.3 Moment and Force Vector Partial

The two previous vector diagrams analyze the control authority of an effector system in terms of its maximum control capability against maximum steady-state wind-shear disturbances defined in terms of maximum aerodynamic angle dispersions and airflow variations from trim. The partial vector diagrams measure gains. They compare the controllability gain of the open-loop effector system against disturbability gain, that is, sensitivity to aerodynamic disturbances. The control partial measures the moment or force produced per acceleration demand in a certain direction. The disturbance partial measures the moment or force produced per alpha variation in pitch or per beta in the lateral axes. The partial vector diagrams compare the moment partials per flight control acceleration demands:  $[C_{m\delta Q}, C_{n\delta R}, C_{l\delta P}]_{FCS}$  per  $(\text{rad}/\text{sec}^2)$  or the force partials per translational acceleration demands:  $[C_{X\delta X}, C_{Y\delta Y}, C_{Z\delta Z}]_{FCS}$  per  $(g)$ , against the moment and force partials the base vehicle per alpha and beta angles  $[C_{m\alpha}, C_{n\beta}, C_{l\beta}, C_{z\alpha}, C_{y\beta}]$  per degree. The control and disturbance partials are plotted together in 2-dimensional vector diagrams because their relative size and directions are important for control design.

Since the flight control demands  $(\delta_P, \delta_Q, \delta_R, \delta_X, \delta_Y, \delta_Z)_{FCS}$  are defined in vehicle body frame, instead of the classical  $(\delta_{\text{elevator}}, \delta_{\text{aireron}}, \delta_{\text{rudder}})$  definition, for good controllability we would like to see the control moment and force vector partials to be greater in magnitude along the control directions, than the moment and force partials per alpha and beta variations. These partials, however, cannot be compared directly because they are different in nature and units. They must be properly scaled in order to be associated in the same diagram.

For example, let us consider the pitch moment equation:  $I\ddot{\theta} = M_\alpha\alpha + M_\delta\delta$ . A good test for pitch controllability is to compare the magnitudes of the partials  $M_\alpha$  and  $M_\delta$ . However, they cannot be compared directly because they are of different substance. The first one is moment per degree of alpha and the second one is moment per angular acceleration demand in  $(\text{rad}/\text{sec}^2)$ . For the vehicle to have good controllability we would like the  $M_\delta\delta$  term to be sufficiently greater than the  $M_\alpha\alpha$  term. This is possible when the control contribution due to  $\delta_{\text{max}}$  is greater than the aerodynamic disturbance due to  $\alpha_{\text{max}}$ . One way to make the control versus alpha partials comparable is to scale the magnitudes of the alpha variation vector by multiplying them with  $(\alpha_{\text{max}}/\delta_{\text{max}})$ . This scaling allows us to compare the two vector partials and to quantify controllability versus disturbability by their relative size and direction. Obviously, the control vector partials should be greater than the scaled moment or force partials per  $\alpha$  or  $\beta$  variation. One might argue that the torque rates rather than the maximum torques are more important in this comparison, especially when you have a divergent vehicle, in which case we would like the  $M_\delta\dot{\delta}_{\text{max}}$  term to be greater than the  $M_\alpha\dot{\alpha}_{\text{max}}$  term, and the scaling factor in this case should be:  $(\dot{\alpha}_{\text{max}}/\dot{\delta}_{\text{max}})$ , where the max actuator rate is defined in the actuator specs and the max vehicle rate can also be estimated.

Let us consider, for example, in Figure 8.10 the partials in two longitudinal directions for a vehicle that has pitch control and also axial force control by means of thrust variation or a speed-brake. The nearly horizontal pitch control blue vector  $(C_{m\delta Q}, C_{x\delta Q})$  represents the pitch moment and axial force partials per pitch control acceleration demand  $\delta Q_{FCS}$ . Similarly, the almost vertical axial force control green vector  $(C_{m\delta X}, C_{x\delta X})$ , represents the pitch moment and axial force partials per axial acceleration demand  $\delta X_{FCS}$ . The partials are calculated at a trim flight condition. The  $(C_{m\alpha}, C_{x\alpha})$  red vector corresponds to the pitch moment and x-force partials per alpha and it is scaled as shown in equations (8.1 & 8.2). This vehicle has a negative  $C_{m\alpha}$  that indicates that it is statically stable, and also a negative  $C_{x\alpha}$  that causes an increase in aft force due to  $\alpha$ . The  $C_{m\alpha}$  component in this vector is scaled by multiplying it with  $(\alpha_{max}/\delta Q_{max})$  so that it can be made comparable with  $C_{m\delta Q}$ , and the  $C_{x\alpha}$  component is scaled by multiplying it with  $(\alpha_{max}/\delta X_{max})$  so that it can be made comparable with  $C_{x\delta Q}$ , and plotted on the same scale. For good controllability in both axes, the directions of the control moment and force partials (blue and green vectors) should be pointing towards their intended directions and their magnitudes should be greater than the scaled moment and force partials per alpha variation (red vector). That is, the pitch control  $C_{m\delta Q}$  should be greater than  $C_{m\alpha}(\alpha_{max}/\delta Q_{max})$  and the axial control  $C_{x\delta X}$  should be greater than  $C_{x\alpha}(\alpha_{max}/\delta X_{max})$ .

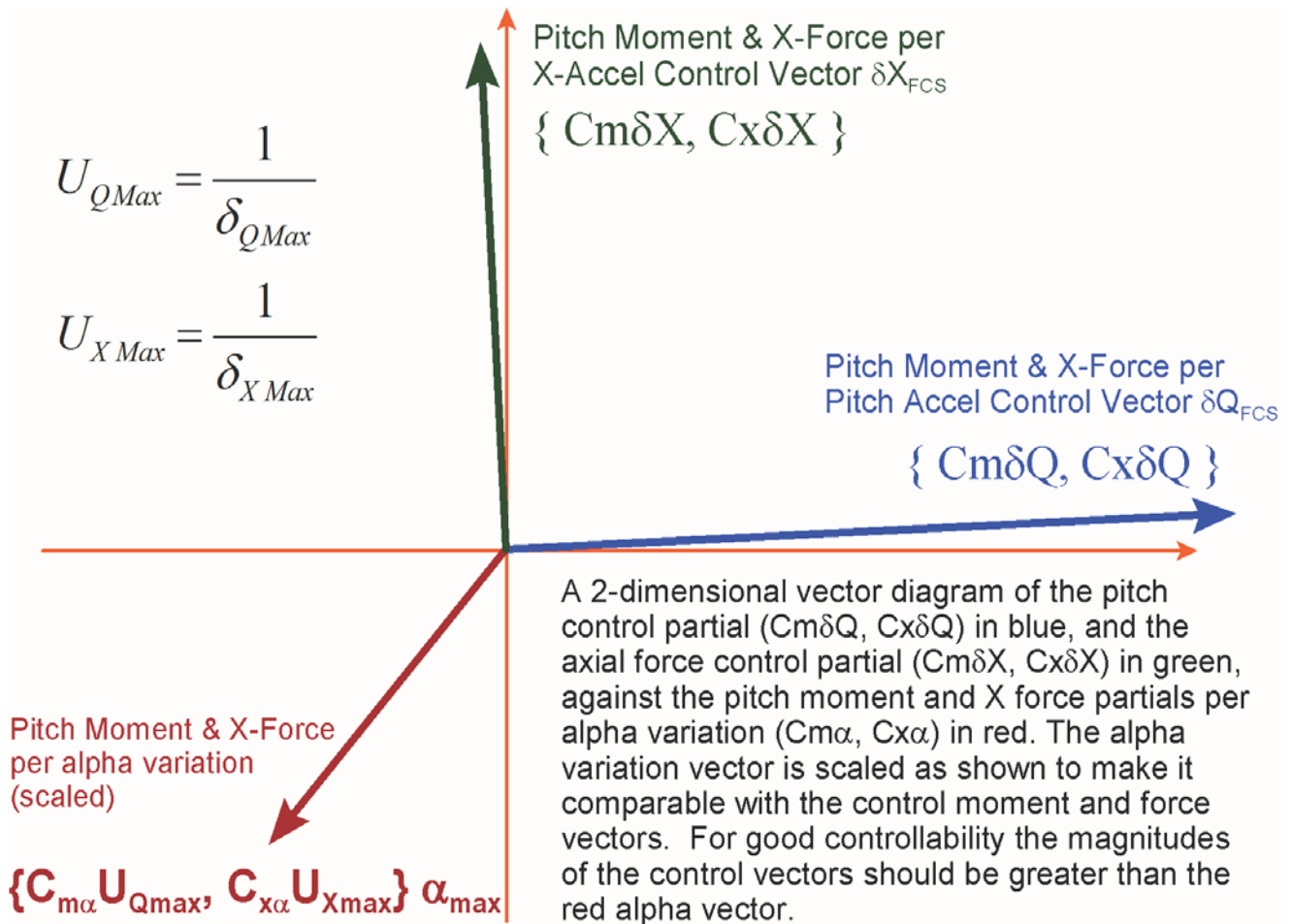


Figure 8.10 Partial Vector Diagram of Pitch Moment and Axial Force per: control, and per alpha

$$|C_{m\alpha}| < \left( \frac{\delta_{Q\max}}{\alpha_{\max}} \right) |C_{m\delta Q}| \quad \text{or} \quad |C_{m\alpha}| < \left( \frac{1}{U_{Q\max} \alpha_{\max}} \right) |C_{m\delta Q}| \quad \text{and} \quad (8.1)$$

$$|C_{A\alpha}| < \left( \frac{\delta_{X\max}}{\alpha_{\max}} \right) |C_{X\delta X}| \quad \text{and} \quad |C_{A\alpha}| < \left( \frac{1}{U_{X\max} \alpha_{\max}} \right) |C_{X\delta X}| \quad (8.2)$$

$$\{C'_{m\alpha} \quad C'_{X\alpha}\} = \{U_{Q\max} C_{m\alpha} \quad U_{X\max} C_{X\alpha}\} \alpha_{\max}$$

A similar vector diagram is shown in Figure 8.11 which is a roll/ yaw moment partials vector diagram in the lateral directions. We plot the roll and yaw control partials (blue and green vectors) against the disturbance partials per beta variation:  $(C_{l\beta}, C_{n\beta})$  red vector. The blue vector represents the roll/yaw moment partials per yaw control demand  $(C_{l\delta R}, C_{n\delta R})$ . This vector is nearly horizontal indicating that the yaw control demand  $\delta R_{FCS}$  affects mainly the yaw direction with very little coupling in roll. Similarly, the vertical green vector represents the moment partials per roll control demand  $(C_{l\delta P}, C_{n\delta P})$ . This vector is almost vertical indicating that roll control demand  $\delta P_{FCS}$  produces mostly a roll torque with very little coupling in yaw. The  $(C_{l\beta}, C_{n\beta})$  vector is scaled as shown in equation 8.4, in order to be made comparable with the control partials.

$$|C_{l\beta}| < \left( \frac{\delta_{P\max}}{\beta_{\max}} \right) |C_{l\delta P}| \quad \text{or} \quad |C_{l\beta}| < \left( \frac{1}{U_{P\max} \beta_{\max}} \right) |C_{l\delta P}| \quad \text{and} \quad (8.3)$$

$$|C_{n\beta}| < \left( \frac{\delta_{R\max}}{\beta_{\max}} \right) |C_{n\delta R}| \quad \text{or} \quad |C_{n\beta}| < \left( \frac{1}{U_{R\max} \beta_{\max}} \right) |C_{n\delta R}| \quad \text{and} \quad (8.4)$$

$$\{C'_{l\beta} \quad C'_{n\beta}\} = \{U_{P\max} C_{l\beta} \quad U_{R\max} C_{n\beta}\} \beta_{\max}$$

We should expect the magnitudes of the two control partials to be greater than the scaled partials per beta variation in both: roll and yaw directions. For good roll controllability the magnitude of  $C_{l\delta P}$  should obviously be greater than  $C'_{l\beta}$  and for good yaw controllability the magnitude of  $C_{n\delta R}$  should be greater than  $C'_{n\beta}$  as shown in equations (8.3 and 8.4).

In Figure 8.11 the two control partials are almost orthogonal and they do not couple much into each other's direction, as they should be. The yaw control partial (blue vector) is pointing mainly in yaw, and the roll control partial (green vector) is pointed mainly in the roll direction. This is because the two axes are nearly decoupled by the mixing-logic matrix. In this type of diagrams we don't need to show negative directions since we are dealing with partials.



Notice that the yaw control partial  $C_n \delta R$  is an order of magnitude bigger than the roll control partial  $C_l \delta P$ , because the roll moment of inertia in this vehicle is much smaller than the yaw inertia, plus this vehicle requires greater controllability in yaw. Notice also that there are two roll and yaw moment partials per beta ( $C'_{l\beta}, C'_{n\beta}$ ), (red vectors). They correspond to two different dispersions. The solid red vector represents  $(C_n \beta & C_l \beta)$  at  $(\alpha_0 + \alpha_{max}$  and  $\beta_0 + \beta_{max})$  and the smaller dashed red vector is calculated at  $(\alpha_0 - \alpha_{max}$  and  $\beta_0 - \beta_{max})$ . This captures the variation of  $(C_n \beta & C_l \beta)$  over the entire range of alpha and beta variations. The disturbance partials (red vectors) are smaller than the control partials in both directions, as they should be, and this is an indication that the vehicle has good controllability against the expected lateral disturbances.

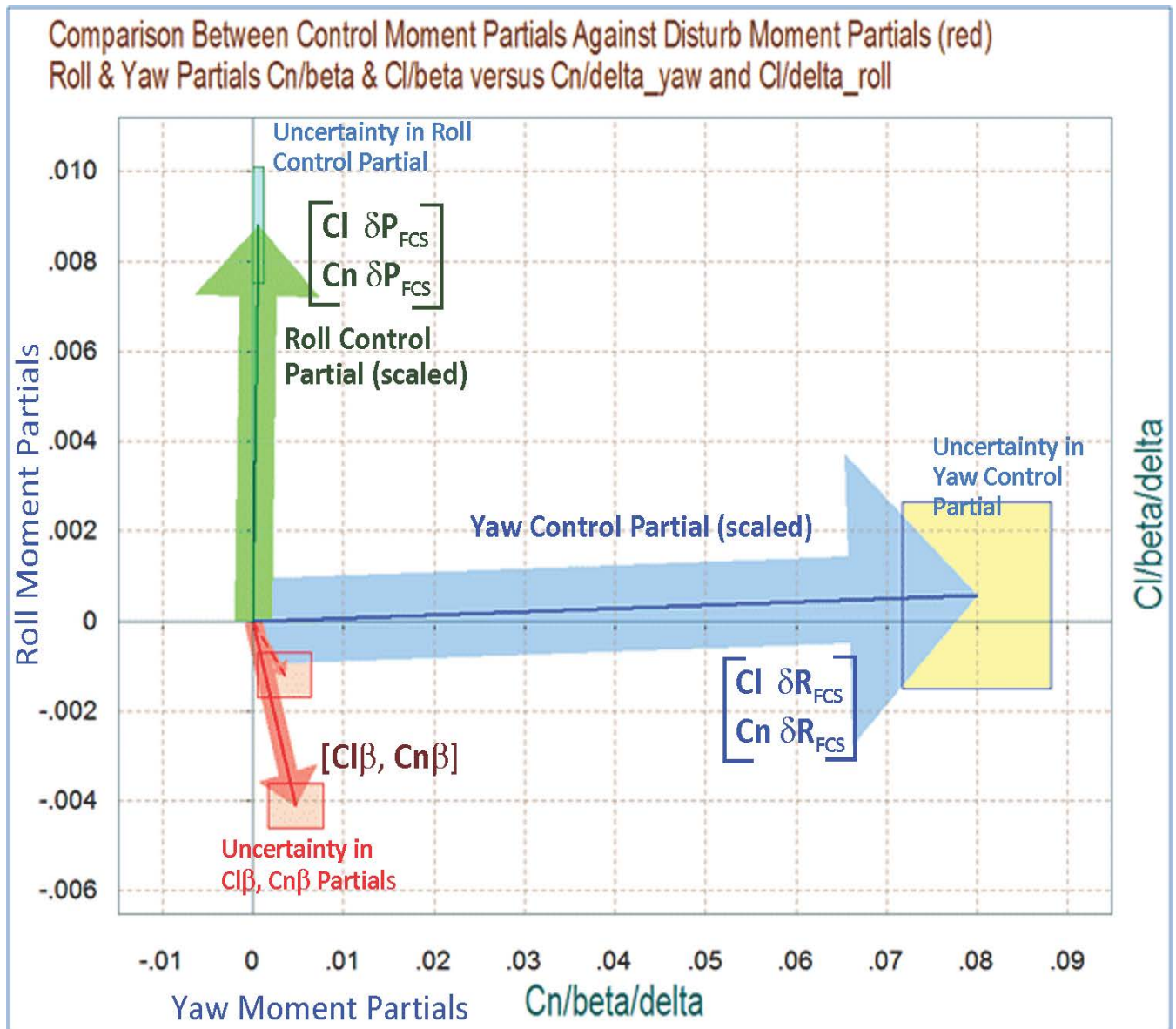


Figure 8.11 Partial of Roll and Yaw Control Moments versus Partial due to Beta

The square rectangles which are centered at the tip of the vectors represent the effects of the uncertainties in the aero derivatives. The uncertainties in  $C_n\beta$  and  $C_l\beta$  are shown by the red rectangles at the tips of the red vectors. The uncertainties in the control surface derivatives are initially defined for each individual aerosurface, as a function of aerosurface deflection. They are converted from individual aerosurfaces to uncertainties per flight control axis demands:  $\delta C_l\delta P$ ,  $\delta C_l\delta R$ ,  $\delta C_n\delta R$ ,  $\delta C_m\delta Q$ , etc. which requires involvement of the mixing logic. For example, the yellow rectangle at the tip of the blue ( $C_n\delta R$ ,  $C_l\delta R$ ) vector represents the possible variations of this vector partial due to the combined uncertainties of all aerosurfaces that contribute in yaw control. Similarly the cyan rectangle at the tip of the green ( $C_n\delta P$ ,  $C_l\delta P$ ) vector represents the possible variations of this vector partial due to the combined uncertainties of all aerosurfaces that contribute in roll. Equations (8.8 and 8.9) describe how we combine the uncertainties from the individual aerosurfaces using the mixing logic matrix.

### 8.3.1 Control versus Airspeed Variation Partial

The airspeed variation vector partials are similar to the  $\alpha$  and  $\beta$  partials. In this case we compare the control moment and forces per control demand against the partials of moments and forces per variation in airspeed. When we plot two different vector types in the same diagram we must scale one of them in order to make them comparable. For example, in a launch vehicle that has pitch and axial acceleration controls we must scale the partials of pitch moment and axial force per velocity variation to make them comparable with the control partials, as shown in the equation below.

$$|C_{m\delta v}| < \left( \frac{\delta_{Q \max}}{v_{\max}} \right) |C_{m\delta Q}| \quad \text{or} \quad |C_{m\delta v} U_{Q \max} v_{\max}| < |C_{m\delta Q}| \quad \text{and}$$

$$|C_{X\delta v}| < \left( \frac{\delta_{X \max}}{v_{\max}} \right) |C_{X \delta X}| \quad \text{or} \quad |C_{X\delta v} U_{X \max} v_{\max}| < |C_{X \delta X}|$$

$$\left\{ C'_{m\delta v} \quad C'_{X\delta v} \right\} = \left\{ U_{Q \max} C_{m\delta v} \quad U_{X \max} C_{X\delta v} \right\} v_{\max}$$

This scaling allows us to compare the pitch control partials  $\{C_{m\delta Q}, C_{X\delta Q}, C_{Z\delta Q}\}$  and the axial force control partials  $\{C_{m\delta X}, C_{X\delta X}, C_{Z\delta X}\}$  against the partials per velocity variation  $\{C_{m\delta v}, C_{X\delta v}, C_{Z\delta v}\}$ . Otherwise, we can't compare them because they are composed of different units. We typically like to see the control partials to be at least twice bigger than the scaled disturbance partials, as shown in the launch vehicle example below.

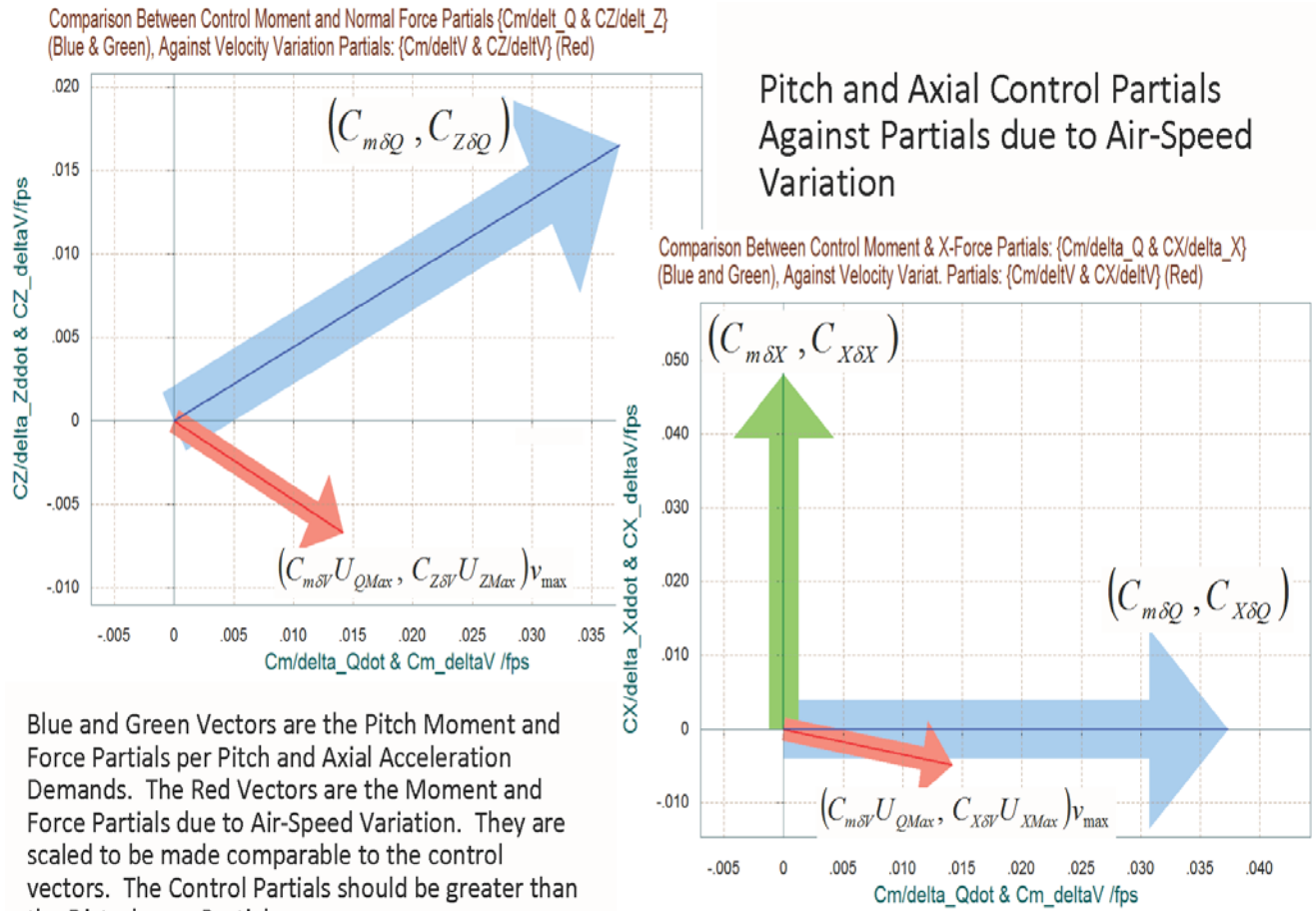


**Figure 8.12** Partial of Pitch Moment, Normal and Axial Forces; Control versus Airspeed Variation Partial

The partial vector diagrams in Figure 8.12 compare the pitch and axial control partials (blue and green vectors) for a launch vehicle that is statically unstable and has a positive angle of attack  $\alpha_0$ , against the moment and force partials per airspeed variation (red vectors). The red vectors are scaled as shown in equation. The vector diagram illustrates that a pitch control demand variation  $\delta Q_{FCS}$  (blue vector) generates mainly a pitching moment  $C_{m\delta Q}$ , as expected, and it does not couple in the axial direction. It generates also a positive z-force  $C_{Z\delta Q}$ . This is because the engines pivot negative (up) to generate the pitch moment and they also produce a +z force. Similarly, the axial control demand variation  $\delta X_{FCS}$  (green vector) generates an axial force  $C_{X\delta X}$  by throttling the engines and it does not couple in the pitch direction, as expected. The scaled red vector is the moment and force partials per airspeed variation. An increase in airspeed causes: a positive pitching moment, a negative z-force (up), and a reduction in x-force (more drag). The control partials are sufficiently greater in magnitude than the velocity partials, as they should be, in order to be able to compensate against airspeed variations.

## 8.4 Acceleration per Acceleration Demand Vector Partial

The fourth type of vector diagrams are partials of accelerations achieved in two control directions per accelerations demanded by flight control in the same directions. They are used for analyzing the vehicle open-loop maneuverability in certain directions by the magnitude and direction of the vehicle response in the control directions relative to the commands. When the mixing-logic is properly designed the vector partial of acceleration per acceleration demand should be pointing towards the demanded direction and its magnitude should be close to unity. This, however, is not a strict requirement but only a guideline because the closed-loop control system compensates for the imperfections in the mixing logic.

In the ideal situation, the open-loop plant is diagonalized by the mixing-logic matrix ( $K_{mix}$ ) and the transfer path between the acceleration demands to vehicle accelerations becomes the identity matrix. It means that the vehicle accelerations become equal to the accelerations commanded by the control system. The controls are unit vectors pointing towards the commanded directions and are orthogonal to each other, meaning that they are perfectly decoupled from each other. This ideal situation of perfect plant diagonalization, however, is not possible to achieve at all times because the vehicle parameters are continuously changing, but a certain amount of diagonal dominance in the controlled directions should at least be attained by the mixing logic because it makes the control system design more efficient. The acceleration partials are used to evaluate the efficiency of the effector mixing logic matrix in achieving the demanded accelerations and also an acceptable amount of decoupling between the control axes.

Going back to Figure 8.4, the moments and forces on the vehicle generated by a flight control input is the vector  $M_\delta = C_M K_{mix} \delta_{FCS}$  where  $\delta_{FCS}$  is the control acceleration demands vector in ( $\text{rad}/\text{sec}^2$ ) for rotational and in ( $\text{feet}/\text{sec}^2$ ) for translational demands. The size of vector  $\delta_{FCS}$  varies from three (for three angular accelerations) to six (including also translational acceleration demands). The matrix  $K_{mix}$  converts the flight control demands to effector deflections or throttle commands. The matrix  $C_M$  converts the deflections to a vector of three moments in (ft-lb) and up to 3 forces in (lb). The rotational and translational accelerations of the vehicle are obtained by multiplying out the 3 matrices in equation 8.5. In the 6x6 mass-matrix, the 3x3 submatrix in the upper left corner is the vehicle inertias dyadic, and the vehicle mass along x, y, and z axes is in the lower right corner. The product of the 3 matrices in equation 8.5 is a matrix that its elements consist of the acceleration partials and its maximum dimension is: (6x6).

$$\begin{bmatrix} \dot{p} \\ \dot{q} \\ \dot{r} \\ \ddot{x} \\ \ddot{y} \\ \ddot{z} \end{bmatrix}_{control} = \begin{bmatrix} I_{XX} & -I_{XY} & -I_{XZ} & 0 & 0 & 0 \\ -I_{XY} & I_{YY} & -I_{YZ} & 0 & 0 & 0 \\ -I_{XZ} & -I_{YZ} & I_{ZZ} & 0 & 0 & 0 \\ 0 & 0 & 0 & M_V & 0 & 0 \\ 0 & 0 & 0 & 0 & M_V & 0 \\ 0 & 0 & 0 & 0 & 0 & M_V \end{bmatrix}^{-1} C_M K_{mix} \begin{pmatrix} \delta_P \\ \delta_Q \\ \delta_R \\ \delta_X \\ \delta_Y \\ \delta_Z \end{pmatrix}_{FCS} \quad (8.5)$$

If we assume that the vehicle has sufficient effectors to span all control directions (three rotations and all three translations) and if the mixing logic matrix is properly designed to provide dynamic decoupling between the axes, based on the vehicle mass properties, geometry, and the effector parameters, the product of 3 matrices in equation 8.5 becomes the 6x6 identity matrix, and the accelerations achieved in all 6 directions will be equal to the accelerations demanded by the control system. In general, however, some of the translational directions are not directly controllable by the FCS and some of the rows in equation 8.5 can be ignored because they are uncontrollable or weakly controllable, plus the mixing-logic is designed to affect mainly the controllable directions. In addition, the selection of the mixing-logic matrix is sometimes influenced by other performance factors, such as the LCDP performance, and it is not always ideal when analyzed from the acceleration partials point of view.

Figure 8.13 is an example showing the accelerations per acceleration demands partials of a flight vehicle in the roll and yaw directions. The solid vertical vector pointing towards roll is the vehicle acceleration response per roll acceleration demand  $\{\dot{P}/\delta P_{FCS}, \dot{R}/\delta P_{FCS}\}$ . The dominant component is in roll with some small coupling into yaw. The dashed horizontal vector pointing towards yaw is the vehicle acceleration response per yaw acceleration demand  $\{\dot{P}/\delta R_{FCS}, \dot{R}/\delta R_{FCS}\}$  where the dominant component is in yaw with a small coupling into roll. The vector units are in (rad/sec<sup>2</sup>) per (rad/sec<sup>2</sup>).

Both angular acceleration partial vectors are pointing towards their commanded directions. They are nearly orthogonal to each other which means, that they are almost decoupled and their magnitudes are close to unity as a result of the effector combination matrix. It is an indication that this vehicle almost perfectly achieves the accelerations demanded, open-loop, with a very small amount of cross-axes coupling.

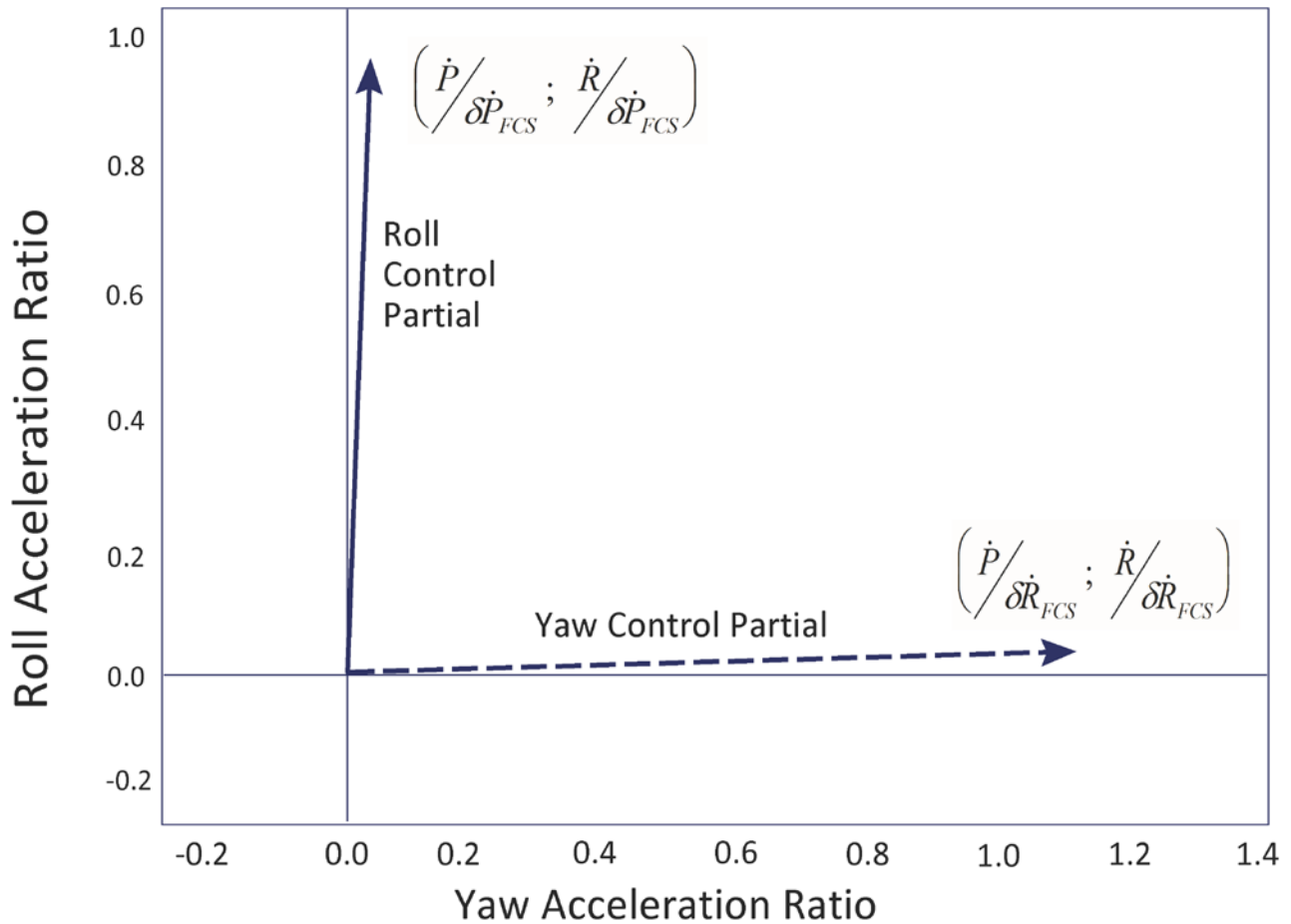


Figure 8.13 Acceleration Partial Vector Diagram in Roll and Yaw showing small coupling between axes

### 8.5 Converting the Aero Uncertainties from Individual Aerosurface Panels to Vehicle Axes

In vector diagram analysis the control moments and force vectors for the combined effector system are calculated in vehicle axes. The uncertainties, however, are generated by the aero group for each individual control surface separately. When many aero-surfaces are used for multiple-axes control, none of these surfaces are specifically dedicated to control a single axis. An acceleration demand is decoded by the mixing-logic matrix and is converted into multiple surface deflections. Since the vector diagrams are presented in vehicle axes the effects of the individual surface uncertainties must also be combined to uncertainties in vehicle axes. The uncertainties from each individual surface must, therefore, be transformed to moment, force, or acceleration uncertainties in body axes and summed up for all surfaces along the vehicle axes according to each surface's participation in the control directions. Since the mixing-logic matrix defines the structure of the effectors combination, the selection of the (Kmix) matrix will also combine the aero-uncertainties and determine the size of the uncertainty rectangles at the tips of the control vector diagrams.

We will now calculate the uncertainty rectangles in the control partial vector diagrams and also in the maximum control moment/ force vector diagrams from the uncertainties in the individual aero-surface derivatives. Let us consider a flight vehicle that is controlled by (n) aero-surfaces which are trimmed at a certain deflections vector:  $\delta_T = (\delta_1 \ \cdots \ \delta_n)$ . The moment and force variations due to the individual aero-surface aerodynamic uncertainties are obtained from matrix equation 8.6, where each element of the matrix is an uncertainty in the moment/ force surface derivative.

$$\begin{bmatrix} \delta L \\ \delta M \\ \delta N \\ \delta F_X \\ \delta F_Y \\ \delta F_Z \end{bmatrix} = \bar{Q} S_r \begin{bmatrix} b \delta C_{l\delta 1} & b \delta C_{l\delta 2} & b \delta C_{l\delta 3} & b \delta C_{l\delta n} \\ \bar{c} \delta C_{m\delta 1} & \bar{c} \delta C_{m\delta 2} & \bar{c} \delta C_{m\delta 3} & \bar{c} \delta C_{m\delta n} \\ b \delta C_{n\delta 1} & b \delta C_{n\delta 2} & b \delta C_{n\delta 3} & b \delta C_{n\delta n} \\ -\delta C_{A\delta 1} & -\delta C_{A\delta 2} & -\delta C_{A\delta 3} & -\delta C_{A\delta n} \\ \delta C_{Y\delta 1} & \delta C_{Y\delta 2} & \delta C_{Y\delta 3} & \delta C_{Y\delta n} \\ \delta C_{Z\delta 1} & \delta C_{Z\delta 2} & \delta C_{Z\delta 3} & \delta C_{Z\delta n} \end{bmatrix} \begin{pmatrix} \delta_1 \\ \delta_2 \\ \vdots \\ \delta_n \end{pmatrix}_T \quad (8.6)$$

The flight control system output demands are related to the individual aerosurface deflections by the mixing logic matrix as shown in equation 8.7, where  $(\delta P \ \delta Q \ \delta R)_{FCS}$  are the FCS rotational acceleration demands and  $(\delta X \ \delta Y \ \delta Z)_{FCS}$  are the translational acceleration FCS demands.

$$\begin{pmatrix} \delta_1 \\ \delta_2 \\ \vdots \\ \delta_n \end{pmatrix} = K_{mix} \begin{pmatrix} \delta_P \\ \delta_Q \\ \delta_R \\ \delta_X \\ \delta_Y \\ \delta_Z \end{pmatrix}_{FCS} \quad (8.7)$$

The number of columns in matrix  $K_{mix}$  varies between 3 and 6, minimum 3 moments plus some translations if the flight vehicle has sufficient effectors to control multiple degrees of freedom including translations. By substituting equation 8.7 to equation 8.6 we obtain a relationship in equation 8.8 that calculates the moment and force uncertainties in body axes as a function of flight control demands. Note that the uncertainties are always positive and, therefore, the absolute value of  $K_{mix}$  is used in equation 8.8 to cover for the worst uncertainty combination.

$$\begin{bmatrix} \delta L \\ \delta M \\ \delta N \\ \delta F_X \\ \delta F_Y \\ \delta F_Z \end{bmatrix} = \bar{Q} S_r \begin{bmatrix} b \delta C_{l\delta 1} & b \delta C_{l\delta 2} & b \delta C_{l\delta 3} & b \delta C_{l\delta 4} \\ \bar{c} \delta C_{m\delta 1} & \bar{c} \delta C_{m\delta 2} & \bar{c} \delta C_{m\delta 3} & \bar{c} \delta C_{m\delta 4} \\ b \delta C_{n\delta 1} & b \delta C_{n\delta 2} & b \delta C_{n\delta 3} & b \delta C_{n\delta 4} \\ -\delta C_{A\delta 1} & -\delta C_{A\delta 2} & -\delta C_{A\delta 3} & -\delta C_{A\delta 4} \\ \delta C_{Y\delta 1} & \delta C_{Y\delta 2} & \delta C_{Y\delta 3} & \delta C_{Y\delta 4} \\ \delta C_{Z\delta 1} & \delta C_{Z\delta 2} & \delta C_{Z\delta 3} & \delta C_{Z\delta 4} \end{bmatrix} abs[K_{mix}] \begin{pmatrix} \delta_P \\ \delta_Q \\ \delta_R \\ \delta_X \\ \delta_Y \\ \delta_Z \end{pmatrix}_{FCS} \quad (8.8)$$

After multiplying out the matrices in equation 8.8, and let us assume, for example, that together with the 3 rotations only one translational direction along x is directly controllable. The uncertainties matrix equation for the 4-dofs becomes.

$$\begin{bmatrix} \delta L \\ \delta M \\ \delta N \\ \delta F_X \\ \delta F_Y \\ \delta F_Z \end{bmatrix} = \begin{bmatrix} \delta L_P & \delta L_Q & \delta L_R & \delta L_X \\ \delta M_P & \delta M_Q & \delta M_R & \delta M_X \\ \delta N_P & \delta N_Q & \delta N_R & \delta N_X \\ \delta X_P & \delta X_Q & \delta X_R & \delta X_X \\ \delta Y_P & \delta Y_Q & \delta Y_R & \delta Y_X \\ \delta Z_P & \delta Z_Q & \delta Z_R & \delta Z_X \end{bmatrix} \begin{pmatrix} \delta_P \\ \delta_Q \\ \delta_R \\ \delta_X \end{pmatrix}_{FCS} \quad (8.9)$$

### Uncertainties in the Control Partial

The uncertainties in the moment and force derivatives with respect to the flight control demands are obtained directly from the matrix elements of equation 8.9. For example, the uncertainty in the pitch moment derivative due to pitch demand (virtual elevon) is  $\delta C_{m\delta Q} = \delta M_Q / \bar{Q} S \bar{c}$ . The uncertainty in rolling moment derivative due to roll demand (virtual aileron) is  $\delta C_{l\delta P} = \delta L_P / \bar{Q} S b$ , and the uncertainty in rolling moment derivative due to yaw demand is  $\delta C_{l\delta R} = \delta L_R / \bar{Q} S b$ , etc. These uncertainties are used in the partial moment per FCS demand or partial force per FCS demand vector diagrams. They define the size of the rectangles at the tips of the control vectors. The rectangles are also scaled proportionally to the vector magnitudes, as described in Figure 8.3, and equations (8.1 to 8.4).

### Uncertainties due to Peak Control Demands

Having calculated the uncertainties in the control vector partials we can now extend the method to calculate the moment and force uncertainties when the flight control demands are maximized either in positive or negative directions. Equation 3.21 calculates the maximum acceleration that can be demanded by the flight control system (due to the effectors position limitations) along a controlled axis before at least one of the effectors saturates, for example, the max pitch control demand is:

$$\delta_{+QMax_{FCS}} = \frac{1}{Q_{QMax}}$$

To calculate, therefore, the magnitude of the maximum moment (or force) uncertainty in a certain direction we must multiply the corresponding row in equation 8.9 with the maximum FCS demand applied in that direction. For example, the uncertainties in the pitch moment and in the x and z forces (non-dimensional) as a result of the uncertainties in the control surface coefficients, when the pitch control demand is at its maximum positive position, are obtained from equation 8.10a. The uncertainties in the same 3 directions when the forward acceleration demand is at its maximum positive position are calculated by equation (8.10b). Notice how they depend on the max demand.



$$\begin{pmatrix} \delta C_M \\ \delta C_X \\ \delta C_Z \end{pmatrix}_{Q_{Max}} = \begin{bmatrix} \delta M_Q / Q \bar{c} S_{ref} \\ \delta X_Q / Q S_{ref} \\ \delta Z_Q / Q S_{ref} \end{bmatrix} \frac{1}{U_{Q_{Max}}}; \quad \begin{pmatrix} \delta C_M \\ \delta C_X \\ \delta C_Z \end{pmatrix}_{X_{Max}} = \begin{bmatrix} \delta M_X / Q \bar{c} S_{ref} \\ \delta X_X / Q S_{ref} \\ \delta Z_X / Q S_{ref} \end{bmatrix} \frac{1}{U_{X_{Max}}} \quad (8.10)$$

Similarly in yaw, equation 8.11a calculate the uncertainty magnitudes in roll and yaw control moments and in side-force caused by uncertainties in the aerosurface coefficients, when the yaw control demand is maximized in the positive direction. Similarly, the uncertainties in the same coefficients are calculated when the roll demand is maximized in the positive direction, using equation 8.11b.

$$\begin{pmatrix} \delta C_L \\ \delta C_N \\ \delta C_Y \end{pmatrix}_{R_{Max}} = \begin{bmatrix} \delta L_R / Q b S_{ref} \\ \delta N_R / Q b S_{ref} \\ \delta Y_R / Q S_{ref} \end{bmatrix} \frac{1}{U_{R_{Max}}}; \quad \begin{pmatrix} \delta C_L \\ \delta C_N \\ \delta C_Y \end{pmatrix}_{P_{Max}} = \begin{bmatrix} \delta L_P / Q b S_{ref} \\ \delta N_P / Q b S_{ref} \\ \delta Y_P / Q S_{ref} \end{bmatrix} \frac{1}{U_{P_{Max}}} \quad (8.11)$$

The above equations are used to calculate the uncertainties in the maximum control moment and force vector diagrams. They define the size of the uncertainty rectangles at the tips of the control vectors generated from a maximum control demand. Notice that the trim positions of the aerosurfaces are not necessarily centered and the max deflection in one direction from trim is not necessarily equal to the max deflection in the opposite direction. For example, in equation 3.23b we proved that the peak FCS demand in the negative pitch direction is different than the max positive pitch FCS demand, and it is defined by equation 8.12, where  $U_{Q_{min}}$  is obtained from equation 3.19b.

$$\delta_{-Q_{Max_{FCS}}} = \frac{1}{Q_{Q_{Min}}} \quad (8.12)$$

This means that the uncertainty rectangles around the tips of the control vectors generated from a peak negative control demand will be different from the rectangles at the tips of the control vectors generated from a max positive control demand, because the size of the two controls are different.

The uncertainties in the pitch moment and in the x and z forces as a result of the uncertainties in the control surface coefficients, when the pitch control demand is at its peak negative position are obtained from equation 8.13a, and the uncertainties in the same 3 directions when the forward acceleration demand is at its peak negative position are obtained from equation 8.13b.

$$\begin{pmatrix} \delta C_M \\ \delta C_X \\ \delta C_Z \end{pmatrix}_{Q Min} = \begin{bmatrix} \delta M_Q / Q \bar{c} S_{ref} \\ \delta X_Q / Q S_{ref} \\ \delta Z_Q / Q S_{ref} \end{bmatrix} \frac{1}{U_{Q Min}} ; \quad \begin{pmatrix} \delta C_M \\ \delta C_X \\ \delta C_Z \end{pmatrix}_{X Min} = \begin{bmatrix} \delta M_X / Q \bar{c} S_{ref} \\ \delta X_X / Q S_{ref} \\ \delta Z_X / Q S_{ref} \end{bmatrix} \frac{1}{U_{X Min}} \quad (8.13)$$

Similarly, the uncertainties in the lateral coefficients when the roll and yaw acceleration control demands are maximized in the negative directions are obtained from equations (8.14).

$$\begin{pmatrix} \delta C_L \\ \delta C_N \\ \delta C_Y \end{pmatrix}_{R Min} = \begin{bmatrix} \delta L_R / Q b S_{ref} \\ \delta N_R / Q b S_{ref} \\ \delta Y_R / Q S_{ref} \end{bmatrix} \frac{1}{U_{R Min}} ; \quad \begin{pmatrix} \delta C_L \\ \delta C_N \\ \delta C_Y \end{pmatrix}_{P Min} = \begin{bmatrix} \delta L_P / Q b S_{ref} \\ \delta N_P / Q b S_{ref} \\ \delta Y_P / Q S_{ref} \end{bmatrix} \frac{1}{U_{P Min}} \quad (8.14)$$

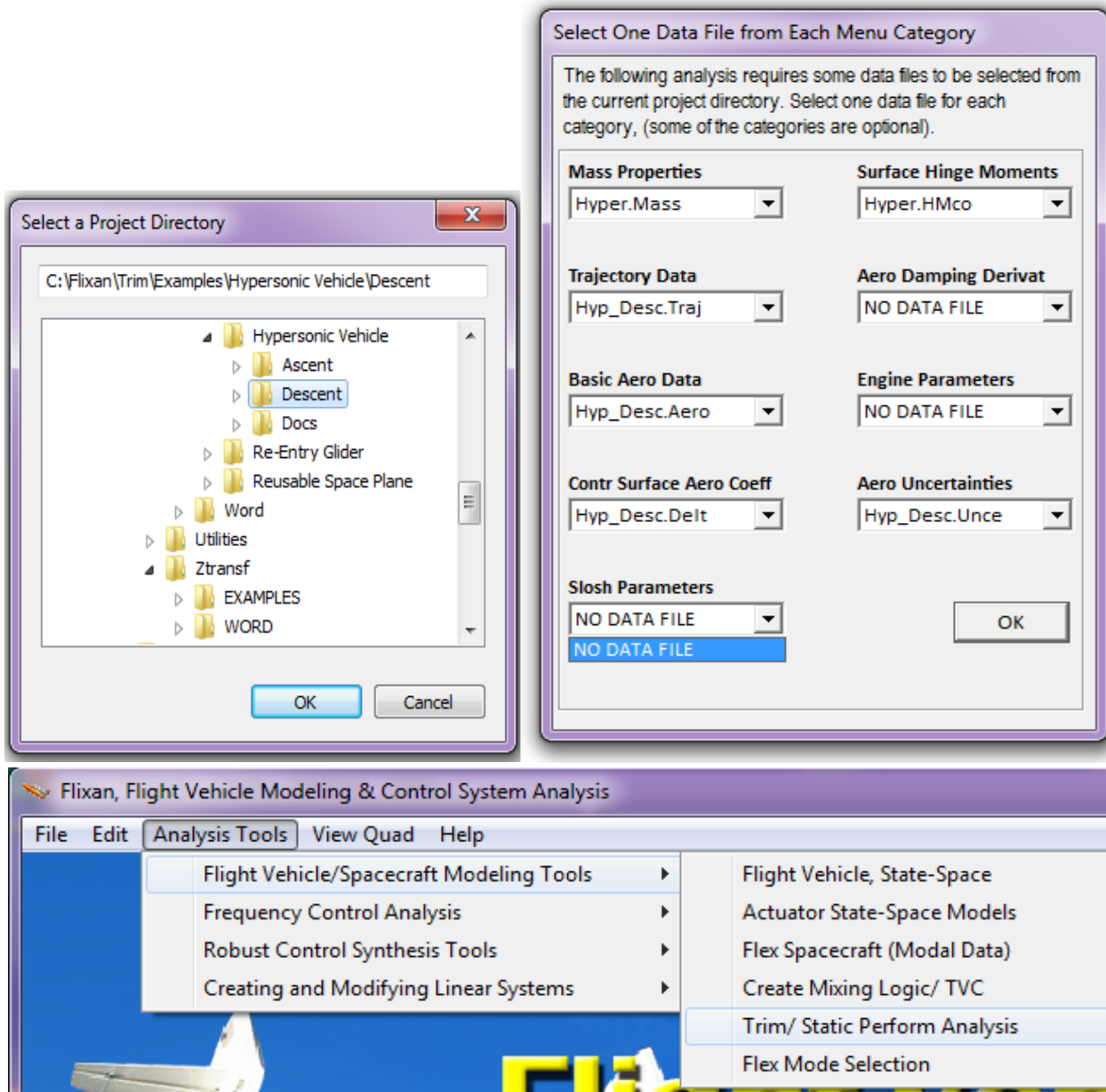
The above equations are also used for calculating the uncertainty rectangles at the tips of the maximum acceleration vector diagrams. In this case the moment and force uncertainties must be converted to acceleration uncertainties by multiplying them with the inverse of the inertias and mass matrix.

$$\begin{bmatrix} I_{XX} & -I_{XY} & -I_{XZ} & 0 & 0 & 0 \\ -I_{XY} & I_{YY} & -I_{YZ} & 0 & 0 & 0 \\ -I_{XZ} & -I_{YZ} & I_{ZZ} & 0 & 0 & 0 \\ 0 & 0 & 0 & M_V & 0 & 0 \\ 0 & 0 & 0 & 0 & M_V & 0 \\ 0 & 0 & 0 & 0 & 0 & M_V \end{bmatrix}$$

## 8.6 Running the Vector Diagrams Program from Flixan

To run the vector diagrams program, start the Flixan program and select the directory that contains the project files, such as: trajectory, mass properties, aerodynamic data, aero uncertainties, engine data, etc. The files must be in the proper format for the program to be able to read them. From the Flixan main menu select "*Analysis Tools*", then "*Flight Vehicle/Spacecraft*

"Modeling Tools", and "Trim/ Static Performance Analysis", as shown below, and from the following file selection menu select the files to be used in the analysis.



The following is the Trim program main menu. If the effectors are already trimmed and a trim file has already been created you may select the Vector Diagrams, which is option-11 in the main menu. Otherwise select option-3 to trim the aerosurfaces and engines before plotting the vector diagrams. In this case we assume that a trim file has already been created and we select option-11. Use the next dialog to enter a flight time along the trajectory to analyze, such as 1200 sec. The following dialog consists of four menus for selecting the vehicle mass, Mach number, alpha, and beta. The default values correspond to the selected flight time, but they can be changed if the user desires to analyze a different flight condition, such as, a combination of parameters that do not correspond to a trajectory time. You may keep those parameters or change them to something different. In this case we select the default values and click "Select".

Main Trim Menu

Select one of the following options

Exit

OK

1. Plot Aero Coefficients, Derivatives, and Control Surface Increments
2. Plot Trajectory Parameters Versus Time from the Trajectory File ".Traj"
3. Trim the Effector Deflections to Balance the Vehicle Moments and Forces
4. Create an Effector Mixing Logic or a TVC Matrix (Kmix)
5. State-Space Modeling of the Flight Vehicle at Selected Times
6. Performance and Stability Parameter Plots Along Trajectory Time
7. Landing and Pull-Up Maneuverability, plus, Inertial Coupling Effects
8. Moments at the Hinges of Control Surfaces Along the Trajectory Time
9. View and Modify Vehicle Data (CG, MRC, TVC, Surfaces) for Dispersion Analysis
10. Contour Plots (Mach versus Alpha) for Performance, Control Authority Analysis
11. Vector Diagrams for Maneuverability & Stability at Selected Flight Conditions
12. Plot and Compare Previous Data Files (Traject, Trim, Perform, Hinge Moment)

Select a Time from: ( 90.000 to 1215.0 ) to Analyze Vehicle Controllability

OK

1200

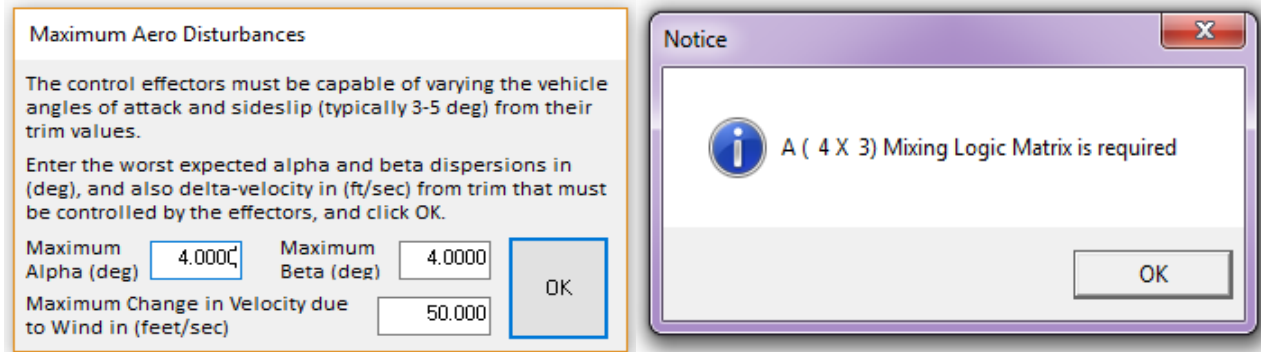
Select the following parameters

Select a Vehicle Mass, Mach Number, Alpha, and Beta from the lists below and click "Select"

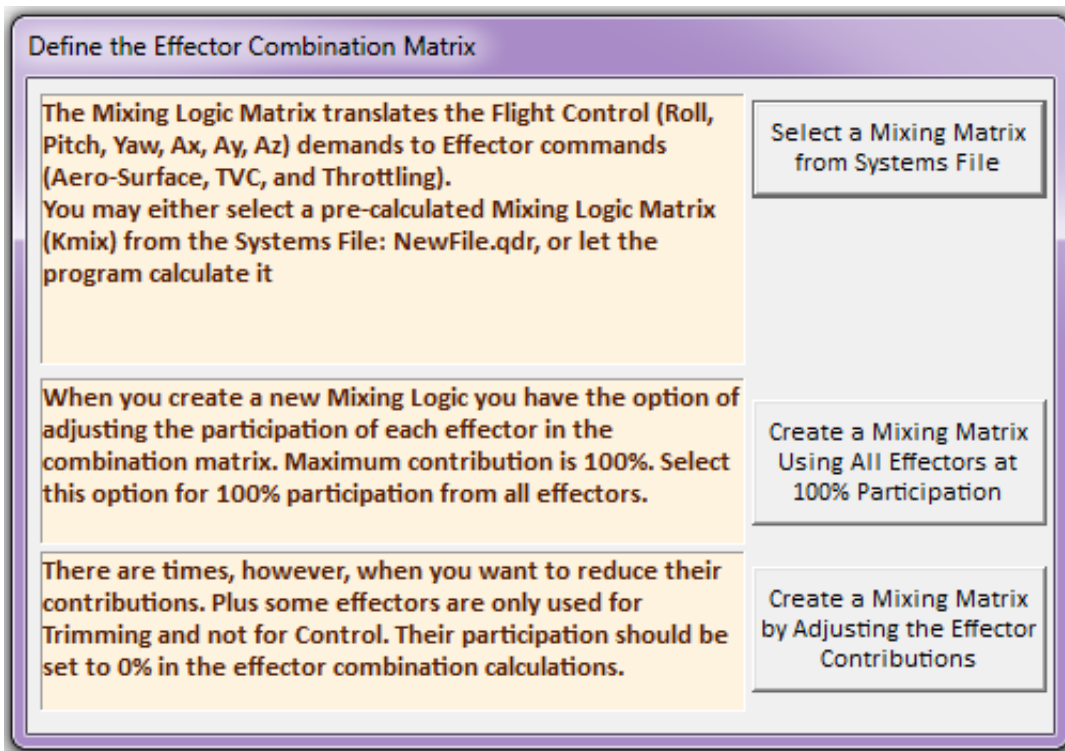
Select

Vehicle Mass (slug)	Mach Number	Angle of Attack (deg)	Angle of Sideslip (deg)
450.00	0.3000	6.00	0.00
827.00	0.3000	6.00	-5.00
777.00	0.6000	8.00	0.00
726.90	0.8000	10.0	5.00
676.90	0.9000	12.0	
626.90	1.200	14.0	
576.80	1.500	16.0	
526.80	2.000	18.0	
522.40	3.000	20.0	
450.00	4.000	25.0	

Wind disturbances are defined by the maximum dispersions in the angles of: attack  $\pm\alpha_{\max}$  and sideslip  $\pm\beta_{\max}$  from trim  $(\alpha_0, \beta_0)$ , due to wind-shear or maneuvering. Wind disturbances also cause variations in the airspeed  $\pm v_{\max}$  relative to nominal speed  $V_0$ . The control authority and other parameters are evaluated by the amount of disturbance moments and forces that the vehicle is capable of tolerating by using its controls. In the following dialog you must enter the maximum dispersions angles which are expected in this flight condition,  $(\alpha_{\max}$  and  $\beta_{\max})=4^\circ$ , and the velocity variation  $v_{\max}=50$  (ft/sec).



A mixing logic matrix is required by the program in order to calculate the proper combination of the effectors. The dialog below allows the user to either select an already existing matrix that is saved in the systems file or to allow the program to calculate a mixing logic matrix from the vehicle data. In this example we do not have a mixing matrix saved in file and we select the second option to let the program calculate a mixing matrix at full participation from all effectors. The user may also define the percentage of effector participation in the third option.



The program begins to plot the vector diagrams, as shown in Figures 8.14. Each plot has a menu bar at the top, and from the menu click on "*Select Vector Diagrams*" to select the type of vector diagrams to plot. Let's choose the 3<sup>rd</sup> option which is "*Partials of Moment/ Force per Alpha Variations against Moment/ Force per Control Partials*". The program calculates several diagrams for different axes. Click on "*Next Plot*" to see them all. The next figure shows the partials in the pitch and axial directions.

The blue vector in Figure 8.14 is the pitch moment and axial force partial per pitch demand  $\delta Q_{FCS}$ , which is the variation in moment and force per pitch control demand  $(Cm\delta Q \ \& \ CX\delta Q)_{FCS}$ . It shows that the response is entirely in the pitch direction and it does not couple in the x-direction. The green vector is the pitch moment and axial force partial per axial control demand  $\delta X_{FCS}$ , which is the variation in moment and force per axial control demand  $(Cm\delta X \ \& \ CX\delta X)_{FCS}$ . The response is entirely in the x-direction and it does not couple in pitch. The vector diagram compares the blue and green control vectors against the red vectors which are moment and force partials per alpha variation  $(Cm\alpha, CX\alpha)$ . The red vectors show that an increase in alpha causes a negative pitching moment variation that means that the vehicle is statically stable in pitch.

Notice that there are two red vector partials, the solid red line is calculated at  $(\alpha_0 + \alpha_{max})$  and the dashed red line is calculated at  $(\alpha_0 - \alpha_{max})$ , where  $\alpha_{max}=4^\circ$ . They are scaled in order to be made comparable with the control vectors, as described in Figure 8.10. The comparison shows that the vehicle is well maneuverable both in pitch and in the axial directions. Figure 8.14 also shows that an increase in alpha causes an increase in drag  $(-C_x)$ . The effects of the uncertainties in the aerosurface derivatives in pitch control are shown by the small yellow rectangle at the tip of the blue pitch control vector. The same applies with the axial acceleration control vector. The uncertainties in the derivatives  $(Cm\alpha \ \& \ Cx\alpha)$  are represented by the red rectangles at the tips of the red vectors.

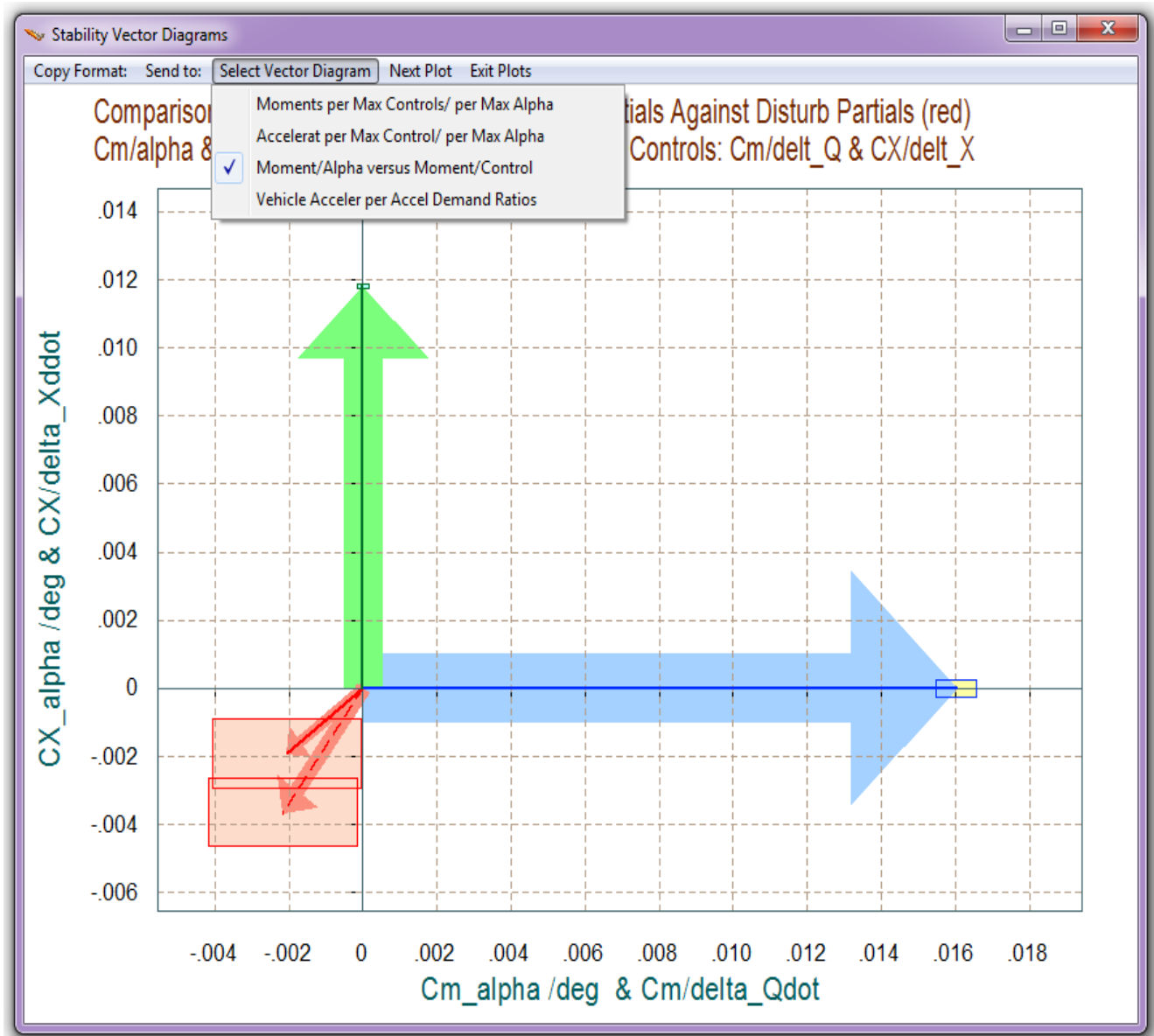
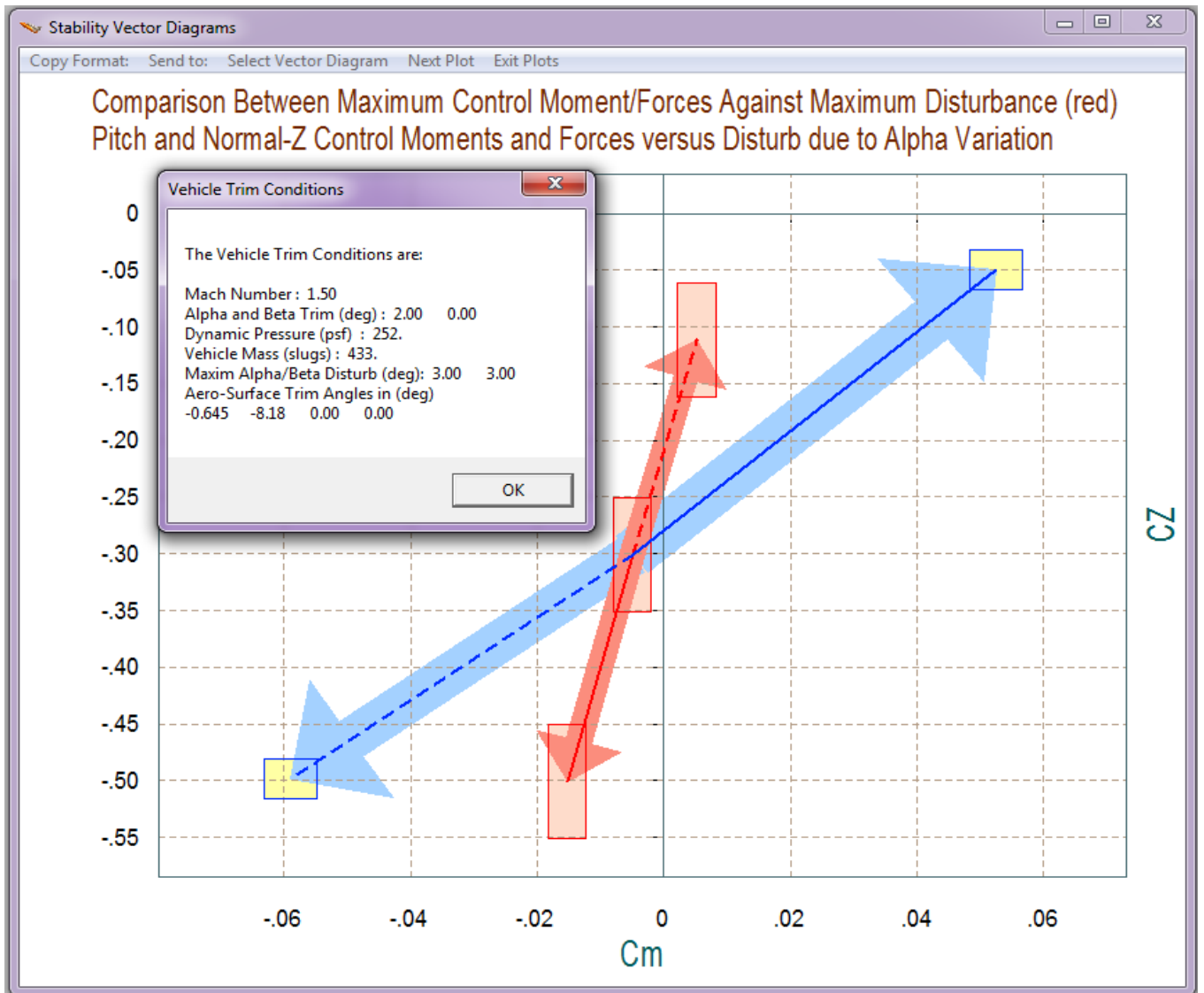


Figure 8.14 Pitch and Axial Control Partial against Partial per Alpha Variations

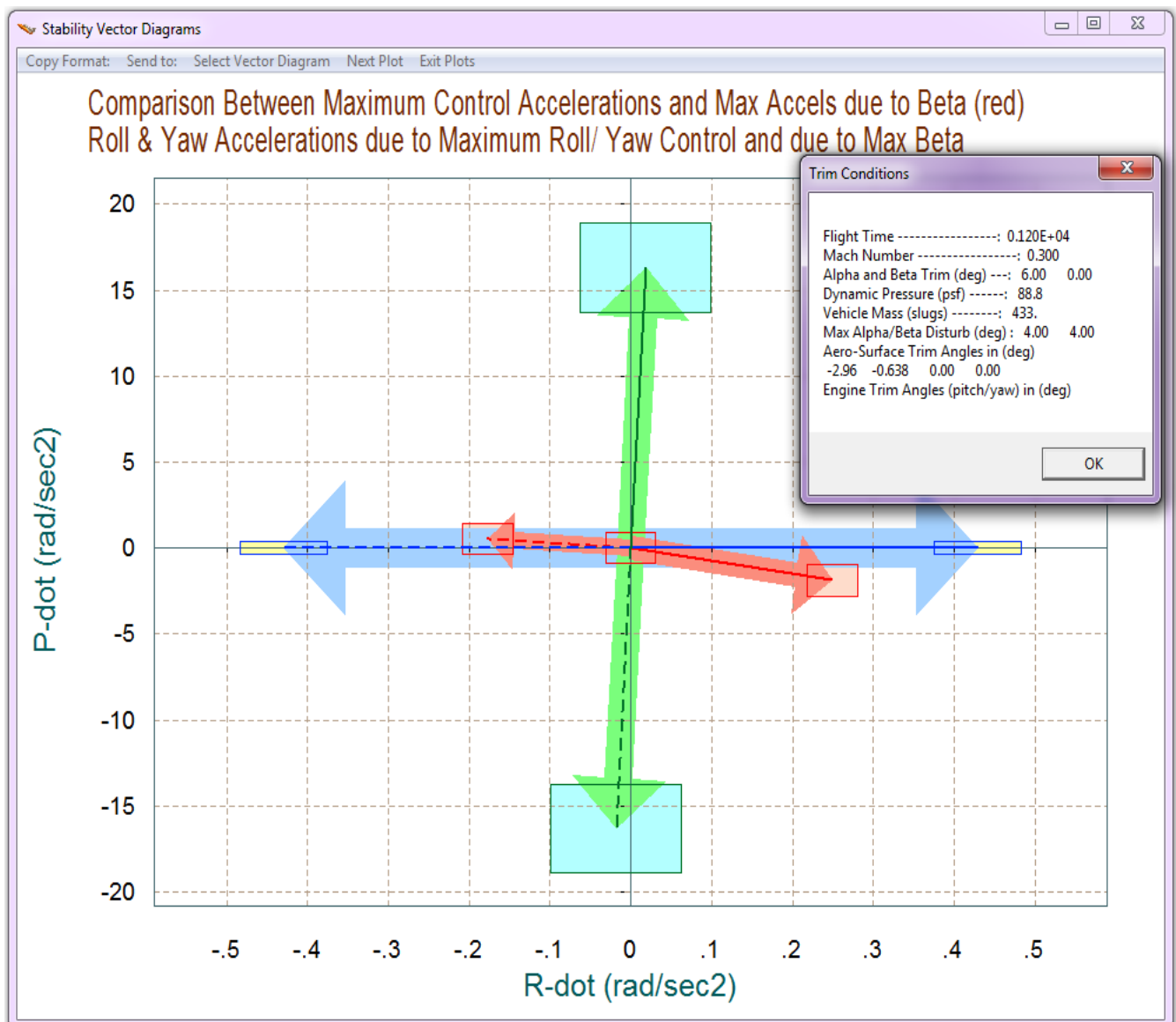
The vector diagram in the next figure corresponds to a different flight condition. The blue vectors show the effects in the pitching moment and in the normal force ( $C_m$  &  $C_z$ ), when the pitch control demand is maximized in the positive and in the negative directions ( $\delta Q_{\pm FCSMax}$ ). The solid blue vector corresponds to max positive pitch demand ( $\delta Q_{+FCSMax}$ ) from trim position and the dashed blue vector corresponds to max negative pitch demand ( $\delta Q_{-FCSMax}$ ). This vehicle does not have normal acceleration control so only the pitch control blue vector is shown. There is no green  $N_z$  control vector in this case. The red vectors correspond to the pitch moment and normal force generated by an  $\alpha_{max} = \pm 3^\circ$  dispersion from trim  $\alpha_0$ . The trim parameters are shown in the dialog that comes up when you click the right mouse button.

The vehicle in this flight condition is trimmed at  $\alpha_0=2^\circ$ . The pitch control consists of blended elevon plus body-flap deflections which is determined by the effector mixing matrix. It has a slightly negative pitching moment that is balanced with negative deflections of the elevon and the body-flap. Since it is trimmed with a positive alpha, the vehicle experiences a negative  $C_z$  force which is actually a lift. A positive pitch demand creates a positive pitching moment (as expected) and a reduction in normal force ( $C_N=-C_z$ ) or lift increase. The red vectors represent the moment and force variations due to the dispersions  $\alpha_{\max}=\pm 3^\circ$  from trim. The solid red vector pointing down represents the pitch moment and z-force generated when  $\alpha=\alpha_0+3^\circ$ , and the dashed vector in the opposite direction is for  $\alpha=\alpha_0-3^\circ$ . An increase in alpha further reduces the pitching moment and increases the normal force ( $C_N=-C_z$ ). The pitch control moment is considerably greater in magnitude than the  $\pm\alpha_{\max}$  dispersion moment. The yellow rectangular blocks at the tips of the blue control vectors represent the size of the aerosurface uncertainties, and the red rectangles at the tips of the red vectors represent the uncertainties ( $\delta C_m$ ,  $\delta C_z$ ) in the basic aero coefficients.



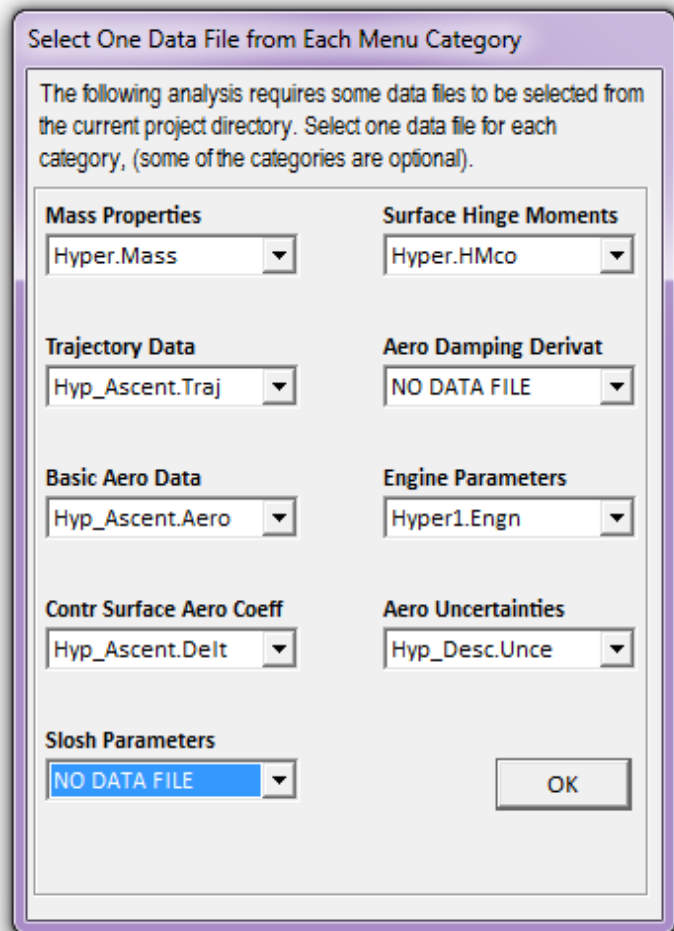


The next vector diagram shows the effects in roll and yaw acceleration in (rad/sec<sup>2</sup>) when the roll and yaw acceleration demands ( $\delta P_{FCS}$  &  $\delta R_{FCS}$ ) are maximized in positive and in negative directions. The two control vectors are almost perfectly orthogonal to each other. The horizontal blue vectors represent the maximum yaw control range. They are symmetric and it shows that the yaw control does not couple in the roll direction. The vertical green vectors represent the roll control range. They are also symmetrical and the roll control couples slightly into yaw acceleration. The two red vectors represent the roll and yaw accelerations due to the  $\pm\alpha_{max}$  and  $\pm\beta_{max}$  dispersions from trim conditions ( $\alpha_0, \beta_0$ ). The solid red vector shows the accelerations at: ( $\alpha_0+\alpha_{max}$  and  $\beta_0+\beta_{max}$ ), and the dashed red vector shows the accelerations at: ( $\alpha_0-\alpha_{max}$  and  $\beta_0-\beta_{max}$ ) dispersions. The yellow and cyan rectangles at the tips of the control vectors represent the uncertainties in roll and yaw accelerations due to the aerodynamic uncertainties in the aerosurface coefficients. The red rectangles at the tips of the red vectors show the possible acceleration spread due to the uncertainties in the aero data.



# 9.9 Data Files and Description

The Trim program uses many different types of data files. Some of them are input data and some files are generated by the program itself. The function and purpose of each data file is categorized by its filename extension. The input data files are: trajectory data, mass properties, propulsion data, aero data (which include basic aero coefficients, control surface increments, damping derivatives, hinge moment coefficients, and aero-uncertainties). The input data files are selected from this menu when you start the program. Some of the input data files are optional and not included, depending on the application. The required files are: the mass, trajectory data, and base aerodynamics. The aerosurfaces and propulsion files are included depending on the type of flight vehicle. For example, for an aircraft you must provide aerosurface coefficients, and optionally damping derivatives, and hinge moment coefficients for sizing the actuators. A launch vehicle does not require aerosurfaces but it needs propulsion data and perhaps fuel sloshing data, although slosh data are not used by the Trim program except for generating dynamic models. To analyze robustness you will also need aero uncertainties. The data files generated by the Trim program are: effector trim deflections and engine throttles, performance parameters, and moments at the hinges of the control surfaces due to aerodynamic loading. These are time histories calculated along the trajectory.



Notice that the Trim program requires that the input data files have a particular format and the users must first devote some time to reshaping their flight vehicle data in this standard Flixan format. This section, therefore, is dedicated to provide detailed description of each type of data file. The files are standard text files and the formats should be very easy to recognize and replicate for other flight vehicle applications. Notice also, that the length of the filenames in Flixan is limited to 20 characters long, including the extension.

## 9.1 Trajectory Data Files

The trajectory files are usually created by trajectory optimization specialists using a point mass trajectory optimization program such as OTIS or POST. They can also be created by control analysts using Matlab simulations, however, not necessarily optimal. The Trim program recognizes trajectory files by the filename extension “.Traj”. They are typical Excel column files converted to text format and they have "time" in the leftmost column. The first line is a title that usually identifies the vehicle and its mission, for example, "*Space Shuttle Entry (Heavy Payload)*". Additional titles or description lines may also be included below the main title. The file contains the following trajectory variables in columns:

1. Trajectory Time in (seconds)
2. Vehicle Mass in (slugs)
3. Vehicle Altitude above sea level (feet)
4. Angle of Attack ( $\alpha$ ) in (degrees)
5. Angle of Sideslip ( $\beta$ ) in (degrees)
6. Flight Path Angle ( $\gamma$ ) in (degrees)
7. Bank Angle ( $\phi$ ) in (degrees)
8. Relative Velocity ( $V_{rel}$ ) in (feet/sec)
9. Mach Number
10. Dynamic Pressure ( $Q$ -bar) in ( $lbf/ft^2$ )
11. Measured Acceleration ( $A_x$ ) along (X) Body Axis (ft/sec)
12. Measured Acceleration ( $A_y$ ) along (Y) Body Axis (ft/sec)
13. Measured Acceleration ( $A_z$ ) along (Z) Body Axis (ft/sec)
14. Roll Rate ( $p$ ) in (deg/sec)
15. Pitch Rate ( $q$ ) in (deg/sec)
16. Yaw Rate ( $r$ ) in (deg/sec)
17. Roll Acceleration ( $\dot{p}$ ) in ( $deg/sec^2$ )
18. Pitch Acceleration ( $\dot{q}$ ) in ( $deg/sec^2$ )
19. Yaw Acceleration ( $\dot{r}$ ) in ( $deg/sec^2$ )
20. Vehicle Lift Force ( $F_L$ ) in (lb)
21. Vehicle Drag Force ( $F_D$ ) in (lb)
22. Vehicle Side Force ( $F_Y$ ) in (lb)
23. Total Engine Thrust ( $T$ ) in (lb)
24. Disturbance Force Along (x) in (lb)
25. Disturbance Force Along (y) in (lb)
26. Disturbance Force Along (z) in (lb)
27. Disturbance Moment About (x) in (ft-lb)
28. Disturbance Moment About (y) in (ft-lb)
29. Disturbance Moment About (z) in (ft-lb)
30. X-CG Location in (ft)
31. Y-CG Location in (ft)
32. Z-CG Location in (ft)

The trajectory file is an input to the Trim program. The Trim program, however, can also generate temporary user-modified trajectory files from the original trajectory data, as it was explained earlier. The modified trajectory file is automatically saved by the program under a different name. For example, if the original trajectory file is "Shuttle.Traj" the user modified trajectory is saved under "Shuttle1.Traj". If there was a previous "Shuttle1.Traj" it is renamed to "Shuttle2.Traj". The title is also changed in the modified trajectories to "Temporary Trajectory". The CG travel (variables 30-32) are not required in the original input trajectory. The CG (x, y, z) position is calculated, however, by the Trim program from the mass properties data as a function of the trajectory time and it is included in the modified trajectories. So the user does not have to include the CG travel.

Rocket-Plane Mission-1, Descent Phase												
Ground Takeoff, Rocket Off, Maxim Q_bar = 1000 psf												
Time	Mass	Altitude	Alpha	Beta	Gamma	Bank	Velocity	Mach	Q_bar	Ax	Ay	Az
(sec)	(slug)	(ft)	(deg)	(deg)	(deg)	(deg)	(ft/sec)	---	(lb/ft^2)	ft/sec^2	ft/sec^2	ft/sec^2
90.0	433.2	76068.0	-1.71	0.00	0.02	-3.26	4388.00	4.50	997.8	-22.522	0.000	-32.174
95.0	433.2	76118.0	-1.63	0.00	0.05	-28.26	4281.00	4.39	947.4	-21.878	0.000	-31.209
98.0	433.2	76110.0	-1.60	0.00	-0.32	-50.00	4191.00	4.30	908.3	-21.235	0.000	-30.565
100.0	433.2	76096.0	-1.59	0.00	-0.42	-50.00	4178.00	4.29	903.2	-21.235	0.000	-30.565
105.0	433.2	75845.0	-1.47	0.00	-1.13	-50.00	4079.00	4.18	871.4	-20.913	0.000	-31.531
110.0	433.2	75354.0	-1.36	0.00	-1.81	-50.00	3983.00	4.09	850.8	-20.913	0.000	-32.817
115.0	433.2	74651.0	-1.25	0.00	-2.45	-50.00	3888.00	3.99	839.0	-20.913	0.000	-34.748
120.0	433.2	73767.0	-1.14	0.00	-3.00	-50.00	3793.00	3.90	833.6	-21.557	0.000	-37.000
125.0	433.2	72743.0	-1.09	0.00	-3.45	-50.00	3697.00	3.80	832.4	-22.200	0.000	-39.574
130.0	433.2	71624.0	-1.00	0.00	-3.77	-50.00	3599.00	3.70	832.9	-22.844	0.000	-42.470
135.0	433.2	70457.0	-0.91	0.00	-3.96	-50.00	3498.00	3.60	832.9	-23.487	0.000	-45.365
140.0	433.2	69290.0	-0.81	0.00	-4.01	-50.00	3394.00	3.50	830.1	-24.131	0.000	-48.261
145.0	433.2	68168.0	-0.71	0.00	-3.91	-50.00	3287.00	3.39	822.6	-24.774	0.000	-51.157
150.0	433.2	67133.0	-0.53	0.00	-3.67	-50.00	3177.00	3.28	808.4	-25.096	0.000	-53.409
155.0	433.2	66219.0	-0.45	0.00	-3.30	-50.00	3065.00	3.17	786.8	-25.096	0.000	-55.339
160.0	433.2	65450.0	-0.39	0.00	-2.83	-50.00	2951.00	3.05	757.3	-24.774	0.000	-56.626
165.0	433.2	64840.0	-0.35	0.00	-2.29	-50.00	2837.00	2.93	720.4	-25.096	0.000	-57.591
170.0	433.2	64397.0	-0.39	0.00	-1.67	-50.00	2719.00	2.81	676.0	-25.096	0.000	-58.235
175.0	433.2	64123.0	-0.34	0.00	-1.02	-50.00	2600.00	2.69	626.1	-24.774	0.000	-58.235
180.0	433.2	64007.0	-0.33	0.00	-0.38	-50.00	2481.00	2.56	573.3	-24.131	0.000	-57.270

## 9.2 Mass Properties Data File

The mass properties data files must have a filename extension ".Mass". They are also Excel type column data converted to text format. They include a title line at the top. The second line defines the gravity acceleration constant 1-g, which is typically 32.2, but the user may wish to use a different acceleration constant if he is using different units or go to another planet. It may be confusing, however, to change the units because the plot labels are all in British units. The vehicle mass in (slugs) is in the leftmost column and it must be in descending magnitude (since the vehicle always loses weight). A mass properties file contains the following data in columns:

1. Vehicle Mass in (slugs)
2. Roll Moment of Inertia ( $I_{xx}$ ) in (slug-ft<sup>2</sup>)
3. Pitch Moment of Inertia ( $I_{yy}$ ) in (slug-ft<sup>2</sup>)
4. Yaw Moment of Inertia ( $I_{zz}$ ) in (slug-ft<sup>2</sup>)
5. Product of Inertia  $I_{xy}$  in (slug-ft<sup>2</sup>)
6. Product of Inertia  $I_{xz}$  in (slug-ft<sup>2</sup>)
7. Product of Inertia  $I_{yz}$  in (slug-ft<sup>2</sup>)
8. CG Location along the X axis (feet)
9. CG Location along the Y axis (feet)
10. CG Location along the Z axis (feet)
11. Vehicle Total Length in (feet)

```

Hyperspeed Rocket Plane Mass Properties
Acceleration due to Gravity, 1g = 32.174
Mass (slg) Ixx (sl-ft^2) Iyy (sl-ft^2) Izz (sl-ft^2) Ixy (sl-ft^2) Ixz (sl-ft^2) Iyz (sl-ft^2) Xcg (ft) Ycg (ft) Zcg (ft)
1.027E+03 1.26E+04 1.32E+05 1.38E+05 0.00E+00 -9.47E+02 0.00E+00 -3.130E+01 0.00E+00 8.604E-01
9.771E+02 1.23E+04 1.29E+05 1.35E+05 0.00E+00 -2.37E+02 0.00E+00 -3.174E+01 0.00E+00 8.979E-01
9.270E+02 1.20E+04 1.25E+05 1.31E+05 0.00E+00 4.00E+02 0.00E+00 -3.224E+01 0.00E+00 9.353E-01
8.770E+02 1.17E+04 1.23E+05 1.29E+05 0.00E+00 7.69E+02 0.00E+00 -3.238E+01 0.00E+00 9.727E-01
8.270E+02 1.14E+04 1.20E+05 1.26E+05 0.00E+00 1.05E+03 0.00E+00 -3.259E+01 0.00E+00 1.010E+00
7.770E+02 1.10E+04 1.16E+05 1.22E+05 0.00E+00 1.18E+03 0.00E+00 -3.274E+01 0.00E+00 1.048E+00
7.269E+02 1.07E+04 1.12E+05 1.19E+05 0.00E+00 1.15E+03 0.00E+00 -3.281E+01 0.00E+00 1.085E+00
6.769E+02 1.04E+04 1.08E+05 1.14E+05 0.00E+00 9.49E+02 0.00E+00 -3.276E+01 0.00E+00 1.123E+00
6.269E+02 1.01E+04 1.03E+05 1.09E+05 0.00E+00 5.65E+02 0.00E+00 -3.257E+01 0.00E+00 1.160E+00
5.768E+02 9.85E+03 9.78E+04 1.04E+05 0.00E+00 -1.10E+01 0.00E+00 -3.221E+01 0.00E+00 1.197E+00
5.268E+02 9.61E+03 9.22E+04 9.84E+04 0.00E+00 -8.21E+02 0.00E+00 -3.161E+01 0.00E+00 1.235E+00
5.224E+02 9.58E+03 9.14E+04 9.75E+04 0.00E+00 -7.05E+02 0.00E+00 -3.155E+01 0.00E+00 1.240E+00
4.500E+02 9.40E+03 8.10E+04 8.50E+04 0.00E+00 -6.14E+02 0.00E+00 -3.156E+01 0.00E+00 1.240E+00

```

### 9.3 Propulsion Data File

A propulsion data file must have an extension ".Engn". This file may contain both: TVC engine propulsion and reaction control thruster information. It includes a title line at the top, a couple of label lines below it, and then it includes the engine or jet thruster data, one effector per line. Each line contains the following parameters for each effector:

1. A short title describing the effector (14 characters long)
2. The Engine nominal thrust or the Jet maximum thrust in (lb)
3. Engine Mass in (slugs), (for gimbaling engines, not required for fixed engines)
4. Engine Inertia about its pivot in (slug-ft<sup>2</sup>), (not required for fixed engines)
5. Distance between the engine CG and its pivot (not required for fixed engines)
6. The location (x, y, z) of the engine pivot or thrust application point in (feet)
7. Engine or Thruster mounting angles (D<sub>y</sub> and D<sub>z</sub>) referenced from -x direction in (deg)
8. Max Pitch and Yaw deflections of a gimbaling engine relative to its mount position (deg)
9. Max Throttling capability relative to nominal thrust (0-1), (0% to 100% variation)

The orientation of the engine nozzle relative to the -x axis defines the direction of thrust. When the nozzle is defined to be mounted at (D<sub>y</sub>=0 and D<sub>z</sub>=0) relative to the -x axis it means that the thrust vector is in the +x direction. When the nozzle of a thruster is rotated at angles (D<sub>y</sub>=0° and D<sub>z</sub>=90°) in azimuth (yaw) the thrust is pointing in the +y direction. When it is rotated in the -pitch direction, let's say, (D<sub>y</sub>=-90° and D<sub>z</sub>=0°) the thrust is pointing towards the +z direction. Big angles are typically used for defining the thrust directions of reaction control jets. Propulsion engine nozzles are typically mounted in the -x direction. Sometimes the engine mounting is slightly tilted by a few degrees in pitch to account for trimming biases. They may also be tilted in yaw for pointing the thrust through the CG and minimizing lateral disturbances in the event of a thrust failure. An engine is defined as gimbaling when its maximum pitch and yaw deflections in the propulsion data file are greater than zero. Otherwise, if the engine's max deflections are zero, it is not gimbaling. Some of the gimbaling engine parameters such as: the engine mass, inertia, and moment arm are not used by Trim directly. They are exported to an input file together with other vehicle data and used for generating vehicle dynamic models and implementing the tail-wags-dog effects. An engine may be defined to be both: gimbaling and throttling. The definition of the maximum throttling capability or throttling parameter of an engine or jet may be a little confusing, but the examples should make it clear.

An engine or a thruster jet is defined to have variable thrust (or throttling) when its throttle parameter ( $p_{thr}$ ) in the engine data is greater than zero and less than or equal to one. The throttle parameter is included in the thruster data file. It is positive and defines the maximum amount of thrust variation. Its interpretation is slightly different for a throttling engine than for an RCS jet. The throttle parameter of a throttling engine determines the percentage of thrust variation above or below nominal thrust  $T_e$ . It should be between zero and less than 1, ( $0 < p_{thr} < 1$ ). For example, if the engine thrust is 1000 and the throttle parameter is 0.5, it means that during trimming the program may vary the engine thrust  $\pm 50\%$  from  $T_e$ . That is, between 500 and 1500, depending on the throttle control input  $\delta_{Thr}(t)$  that varies between -1 and +1. The thrust is equal to  $T_e$  when  $\delta_{Thr} = 0$ . The throttle control input  $\delta_{Thr}(t)$  for each engine is calculated by the Trim program as a function of time. It varies between zero and  $\pm 1$  and controls the thrust in order to balance the vehicle moments and forces.

Otherwise, when the throttle parameter is exactly 1, it defines that the thruster is an RCS jet. This is interpreted by the program as a pair of reaction control jets firing back-to-back with zero nominal thrust. The actual thrust at any time can be either positive or negative. It means that the thrust variation is limited between  $-T_{max}$  and  $+T_{max}$  depending on the throttle control input  $\delta_{Thr}(t)$  that may vary between -1 and +1. The jet thrust is zero when  $\delta_{Thr} = 0$ . For example, if the jet thrust is defined to be 1000, during trimming the program may vary the thrust between -1000 to +1000 continuously as the throttle control varies between -1 to +1. Notice, that the jet thrust during trimming is continuous (not bang-bang) because the purpose of the Trim program is for sizing the thrust requirements and not for analyzing the dynamic behavior of the closed-loop system. Dynamic analysis is performed later by means of the state-space models which are generated by the FVMP. The dynamic models include detailed representation of the reaction control system with throttle control inputs for each jet. Non-linear dynamic analysis and closed-loop simulations are also performed to analyze the system's response with bang-bang reaction control jets. The user may take a look at the RCS examples presented in the Flixan examples section.

Rocket Plane Propulsion Data											
Engine Description, Thrust	Mass (lb)	Mass (slug)	Ieng (slug-ft2)	Mom Arm (ft)	Location (x,y,z) (feet)			Mounting Angles (Dy, Dz) Elevat, Azimuth (degr)		Max Deflection Dym,Dzm (deg)	Max Throttle (0-1)
Main Engine	62000.0	160.0	3500.0	3.5	-47.0	0.0	-0.492	0.0	0.0	5.0 5.0	0.4
+Z RCS Jet	4000.0	0.0	0.0	1.0	+1.0	0.0	0.0	-90.0	0.0	0.0 0.0	1.0
+Y RCS Jet	4000.0	0.0	0.0	1.0	+1.0	0.0	0.0	0.0	+90.0	0.0 0.0	1.0

## 9.4 Base Aero Data File

The basic aero data file contains the information necessary for calculating the aerodynamic forces and moments of the base vehicle assuming the aerosurface deflections are zero. The filenames extension is ".Aero". The first line contains the vehicle configuration title. The second line contains the vehicle reference area in (feet<sup>2</sup>), the mean aerodynamic chord, and the wing span in (feet). The third line contains the location of the moments reference center (MRC) with respect to the vehicle reference axes, in (feet). The aero moment coefficients are calculated relative to the MRC and they are converted by the program to the vehicle CG. The fourth line contains the number of Mach #s, the number of betas and the number of alphas which are included in the data set.

A basic aero data file consists of groups of data separated by blank lines that make it easier to read. Each group corresponds to a fixed Mach number and beta and contains a full set of alphas followed with the corresponding force and moment coefficients in one line. The aero coefficients consist of 3 base forces and 3 base moments (non-dimensional), in the following sequence:  $C_A$  (along the -x axis),  $C_Y$ ,  $C_Z$  (along the vehicle z axis),  $C_l$ ,  $C_m$ ,  $C_n$ . They are functions of: (Mach,  $\beta$ , and  $\alpha$ ) and they are listed as blocks of column data, as shown below. The first column in the data file is the Mach number, the second column is the angle of sideslip  $\beta$  in degrees, the third column is the angle of attack  $\alpha$  in degrees, and they are followed by the 6 aero coefficients. They are originally Excel files that have been converted into text format. The sequence of Mach,  $\beta$ , and  $\alpha$  must be in ascending order. The pattern is pretty obvious and easy to reproduce for other applications by replicating some of the data files which are included in the examples folder.

```

Hyperspeed Rocket Plane, Basic Descent Aero Data
S_reference, Aero Chord, Span (ft) 390.64 50.0 30.809
Moment Reference Center, (MRC) (ft) -31.5 0.0 0.0
Numbers of: Mach, Beta, Alpha= 12, 3, 16
(deg) (deg) Aero Force Coefficients ..... Aero Moment Coefficients .....
Mach#Beta Alpha Ca (-Cx), Cy, Cz (-CN), Cl, Cm, Cn
-----
0.3 -5 -6 1.283E-02 6.524E-02 1.832E-01 -8.033E-03 -8.422E-03 -1.829E-02
0.3 -5 -4 2.285E-02 6.353E-02 7.422E-02 -5.588E-03 -8.796E-03 -1.794E-02
0.3 -5 -2 2.827E-02 6.182E-02 -3.505E-02 -3.143E-03 -9.169E-03 -1.759E-02
0.3 -5 0 2.971E-02 6.239E-02 -1.445E-01 0.000E+00 -9.543E-03 -1.666E-02
0.3 -5 2 3.104E-02 6.125E-02 -2.554E-01 3.493E-03 -9.916E-03 -1.738E-02
0.3 -5 4 3.365E-02 6.182E-02 -3.728E-01 6.636E-03 -1.029E-02 -1.816E-02
0.3 -5 6 3.806E-02 6.125E-02 -4.953E-01 1.083E-02 -1.066E-02 -1.966E-02
0.3 -5 8 4.406E-02 6.239E-02 -6.264E-01 1.432E-02 -1.104E-02 -2.293E-02
0.3 -5 10 5.119E-02 5.897E-02 -7.678E-01 1.816E-02 -1.141E-02 -2.366E-02
0.3 -5 12 5.384E-02 5.043E-02 -9.195E-01 2.096E-02 -1.178E-02 -2.135E-02
0.3 -5 14 5.664E-02 4.188E-02 -1.057E+00 2.410E-02 -1.088E-02 -1.819E-02
0.3 -5 16 5.890E-02 3.219E-02 -1.195E+00 2.585E-02 -8.449E-03 -1.859E-02
0.3 -5 18 6.136E-02 2.251E-02 -1.328E+00 2.908E-02 -5.695E-03 -1.899E-02
0.3 -5 20 6.074E-02 1.283E-02 -1.464E+00 3.231E-02 -2.246E-03 -1.939E-02
0.3 -5 25 2.471E-02 -1.139E-02 -1.787E+00 4.038E-02 4.439E-03 -2.040E-02
0.3 -5 30 -2.264E-02 -3.560E-02 -2.032E+00 4.846E-02 1.112E-02 -2.141E-02

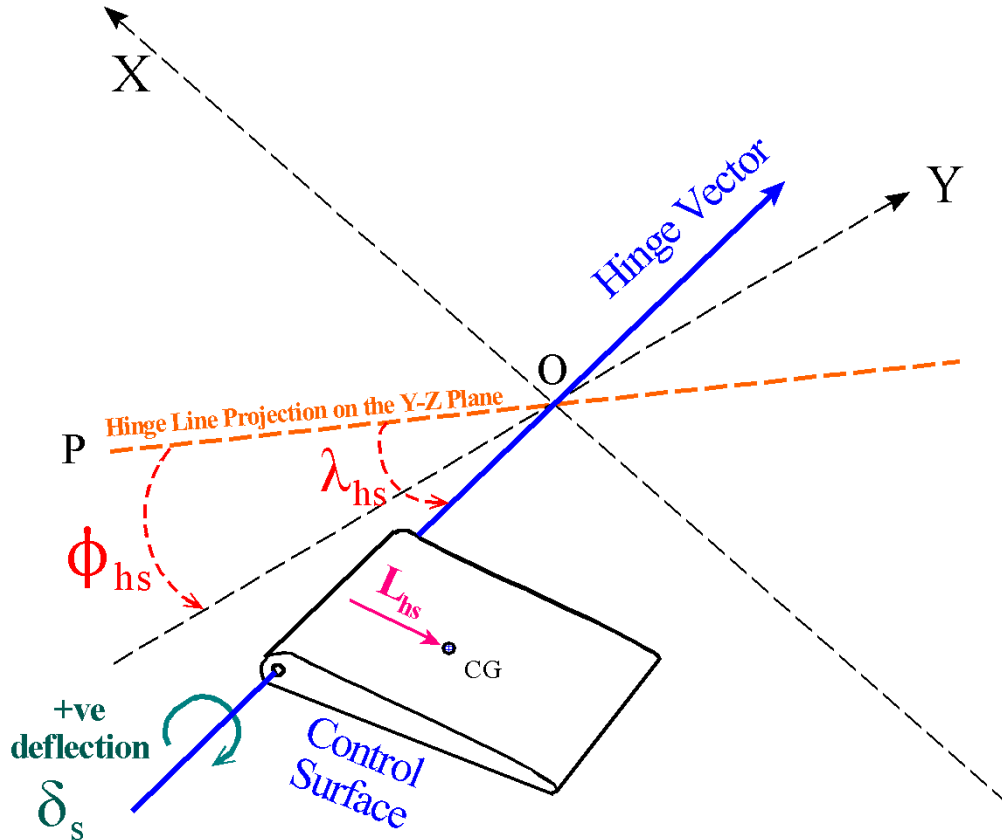
0.3 0 -6 1.283E-02 0.000E+00 1.832E-01 0.000E+00 -8.422E-03 0.000E+00
0.3 0 -4 2.285E-02 0.000E+00 7.422E-02 0.000E+00 -8.796E-03 0.000E+00
0.3 0 -2 2.827E-02 0.000E+00 -3.505E-02 0.000E+00 -9.169E-03 0.000E+00

```

## 9.5 Control Surface Increment Coefficients File

The aerosurfaces data file contains the increment coefficients required for calculating the aerodynamic forces and moments on the vehicle as a function of aerosurface deflections ( $\delta_i$ ) in (degrees). These aero forces and moments are additional increments to the moments and forces generated by the base vehicle aerodynamics. The control surfaces filename has an extension ".Delt" and it includes the aero data of all vehicle aerosurfaces. They are separated in sets, one set of data per surface. The first line in the aerosurfaces file includes a title and the second line includes the number of aerosurface sets which are in this file. The first line of each aerosurface data set includes the surface title, for example, "Elevon, Surface No 1". The next two lines are labels, see examples. The fourth line contains parameters related to the aerosurface panel itself, assuming that it is a separate panel and not a combination of panels. These are:

1. Aerosurface area in (feet<sup>2</sup>),
2. Aerosurface chord in (feet)
3. Aerosurface span in (feet).
4. Hinge Line orientation angle  $\lambda_{hs}$  (deg)
5. Hinge Line orientation angle  $\phi_{hs}$  (deg)
6. Location (x, y, z) of the center of the hinge in (ft)
7. Bias deflection, is the surface position when the command input is zero (deg)
8. Minimum and Maximum surface positions relative to zero position in (deg)
9. Aerosurface Mass (slugs), (for TWD modeling)
10. Aerosurface Moment of Inertia about its hinge (slug-ft<sup>2</sup>), (for TWD modeling)
11. Distance between the surface CG and its hinge (feet), (for TWD modeling)
12. Number of Mach numbers for this aerosurface
13. Number of betas for this aerosurface
14. Number of alphas for this aerosurface
15. Number of increments for this aerosurface



Some of the aerosurface parameters included in the ".Delt" file are not used for static analysis by the Trim program and initially they may be set to zero. They are only used for the creation of vehicle dynamic models by the FVM program and specifically for modeling the tail-wag-dog dynamics. When the dynamic modeling option is selected from Trim, these parameters are included in a dataset, in the flight vehicle input data file ".Inp", together with other vehicle data. Some of these parameters include the direction of the hinge line relative to the vehicle reference axes which is defined by two angles ( $\lambda_{hs}$  and  $\phi_{hs}$ ), as shown in figure. This is the line about which the aerosurface is rotating clockwise for a positive surface deflection. The aerosurface area, chord,



span, location, mass, inertia, and the distance between the aerosurface CG and the hinge line, are also transferred to the vehicle input data file, although not directly used by the Trim program. When requesting aerosurface data from the aero group, it is recommended to request the aero coefficients as separate aerosurface panels and not as a combination of panels, such as aileron, etc. It is not that panel combinations will not work in Trim but some of those TWD parameters cannot be defined when you combine multiple surfaces together. Some information is lost when panels are defined in pairs and this will affect the quality of the dynamic models. This guideline, obviously, does not affect the Trim static analysis or even the creation of rigid-body dynamic models but only when you start developing high order dynamic models. Specifically, the modeling of structural flexibility, tail-wag-dog, and the dynamic coupling between vehicle and actuator dynamic models (load-torque), may be inaccurate when the surfaces are defined in pairs. It is more efficient to define them separately and to combine them with the mixing logic matrix. But this is further down the line and there is no need to worry about this for now.

Returning to the aerosurface data file, skip a couple more lines down the file, and the surface coefficients begin. The coefficients for each aerosurface set are listed in columns and they are separated into groups of data, just like the basic aero data. The first four columns contain: the Mach number, the angle of sideslip  $\beta$  in degrees, the angle of attack  $\alpha$  in degrees, and the control surface deflection  $\delta$  in degrees. They are followed by 6 columns of force and moment coefficients,  $C_A$  (along the negative x axis),  $C_Y$  (along the y axis),  $C_Z$  (along the vehicle z axis), and  $C_l$ ,  $C_m$ ,  $C_n$  (about the roll, pitch and yaw axes). They are four dimensional arrays of: (Mach,  $\beta$ ,  $\alpha$ ,  $\delta$ ). The groups are separated by a blank line which makes it easier to read. Each group of data corresponds to a fixed Mach#,  $\beta$ , and deflection  $\delta$ , and contains a full set of alphas, followed by the aero force moment coefficients corresponding to the (Mach,  $\beta$ ,  $\alpha$ , and  $\delta$ ). The Mach,  $\beta$ ,  $\alpha$ , and  $\delta$  data sequence should be in ascending order. The moment coefficients in the data file are referenced relative to the moments reference center (MRC), but the Trim program transforms them to the vehicle CG.

Aero-Surface Coefficients for the Rocket Plane													
Number of Aero-Surfaces = 4													
-----													
Elevon	Surface No 1			Hinge Line Angles, Location,			Bias Defl.	Deflect Min, Max,	Surf Mass, In, Mom Arm, Numb: Mach, Beta, Alpha, Delta				
Surface Area, (ft^2)	Chord (ft)	Span (ft)	Lambda, Phi (deg)	x, y, z (ft)	(degrees)	(degrees)	(degrees)	Mas, Ias, Las, (slugs), (ft)					
11.81	2.36	10.5	0.0	0.0	-41.4, 0., +2.	0.0	-20.0, +20.0,	10. 100. 2.	12, 3, 16, 5				
Angles in (degrees)													
Mach#	Beta	Alpha	Delta	$C_A$ (-Cx)	$C_Y$	$C_Z$ (-Cn)	$C_l$	$C_m$	$C_n$				
-----													
0.3	-5	-6	-20	-1.782E-02	0.000E+00	3.925E-01	0.000E+00	5.486E-02	0.000E+00				
0.3	-5	-4	-20	-1.362E-02	0.000E+00	3.922E-01	0.000E+00	5.502E-02	0.000E+00				
0.3	-5	-2	-20	-9.447E-03	0.000E+00	3.921E-01	0.000E+00	5.518E-02	0.000E+00				
0.3	-5	0	-20	-5.288E-03	0.000E+00	3.922E-01	0.000E+00	5.534E-02	0.000E+00				
0.3	-5	2	-20	-1.122E-03	0.000E+00	3.925E-01	0.000E+00	5.550E-02	0.000E+00				
0.3	-5	4	-20	3.067E-03	0.000E+00	3.930E-01	0.000E+00	5.565E-02	0.000E+00				
0.3	-5	6	-20	7.300E-03	0.000E+00	3.936E-01	0.000E+00	5.581E-02	0.000E+00				
0.3	-5	8	-20	1.159E-02	0.000E+00	3.945E-01	0.000E+00	5.597E-02	0.000E+00				
0.3	-5	10	-20	1.597E-02	0.000E+00	3.955E-01	0.000E+00	5.613E-02	0.000E+00				
0.3	-5	12	-20	2.043E-02	0.000E+00	3.967E-01	0.000E+00	5.629E-02	0.000E+00				
0.3	-5	14	-20	2.502E-02	0.000E+00	3.980E-01	0.000E+00	5.645E-02	0.000E+00				
0.3	-5	16	-20	2.973E-02	0.000E+00	3.995E-01	0.000E+00	5.660E-02	0.000E+00				
0.3	-5	18	-20	3.459E-02	0.000E+00	4.012E-01	0.000E+00	5.676E-02	0.000E+00				
0.3	-5	20	-20	3.961E-02	0.000E+00	4.030E-01	0.000E+00	5.692E-02	0.000E+00				
0.3	-5	25	-20	5.298E-02	0.000E+00	4.081E-01	0.000E+00	5.732E-02	0.000E+00				
0.3	-5	30	-20	6.771E-02	0.000E+00	4.138E-01	0.000E+00	5.771E-02	0.000E+00				
-----													
0.3	-5	-6	-10	-1.538E-02	0.000E+00	1.956E-01	0.000E+00	2.824E-02	0.000E+00				
0.3	-5	-4	-10	-1.330E-02	0.000E+00	1.957E-01	0.000E+00	2.832E-02	0.000E+00				
0.3	-5	-2	-10	-1.123E-02	0.000E+00	1.958E-01	0.000E+00	2.840E-02	0.000E+00				
0.3	-5	0	-10	-9.155E-03	0.000E+00	1.961E-01	0.000E+00	2.847E-02	0.000E+00				
0.3	-5	2	-10	-7.068E-03	0.000E+00	1.965E-01	0.000E+00	2.855E-02	0.000E+00				
0.3	-5	4	-10	-4.961E-03	0.000E+00	1.969E-01	0.000E+00	2.863E-02	0.000E+00				
0.3	-5	6	-10	-2.825E-03	0.000E+00	1.975E-01	0.000E+00	2.871E-02	0.000E+00				
0.3	-5	8	-10	-6.504E-04	0.000E+00	1.981E-01	0.000E+00	2.879E-02	0.000E+00				
0.3	-5	10	-10	1.571E-03	0.000E+00	1.989E-01	0.000E+00	2.887E-02	0.000E+00				
0.3	-5	12	-10	3.849E-03	0.000E+00	1.997E-01	0.000E+00	2.895E-02	0.000E+00				
0.3	-5	14	-10	6.191E-03	0.000E+00	2.006E-01	0.000E+00	2.903E-02	0.000E+00				
0.3	-5	16	-10	8.605E-03	0.000E+00	2.016E-01	0.000E+00	2.911E-02	0.000E+00				
0.3	-5	18	-10	1.110E-02	0.000E+00	2.026E-01	0.000E+00	2.919E-02	0.000E+00				
0.3	-5	20	-10	1.369E-02	0.000E+00	2.037E-01	0.000E+00	2.927E-02	0.000E+00				
0.3	-5	25	-10	2.059E-02	0.000E+00	2.068E-01	0.000E+00	2.946E-02	0.000E+00				
0.3	-5	30	-10	2.822E-02	0.000E+00	2.102E-01	0.000E+00	2.966E-02	0.000E+00				

## 9.6 Hinge Moment Coefficients File

The Hinge Moment coefficients file contains the data required to calculate the static moments at the aerosurface hinges after trimming. These moments are used for sizing the actuator torques that control the aerosurfaces. The Hinge Moment coefficients file is identified by the filename extension ".HMco". Its format structure is very similar to the aerosurfaces file, except that it contains only one coefficient per line instead of 6. The first line in this file includes the flight vehicle title, and the second line shows the number of aerosurface data sets which are included in the same file. The first line of each aerosurface data set includes the surface title, for example, "Left Flapper, Surface No 1". The next two lines are labels, see examples. The fourth line contains parameters associated with the aerosurface panel itself, assuming that it is a separate panel and not a combination of panels. These are:

1. Aerosurface area in (feet<sup>2</sup>),
2. Aerosurface chord in (feet)
3. Aerosurface span in (feet).
4. Number of Mach numbers for this aerosurface
5. Number of betas for this aerosurface
6. Number of alphas for this aerosurface
7. Number of increments for this aerosurface

The HM coefficients data for each aerosurface set is in columns and they are separated in groups of data just like the aerosurface increments data. The first four columns contain: the Mach number, the angle of sideslip  $\beta$  in degrees, the angle of attack  $\alpha$  in degrees, and the control surface deflection  $\delta$  in degrees. The fifth column contains the corresponding HM coefficient, see below.

```

Hinge Moment Coefficients for the Re-Entry Vehicle Control Surfaces
Number of Aero-Surfaces = 5
-----
Left Flapper      Surface No 1
Surface Area,    Chord,   Span,   Numbers of: Mach, Beta, Alpha, Delta
(ft^2)           (ft)    (ft)
5.553           1.207   3.1
                27      3      28      7
Angles in (degrees)
Mach#           Beta    Alpha   Delta   Hinge Moment Coefficients .....
-----
0.20  -5.00  -4.00  -30.00  0.25293E+00
0.20  -5.00  -2.00  -30.00  0.24882E+00
0.20  -5.00   0.00  -30.00  0.22104E+00
0.20  -5.00   2.00  -30.00  0.19332E+00
0.20  -5.00   4.00  -30.00  0.16981E+00
0.20  -5.00   6.00  -30.00  0.14586E+00
0.20  -5.00   8.00  -30.00  0.11476E+00
0.20  -5.00  10.00  -30.00  0.86070E-01
0.20  -5.00  12.00  -30.00  0.71250E-01
0.20  -5.00  14.00  -30.00  0.11090E+00
0.20  -5.00  16.00  -30.00  0.10496E+00
0.20  -5.00  18.00  -30.00  0.89430E-01
0.20  -5.00  20.00  -30.00  0.89710E-01
0.20  -5.00  22.00  -30.00  0.93000E-01
0.20  -5.00  24.00  -30.00  0.10751E+00
0.20  -5.00  26.00  -30.00  0.10751E+00
0.20  -5.00  28.00  -30.00  0.10751E+00
0.20  -5.00  30.00  -30.00  0.10751E+00
0.20  -5.00  32.00  -30.00  0.10751E+00
0.20  -5.00  34.00  -30.00  0.10751E+00
0.20  -5.00  36.00  -30.00  0.10751E+00
0.20  -5.00  38.00  -30.00  0.10751E+00
0.20  -5.00  40.00  -30.00  0.10751E+00
0.20  -5.00  42.00  -30.00  0.10751E+00
0.20  -5.00  44.00  -30.00  0.10751E+00
0.20  -5.00  46.00  -30.00  0.10751E+00
0.20  -5.00  48.00  -30.00  0.10751E+00
0.20  -5.00  50.00  -30.00  0.10751E+00

0.20  -5.00  -4.00  -20.00  0.13177E+00
0.20  -5.00  -2.00  -20.00  0.12571E+00
    
```

## 9.7 Damping Derivatives File

The damping derivatives calculate the increments in the aerodynamic moments and forces as a function of the vehicle pitching, rolling and yawing rates. They are: Cm<sub>q</sub>, Cl<sub>p</sub>, C<sub>np</sub>, Cl<sub>r</sub>, C<sub>nr</sub>, C<sub>zq</sub>, C<sub>Aq</sub>, C<sub>yp</sub>, and C<sub>yr</sub>. The coefficients are dimensionless and they are converted to actual forces and moments by the following equations (shown partially):

$$\text{Increment in pitching moment} = \bar{Q} S_{ref} \bar{c} C_{mq}(\alpha, M) \times \frac{\bar{c}}{2V_T} \times q$$

$$\text{Increment in rolling moment} = \bar{Q} S_{ref} b C_{lp}(\alpha, M) \times \frac{b}{2V_T} \times p$$

$$\text{Increment in yawing moment} = \bar{Q} S_{ref} b C_{nr}(\alpha, M) \times \frac{b}{2V_T} \times r$$

Where: V<sub>T</sub> is the vehicle relative velocity in (ft/sec), b is the wing span in (ft),  $\bar{c}$  is the mean aero chord in (ft), and the body rates (p, q, r) are in (rad/sec).

The damping derivatives filenames have an extension ".Damp". They contain the damping derivatives as a function of Mach and alpha. The first line is a title and the second line includes the number of Mach and alpha points. The data is in columns and they are separated into groups, and the groups are separated by blank lines. The first two columns contain the Mach numbers and the angles of attack. Each group corresponds to a fixed Mach and contains a full range of alphas, followed by 9 columns of the corresponding damping derivatives in the order shown below.

Aero Damping Derivatives for the Space Shuttle Vehicle											
Numbers of: Mach, Alpha= 25 28											
Mach,	Alpha,	Cmq	Clp	Cnp	Clr	Cnr	Czq	CAq	Cyp	CYr	
0.20	-4.00	-0.10707E+02	-0.43896E+00	0.33093E+00	0.40549E+00	-0.13852E+01	-0.91826E+01	0.22219E+00	-0.46756E+00	0.18613E+01	
0.20	-2.00	-0.10925E+02	-0.41797E+00	0.27946E+00	0.40132E+00	-0.13722E+01	-0.93146E+01	0.91030E-01	-0.30639E+00	0.18409E+01	
0.20	0.00	-0.11131E+02	-0.39796E+00	0.22889E+00	0.39790E+00	-0.13561E+01	-0.94353E+01	-0.40248E-01	-0.14704E+00	0.18092E+01	
0.20	2.00	-0.11322E+02	-0.37884E+00	0.17944E+00	0.39540E+00	-0.13370E+01	-0.95445E+01	-0.17147E+00	0.97078E-02	0.17666E+01	
0.20	4.00	-0.11500E+02	-0.36047E+00	0.13130E+00	0.39394E+00	-0.13151E+01	-0.96421E+01	-0.30250E+00	0.16310E+00	0.17130E+01	
0.20	6.00	-0.11664E+02	-0.34271E+00	0.84647E-01	0.39364E+00	-0.12905E+01	-0.97278E+01	-0.43315E+00	0.31239E+00	0.16490E+01	
0.20	8.00	-0.11814E+02	-0.32539E+00	0.39636E-01	0.39462E+00	-0.12634E+01	-0.98018E+01	-0.56327E+00	0.45684E+00	0.15746E+01	
0.20	10.00	-0.11934E+02	-0.31154E+00	0.81278E-02	0.39462E+00	-0.12337E+01	-0.98523E+01	-0.77263E+00	0.55795E+00	0.14631E+01	
0.20	12.00	-0.12030E+02	-0.30046E+00	-0.13928E-01	0.39462E+00	-0.12010E+01	-0.98703E+01	-0.10757E+01	0.62873E+00	0.12958E+01	
0.20	14.00	-0.12107E+02	-0.29160E+00	-0.29366E-01	0.39462E+00	-0.11651E+01	-0.98591E+01	-0.14276E+01	0.67828E+00	0.10449E+01	
0.20	16.00	-0.12168E+02	-0.28451E+00	-0.40174E-01	0.39462E+00	-0.11256E+01	-0.98288E+01	-0.17782E+01	0.71296E+00	0.79403E+00	
0.20	18.00	-0.12168E+02	-0.28451E+00	-0.40174E-01	0.39462E+00	-0.11256E+01	-0.98288E+01	-0.17782E+01	0.71296E+00	0.79403E+00	
0.20	20.00	-0.12207E+02	-0.27997E+00	-0.45469E-01	0.39462E+00	-0.10822E+01	-0.96968E+01	-0.24653E+01	0.72996E+00	0.59330E+00	
0.20	22.00	-0.12207E+02	-0.27997E+00	-0.45469E-01	0.39462E+00	-0.10822E+01	-0.96968E+01	-0.24653E+01	0.72996E+00	0.59330E+00	
0.20	24.00	-0.12207E+02	-0.27997E+00	-0.45469E-01	0.39462E+00	-0.10822E+01	-0.95012E+01	-0.31357E+01	0.72996E+00	0.43272E+00	
0.20	26.00	-0.12207E+02	-0.27997E+00	-0.45469E-01	0.39462E+00	-0.10822E+01	-0.95012E+01	-0.31357E+01	0.72996E+00	0.43272E+00	
0.20	28.00	-0.12207E+02	-0.27997E+00	-0.45469E-01	0.39462E+00	-0.10822E+01	-0.92593E+01	-0.37909E+01	0.72996E+00	0.30426E+00	
0.20	30.00	-0.12207E+02	-0.27997E+00	-0.45469E-01	0.39462E+00	-0.10822E+01	-0.92593E+01	-0.37909E+01	0.72996E+00	0.30426E+00	
0.20	32.00	-0.12207E+02	-0.27997E+00	-0.45469E-01	0.39462E+00	-0.10822E+01	-0.89723E+01	-0.44276E+01	0.72996E+00	0.30426E+00	
0.20	34.00	-0.12207E+02	-0.27997E+00	-0.45469E-01	0.39462E+00	-0.10822E+01	-0.89723E+01	-0.44276E+01	0.72996E+00	0.30426E+00	
0.20	36.00	-0.12207E+02	-0.27997E+00	-0.45469E-01	0.39462E+00	-0.10822E+01	-0.86416E+01	-0.50427E+01	0.72996E+00	0.30426E+00	
0.20	38.00	-0.12207E+02	-0.27997E+00	-0.45469E-01	0.39462E+00	-0.10822E+01	-0.86416E+01	-0.50427E+01	0.72996E+00	0.30426E+00	
0.20	40.00	-0.12207E+02	-0.27997E+00	-0.45469E-01	0.39462E+00	-0.10822E+01	-0.82688E+01	-0.56332E+01	0.72996E+00	0.30426E+00	
0.20	42.00	-0.12207E+02	-0.27997E+00	-0.45469E-01	0.39462E+00	-0.10822E+01	-0.82688E+01	-0.56332E+01	0.72996E+00	0.30426E+00	
0.20	44.00	-0.12207E+02	-0.27997E+00	-0.45469E-01	0.39462E+00	-0.10822E+01	-0.77463E+01	-0.63325E+01	0.72996E+00	0.30426E+00	
0.20	46.00	-0.12207E+02	-0.27997E+00	-0.45469E-01	0.39462E+00	-0.10822E+01	-0.77463E+01	-0.63325E+01	0.72996E+00	0.30426E+00	
0.20	48.00	-0.12207E+02	-0.27997E+00	-0.45469E-01	0.39462E+00	-0.10822E+01	-0.71649E+01	-0.69835E+01	0.72996E+00	0.30426E+00	
0.20	50.00	-0.12207E+02	-0.27997E+00	-0.45469E-01	0.39462E+00	-0.10822E+01	-0.71649E+01	-0.69835E+01	0.72996E+00	0.30426E+00	

Figure 9.1 Damping Derivatives Data

## 9.8 Aerodynamic Uncertainties File

The aerodynamic uncertainty files have an extension ".Unce". They contain additive uncertainties in three types of aero coefficients: (a) the basic aero coefficients, (b) the basic aero derivatives, and (c) in the control surface derivatives for each aerosurface on the vehicle. They are functions of Mach number. For example, the yawing moment coefficient is  $C_n(\alpha, \beta, M)$ . With the addition of the uncertainty it becomes:  $C_n(\alpha, \beta, M) \pm \delta C_n(M)$ . The uncertainties are used in the vector diagram plots, described earlier, for calculating the size of the uncertainty rectangle at the tips of the vectors. The uncertainty rectangles provide a visual interpretation of the uncertainty size in the control effectors and also in the aero disturbance vectors. The uncertainties are also used for analyzing system robustness by means of mu-analysis using robustness analysis models generated by Flixan. The data in the uncertainties file are arranged into groups and separated by blank lines. The first set contains the uncertainty magnitudes in the six basic aero coefficients, as a function of Mach. The second set contains the uncertainty magnitudes in the six basic aero derivatives ( $CA_\alpha$ ,  $CY_\beta$ ,  $CZ_\alpha$ ,  $Cl_\beta$ ,  $Cm_\alpha$ ,  $Cn_\beta$ ), as a function of Mach. The remaining sets contain the uncertainties in the control surface derivatives, ex. ( $CA_{\delta elev}$ ,  $CZ_{\delta elev}$ ,  $Cm_{\delta elev}$ , etc), for each control surface, which are also functions of Mach number. The top line in this file includes a title. The second line includes the number of Mach #s and the number of aerosurfaces, as shown below.

```
Variations of Aerodynamic Coefficient for the Hypersonic Vehicle
Number of Mach Numbers, Control Surfaces = 8, 4

Basic Aero Uncertainties as a function of Mach Number
Mach CA CY CZ Cl Cm Cn
0.30 0.002 0.000 0.050 0.008 0.004 0.003
0.60 0.002 0.000 0.050 0.008 0.004 0.003
0.80 0.002 0.000 0.050 0.008 0.004 0.003
0.95 0.002 0.000 0.050 0.008 0.004 0.003
1.10 0.002 0.000 0.050 0.008 0.004 0.003
1.15 0.003 0.000 0.050 0.008 0.003 0.003
2.00 0.003 0.000 0.060 0.008 0.003 0.003
3.00 0.003 0.000 0.060 0.008 0.003 0.003

Uncertainties in the Base Derivatives
Mach CA_alpha CY_beta CZ_alpha Cl_beta Cm_alpha Cn_beta
0.30 0.0020 0.0030 0.0100 0.0005 0.0020 0.0030
0.60 0.0040 0.0030 0.0100 0.0005 0.0020 0.0030
0.80 0.0040 0.0030 0.0100 0.0005 0.0020 0.0030
0.95 0.0040 0.0040 0.0100 0.0005 0.0020 0.0030
1.10 0.0040 0.0040 0.0100 0.0005 0.0020 0.0030
1.15 0.0040 0.0050 0.0100 0.0005 0.0020 0.0030
2.00 0.0040 0.0050 0.0080 0.0003 0.0015 0.0030
3.00 0.0040 0.0055 0.0080 0.0003 0.0010 0.0030

Uncertainties in the Elevon Derivatives
Mach CA_elev CY_Elev CZ_Elev Cl_Elev Cm_Elev Cn_Elev
0.30 0.0020 0.0000 0.0200 0.0000 0.0035 0.0000
0.60 0.0020 0.0000 0.0200 0.0000 0.0035 0.0000
0.80 0.0020 0.0000 0.0200 0.0000 0.0035 0.0000
0.95 0.0020 0.0000 0.0200 0.0000 0.0035 0.0000
1.10 0.0020 0.0000 0.0200 0.0000 0.0035 0.0000
1.15 0.0020 0.0000 0.0300 0.0000 0.0035 0.0000
2.00 0.0020 0.0000 0.0300 0.0000 0.0030 0.0000
3.00 0.0020 0.0000 0.0300 0.0000 0.0030 0.0000
```

Figure 9.2 Aero-Uncertainties Data: (Basic, Derivatives, Surface Derivatives)

## 9.9 Propellant Sloshing Data File

The propellant slosh data filename extension is ".Slsh" and it contains information for modeling slosh dynamics in a flight vehicle that uses liquid propellant tanks. It is a look-up table used to calculate the slosh parameters at the selected trajectory time as a function of the corresponding vehicle mass. This type of file is not used for static analysis, but it is used by the dynamic modeling option of the Trim program to transfer the slosh parameters, that correspond to the selected flight condition, to an input file ".Inp" together with the other vehicle data. The vehicle input file will then be processed by the Flixan Flight Vehicle Modeling program to generate the vehicle dynamic model that will include fuel sloshing. The slosh file may include more than one sloshing tank. The data for each sloshing tank consist of: the propellant sloshing mass in (slugs), the frequency in (rad/sec), the damping coefficient ( $\zeta$ ), and the slosh mass steady-state location (feet) in vehicle coordinates (x, y, z).

The following slosh data file includes two sloshing tanks of liquid oxygen and liquid hydrogen propellants. The first line is a title. The second line contains the number of sloshing tanks (2 in this case). The next few lines before the data are just label lines. The parameters in the slosh file are listed in columns as a function of the vehicle mass in (slugs), which is included in the first column. It is followed by columns of the corresponding slosh parameters. That is: 2 slosh masses, 2 frequencies in (rad/sec), 2 damping coefficients ( $\zeta$ ), 2 slosh-mass X-locations, 2 Y-locations, and 2 Z-locations of the slosh masses that correspond to the LOX and the LH2 tanks. The slosh frequencies are calculated under 1-g loading. They are converted to the proper frequency by the modeling program (according to the acceleration). Note the slosh masses should not be included in the vehicle mass properties (mass, CG and inertias) because their effect is introduced by the forces they exert on the vehicle.

Slosh Data for a Re-Usable Launch Vehicle with Liquid Oxygen and Hydrogen Tanks												
Number of Slosh Masses= 2												
Vehicle Mass (slugs)	Slosh Masses (slug)		Slosh Frequencies (rad/sec) 1-g Load		Damping Zetas		X-Slosh (ft)		Y-Slosh (ft)		Z-Slosh (ft)	
8485.9	5.9	0.7	5.3	6.8	0.001	0.0004	-82.2	-37.4	0.0	0.0	0.0	0.0
7831.7	776.0	12.5	4.56	5.12	0.001	0.0004	-82.7	-38.2	0.0	0.0	0.0	0.0
7365.0	1256.0	43.5	4.1	4.19	0.001	0.0004	-83.5	-38.9	0.0	0.0	0.0	0.0
6484.0	1490.0	69.1	3.9	3.81	0.001	0.0004	-83.9	-39.7	0.0	0.0	0.0	0.0
6176.0	1521.0	89.3	3.78	3.72	0.001	0.0004	-84.4	-40.5	0.0	0.0	0.0	0.0
5353.0	1631.0	103.5	3.68	3.6	0.001	0.0004	-84.8	-41.2	0.0	0.0	0.0	0.0
4355.0	1622.0	105.2	3.57	3.4	0.001	0.0004	-85.2	-41.9	0.0	0.0	0.0	0.0
3358.0	1292.0	63.0	3.36	2.9	0.001	0.0004	-85.8	-42.4	0.0	0.0	0.0	0.0

Figure 9.3 Propellant Sloshing Data

## 9.10 Output Data Files

There are three different types of data files generated by the Trim program mainly for vehicle analysis. The effector trim data (.Trim), the performance parameters (.Perf), and the hinge moment files (.Himo). These files are also used as inputs to Trim, for plotting, analyzing, and comparing vehicle performance. Option-12 is used to overlay, plot, and compare the data files.

### 9.10.1 Effector Trim Data File

The effectors trim data file contains the effector trim deflections and throttles as a function of the trajectory time after balancing the 3 moments and possibly some of the vehicle accelerations. It is generated by the Trim program by selecting the effector trimming option-3 from the Trim main menu. It contains the deflection angles of the control surfaces, the TVC nozzle deflections, and the throttle positions of the throttling engines or jets, as a function of time. It includes also the maximum and minimum deflections, and throttle limits of each effector as a function of time. It includes also the trim directions (dofs) and the effector bias positions. It is used as input to other programs in Trim for analyzing performance or plotting the trim data versus time. It is also used as an initialization file for re-trimming to influence and adjust the new trim results. The effector positions and limits of a trim file can be modified interactively prior to re-trimming in order to manipulate the new trim results, whenever possible.

The default filename of a trim data file is the same as the trajectory filename but it has an extension ".Trim". When a new trim is performed the previous trim file is renamed by including an extension "1". For example, if "Shuttle.Trim" was the original trim filename, after trimming again the previous trim file is renamed to "Shuttle1.Trim" and "Shuttle.Trim" now includes the latest trim data. The previous trim file "Shuttle1.Trim" is also renamed to "Shuttle2.Trim", but this pattern does not continue forever, the last filename saved is "Shuttle2.Trim". To preserve a trim filename from being overwritten for later analysis or plotting the user must rename it. The filenames length in Flixan should not exceed 20 characters.

```
EFFECTOR TRIMMING POSITIONS FOR: Rocket-Plane, Mission-1, Ground Takeoff
Number of Gimbal Engines (Pitch)= 1; Total Deflection (degr): Dy_Engine 1,
Number of Gimbal Engines (Yaw) = 1; Total Deflection (degr): Dz_Engine 1,
Number of Throttling Engines/RCS= 3; Total Thrust in (lb) : Throttle 1, Throttle 2, Throttle 3,
Number of Control Surfaces = 4; Total Deflection (degr): Elevon , Body Flap , Aileron , Rudder ,
Number of Directions Balanced = 6 1 2 3; Degrees of Freedom Trimmed (Minimum 3, Maximum 6), Translation Index (1=x, 2=y, 3=z)
Max Control/Bias 5.00 0.000 5.00 0.000 0.400 0.6200E+05
Time(sec) Dy_Engine 1 Max Deflect. Min Deflect. Dz_Engine 1 Max Deflect. Min Deflect. Throttle 1 Max Deflect. Min Deflect
0.00 -2.1186 5.0000 -5.0000 0.58076E-13 5.0000 -5.0000 -0.68152E-01 0.40000 -0.40000
4.00 -3.6317 5.0000 -5.0000 0.13276E-10 5.0000 -5.0000 -0.51537E-01 0.40000 -0.40000
5.00 -0.89407 5.0000 -5.0000 0.24906E-10 5.0000 -5.0000 -0.65525E-01 0.40000 -0.40000
8.00 -0.21961 5.0000 -5.0000 0.58132E-10 5.0000 -5.0000 -0.56952E-01 0.40000 -0.40000
10.0 0.17310 5.0000 -5.0000 0.10147E-09 5.0000 -5.0000 -0.68238E-01 0.40000 -0.40000
15.0 0.25138 5.0000 -5.0000 0.25299E-09 5.0000 -5.0000 -0.15462 0.40000 -0.40000
20.0 0.14113 5.0000 -5.0000 0.58865E-10 5.0000 -5.0000 -0.41879E-01 0.40000 -0.40000
23.0 0.53443E-01 5.0000 -5.0000 0.93840E-10 5.0000 -5.0000 -0.31535E-01 0.40000 -0.40000
25.0 -0.91678E-02 5.0000 -5.0000 0.12770E-09 5.0000 -5.0000 -0.45381E-01 0.40000 -0.40000
30.0 -0.28135E-01 5.0000 -5.0000 0.14218E-09 5.0000 -5.0000 -0.13748 0.40000 -0.40000
35.0 0.38297E-01 5.0000 -5.0000 0.45452E-10 5.0000 -5.0000 -0.43371E-01 0.40000 -0.40000
```

### 9.10.2 Performance Parameters File

The performance parameters file contains the parameters described in Section 3 as a function of the trajectory time. It is generated by selecting the option "6-Performance and Stability Parameters" from the main Trim menu. It is used for plotting the performance data versus time. Its default filename is the same as the trajectory filename but the extension is changed to ".Perf". When a new performance analysis is completed the previous performance data file is renamed by including an extension "1". For example, if "Shuttle.Perf" was the original performance data file, after running the performance analysis again, the previous file is renamed to "Shuttle1.Perf" and "Shuttle.Perf" now contains the latest performance data. The previous "Shuttle1.Perf" is also renamed to "Shuttle2.Perf". This pattern, however, does not continue forever and the last filename saved is "Shuttle2.Perf".

PERFORMANCE PARAMETERS FOR: Rocket-Plane, Mission-1, Ground Takeoff												
Number of Directions Balanced = 3 0 0 0; Degrees of Freedom Trimmed (Minimum 3, Maximum 6), Translation Index (1=x, 2=y, 3=z)												
Time (sec)	Static_Margn (%)	Centr_Pressr (feet)	Cm_alpha (1/deg)	Pitch_T2I (1/sec)	Lateral_T2I (1/sec)	Q_alpha_beta (deg-lb/ft^2)	Roll_Effort (-)	Pitch_Effort (-)	Yaw_Effort (-)	Bankangl_phi (deg)	LCDF_Ratio (-)	
0.00000E+00	-0.10759E+01	-0.32291E+02	0.79478E-03	0.12144E-02	-0.21296E-02	0.70900E-03	0.54669E-01	-0.88011E-07	-0.25744E+00	0.00000E+00	0.48498E+00	
0.40000E+01	-0.14014E+01	-0.32291E+02	0.10460E-02	0.12052E+01	-0.18399E+01	0.52611E+03	0.54463E-01	-0.32725E-01	-0.25307E+00	0.00000E+00	0.47381E+00	
0.50000E+01	-0.14054E+01	-0.32291E+02	0.10396E-02	0.14976E+01	-0.22939E+01	0.81579E+03	0.54424E-01	-0.36066E-01	-0.25217E+00	0.00000E+00	0.47148E+00	
0.80000E+01	-0.14654E+01	-0.32291E+02	0.10693E-02	0.23481E+01	-0.35455E+01	0.19383E+04	0.54302E-01	-0.43418E-01	-0.24944E+00	0.00000E+00	0.46447E+00	
0.10000E+02	-0.10896E+01	-0.32497E+02	0.79618E-03	0.24210E+01	-0.37250E+01	0.24712E+04	0.39106E-01	-0.32537E-01	-0.19247E+00	0.00000E+00	0.50636E+00	
0.15000E+02	-0.12690E+01	-0.32705E+02	0.85315E-03	0.31242E+01	-0.37481E+01	0.20251E+04	0.26383E-01	-0.35733E-01	-0.17547E+00	0.00000E+00	0.70764E+00	
0.20000E+02	-0.72571E+00	-0.33729E+02	0.48356E-03	0.27704E+01	-0.36336E+01	0.51731E+03	0.54962E-02	-0.17954E-01	-0.16512E+00	0.00000E+00	0.96854E+00	
0.23000E+02	-0.20805E+00	-0.37019E+02	0.18678E-03	0.18678E+01	-0.42127E+01	0.12855E+04	0.20544E-02	-0.35242E-02	-0.16515E+00	0.00000E+00	0.10105E+01	
0.25000E+02	-0.26233E+00	-0.37019E+02	0.22206E-03	0.20799E+01	-0.42917E+01	0.16317E+04	0.20820E-02	-0.65915E-02	-0.16482E+00	0.00000E+00	0.10145E+01	
0.30000E+02	0.31501E+01	-0.28992E+02	-0.21683E-02	-0.45118E+01	-0.42986E+01	0.19807E+04	-0.71793E-02	0.65106E-01	-0.16957E+00	0.00000E+00	0.96503E+00	

### 9.10.3 Hinge Moment Files

The hinge moments file contains the moments at the aerosurface hinges versus trajectory time. It is generated by the program and used for sizing the actuator moment and power required to keep the aerosurfaces trimmed along the flight trajectory. It is selected from Option-8 of the Trim main menu. However, a hinge-moment coefficients file: ".HMco" is required in order to calculate the hinge moments. The default hinge moments filename is the same as the trajectory filename but the extension is ".HiMo". When the hinge moments calculation is repeated the previous hinge moments data file is renamed with an extension "1". For example, if "Shuttle.HiMo" was the original hinge moments data file, after calculating the hinge moments again the previous data is renamed to "Shuttle1.HiMo", and "Shuttle.HiMo" now contains the latest hinge moments data. The previous "Shuttle1.HiMo" is also renamed to "Shuttle2.HiMo".

Aero-Surface Hinge Moments for: Rocket-Plane, Mission-1, Ground Takeoff					
4	Time (sec)	Elevon (ft-lb)	Body Flap	Aileron	Rudder
	0.00000E+00	0.59386E-03	0.59206E-03	-0.32312E-03	0.00000E+00
	0.40000E+01	0.43992E+03	0.22080E+03	-0.23956E+03	0.00000E+00
	0.50000E+01	0.36314E+03	0.13130E+03	-0.37147E+03	0.00000E+00
	0.80000E+01	-0.15207E+03	0.15353E+03	-0.88260E+03	0.00000E+00
	0.10000E+02	-0.46791E+03	0.18754E+03	-0.12034E+04	0.00000E+00
	0.15000E+02	-0.80181E+03	0.39630E+03	-0.16235E+04	0.00000E+00
	0.20000E+02	-0.86731E+03	0.75884E+03	-0.20695E+04	0.00000E+00
	0.23000E+02	-0.14727E+04	0.79903E+03	-0.25832E+04	0.00000E+00
	0.25000E+02	-0.23137E+04	0.78087E+03	-0.31656E+04	0.00000E+00
	0.30000E+02	-0.33494E+04	0.17225E+04	-0.39492E+04	0.00000E+00
	0.35000E+02	-0.43188E+04	0.58161E+03	-0.41476E+04	0.00000E+00
	0.40000E+02	-0.47558E+04	-0.47765E+03	-0.38816E+04	0.00000E+00
	0.45000E+02	-0.41076E+04	-0.11005E+04	-0.22407E+04	0.00000E+00
	0.50000E+02	-0.39756E+04	-0.10437E+04	-0.16166E+04	0.00000E+00
	0.55000E+02	-0.40076E+04	-0.66777E+03	-0.14034E+04	0.00000E+00

# 10. Design Examples

---

The following examples are included in this document for the purpose of demonstrating the capability of the Trim program to analyze a variety of flight vehicle types and to create dynamic models for control analysis and design.

1. **Hypersonic Rocket-Plane Analysis during Ascent and Descent phases.**
2. **F-16 Fighter Aircraft Analysis, Control Design, and 6-dof Simulation**
3. **Air-Launched Vehicle with Wings and Tails Design in Multiple Phases**
4. **Re-Usable Launch Vehicle with Multiple-Engines During Ascent and Descent**
5. **Lifting-Body Aircraft Descent from Space, Vertical Take-Off, and 6-dof Simulation**
6. **Re-Entry Vehicle Design and Analysis Using Aero-Surfaces and RCS Jets**

The examples presented, in addition to trimming and performance analysis, they demonstrate also the following methodologies and capabilities of the Flixan/ Trim program.

- Capability of the Trim algorithm to automatically allocate trim control authority based on the individual effector capabilities in specific directions.
- How to graphically modify the trimming conditions and to trade off activity of some effector against others in situations where multiple effectors are available.
- How to analyze the effects of parameter dispersions on vehicle performance.
- Generating dynamic models at selected flight conditions along the trajectory.
- Using the Flixan program to create various types of design models for synthesizing control systems, time-domain simulations, models for stability analysis using Matlab.
- Using Flixan to generate models for Robustness Analysis to Structured Uncertainties, and how to use these models to perform  $\mu$ -Analysis.
- Using Flixan derived models to synthesize flight control laws. Evaluate control designs using analysis and simulations. The dynamic models, vehicle data files, design software, detailed methodologies, Flixan & Matlab files, etc, are included in the example packages.
- Developing 6-dof Non-Linear Simulations using Flixan derived control laws, interpolated between design points. Using the 6-dof simulations to generate trajectories.
- Demonstrating interactive graphics using vector diagrams, contour plots, overlays, user interactive trajectory modifications, interactive features (menus, dialogs, etc).
- How to efficiently combine effectors in vehicles that use multiple types of effectors by creating effector combination matrices that produce the demanded accelerations, and reduce the dynamic coupling between the control axes.
- Huge amount of flight vehicle design information is available, including data files, Matlab scripts, Simulink files, and 6-dof non-linear simulations.

The user/ analysts are encouraged to study, repeat, and run some of these examples in their own computers in order to familiarize themselves with the process and tool. They may begin with the examples which are similar to their flight vehicle application and gradually modify them by introducing data from their own applications.